BUILDING TOXICITY PATHWAY MODELS AND ESTIMATING TRANSCRIPTOMIC POINTS-OF-DEPARTURE (tPODs) IN THREE PHYLOGENETICALLY DISTANT RAY-FINNED FISHES EXPOSED TO 17α-ETHINYLESTRADIOL AND FLUOXETINE

A Thesis Submitted to the

College of Graduate and Postdoctoral Studies

In Partial Fulfillment of the Requirements

For the Degree of Doctor of Philosophy

In the Toxicology Graduate Program

University of Saskatchewan

Saskatoon

By

ALPER JAMES G. ALCARAZ

PERMISSION TO USE

In presenting this thesis/dissertation in partial fulfillment of the requirements for a Postgraduate degree from the University of Saskatchewan, I agree that the Libraries of this University may make it freely available for inspection. I further agree that permission for copying of this thesis/dissertation in any manner, in whole or in part, for scholarly purposes may be granted by the professor or professors who supervised my thesis/dissertation work or, in their absence, by the Head of the Department or the Dean of the College in which my thesis work was done. It is understood that any copying or publication or use of this thesis/dissertation or parts thereof for financial gain shall not be allowed without my written permission. It is also understood that due recognition shall be given to me and to the University of Saskatchewan in any scholarly use which may be made of any material in my thesis/dissertation.

Requests for permission to copy or to make other uses of materials in this thesis/dissertation in whole or part should be addressed to:

Chair of the Toxicology Graduate Program

44 Campus Drive

University of Saskatchewan

Saskatoon, Saskatchewan S7N5B3 Canada

OR

Dean

College of Graduate and Postdoctoral Studies

University of Saskatchewan

116 Thorvaldson Building, 110 Science Place

Saskatoon, Saskatchewan S7N 5C9 Canada

ABSTRACT

The continuous development and production of new chemicals to meet societal needs results in their increasing release and prevalence in the environment. These contaminants of emerging concern (CECs) are continuously discharged from wastewater treatment plants and other sources that are often not equipped to remove these classes of compounds. Thus, the pseudo-persistence of these CECs poses potential toxicological risks to aquatic organisms and, therefore, constitute a significant issue in many aquatic environments. However, current testing frameworks supporting chemical and environmental risk assessment (ERA) are falling short of the global need to rapidly test the increasing numbers of CECs because they rely on the extensive use of live animals, which is time-consuming, costly, and presents significant ethical concerns. Thus, there is an urgent need for the development and implementation of new approach methodologies (NAMs) aimed to replace, reduce, and refine (3Rs) live animal testing while increasing throughput and decreasing costs to improve hazard assessment strategies and support regulatory decision-making. This dissertation aimed to develop and evaluate a NAM system based on short-term embryonic exposure assays to (1) characterize the toxicity pathways of two priority CECs, 17α-ethinylestradiol (EE2) and fluoxetine (FLX) as model chemicals, through cross-organizational level assessments linking molecular mechanistic response patterns with physiological/apical outcomes; and (2) derive transcriptomics points-of-departure (tPODs) that can support quantitative hazard assessment across phylogenetically distant fish. Specifically, fathead minnow (FHM), rainbow trout (RBT), and white sturgeon (WS) were exposed to graded concentrations of each CEC from an early embryonic stage. At 4 days post-hatch (dph), changes across the whole transcriptome and proteome were characterized, and higher organizational-level responses were evaluated at 28 dph (FHM) and 60 dph (RBT and

WS). Molecular alterations were then compared to downstream responses to build toxicity pathway models for each chemical. In addition, transcriptomic datasets from 4 dph were used to model dose-response for genes/transcripts and calculate benchmark concentrations (geneBMCs) of toxicant-responsive genes/transcripts. These geneBMCs were used to derive transcriptomics points-of-departure (tPODs) using a number of statistical strategies. These tPODs were then compared to chronic and physiological/apical PODs obtained in this study and from the literature. tPOD estimates were also compared across species.

Results demonstrated that when exposed to EE2, transcriptomic and proteomic profiles of FHM at 4 dph were predictive of histological and apical outcomes at 28 dph. Similarly, transcriptomic profiles of RBT at 4 dph were predictive of histological and apical responses at 60 dph, when exposed to EE2, although proteomic profiles at 4 dph did not correlate well with transcriptomics and apical outcomes. On the other hand, FLX-target genes and proteins were not significantly altered in FHM at 4 dph, but integrated functional analyses of transcriptomics and proteomics revealed molecular processes that were predictive of apical outcomes observed in this study and those reported in the literature. Overall, results showed that transcriptomic responses from whole-body early-life stage (ELS) fish were related to downstream and apical outcomes observed at more advanced life stages. Proteomic responses were limited in predicting relevant responses but added a valuable layer of biological information that enhanced the understanding of the connectivity between molecular events and apical outcomes. Hence, proteomics provided an additional line-of-evidence in support of enhancing our understanding of the mode of action of the tested CECs across biological levels.

Estimated tPODs in all species closely approximated and were protective of chronic apical PODs observed in this study and in the literature, both for EE2 and FLX. tPODs derived

from the median of the 20 most sensitive active genes ($omicBMC_{20}$) were the most protective among tPOD estimates within a species, with FLX tPOD values of 0.02, 0.02, and 0.56 µg/L, and with EE2 tPOD values of 0.06, 0.12, and 2.39 ng/L for WS, RBT, and FHM, respectively. These values were significantly more sensitive than pathway-level BMCs (pathBMC) and were independent of species annotations, which is one of the main limitations when working with non-model species for which no functionally annotated genomes or transcriptomes are available. In general, RBT appeared to be the most sensitive species in terms of tPOD estimates, closely followed by WS, with FHM being the least sensitive to exposure to both chemicals. Regardless, tPOD estimates from ELS fish were within a tight range of concentrations despite minor differences in exposure conditions and data analysis workflow. Overall, this dissertation demonstrated that the fish embryo assays established in this thesis project represent a promising approach to (1) characterize toxicity pathways for CECs that can inform cross-species and chemical hazard assessment, and (2) derive quantitative BMCs (tPODs) that are protective of apical PODs, and therefore show significant promise as a NAM to support chemical hazard assessment and regulatory decision making. Future studies should be directed towards the optimization and validation of this approach using more chemicals and other species that are relevant to ERA.

ACKNOWLEDGEMENTS

My sincerest gratitude to my supervisor, Dr. Markus Hecker, for all the knowledge and wisdom he imparted to me throughout my degree. Markus has shaped me these past years to become the scientist that I am right now; he encouraged a free-thinking, holistic, and optimistic environment where one can grow by pushing boundaries and trying/doing seemingly unmanageable tasks; for giving endless opportunities to attend conferences, meet distinguished scientists, train and work outside our comfort zones, and collaborate with capable and experienced scientists and institutions. This thesis, and the whole experience of this PhD degree, would not have been possible without Markus' immeasurable support. I would also like to thank Dr. David Janz, the Chair of my graduate committee, for the many words of encouragement and wisdom, and for always reminding me that I'm doing good. Sincerest gratitude also goes to all the members of my graduate committee: Dr. Suraj Unniappan, Dr. Lynn Weber, Dr. Steve Wiseman, and Dave Schneider for the continuous support, advice, and for the challenges they provided throughout the years of my graduate studies that made me a better student and scientist. And to Dr. Daniel Schlenk, who did not hesitate to lend his expertise to give the final challenge and share his wisdom, and be the external examiner of my dissertation.

Very special thanks to soon-to-be Drs. Taylor Lane, Phillip Ankley, and Dayna Schultz, and to Nicole Baldwin, Katherine Raes, Saurabh Prajapati, and Sydney Murray for the collaborations, friendship, and for keeping me company during late nights to early mornings in and outside grad school, and most especially for making this journey fun, exciting, and enjoyable, and for keeping my sanity intact when things seem to fall apart. Much appreciation to all of you; these will never be forgotten. As well, thanks to Dr. Kamran Shekh, Dr. Jon Doering, Dr. Markus Brinkmann, and Dr. Marek Pipal for the many collaborations, the inspiration to

finish, and advises on how to survive and thrive in grad school, research, and beyond. To Dr. Song Tang, Connor Burbridge, Dr. Othman Soufan, and Jessica Ewald for the discussions and help in bioinformatics. To present and previous colleagues who contributed a lot towards the completion of my project(s): Bryanna Eisner, Anita Masse, Susari Mala Irugal Bandaralage, Dr. Natacha Hogan, Dr. Klara Hilscherova, Dr. Jason Raine, Derek Green, Dr. Kerstin Bluhm, Kamil Mikulasek, David Potesil, Dr. Zbynek Zdrahal, Carly Colville, Ulyana Fuchylo, Mikayla Oldach, and Dr. Shreyas Jois. To Adriana Brown, Fiona Price, and Tina Klein for the administrative help and for going beyond what was required for them to help me out throughout my stay in Toxicology Centre, all of these are very much appreciated.

I would also like to take this opportunity to thank the sources of funding for my degree and research: the U of S Dean's International Scholarship, Toxicology Devolved Scholarship, Mitacs Globalink Research Award, Genome Canada, and Oceans and Fisheries Canada. Similarly, I would like to thank our collaborators from McGill University, Environment and Climate Change Canada, RECETOX and CEITEC in Masaryk University, University of Lethbridge, the Genome Project, the Hogan and Hecker Labs, and all the past and present students, faculty, postdocs, our many trainees and technicians, and visiting students at the Toxicology Centre.

And to Kuya Alper John, Paul Alper, Peter Alper, Nanay and Tatay, this is for you.

TABLE OF CONTENTS

LIST OF TABLES

LIST OF FIGURES

LIST OF ABBREVIATIONS

|log2FC|	absolute value of the log2 fold-change
µg	microgram
µg/L	microgram per liter
3R	replace, reduce, refine
A. transmontanus	*Acipenser transmontanus*
ABIRD	Active Background Ion Reduction Device
AB	ammonium bicarbonate
ahcyl1	adenosylhomocysteinase-like 1 gene
ahsg2	alpha-2-hs-glycoprotein 2 gene
AIC	Akaike information criterion
ANOVA	analysis of variance
AOP	adverse outcome pathways
BMC	benchmark concentration
BMD	benchmark dose
bp	base-pair
BP	biological process
bw	body weight
CC	cellular component
cDNA	complementary DNA
CEC	chemicals of emerging concern
cplx2l	complexin 2 gene
CPM	counts per million

cRAP	common Repository of Adventitious Proteins
CRediT	Contributor Roles Taxonomy
ctnnd2a	catenin (cadherin-associated protein), delta 2a gene
ctsa	cathepsin A gene
ctsz	cathepsin Z gene
cyp19a1b	cytochrome P450, family 19, subfamily A, polypeptide 1b gene (aromatase B)
D. rerio	*Danio rerio*
d4-EE2	d4-17α-ethinylestradiol (deuterated)
d5-FLX	d5-fluoxetine (deuterated)
DA	differentially abundant
DAP	differentially abundant protein
DE	differentially expressed
DEG	differentially expressed genes
DMSO	dimethylsulfoxide
DNA	deoxyribonucleic acid
DO	dissolved oxygen
dpf	days post-fertilization
dph	days post-hatch
dsDNA	double-stranded deoxyribonucleic acid
DTT	dithiothreitol
E2	estradiol
EC50	concentration of chemical causing 50% effect

EDC	endocrine disrupting compound
EE2	17α-ethinylestradiol
ELISA	enzyme-linked immunosorbent assay
ELS	early life stage
epn2	epsin 2 gene
ER	estrogen receptor
ERA	environmental risk assessment
ers	earlyriser gene
ERα	estrogen receptor alpha protein
esr1	estrogen receptor 1 gene
f13a	coagulation factor XIIIA gene
f13a1a	coagulation factor XIII, A1 polypeptide a gene
FA	formic acid
fam20c	extracellular serine/threonine protein kinase FAM20C gene
FASP	filter-aided sample preparation
fbln1	fibulin 1 gene
FC	fold-change
FDR	false discovery rate
FHM	fathead minnows
FLC	full life cycle
FLX	fluoxetine
fn1a	fibronectin 1a gene
GDRS	genomic dose-response studies

geneBMC	gene-level benchmark concentration
geneBMD	gene-level benchmark dose
GEO	Gene Expression Omnibus
GH/IGF-I	growth hormone/Insulin-like growth hormone
GO	Gene Ontology
HCD	higher-energy collisional dissociation
HP	Human Phenotype Ontology
hpf	hours post-fertilization
HPLC	high performance liquid chromatography
H_TPCs	Human Therapeutic Plasma concentrations
IGF	insulin-like growth factor
IGFBP	insulin-like growth factor binding protein
inpp5kb	inositol polyphosphate-5-phosphatase Kb gene
IPL	inner plexiform
kDa	kiloDalton
KEGG	Kyoto Encyclopedia of Genes and Genomes
KNIME	Konstanz Information Miner
LC50	concentration of chemical causing 50% mortality
LC-MS/MS	Liquid chromatography with tandem mass spectrometry
LMWHC	low molecular weight hydrocarbons
LOEC	lowest observed effect concentration
m/z	mass-to-charge ratio
MA plot	plot of M (log ratio) and A (mean average) scales

MF	molecular function
mg CaCO3/L	milligrams calcium carbonate per liter (equivalent)
mg/L	milligrams per liter
mM	millimolar
MOA	mode of action
mRNA	messenger RNA
MS222	tricaine methanesulfonate
mta3	metastasis associated 1 family, member 3 gene
mtdha	metadherin a gene
NAM	new approach method/methodology
nbeaa	neurobeachin a gene
NCBI	National Center for Biotechnology Information
ND	not detectable
ng/L	nanogram per liter
NH_4OH	ammonium hydroxide
NOEC	no observed effect concentration
nots	nothepsin gene
nr2f2	nuclear receptor subfamily 2, group F, member 2 gene
NTP	National Toxicology Program
O. mykis	*Oncorhynchus mykiss*
^oC	degree Celsius
OCD	obsessive-compulsive disorder
OCD	obsessive-compulsive disorder

OECD	Organisation for Economic Co-operation and Development
OLS	ordinary least-squares
omicBMC$_{10th}$	the value of the benchmark concentration of the tenth percentile of all active genes
omicBMC$_{20}$	the median of the benchmark concentration of the 20 most sensitive active genes
omicBMC$_{mode}$	the mode of the first peak of the geneBMC distribution
omicBMD$_{10th}$	the value of the benchmark dose of the tenth percentile of all active genes
omicBMD$_{20}$	the median of the benchmark dose of the 20 most sensitive active genes
omicBMD$_{mode}$	the mode of the first peak of the geneBMD distribution
OPL	outer plexiform
P.promelas	*Pimephales promelas*
pathBMC	the most sensitive pathway based on the median of geneBMCs in a pathwaywith at least three active genes
pathBMD	the most sensitive pathway based on the median of geneBMDs in a pathwaywith at least three active genes
pax6a	paired box 6a gene
PNEC	predicted no-effect concentration
POD	point-of-departure
Poly2	2^o polynomial
PPCP	pharmaceuticals and personal care products

PPI	Protein-protein interaction
PRIDE	Proteomics Identification Database - EMBL-EBI
PRL	photoreceptor
qki2	paired box 6a gene
qRT-PCR	quantitative Reverse Transcription Polymerase Chain Reaction
QSAR	quantitative structure–activity relationship
RBT	rainbow trout
REAC	Reactome
RIN	RNA integrity number
RNA	ribonucleic acid
SD	standard deviation
sdcbp2	syndecan binding protein (syntenin) 2 gene
SDS	sodium dodecyl sulfate
SDS-PAGE	sodium dodecyl sulphate–polyacrylamide gel electrophoresis
SDT	SDS/DTT/Tris-HCl
SE	standard error of the mean
SSRI	serotonin reuptake inhibitor
TMM	trimmed mean of M
tPOD	transcriptomic point-of-departure
try/prss1	serine protease 1 gene
USFDA	US Food and Drug Administration
v/v	volume to volume
vtg	vitellogenin gene/transcript

Vtg	vitellogenin protein
vwa2	von Willebrand factor A domain containing 2 gene
WS	white sturgeon
WWTP	wastewater treatment plant
Zp	Zona pellucida glycoprotein
zp2.3	zona pellucida glycoprotein 2 gene
µS/cm	microSiemens per centimeter

*This thesis followed the ZFIN Zebrafish Nomenclature Convensions (zfin.atlassian.net) for naming genes/transcripts and proteins:

a. Gene nomenclature: full gene names and gene symbols are in lowercase and italics.

b. Protein nomenclature: protein names and symbols are non-italic and the first letter is uppercase.

NOTE TO READERS

This thesis is organized to follow the University of Saskatchewan College of Graduate and Postdoctoral Studies guidelines for manuscript style thesis. Chapter 1 is the general introduction of the thesis topic. Chapter 2-5 are organized as manuscripts for publication in peer-reviewed scientific journals. Chapter 6 contains the overall discussions and conclusion of this thesis. Chapter 2 and 3 have been published in *Environmental Science and Technology*, Chapter 4 is currently under review (after minor revision) in *Environmental Pollution,* and Chapter 5 is in preparation for submission to *Environmental Science and Technology*. Full citations of published papers and author contributions are provided following the preface of each chapter. As a result of the manuscript style format, there is some repetition of materials in the introduction and materials and methods sections across the different chapters of this thesis. The tables, figures, supporting information, and references cited in each chapter have been reformatted here to be consistent with the thesis style requirements of the University of Saskatchewan. References cited in each chapter are combined and listed in the References section of this thesis. Supporting information associated with research chapters are presented in the "Appendices" section at the end of this thesis as X.Sy, where X indicates the Appendix letter and Sy indicates the table or figure number. The descriptions of Supplemental Files for each research chapter are listed in their respective section of "List of Supporting Information". The Supplemental Files can be found in the associated publications.

1 CHAPTER 1: GENERAL INTRODUCTION

1. 1. Introduction

The number of chemical substances for which toxicity data is required has been exponentially increasing over the past decades, with new compounds being introduced almost every day. These chemicals of emerging concern (CECs) typically end up in surface water systems, with effluents of municipal wastewater facilities that are not equipped to treat these compounds constituting one of their main sources (Petrie *et al*., 2015; Sauvé and Desrosiers, 2014; Templeton *et al*., 2009; USEPA OW/ORD Emerging Contaminants Workgroup, 2008; Vidal-Dorsch *et al*., 2012). CECs include a wide range of different substance groups that include brominated flame retardants, nanoparticles, microplastics, and pharmaceuticals and personal care products (PPCP), among others, which may consequently affect non-target organisms in impacted environments (Patel *et al*., 2019; Sehonova *et al*., 2018). Many CECs, particularly PPCPs, are considered pseudo-persistent – compounds that may have short half-lives and are released at low concentrations but are consistently and continually infused into the aquatic environment, thus essentially becoming persistent (Daughton, 2003). Aquatic organisms are then chronically exposed to these low sub-lethal concentrations of CECs that do not result in immediate lethal or acute outcomes. However, subtle short-term molecular changes that do not immediately manifest at the physiological level may affect populations and communities of organisms under sub-chronic or chronic environmental exposure (Kidd *et al*., 2014; Liney *et al*., 2006).

Environmental quality criteria under current regulatory frameworks to support environmental risk assessments (ERA) are mostly based on endpoints that have direct ecological and/or regulatory relevance such as survival, reproduction, growth, and development. These endpoints rely heavily on the use of extensive tests with live vertebrate animals, which is increasingly becoming of ethical concern. Furthermore, lengthy-time requirements render the

current process of chemical hazard assessment tedious, resource-intensive, and prone to uncertainty (Hecker, 2018). It is therefore apparent that there is an urgent need to establish alternative, high-throughput approaches for screening and prioritizing of chemicals to improve the current ERA process. In addition, traditional testing approaches in support of ERA, by and large, utilize a few select model organisms, which may not necessarily assure protectiveness towards the huge diversity of native species living in local ecosystems of concern because of our limited understanding of their sensitivity and vulnerability. For instance, there have only been a few studies investigating the effects of CECs on fishes of commercial, cultural, and recreational importance to Canadians (Beitel *et al*., 2015, 2014; Schultz *et al*., 2021). Questions have been raised on whether values derived from model organisms are protective of native organisms and whether they respond similar to organisms of different ancestral origin, and therefore, would be able to predict impacts on ecological species, which is the ultimate protection goal (Doering *et al*., 2018; Schultz *et al*., 2021).

Recent developments in the field of predictive ecotoxicology advocate alternative toxicity testing approaches such as the use of *in vitro*, *in silico* or embryonic assays combined with mechanism-based testing as promising new approach methods (NAMs), particularly for prioritizing chemicals for further testing (Basu *et al*., 2019). Advances in 'omics technologies offer high-throughput and cost-effective approaches by examining patterns of mechanisms of toxicity that could guide tests and endpoint selection across species in predictive ERA (Villeneuve *et al*., 2012; Waters & Fostel, 2004). In particular, next-generation whole systems technologies allow the interrogation of a full suite of molecular families (i.e., transcripts, proteins, etc.) of an organism without *a priori* knowledge of the chemical's mode of action (MOA). For instance, molecular toxicity pathways from non-target gene and protein expression analyses, when developed as

extrapolative models, could be used as diagnostic tools in predicting apical responses across biological organizations that are of ecological and regulatory relevance. Similarly, the use of the earliest life stages (ELS) of animals, specifically in fish, has been proven effective in deriving benchmark concentrations that are protective of a chemical's effects at more advanced life stages (Wheeler *et al*., 2014). Life stages of oviparous vertebrates, such as fish, prior to independent exogenous feeding are not considered live animals under current legislations (Canadian Council on Animal Care, 2005; European Union, 2010; Strähle *et al*., 2012; UK, 1993). Thus, short-term ELS assays utilizing 'omics technologies show great promise in advancing efforts that aim to replace, reduce and refine (3Rs) live animal testing while increasing throughput to improve hazard assessment strategies and support regulatory decision-making.

1.2. Objectives and hypotheses

The current paradigm shift necessitated by the need for the reduction of the use of live vertebrate animals in toxicity testing is resulting in the accelerated development of NAMs to streamline chemical hazard assessment. Most NAMs are based on mechanistic toxicity models to identify molecular and cellular events that could lead to adverse apical outcomes of regulatory relevance (Ankley *et al*., 2010; Villeneuve *et al*., 2014). While mechanistic molecular analyses in support of chemical hazard assessment have been conducted for decades, only a few focused on the quantitative derivation of toxicity thresholds and most of these developments have relied on *in silico* (Brinkmann *et al*., 2014), *in vitro* (Doering *et al*., 2020), and *ex vivo* (Rahman *et al*., 2020) studies. However, many of these approaches are limited in estimating apical toxicity thresholds as they do not represent the complex interactions occurring within an organism after a toxic insult;

hence, there is a need to quantitatively anchor these models to relevant apical outcomes to fully realize their predictive capability in regulatory ecotoxicology.

Therefore, the overall objective of this dissertation was to develop and evaluate short-term embryonic exposure assays to derive protective points-of-departure (POD) from transcriptomic datasets across phylogenetically distant fish species using 17α-ethinylestradiol (EE2) and fluoxetine (FLX) as model CECs. EE2 is a synthetic estrogenic compound frequently used as an active ingredient in contraceptives while FLX is one of the most highly prescribed selective serotonin reuptake inhibitors (SSRI). These compounds are commonly found in surface waters and their toxicities are well described in the literature (reviewed in Brooks, 2014 and Laurenson *et al*., 2014), and therefore, there is a wealth of information on their respective MOAs. Empirically derived apical PODs for these compounds across several fish species have also been reported previously, allowing comparisons to transcriptomics PODs (tPODs). Specifically, this project aimed to (1) develop short-term ELS assays to assess the toxicity of CECs, (2) construct toxicity pathway models for EE2 and FLX using the embryo assays developed in (1), (3) calculate tPODs for EE2 and FLX from short-term ELS assays using molecular benchmark dose/concentration (BMD; BMC) modeling, and (4) apply the transcriptomics benchmark models established under the earlier objectives to derive tPODs for three phylogenetically distant ray-finned fish species – fathead minnow (FHM; *Pimephales promelas*), rainbow trout (RBT; *Oncorhynchus mykiss*), and white sturgeon (WS; *Acipenser transmontanus*). This research utilized non-targeted techniques such as the evaluation of the effects of the two chemicals on the whole transcriptome and the global proteome with the goal of linking molecular perturbations to adverse apical outcomes and to derive tPODs to approximate protective apical thresholds. This study serves as a proof-of-concept in the use of short-term embryonic assays in deriving tPODs as alternative testing strategy to support

regulatory decision-making. The main objectives and testable hypotheses for each chapter were as follow:

Objective 1. *To build a toxicity pathway model for embryo-larval stages of fathead minnows (Pimephales promelas) exposed to EE2, using a combination of whole transcriptomics, non-target proteomics, and physiological/histological/apical analyses. (Chapter 2)*

1. H_o: There are no statistical differences in the expression of transcripts across treatment groups after exposure of embryonic FHM to EE2 from <6 hours post-fertilization (hpf) to 4 days post-hatch (dph).
2. H_o: There are no statistical differences in the abundance of proteins between the control and high treatment groups after exposure of embryonic FHM to EE2 from <6 hpf to 4 dph.
3. H_o: There is no statistical correlation between the transcriptomic and proteomic responses after exposure of embryonic FHM to EE2 from <6 hpf to 4 dph.
4. H_o: There are no statistical differences in apical responses across treatment groups after exposure of embryo-larval FHM to EE2 from <6 hpf to 28 dph.
5. H_o: There are no statistical differences in survival rates across treatment groups after exposure of embryo-larval FHM to EE2 from <6 hpf to 28 dph.

Objective 2. *To establish a 4-day embryo-alevin assay for rainbow trout **(**RBT**)** to characterize the effects of EE2 across biological levels of organization and to calculate tPODs using a transcriptomic BMD approach. (Chapter 3)*

1. H_o: There are no statistical differences in the expression of transcripts across treatment groups after exposure of embryo-alevin RBT to EE2 from hatch to 4 dph.
2. H_o: There are no statistical differences in the abundance of proteins across treatment groups after exposure of embryo-alevin RBT to EE2 from hatch to 4 dph.
3. H_o: There is no statistical correlation between the transcriptomic and proteomic responses after exposure of embryo-alevin RBT to EE2 from hatch to 4 dph.
4. H_o: There are no statistical differences in the apical responses across treatment groups after exposure of embryo-alevin RBT to EE2 from hatch to 4 dph or to swim-up stage (21 dph).
5. H_o: There are no statistical differences in survival rates across treatment groups after exposure of embryo-alevin RBT to EE2 from hatch to 4, 21, or 60 dph.

Objective 3. *To characterize the effects of FLX to early-life stage FHM across biological levels of organization and to develop and validate the utility of a short-term embryo-larval FHM assay to estimate tPODs using FLX. (Chapter 4)*

1. H_o: There are no statistical differences in the expression of transcripts across treatment groups after exposure of embryo-larval FHM to FLX from <6 hpf to 4 dph.
2. H_o: There are no statistical differences in the abundance of proteins between the control and medium treatment groups after exposure of embryo-larval FHM to FLX from <6 dpf to 4 dph.
3. H_o: There are no statistical differences in apical responses across treatment groups after exposure of embryo-larval FHM to FLX from <6 dpf to 28 dph.

4. H_o: There is no statistical correlation between the transcriptomic and proteomic responses after exposure of embryonic FHM to FLX from <6 hpf to 4 dph.
5. H_o: There are no statistical differences in locomotor responses across treatment groups after exposure of embryo-larval FHM to FLX from <6 dpf to 4 dph.
6. H_o: There are no statistical differences in survival rates across treatment groups after exposure of embryo-larval FHM to FLX from <6 hpf to 28 dph.

Objective 4. *To derive tPODs from three phylogenetically distant ray-finned fish species – FHM, RBT and WS – at embryo-larval/alevin stages, using EE2 and FLX. (Chapter5)*

1. H_o: There are no statistical differences in the abundance of transcripts across treatment groups after exposure of embryo-larval FHM to FLX and EE2 from <6 hpf to 4 dph.
2. H_o: There are no statistical differences in the abundance of transcripts across treatment groups after exposure of embryo-alevin RBT to FLX and EE2 from hatch to 4 dph.
3. H_o: There are no statistical differences in the abundance of transcripts across treatment groups after exposure of embryo-larval WS to FLX and EE2 from hatch to 4 dph.

1.3. Review of related literature

1.3.1 Contaminants of emerging concern (CEC)

Contaminants of emerging concern (CECs) are pollutants that have recently been detected or which have been previously reported in the environment but that had only recently been discovered to have adverse effects. They also include well-known chemicals that have recently become a toxicological concern due to the potential adverse effects they may have on non-target organisms (Sauvé and Desrosiers, 2014). CECs do not have regulatory standards and are usually

not included in routine monitoring activities but may be candidates for future monitoring programs due to their potential adverse effects and ubiquity (USEPA OW/ORD Emerging Contaminants Workgroup, 2008). The qualification of a chemical contaminant as "emerging" is relative to its importance as a contamination issue at present, as chemicals are continuously synthesized and discovered in the environment.

Many CECs are introduced into aquatic ecosystems through municipal wastewater effluents, or as runoff from agricultural and urban areas. The ubiquity of most of these compounds in surface waters was not recognized until recent developments of more advanced chemical analytical methods that improved our ability to detect these compounds with greater sensitivity in the environment (Anderson *et al*., 2013; Comerton *et al*., 2009; Martín-Pozo *et al*., 2019). For instance, CECs such as pharmaceuticals have been used for a long time but have only been recognized as contaminants of concern in the past decade or two due to the limitations of traditional analytical technologies. This is true for many natural and degradation products, as well as newly synthesized compounds that were not previously known in the scientific literature. Based on CAS registry alone, more than 159 million unique chemicals have been registered as of 2020, and 250 million unique chemical substances were registered in April 2021 (www.cas.org). These numbers are expected to increase further as the demands for improved raw materials and active ingredients intensify, resulting in more common occurrences of CECs.

Pharmaceuticals and personal care products (PPCPs) are one of the major categories of CECs, which includes a suite of human-prescribed and over-the-counter drugs and medications, steroids and hormones, disinfectants, synthetic musks, etc. Significant concerns have been raised about CECs due to their unintentional presence and their inherent ability to induce effects at low doses/concentrations, as well as their persistent input and potential threats to human and ecological

health (Ebele *et al*., 2017). These chemicals find their way into the aquatic environment mainly through municipal wastewater and sewage treatment effluents. Relatively little is known about the occurrence of these compounds in freshwater environments compared to other pollutants, and while many of these compounds are broken down and degraded, parent compounds and degradation products could persist and create potential hazards to the environment and human life. Two PPCPs of particular interest are the endocrine disrupting compound (EDC), EE2, and the selective serotonin reuptake inhibitor (SSRI), FLX, due to their wide use and their reported occurrence in surface waters in North America.

1.3.1.1. CEC in focus: 17α-ethinylestradiol

Perhaps one of the most studied endocrine disrupting compounds (EDC) is 17α-ethinylestradiol (EE2). EE2 is a synthetic hormone modeled after the endogenous estrogen estradiol (E2), and is used as a contraceptive, as well as a treatment for menopausal and postmenopausal syndrome, prostatic cancer, and breast cancer in postmenopausal women, and osteoporosis (Aris *et al*., 2014). It alters processes of the endocrine system by mimicking or antagonizing the effects of endogenous hormones, disrupting the synthesis and metabolism of endogenous hormones, or disrupting the synthesis of specific hormone receptors. It is generally known that estrogens in the environment originate from poorly or untreated sewage discharged into water bodies, with approximately 40% of the hormones entering a conventional wastewater treatment plant not being removed in secondary treated effluents (Froehner *et al*., 2011). Due to its lipophilic and persistent properties, EE2 can bioaccumulate and biomagnify in aquatic organisms (Matozzo *et al*., 2008). The occurrence of EE2 in water, sediment, and biota has been observed globally (Aris, 2014; Laurenson *et al*., 2014), with the highest concentration of 129.8

206 ng/g having been reported in surface sediments in a mangrove forest in Brazil (Froehner *et al*.,
207 2012). When detected in waterways, EE2 is typically found in single digit or sub ng/L range, but
208 concentrations in WWTP effluents from urbanized areas of up to 62 ng/L have been reported (Aris
209 *et al*., 2014).

210 Research on the effects of EE2 in fish has been extensive (Aris, 2014; Overturf *et al*.,
211 2015). EE2 is known to affect reproductive function in fish, specifically affecting endocrine
212 pathways influencing behaviour, gonadal differentiation, and the production of vitellogenin (Vtg)
213 (Zhang *et al*., 2008). It has been shown to alter molecular signaling cascades resulting in increased
214 plasma vitellogenin concentrations in male and female fish, increased proportions of intersex fish,
215 decreased egg and sperm production, reduced gamete quality, complete feminization of male fish,
216 and reduced fertility (Andersson *et al*., 2007; Kidd *et al*., 2007; Partridge, Boettcher, & Jones,
217 2010). Aquatic organisms are sensitive to the exposure with EE2 throughout their life, and
218 particularly during embryonic and juvenile stages (van Aerle *et al*., 2002). However, while overall
219 types of responses are similar, species-specific differences in sensitivities exist among fishes. For
220 instance, while it has generally been shown that EE2 reduces reproductive capability of fish
221 populations (Schwindt *et al*, 2014), certain species such as the mummichog do not show
222 comparable impacts on egg production as was observed in other fishes (Bosker *et al*., 2016). Even
223 an improved egg production occurred in Gulf pipefish (Rose *et al*., 2013). In fish species native to
224 North America, it has been reported that EE2 altered *vtg* transcript abundance *in vitro* but there
225 were great differences in sensitivities among species (Beitel *et al*., 2015, 2014). Therefore, while
226 there have been extensive research efforts in the assessment of the effects of EE2, there is still a
227 great deal of remaining uncertainties and issues concerning the hazard assessment of this
228 compound in freshwater ecosystems (Hecker and Hollert, 2011). To date, there is no official water

quality guideline for EE2, albeit there are recommendations in the literature (European Commission, 2011; Caldwell *et al*., 2012). Further research is necessary to ascertain that values set for environmental quality criteria are robust and protective of non-model organisms.

1.3.1.2. CEC in focus: Fluoxetine

Fluoxetine was first introduced as Lilly 110140 (Wong *et al*., 1974). It was approved by the US Food and Drug Administration (FDA) as an antidepressant drug, treatment for obsessive-compulsive disorder (OCD), and recommended for treatment of bulimia. This drug exerts its action within the central nervous system by reducing the clearance rate of serotonin (5-hydroxytrypamine), a neurotransmitter, through binding to presynaptic serotonin reuptake receptors, potentiating the effects of serotonin in the post synaptic cleft. While the mechanism of action of FLX is not fully understood, Guest *et al*. (2004) suggested that FLX alters cortical expression of multiple heat shock protein 60 forms along with neurofilaments and related proteins that are critical determinants of synaptic structure and function.

In the US, more than 27 million prescriptions of FLX were issued in 2019 (https://clincalc.com/DrugStats/Drugs/Fluoxetine). On average, 80% of FLX administered is excreted through the urine and feces (Gracia, 2005). At this rate, and with increasing global usage, an increasing amount of trace FLX has been detected in the environment, with concentrations likely to further increase in the future (Mole and Brooks, 2019). In general, aquatic discharges are usually from domestic pharmaceutical consumption, which pass through wastewater treatment plants mostly at sub-therapeutic levels that are of negligible acute toxicological risk, but with elevated concentrations in areas where manufacturing plants are located (Bringolf *et al*., 2010). Unfortunately, FLX is not readily biodegradable in wastewater treatment plants. A summary of

published reports on the distribution of FLX shows a median concentration of 17.9 ng/L with a maximum concentration reported at 596 ng/L in freshwater ecosystems (Hughes *et al*., 2013). The compound is hydrolytically and photolytically stable (photodegradation $t_{1/2}$ of ~160 days) in aqueous environments but is rapidly adsorbed in sediment systems, hence, concentrations in the aqueous phase will be lower and the potential impacts of FLX in the aquatic environments are decreased (Black and Armbrust, 2007; Kwon and Armbrust, 2006). However, since FLX is recalcitrant against physico-chemical and biological degradation processes, it is persistent as a substrate-adsorbed compound, and therefore, poses a significant threat to bottom-dwelling organisms.

Read-across hypotheses have driven much of the research on the likely effects of pharmaceuticals to non-target organisms. The read-across hypothesis stipulates that if a drug's molecular targets are conserved and plasma concentrations are similar to human therapeutic concentrations in non-target organisms, it is expected that the drug will have a similar effect (Rand-Weaver *et al*., 2013). It should therefore be possible to predict potential environmental impacts of a drug using model organisms. For instance, effects on active avoidance behaviour were observed in fish exposed to FLX, as previously observed in rats, suggesting that serotonin mechanisms were highly conserved among vertebrates (Beulig and Fowler, 2008). Fish elicited anxiolytic responses when exposed to an equal range of Human Therapeutic Plasma concentrations (H_TPCs) of FLX, showing comparable sensitivity to that observed in human patients affected by general anxiety disorder (Margiotta-Casaluci et al., 2014a). Even at concentrations as low as 1 μg/L, FLX significantly impacted mating behaviour in male freshwater fish, displaying increased aggression, isolation, and repetitive behaviors at higher concentrations, as well as lack of predator avoidance behaviors (Beulig & Fowler, 2008; Painter *et al*., 2009; Winder *et al*., 2009). There were also

effects observed that went beyond what was expected from the read-across approach. Acute and chronic exposure of other fishes to FLX were reported to cause endocrine disruption (Mennigen *et al*., 2010a; Schultz *et al*., 2011), impaired energy metabolism (Mennigen *et al*., 2010) and altered nitrogen waste excretion and osmoregulation (Morando *et al*., 2009). At the genomic level, transcriptomic studies showed FLX-induced alteration in stress- and behaviour-linked pathways, lipid and amino acid metabolic processes, and steroid biosynthesis (Mercier *et al*., 2004; Wong *et al*., 2013). However, the absence of lethal effects and the diversity of behavioral and biomarker response endpoints in FLX toxicity makes it difficult for regulatory bodies to set reliable standard criteria for FLX in the aquatic environment (Kumar *et al*., 2016). Therefore, at present, freshwater guideline values are still scarce, if there are any, and are still at the recommendatory stage (European Commission, 2011). Nevertheless, the diverse adverse side effects of FLX attest that exploration of FLX-induced mechanisms merits further investigation through untargeted and unbiased approaches.

1.3.2. Transcriptomic points-of-departure (tPOD) as a toxicogenomic tool in chemical hazard assessment

Toxicogenomics play an important role in the current efforts to reduce, refine and eliminate live animal-based conventional toxicity testing, which is expensive, lengthy, and ethically questionable. It exploits rapidly evolving genomic technologies that serve as powerful tools in mechanism-based and predictive toxicology. Approaches such as RNA sequencing and ultra-high resolution liquid chromatography tandem-mass spectroscopy (LC-MS/MS) enable exploration of the interconnections of changes in molecular circuitry across different molecular families (e.g., genome, proteome, metabolome, etc.), without *a priori* knowledge of a compound's mode of

action (MOA) (Health Canada, 2018; Liu *et al*., 2019). While apical responses may not be apparent immediately, toxicogenomic responses may reveal toxicological effects at earlier time points. In particular, transcriptional profiling enables the detection of a snapshot of the earliest cellular responses following an exposure scenario, which generally correlate with a system's response to a stressor. Thus, these responses may be linked to overt health effects typically observed at later time points. In the context of chemical hazard assessment, toxicogenomics is currently being used to complement traditional toxicological approaches as it enables assessment of toxicity endpoints for which there are no current conventional toxicity tests. The approaches show promise with regard to the assessment of probable human relevance and provide weight-of-evidence and insights into the linkage of MOA and apical outcomes (Health Canada, 2018).

Recently, toxicogenomics have evolved from a tool primarily used for mechanistic inquiry to one that is focused on the assessment of biological potency (Auerbach and Paules, 2018). In particular, genomic dose-response studies (GDRS) have gained significant interest as they generally provided good approximation of toxicological potencies typically observed in long-term and expensive traditional toxicity studies (Thomas *et al*., 2013a). GDRS leverages genome-/transcriptome-wide inquiry that is identical to assessing nearly all biological responses, and can be applied to both *in vivo* and *in vitro* studies by assessing alterations in mRNA expression following chemical exposure. It uses the traditional benchmark dose (BMD) approach to determine a point-of-departure (POD) at the molecular level. The process involves the identification of genes that were responsive to treatments, then fitting a dose-response model to identify a benchmark dose/concentration level that caused gene expression change relative to the control group, much similar to how traditional apical dose-response modelling is conducted. To identify the transcriptome-wide POD (transcriptomic point-of-departure; tPOD), the US National Toxicology

Program (NTP) recommended the use of the most sensitive set of genes based on functional annotation, which are assumed to best approximate the doses at which adverse apical effects occur. However, due to the limited number of species with annotations and the very nature of gene annotation itself where less studied processes are less represented and most ontologies are human-centric, this approach is not feasible for most ecological receptors of concern. Hence, there is currently no consensus on the process to derive tPODs. Keeping these limitations in mind, a variety of approaches have been suggested to derive reproducible tPODs that closely approximate PODs from traditional methods for ecological risk assessment. These include the mean of gene-level BMDs (geneBMD) of the 20 genes that contribute to the greatest number of enriched pathways, the mean of 20 geneBMDs with the largest fold-change (FC) relative to the control, and the mean of 20 significantly enriched pathways with the lowest BMD (Farmahin *et al*., 2017).

While most BMD approaches result in tPODs that are within one order of magnitude of empirically derived chronic apical PODs, the most sensitive and protective tPODs were those derived from the mode of the first peak of the geneBMD distribution, the median of the 20 most sensitive geneBMDs, and the tenth percentile of the all geneBMDs (Pagé-Larivière *et al*., 2019). Still, the advantage of pathway-level BMDs cannot be discounted as these values present the most plausible biological interpretation, and therefore, the possible link to apical PODs, which is important information in providing weight-of-evidence in the regulatory acceptance of GDRS. Nevertheless, it should be noted that the main purpose of GDRS is to identify the concentration that would significantly perturb biology and would potentially result in a phenotypic outcome; the mechanism or identification of this phenotypic outcome is secondary due to often limited information particularly when testing new compounds.

1.3.3. Early-life stages of fish as models for toxicity testing

Full life cycle (FLC) and partial life cycle toxicity testing strategies are animal- and resource-intensive and logistically challenging. Thus, there have been significant efforts in developing NAMs that would closely approximate responses typically observed in chronic scenarios while reducing the need for live animals. To date, many NAMs rely on *in silico* (Brinkmann *et al*., 2014), *in vitro* (Doering *et al*., 2020), and *ex vivo* (Rahman *et al*., 2020) studies. While some of these models have proven successful in predicting downstream effects of specific molecular key events (Doering *et al*., 2018), many of the abovementioned approaches are limited in estimating apical toxicity thresholds as they do not represent the complex interactions occurring within an organism after a toxic insult; hence, there are still gaps in the predictive capability of these models as they need to be anchored quantitatively to relevant apical outcomes to fully realize their potential applications in regulatory ecotoxicology. In this light, much attention has been given to the use of fish embryos as surrogate for juvenile and adult fish as the ELS has the advantage of being the most sensitive stages in the fish life cycle that already express the majority of molecular features characteristic of adult fish (Lillicrap *et al*., 2016; Sobanska *et al*., 2018). In many jurisdictions, ELS are not considered to be a protected life stage (i. e., life stage prior to independent exogenous feeding) (Canadian Council on Animal Care, 2005; European Union, 2010; Strähle *et al*., 2012; UK, 1993). Furthermore, it has been shown that ELS assays, along with the inclusion of other test endpoints such as developmental abnormalities and gene expression, are more sensitive than FLC (Jeffries *et al*., 2015, 2014; Lillicrap *et al*., 2016; Roush *et al*., 2018; Wheeler *et al*., 2014). Gene expression analyses using ELS of model fish species such as zebrafish have been previously proposed (Wang *et al*., 2018; Weil *et al*., 2009; Zhang *et al*., 2020), although they have not gained regulatory acceptance. Nevertheless, ELS represent a promising alternative

to adult fish tests and may possibly bridge regulatory acceptance and utility of other prospective animal alternatives such as cell-based assays and quantitative structure–activity relationship (QSAR) models (Halder *et al*., 2010).

1.4. Scope and limitations

This dissertation implemented six separate ELS exposure experiments using three (representative) species of ray-finned fishes, and which were conducted based on the availability of fish embryos. The differences in the start time and study duration were due to logistical limitations (FHM were bred in-house, RBT arrived as eyed-up eggs, WS were spawned in a hatchery from wild populations, and therefore, needed to be quarantined) and differences in natural growth rates of the fishes. Nevertheless, whole embryo transcriptomics and non-target proteomics were conducted at 4 dph for all species. A range of apical responses were measured/observed at different time points whenever logistically possible: at 4 dph, at swim up, and at early fry/juvenile life stages. Some observations were also opportunistic and qualitative, and thus, statistical tests were not possible. Lastly, this research did not aim to develop and establish new statistical methods and bioinformatics workflows. Instead, it used well established methods, software, and workflows recommended by reputable groups and organizations and which are well cited in the literature. This dissertation leveraged the use of these existing tools and applied these to datasets derived from ELS fish. It is acknowledged that these bioinformatics workflows can be further optimized specifically for use in MOA characterization and derivation of tPODs.

CHAPTER 2: DEVELOPMENT OF A COMPREHENSIVE TOXICITY PATHWAY MODEL FOR 17α-ETHINYLESTRADIOL IN EARLY LIFE STAGE FATHEAD MINNOWS (*PIMEPHALES PROMELAS*)

PREFACE

While there is a huge body of literature on the toxicity of EE2 in fish, little research has been done to characterize and link the molecular toxicity pathways from early life stages (ELS) of fish to apical outcomes at later life stages. This chapter aimed to test the hypothesis that early embryonic life stages could be used as an alternative to live animal testing, with "live animals" being defined as those capable of independent exogenous feeding (reviewed in Halder *et al*., 2010). Sequence-by-synthesis mRNA sequencing and non-target proteomics were used to characterize molecular responses (changes in the abundance of transcripts and proteins) at 4 dph and were subsequently linked to apical outcomes of regulatory relevance measured at later life stage (histology, survival, length, weight). This chapter sets the stage for the use of ELS transcriptomic data in deriving tPODs to approximate apical PODs presented in the subsequent chapters.

The content of Chapter 2 was reprinted (adapted) from Alcaraz, A.J.G., Potěšil, D., Mikulášek, K., Green, D., Park, B., Burbridge, C., Bluhm, K., Soufan, O., Lane, T., Pipal, M., Brinkmann, M., Xia, J., Zdráhal, Z., Schneider, D., Crump, D., Basu, N., Hogan, N., Hecker, M., 2021. Development of a Comprehensive Toxicity Pathway Model for 17α-Ethinylestradiol in Early Life Stage Fathead Minnows (*Pimephales promelas*). *Environ. Sci. Technol.* 55, 5024–5036. https://doi.org/10.1021/acs.est.0c05942. Copyright (2021), with permission from the American Chemical Society.

Author Contributions:

Alper James G. Alcaraz (University of Saskatchewan) - Conceptualization, Methodology, Software, Validation, Formal Analysis, Investigation, Data Curation, Writing - Original Draft, Review and Editing, Visualization.

Dr. David Potěšil (Masaryk University) - Methodology, Software, Formal Analysis, Investigation, Supervision, Review and Editing.

Dr. Kamil Mikulášek (Masaryk University) - Methodology, Formal Analysis, Investigation, Review and Editing.

Derek Green (University of Saskatchewan) - Methodology, Investigation.

Bradley Park (University of Saskatchewan) - Methodology, Formal Analysis, Investigation, Review and Editing.

Connor Burbridge (University of Saskatchewan) - Methodology, Software, Review and Editing.

Dr. Kerstin Bluhm (University of Saskatchewan) - Methodology, Investigation, Review and Editing.

Dr. Othman Soufan (McGill University; St. Francis Xavier University) - Methodology, Software, Review and Editing.

Taylor Lane (University of Saskatchewan; University of York) - Methodology, Investigation, Review and Editing.

Dr. Marek Pipal (Masaryk University) - Methodology, Investigation, Review and Editing.

Dr. Markus Brinkmann (University of Saskatchewan) - Methodology, Investigation, Review and Editing.

Dr. Jianguo Xia (McGill University) - Resources, Review and Editing, Supervision.

Dr. Zbyněk Zdráhal (Masaryk University) - Resources, Review and Editing, Supervision, Project Administration, Funding Acquisition.

David Schneider (University of Saskatchewan) - Resources, Supervision, Review and Editing.

Dr. Doug Crump (Environment and Climate Change Canada) - Conceptualization, Review and Editing, Project Administration, Funding Acquisition.

Dr. Niladri Basu (McGill University) - Conceptualization, Review and Editing, Project Administration, Funding Acquisition.

Dr. Natacha Hogan (University of Saskatchewan) - Conceptualization, Review and Editing, Project Administration.

Dr. Markus Hecker (University of Saskatchewan) - Conceptualization, Resources, Writing – Original Draft, Review and Editing, Project Administration, Funding Acquisition.

*__Appendix A__ Summarizes the definitions of CRediT (Contributor Roles Taxonomy) Author Statement, used by Elsevier.

2.1. Abstract

There is increasing pressure to develop alternative ecotoxicological risk assessment approaches that do not rely on expensive, time-consuming and ethically questionable live animal testing. This study aimed to develop a comprehensive early-life stage toxicity pathway model for the exposure of fish to estrogenic chemicals that is rooted in mechanistic toxicology. Embryo-larval fathead minnows (FHM; *Pimephales promelas*) were exposed to graded concentrations of 17α-ethinylestradiol (water control, 0.01% DMSO, 4, 20, and 100 ng/L) for 32 days. Fish were assessed for transcriptomic and proteomic responses at four days post-hatch (dph), and for histological and apical endpoints at 28 dph. Molecular analyses revealed core responses that were indicative of observed apical outcomes, including biological processes resulting in overproduction of vitellogenin and impairment of visual development. Histological observations indicated accumulation of proteinaceous fluid in liver and kidney tissues, energy depletion, and delayed or suppressed gonad development. Additionally, fish in the 100 ng/L treatment group were smaller than controls. Integration of omics data improved the interpretation of perturbations in early-life stage FHM, providing evidence of conservation of toxicity pathways across levels of biological organization. Overall, mechanism-based embryo-larval FHM model showed promise as a replacement for standard adult live animal tests.

Keywords: fathead minnow; transcriptomics; proteomics; histology; estrogen; toxicity pathway

2.2. Introduction

Contaminants of emerging concern (CEC) constitute a significant issue in many aquatic environments due to their continuous discharge from wastewater treatment plants that are often not equipped to remove these classes of compounds. Their unabating discharge to surface water systems results in the pseudo-persistence of many CECs, posing potential toxicological risks to aquatic organisms, including fish (Nilsen *et al*., 2019). Fishes are among the most sensitive aquatic organisms chronically exposed to sub-lethal concentrations of CECs that often do not cause immediate lethal or acute effects but may result in long-term impacts such as alterations in reproductive success, abnormal growth/development, and disruption of normal behaviour (Rose *et al*., 2013). Furthermore, studies suggest that subtle and seemingly unimportant short-term molecular changes that do not immediately manifest at the physiological level may affect populations and communities of organisms under sub-chronic or chronic environmental exposure (Matthiessen *et al*., 2018).

One CEC of particular concern is the xenoestrogen, 17α-ethinylestradiol (EE2). There is ample evidence that EE2 affects the endocrine system by mimicking or antagonizing the actions of endogenous hormones, resulting in the disruption of reproductive functions at concentrations between 0.47 and 117 ng/L (summarized in Armstrong *et al*., 2016). Xenoestrogens in the environment originate from poorly and/or untreated sewage discharged into water bodies, with approximately 55% of the hormones entering a wastewater treatment plant (WWTP) not being removed by conventional secondary wastewater treatment (Froehner *et al*., 2011). When detected in waterways, EE2 is typically found in the single digit or sub ng/L range, but concentrations in WWTP effluents from urbanized areas of up to 62 ng/L have been reported (Aris *et al*., 2014).

Current risk assessment approaches for CECs, including endocrine disruptors such as EE2, rely heavily on live animal testing and are therefore expensive, time-consuming, prone to uncertainty and of significant ethical concern (Hecker, 2018). National and international regulatory communities have recognized these concerns, which has triggered a paradigm shift towards the development of alternative approaches rooted in mechanistic toxicology. Examples of emerging approaches under this paradigm shift are *in vitro* systems (Beitel *et al*., 2015), the utilization of embryos as surrogate models for adults (Capela *et al*., 2020) and the use of toxicogenomics technologies to elucidate mechanisms of toxicity with the aim to predict apical outcomes of regulatory relevance (Brockmeier *et al*., 2017; National Research Council, 2007). The opportunities that these advancements provide are expected to guide the future of regulatory ecotoxicology as they promise to lower the cost, save time, and reduce uncertainties of chemical hazard evaluations, while significantly reducing the need for live animal testing (Villeneuve and Garcia-Reyero, 2011). However, there is a lack of calibrated and validated approaches and tools that can conclusively and reliably link mechanistic information to toxic outcomes (Basu *et al*., 2019).

The main objective of this study was to develop a comprehensive toxicity pathway model for embryo-larval stages of a model fish species, fathead minnow (FHM; *Pimephales promelas*), exposed to EE2, using a combination of non-targeted transcriptomics and proteomics, and physiological/histological/apical analyses. Furthermore, this study tested the hypothesis that early embryonic life stages, which are not considered live animals under current legislations (Halder *et al*., 2010), could be used as an alternative to live animal testing. This work is part of a series of studies that aim to establish an alternative testing approach using embryonic FHM and other species for chemical testing and prioritization (Basu *et al*., 2019).

2.3. Materials and Methods

2.3.1. Test organisms

FHM (source: Aquatic Research Organisms Inc., NH, USA) were reared from in-house cultures at the Aquatic Toxicology Research Facility, Toxicology Centre, University of Saskatchewan. Sexually mature FHM were maintained and bred following the procedures described previously (Lane *et al*., 2019). Fertilized eggs from different breeding groups were collected (< 6 hours post-fertilization, hpf), sorted for quality, and randomly assigned to treatment groups.

2.3.2. Exposure conditions

FHM embryos were exposed to graded concentrations (water control, solvent control, low = 4, medium = 20, high = 100 ng/L) of EE2 (≥ 98% purity, Sigma-Aldrich, MO, USA) (**Figure B.S1**). The final concentration of DMSO in all treatments was 0.01%, except for the water only controls. Exposures were initiated by placing late cleavage to high blastula stage embryos in Petri dishes containing the corresponding test solutions. Separate Petri dishes were used for each endpoint. Transcriptomics were conducted in quintuplicates for each treatment group, with 20 embryos per replicate. For proteomics and apical assessments, there were six and five replicates per treatment group, respectively, each containing 30 embryos. All Petri dishes were maintained under static renewal conditions (> 50% of test solution was replaced daily), a 16:8 light:dark cycle, and at a temperature of 24±1^{o}C.

Embryos for omics analyses were reared to four days post-hatch (dph) and sampled by pooling all larvae in each Petri dish. Pooled larvae were flash-frozen in liquid nitrogen and kept at -80^{o}C until further analyses. Larvae for apical assessments were then transferred to 9L glass

aquaria and maintained under flow-through conditions using a randomized design, where they were exposed to the same test concentrations and physico-chemical conditions until 28 dph following OECD 210 (OECD, 2013). Each tank was monitored daily for temperature, pH, conductivity and dissolved oxygen, and weekly for ammonia, nitrates, nitrite, hardness and alkalinity, following the procedures described in Lane *et al*. (2019). Surviving larvae at the end of the exposure period were euthanized using buffered tricaine methanesulfonate (MS222; Sigma-Aldrich). Length and weight of each larva were measured and overt morphological abnormalities were qualitatively recorded during takedown by a designated subjective observer. From each replicate, randomly selected whole larvae were then decalcified and fixed for 24 hours using Cal-Ex™ (≥98.5%; Fisher Scientific, MA, USA), and stored in 70% ethanol for histological analyses. All methods reported here were approved by the Animal Research Ethics Board of the University of Saskatchewan (Protocol #20160090).

2.3.3. Chemical analyses

Water samples from exposure tanks were collected at three time points during the exposure experiment (4, 14 and 28dph). EE2 was quantified by SGS AXYS Analytical Services Ltd. (BC, Canada) using a protocol published previously (Long *et al*., 2013). Water samples were extracted by solid-phase extraction and were spiked with d4-17α-ethinylestradiol (d4-EE2; CDN Isotopes, QC, Canada). Concentrations of EE2 were measured using a Waters LC-MS/MS system, operating in negative ion electrospray mode at unit resolution. Measured concentrations were corrected for % recovery of d4-EE2. The limit of detection was 6.46 ng/L.

2.3.4. Transcriptomics

Only samples from the solvent control, medium, and high treatment groups were used to assess transcriptional responses. Total RNA was extracted from each replicate pool using the RNEasy Plus Universal Mini Kit (Qiagen, Germany) following the manufacturer's protocol. Samples with a RIN > 8 were sent to the McGill University and Génome Québec Innovation Centre for 200 base-pair paired-end (100x2) sequencing using a HiSeq 4000 instrument (Illumina, CA, USA).

Raw fastq files were assessed for quality, trimmed, and aligned to the latest FHM genome assembly (NCBI Acc# WIOS00000000). Expression levels of genes were estimated and then filtered to remove features with less than five counts per million in at least five samples. edgeR (Robinson *et al*., 2010) was used to assess the significance of differentially expressed genes (DEG) using the quasi-likelihood pipeline and scored with a cut-off false discovery rate (FDR; Benjamini-Hochberg) ≤ 0.05 and a minimum effect size threshold fold-change $|FC| > 1.5$ relative to the solvent control group. Raw fastq files are available through the NCBI GEO accession# GSE156916.

2.3.5. Proteomics

Transcriptomic analyses showed more pronounced perturbations in the high treatment group; thus, only the samples from the solvent and high treatment groups were selected for non-targeted proteomics analysis. Protein samples were processed by filter-aided sample preparation (FASP) (Wiśniewski *et al*., 2009) using Microcon filters with molecular weight cut-off size of 30 kDa (Merck Millipore, MA, USA) covering alkylation and digestion steps. LC-MS/MS analyses of peptide mixtures were done using an RSLCnano system (Thermo Fisher Scientific, MA, USA)

connected to an Orbitrap Fusion™ Lumos™ hybrid spectrometer (Thermo Fisher Scientific). MS data were acquired in a data-dependent strategy selecting up to top 20 precursors for HCD fragmentation. The analysis of the mass spectrometric data was carried out using MaxQuant. MS/MS ion searches were done against the modified cRAP database (http://www.thegpm.org/crap/, accessed January 2020; 246 sequences) and the FHM reference proteome (NCBI Acc# WIOS00000000, number of protein sequences: 35,108). Peptides and proteins with an FDR (q-value) < 1% and at least one razor peptide were selected for downstream analyses. Differential protein abundance analyses were done in KNIME (Berthold *et al*., 2008) using the OmicsWorkflow (https://github.com/OmicsWorkflows). Median normalization strategy was applied to all protein group intensities across samples (**Figure B.S2**). Significance of differentially abundant protein (DAP) groups was assessed using *limma* (Ritchie *et al*., 2015), with a cut-off moderated p-value ≤ 0.05 and a minimum effect size threshold |FC| > 1.5 relative to the solvent control. The MS proteomics data have been deposited to the ProteomeXchange Consortium via the PRIDE (Perez-Riverol *et al*., 2019) partner repository with the dataset identifier PXD021155.

2.3.6. Enrichment and interaction network analyses

Enrichment analyses were conducted in g:Profiler(Raudvere *et al*., 2019) using databases for *Danio rerio* (Gene Ontology, REACTOME pathways, KEGG, and Human Phenotype Ontology). Significantly dysregulated genes or proteins were ordered based on FC and assessed for enrichment using modified Fisher's test with statistical domain based on annotated zebrafish genes only, and with a g:SCS significance cut-off threshold (p-value) < 0.05.

Protein-protein interaction (PPI) networks were built using STRING (Szklarczyk *et al*., 2019) with a medium confidence level ($P < 0.05$). Further analyses to assess network topological parameters of DEGs and DAPs were conducted using NetworkAnalyzer (Assenov *et al*., 2008) in Cytoscape (Shannon *et al*., 2003).

Evaluation of RNA-seq and MS-based proteomics data set concordance was done using QuanTP (Kumar *et al*., 2019) in usegalaxy.eu (Afgan *et al*., 2018). Since the number of detected proteins was limited to the detected protein groups, the protein IDs were used to filter the list of genes for concordance analyses. Gene abundance ratios were plotted against protein abundance ratios in a scatterplot of individual gene-protein pairs. Correlation coefficients were calculated to assess the relative correspondence of gene–protein abundance ratios across the data set. Regression analysis was conducted using the least square method.

2.3.7. Histology

A subset of three fixed whole embryos from each replicate of the solvent control, medium, and high treatment groups were dehydrated in graded concentrations of alcohol, cleared in xylene, and infiltrated with molten paraffin using a Belair RVG/1 Vacuum Tissue Processor (Adelsus, OH, USA), and subjected to 5-µm longitudinal step-sectioning in frontal plane. For each individual, representative sections were taken at a minimum of eight different levels through the body cavity at approximately 75 µm intervals, mounted on glass slides, and stained with Harris' hematoxylin and eosin.

Gonadal sex was determined based on the criteria of Van Aerle *et al*. (2004). All liver sections were assessed for the presence/absence of glycogen-type and lipid-type vacuolation (Wolf and Wheeler, 2018), eosinophilic or basophilic staining of the hepatocyte parenchyma, and

presence of excessive proteinaceous intravascular fluid in the sinusoids of the liver parenchyma. Histology of both the head kidney and posterior kidney were assessed at multiple levels for overall structure and relative sizes of tubules and epithelial cells, as well as glomeruli. An opportunistic assessment of eye histology was also conducted on selected embryos with acceptable eye sections from the solvent control and high treatment groups, whenever possible. Total cross-sectional area, total retinal thickness and thickness of retinal layers (photoreceptor, outer plexiform, inner plexiform), and the eye index (eye size relative to body size) were measured.

2.3.8. Statistical Analyses

Apical outcomes (length, weight, condition factor, and survival rates) were assessed for significant differences across treatment groups using a one-way analysis of variance (ANOVA), followed by Tukey's multiple comparison post-hoc test, with a cut-off adjusted p-value < 0.05. Regression analyses were done on all treatment groups, excluding the water control group, using ordinary least-squares (OLS) linear regression. Significant differences of the measurements in eye histology were assessed using student's t-test, with cut-off p-value < 0.05. All non-omics statistical analyses were carried out in GraphPad Prism.

Detailed description of Materials and Methods can be found in the **Appendix B1-B3**. All software versions used in this study are summarized in **Table B.S1**.

2.4. Results and Discussion

2.4.1. Chemical analysis

The average measured concentrations of EE2 in medium (23.5 ± 8.1 ng/L) and high (96.0. ± 19.6 ng/L) treatment groups were within 20% of the nominal concentrations, while water, solvent, and low were below the method detection limit (**Table B.S2**). Measured physico-chemical characteristics of exposure solutions were generally in accordance with OECD 210 (OECD, 2013); however, measured temperature was 23.12 ± 0.77 ^{o}C, which was slightly lower than the prescribed 25.0 ± 1.5 ^{o}C (**Table B.S3**).

2.4.2. Global gene expression at four days post-hatch

The abundance of 505 and 11 transcripts in the high and medium treatment groups, respectively, were significantly altered compared to the solvent control group (**Dataset S1**). All DEGs in the medium treatment group were upregulated and also highly dysregulated in the high treatment group (**Figure 2.1A**). Furthermore, all commonly dysregulated genes exhibited a concentration-dependent response, suggesting that core responses were activated at medium and high concentrations of EE2. For instance, genes encoding for egg yolk precursor proteins, *vtg* and *vtg*-like variants, were highly dysregulated with > 1900-FC and > 49-FC for every variant in the high and medium treatment groups, respectively. The overexpression of *vtg* is a classic biomarker for the exposure of fish to estrogens (Denslow *et al*., 1999; Jones *et al*., 2000). Additionally, in accordance with a previous study that exposed FHM to EE2 (Villeneuve *et al*., 2006), *cyp19a1b*, which encodes the enzyme aromatase that catalyzes estrogen biosynthesis, was also significantly upregulated in both treatment groups. Similarly, three forms of the *f13a1a* gene were highly dysregulated in both treatment groups. While the role of *f13a1a* in normal endocrine functioning

has not been fully elucidated, it was associated with the prothrombotic effects of estrogens in higher mammals (Reiner *et al*., 2003). Furthermore, *f13a1a* was highly upregulated (> 20-fold change) in the testis of EE2-exposed male FHM (Feswick *et al*., 2016) and in whole-tissue of estradiol-treated adult zebrafish (Hao *et al*., 2013). The dysregulation of multiple variants of some notable genes (e.g. *vtg* and *f13a1a*) highlights the advantage of RNA-seq technology for characterizing transcriptional responses. That is, multiple, if not all, forms of a certain gene were captured, which might have been missed in targeted analyses like qRT-PCR or microarrays, potentially rendering false-negative results. This is particularly important as gene expression may have high variability among individuals as has been previously observed for the expression of *vtg* in FHM (Biales *et al*., 2007).

The majority of other genes that were significantly dysregulated in the high treatment group are involved in less-specific molecular functions and biological processes typically observed in organismal stress response including regulatory functions, biosynthetic processes, and metabolism. The significant increase in the number of dysregulated genes in the high treatment group could, therefore, be due to the very high concentration of EE2 having started to overwhelm the organisms' ability to maintain homeostasis of systemic processes. Overexpression of core genes in our study using whole FHM embryos corroborates previously reported transcriptional estrogenic responses observed in later life stages despite reported high tissue-specificity of gene expression (Mohamed *et al*., 2018).

Transcriptomics-based PPI network for DEGs in the high treatment group showed a high degree of connectedness of genes that are relevant to estrogenic responses (**Figure File S1; Dataset S2**). *fn1a*, *pax6a*, *try*/*prss1*, and *ctsz* had the highest degree of centrality, with 21, 18, 14, and 14 nodes directly connected, respectively. Isoforms of *fn1a*, *pax6a*, and *prss1* were associated

with the estrogen receptor (ER) in human cancer studies (Chan *et al*., 2012; Sampayo *et al*., 2018; Zong *et al*., 2011), while isoforms of *ctsz* have been implicated in the proteolysis of *vtg* in aquatic animals (Hiramatsu *et al*., 2002). Though these hub genes have not often been associated with EE2 toxicity, they are well connected to each other and are connected to highly dysregulated genes associated with xenoestrogen exposure such as *vtg*, *esr*, *nots*, and *f13a1a*. These connections mean that effects on a node may directly or indirectly affect neighboring nodes (Koschützki and Schreiber, 2008); however, the relative impacts of changes on a connected node towards the hub gene have yet to be investigated.

There were a total of 62 (44 from up- and 18 from down-regulated genes) and four significantly enriched GO terms (all from upregulated genes) in the high and medium treatment groups, respectively (**Figure 2.1B-1C**; **Figure B.S3.1-B.S3.3**). In the high treatment group, enriched GO terms included 38 biological processes, 12 molecular functions, and 12 cellular components. Enrichment analyses revealed all significantly enriched GO terms in the medium treatment group were also significantly enriched in the high treatment group (response to estradiol, cellular response to estrogen stimulus, response to estrogen, and lipid transporter activity). These GO terms have also been observed by Colli-Dula *et al*. (2014) in largemouth bass exposed to dietary EE2, while Hultman *et al*. (2015) observed lipid-related molecular functions and processes moderated by EE2 in rainbow trout primary hepatocytes. The intersection of significantly enriched terms in medium and high treatments suggests that these GO terms represent the core transcriptional response of embryonic FHM to EE2. This hypothesis is further supported by > 20-FC in contributing genes in both treatment groups while the remaining significantly dysregulated genes found in the high group had relatively lower dysregulation (< 6-FC), with few exceptions: *fam20cl* (25-FC), *nots* (203-FC), and *esr1* (20-FC), which are also involved in cellular

response to estrogen stimulus. Additionally, there were significantly enriched GO terms in the high treatment group that are associated with nervous and visual system development. EE2 has been implicated in disruptions in brain and nervous system-specific gene expression in medaka (Kitagawa *et al*., 2009). While there were no reports in the literature showing direct effects of EE2 to visual development, the increase in plasma levels of 17β-estradiol, a closely related estrogen, was concomitant with the increase in ERα and ERβ transcripts in the choriocapillary layer and photoreceptor in artificially-induced maturation of Japanese eel (Hyeon *et al*., 2019). Furthermore, it has been reported that estrogen signaling is involved in retinal development in developing embryos of zebrafish (Hamad *et al*., 2007). This would suggest a possible physiological effect of elevated estrogen exposure on eye development.

2.4.3. Proteome-wide responses to the high concentration of EE2

There were 3767 protein groups identified, with the intensities of 244 protein groups (consisting of a total of 378 proteins) having been significantly altered in the high treatment group compared to the solvent control group (**Dataset S3**). The most upregulated protein was Selenof, a stress-regulated selenoprotein found in the endoplasmic reticulum that is functionally associated with protein folding and selenium-mediated antioxidative process (Ren *et al*., 2018). In mice, Selenof is involved in the regulation of non-functional immunoglobulins and in redox quality control of other client proteins exiting the endoplasmic reticulum (Yim *et al*., 2018); thus, it may also have a role in the complex sub-cellular secretome gatekeeping in other species like fish. However, there have been no reports that directly link Selenof to elevated levels of estrogen. The most downregulated protein was Vtnb, a member of the mutifunctional glycoprotein family, which is predicted to be involved in immune response and scavenger receptor activity. While there have

been no studies on the direct effects of EE2 on the expression of Vtnb, 17β-estradiol decreased the expression of the Vtnb receptor, resulting in the inhibition of the development of human osteoclasts *in vitro* (Chen *et al*., 2009). Hence, the associated decrease in abundance of Vtnb protein may have implications in bone formation in developing FHM, although this hypothesis remains to be investigated. Three variants of the estrogenic biomarker protein Vtg were significantly upregulated (4- to 8-FC), showing steroidogenic plasticity as an early response of embryo-larval FHM at the proteome level. While the relative abundance of Vtg proteins was lower than their transcript counterparts, it should be noted that basal Vtg protein levels were also high. The likely reason for this high background level is that Vtg is one of the main components of the yolk sac, and therefore, found at high concentrations in developing larvae, which likely led to the seemingly low differential protein abundance. Furthermore, the induction of Vtg protein synthesis may not have immediately occurred at the early embryonic stage, but rather at the later stages when the yolk sac was almost absorbed (Andersen *et al*., 2003); thus, at 4dph, larvae may have just actively started producing Vtg protein. The abundance of Vtg proteins in larval fish exposed to xenoestrogens has been rarely reported, unlike in their adult counterparts; moreover, recent studies showed organ- and sex-specific proteomic responses of adult fish exposed to EDCs (Ayobahan *et al*., 2019; Voisin *et al*., 2019). Thus, the use of pooled whole embryos might have diluted the relative abundance levels, resulting in lower DAP. Other dysregulated proteins associated with EE2 exposure are involved in cellular growth, organization and transport, metabolic processes, biosynthetic processes, and development; however, most of these proteins had low differential abundance and are not functionally specific, which may suggest that there was a delayed onset of responses at the proteome level.

Enrichment analysis showed only one significantly enriched GO term - response to estradiol (**Figure 2.1D**; **Figure B.S4**). This GO term was also found to be significantly enriched at the transcriptome level suggesting that it is well conserved and a major response across the two omics layers, even after a short exposure at very early life stages. While the lone enriched GO term may indicate possible delayed response at the proteome level, this would also imply a highly specific and immediate response to EE2. Proteomics-based PPI network analysis showed Ddx49, Wdr18, and Rrs1 proteins had the highest degree of centrality, with 12, 11 and 10, respectively (**Figure File S2; Dataset S4**). A Ddx isoform serves as a co-activator of ERα while ribosome biogenesis has previously been observed in response to estrogen exposure in brown trout (Uren Webster *et al*., 2015), albeit as an enriched term based on transcriptional response. While these proteins have high centrality, there have not been reports directly linking them to xenoestrogen toxicity. Furthermore, the magnitude of dysregulations of these proteins was relatively low, rendering their biological relevance uncertain; nevertheless, it would be interesting to investigate the potential roles these proteins may play in EE2-induced toxicity response mechanisms.

2.4.4. Analysis of gene-protein pair concordance

There were 22 features significantly dysregulated at both the transcriptome and proteome levels (**Figure 2.1E**). The direction (up- or down-) of dysregulation in most of these gene-protein pairs was the same, with only four exceptions. However, correlation analysis of gene-abundance ratios and protein-abundance ratios showed weak concordance (Pearson's $\rho = 0.130$). This is not uncommon, because there are many post-translational factors that influence protein product abundance (Liu *et al*., 2016). In zebrafish, De Wit *et al*. (2010) observed limited concordance between the transcriptomic and proteomic response to EE2, but noted that affected signaling

pathways perturbed at the transcriptome level were projected at the protein level. Nonetheless, combined transcriptomic and proteomic analyses have been instrumental in providing a more comprehensive understanding of certain mechanisms of toxicity in fish; for example, the connection of TBCO-induced molecular perturbations to cardiac and vision toxicity in medaka (Sun *et al*., 2016).

Dysregulated gene-protein pairs included features that are linked to estrogen signaling. There were three forms of Vtg where the levels of abundance ratios were among the highest at both the transcriptome and proteome levels. Isoforms of Chymotrypsin, Ankyrin repeat domain-containing protein, Phospholipase B, Carboxylic ester hydrolase, and N-acetylserotonin O-methyltransferase, among others, were all associated with the regulation of the estrogen receptor signaling pathway. Combined transcriptomics- and proteomics-based PPI network analysis reinforced the observed high degrees of centralities of several gene and protein products from separate PPI network analyses, including Fn1a, Grb2b, and Pax6a, suggesting the relative importance of these features in the regulation of molecular processes in response to EE2 (**Figure File S3**). Nonetheless, our current results suggest that while many post-transcriptional modifications occur, certain processes are still conserved and are projected from the transcriptomic response to changes at the proteome level.

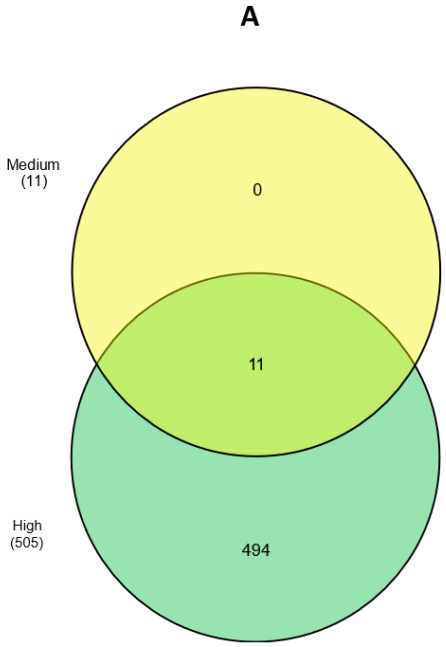

B

source	term_name	adj_p_value
GO:BP	response to estradiol	2.41E-03
GO:BP	cellular response to estrogen stimulus	5.37E-03
GO:BP	response to estrogen	6.05E-03
GO:MF	lipid transporter activity	4.57E-02

C

source	term_name	adj_p_value
GO:BP	cellular response to estrogen stimulus	3.14E-09
GO:BP	response to estrogen	4.28E-09
GO:BP	sensory organ development	3.00E-05
GO:BP	cellular response to hormone stimulus	5.51E-05
GO:BP	sensory system development	7.73E-05
GO:BP	regulation of transcription, DNA-templated	8.79E-05
GO:BP	response to hormone	1.01E-04
GO:BP	visual system development	1.02E-04
GO:BP	eye development	1.02E-04
GO:BP	regulation of nucleic acid-templated transcription	1.22E-04

D

source	term_name	adj_p_value
GO:BP	response to estradiol	4.97E-02

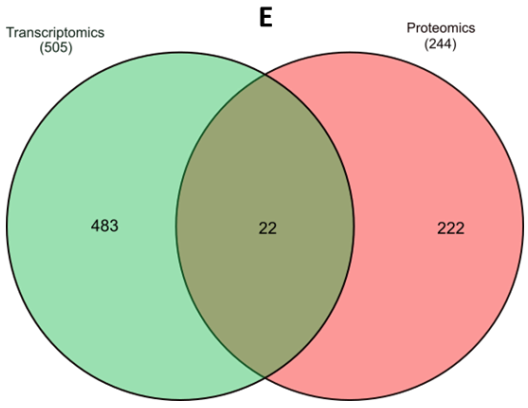

792

793 **Figure 2.1.** Intersections of molecular responses and list of significantly overrepresented GO
794 terms. (**A**) Intersection of DEGs in medium (yellow) and high (green) treatment groups. All
795 significantly dysregulated genes (FDR <0.05; |FC| > 1.5) in the medium treatment (11) were also

significantly dysregulated (FDR <0.05; |FC| > 1.5) in the high treatment (505) group. (**B**) Manhattan plot and list of overrepresented GO terms based on DEGs in medium treatment group. (**C**) Manhattan plot and list of 10 most overrepresented (sorted based on adj p-value) GO terms based on DEGs in high treatment group. (**D**) Manhattan plot and list of overrepresented GO terms based on DAPs in high treatment group. (**E**) Intersection of DEGs (green) and DAPs (red) in the high treatment group. The abundance of 22 features (gene-protein pairs) were altered at both the transcriptome and proteome levels. (Note: sizes of the circles of Venn diagrams do not reflect the relative numbers of DEGs or DAPs in their respective group. Venn diagrams were constructed using InteractiVenn (Heberle *et al*., 2015); complete list of overrepresented GO terms are in **Figure B.S3**). GO – Gene Ontology; BP – Biological Process; CC – Cellular Component, MF – Molecular Function; REAC – REACTOME Pathways; KEGG – Kyoto Encyclopedia of Genes and Genomes; HP – Human Phenotype Ontology; DEG – differentially expressed genes; DAP – differentially abundant proteins.

2.4.5. Physiological and histological responses

2.4.5.1. Survival, length, weight, and condition factor

Exposure to EE2 significantly altered length and weight but neither survival nor the overall condition of FHM at 28dph (**Figure 2.2**; **Dataset S5**). The lack of acute toxicity of EE2 in early-life stage FHM, even at high concentrations, is consistent with previous studies in teleosts. In contrast, significant and linear concentration-dependent decreases were observed for standard lengths (R^2 = 0.8486, p<0.0001) and weights (R^2 = 0.6038, p=0.0004) (**Dataset S6**), suggesting direct effects of EE2 on growth in terms of length and weight (Shved *et al*., 2008). This decrease in fish size may also be explained by the significant energy requirements of xenobiotic metabolism and massive overproduction of Vtg protein (Tompsett *et al*., 2012). However, Fulton's condition factor was not significantly affected. Similar observations have been reported previously (Hill and Janz, 2003; Papoulias *et al*., 2000; Schäfers *et al*., 2007). Lastly, there was no indication of gross abnormal development in any of the EE2-treated FHM.

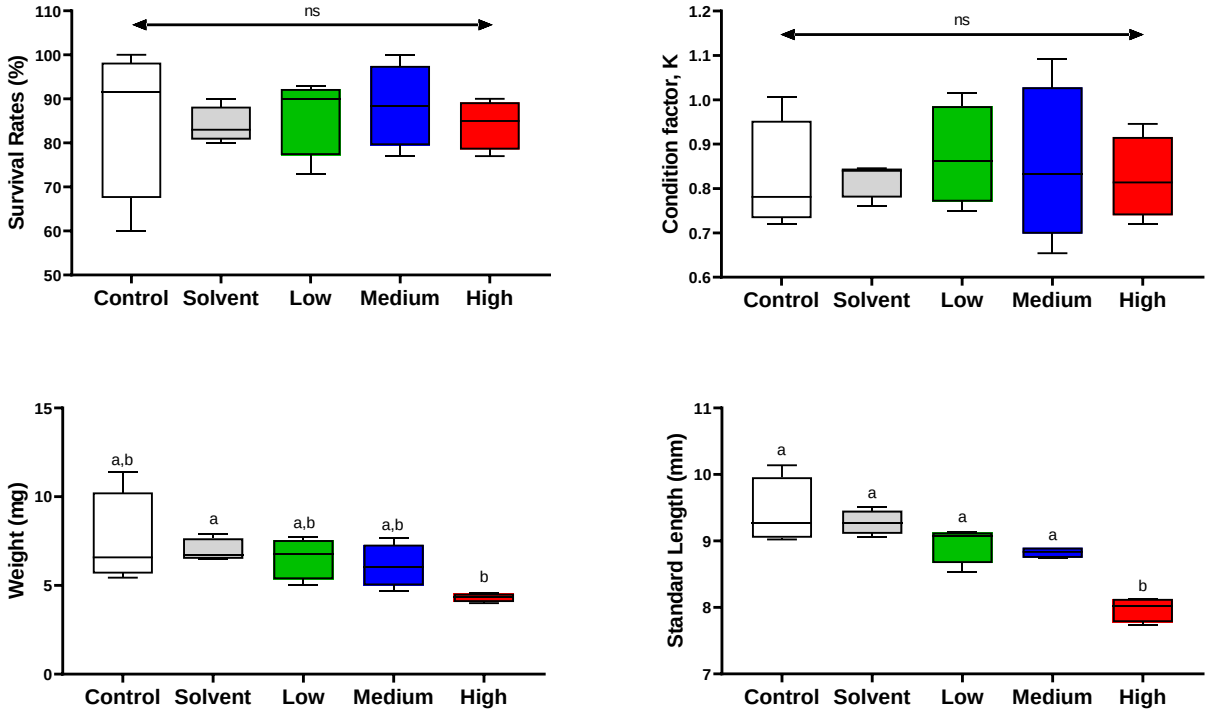

Figure 2.2. Survival, condition factor, weight, and standard length at 28dph of FHM exposed to graded concentrations of EE2. There was no significant difference in survival rates ($p = 0.9709$) and overall condition factor ($p = 0.9590$) across all treatment groups, while significant differences were observed in weight (Kruskal-Wallis $p = 0.0314$) and standard length ($p < 0.0001$). ns = not significant; Control = facility water; Solvent = 0.01% DMSO; Low < limit of detection; Medium = 23.46 ± 8.13; High = 95.99 ± 19.58. Whiskers represent minimum and maximum values, boxes represent 1st and 3rd quartile, lines at the middle of the boxes represent the median.

2.4.5.2. Histological Observations

Gonadal sex differentiation in larval FHM was affected in treated groups (**Figure 2.3A-3D**). Differentiated gonads were present in all larvae from the solvent control group, with sex ratios of 6 males and 9 females. In contrast, only 1 individual each from the high and medium treatment groups exhibited a differentiated gonad (female), whereas remaining individuals had gonads that were either undifferentiated and poorly developed or not detected (**Table B.S4**). This result is consistent with previously reported EE2-concentration-associated impaired juvenile growth, delayed time to sexual maturity (Weber *et al.*, 2003) and increase of undeveloped gonads in zebrafish (Hill and Janz, 2003). While reduced overall fish size or development may have contributed to the delayed gonad development, EE2 exposure is known to directly affect the hepatic GH/IGF-I system, which causes inhibitory effects to both fish size and gonad development (Shved *et al*., 2008, 2007). However, in this study, genes and pathways involved in the GH/IGF-I system were not found to be significantly dysregulated, which may be due to the dilution effect of analyzing whole larval tissues instead of liver tissues.

Exposure to EE2 caused concentration-associated incidence of histological changes to the liver and kidneys of FHM (**Figure 2.3E-2.3H**, **Table B.S4**). Glycogen-type vacuolation of hepatocytes was evident in the majority of solvent control fish, whereas it was absent in all of the medium and high dose fish. Loss of hepatic glycogen was reported previously in EE2-exposed adult FHM (Palace *et al*., 2002), suggesting the occurrence of high energy consumptive processes (e.g. Vtg production, xenobiotic metabolism), which result in more rapid degradation of glycogen. Furthermore, livers from treated groups exhibited increased hepatocyte basophilia relative to the solvent controls. Thus, our findings are in accordance with previous studies, which demonstrated that basophilic hepatocytes are highly correlated to estrogen-induced excessive production of Vtg

(Bogers *et al*., 2006; Wolf and Wheeler, 2018). Intravascular proteinaceous fluid was also observed in treated groups but was completely absent in the control group, which may suggest the presence of excess Vtg in the extracellular fluid, as previously identified by Van den Belt *et al*. (2002) and Tompsett *et al*. (2012) Furthermore, individuals in treated groups had relatively larger and distorted kidney tubules with dilated lumens containing eosinophilic fluids. Tubule epithelial cells were hypertrophied, vacuolated, and swollen. An increase in number and size of glomeruli were observed, as well as the presence of eosinophilic fluid in the cells. These observations were consistent with previous studies of Palace *et al*. (2002) and Weber *et al*. (2003) where tubule enlargement, necrosis, glomerular dilation, and the presence of eosinophilic amorphous deposits were observed in the kidney tubules of adult male FHM and larval zebrafish, respectively, after exposure to EE2.

Amorphous eosinophilic staining in the spaces adjacent to organs was observed in all individuals from treated groups but was absent in the body cavities of individuals from the solvent control group. The degree of fluid accumulation in EE2-exposed individuals ranged from one to a few localized spots in a few sections, to extensive accumulation throughout the majority of the sections. Similar to the eosinophilic staining in the livers, this staining is presumed to be extracellular fluid that is laden with excess protein, presumptively Vtg (Weber *et al*., 2003).

Based on the conservation of some molecular features associated with visual development, inspection of eye sections was conducted, whenever possible. Cross-sectional histological analysis of the eyes showed decrease in retinal thickness, OPL and IPL, and a decreasing trend in eye area, eye index, and PRL (**Dataset S7**). Estrogens promote retinal development in developing zebrafish (Hamad *et al*., 2007), although the consequences of its excess are still unknown. In humans, limited evidence suggests the role of sex hormones in optic nerve functions and ocular hemodynamics

(reviewed in Nuzzi *et al*., 2019). It has been suggested that the effects of EDCs on eye development were due to perturbations in the retinoid pathway (Martínez *et al*., 2018); still, the implications of elevated estrogen levels in visual development and its mechanism are poorly understood. While it is interesting to characterize the physiological effects of EE2 in visual development of FMH, eye histology was not part of our original experimental design and thus the analysis presented here was opportunistic in nature; hence, there is a need for a more thorough investigation of the possible damages and impairments in visual development in embryo-larval FHM, especially as it cannot be excluded that the observed differences were due to the overall delayed development observed in exposed larvae.

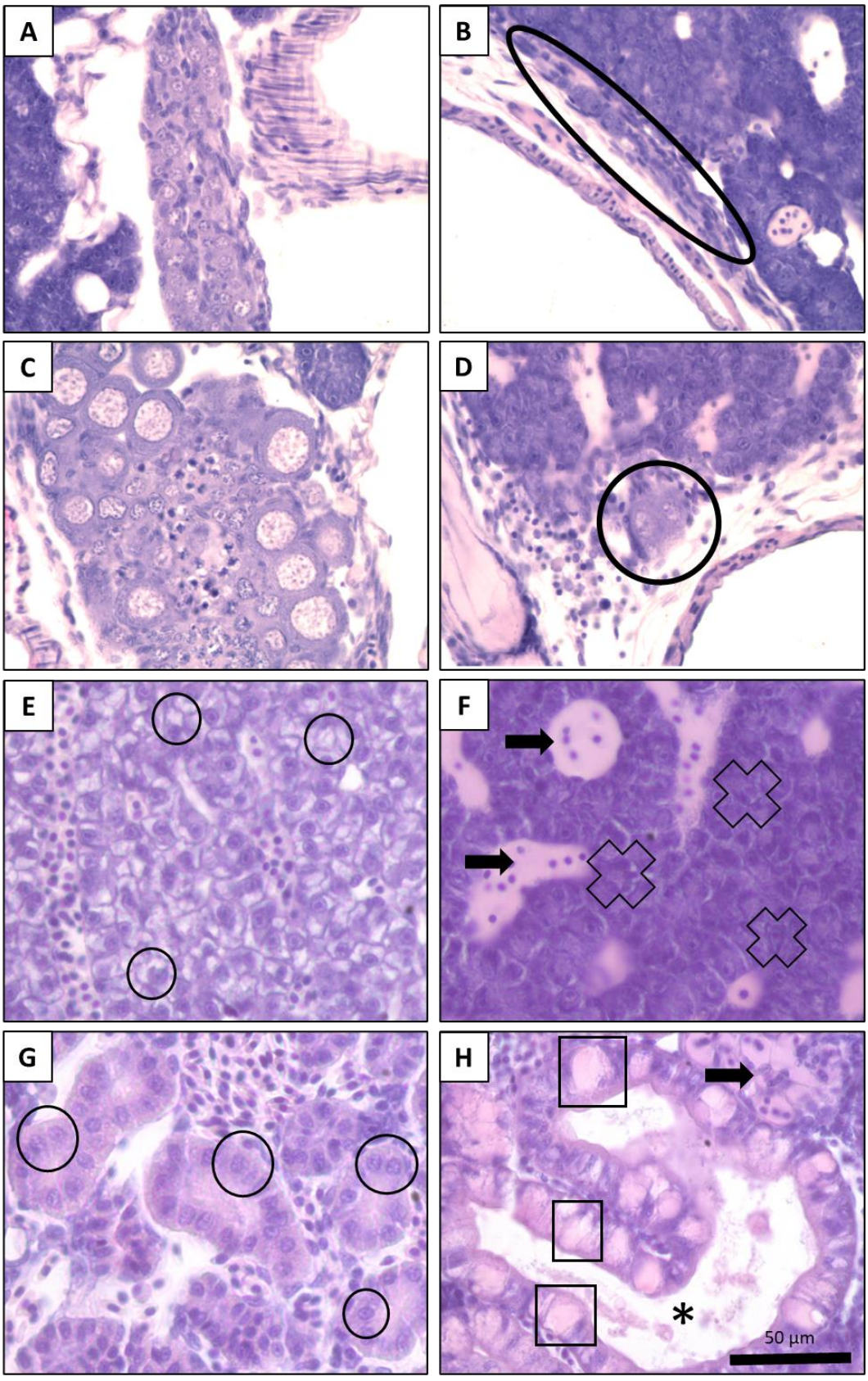

886

887 **Figure 2.3.** Photomicrographs of FHM gonads, liver, and kidney tissues (hematoxylin and eosin
888 stain). (**A**) Solvent control male gonad. Somatic cells are interspersed among germ cells. (**C**)
889 Solvent control female. Meiotic germ cells are present up to the primary oocyte stage. Somatic
890 cells are at the gonad periphery. (**B**) and (**D**) EE2-exposed gonads (circled); small with inhibited
891 development, not clearly differentiated. (**E**) Solvent control liver. Hepatocytes have normal
892 appearance with abundant glycogen-type vacuolation (◯). (**F**) EE2-exposed liver. Hepatocytes
893 are strongly basophilic, characterized by dark blue stain (X) and lack glycogen-type vacuolation.
894 Eosinophilic (pink-staining) proteinaceous fluid is evident in the sinusoids (→). (**G**) Solvent
895 control kidney. Normal-appearing tubules have regular structure, and are lined with cuboidal
896 epithelial cells (◯). (**H**) EE2-exposed kidney. Tubules are large and distorted, with dilated lumens
897 (*). Tubule epithelial cells are hypertrophied with vacuolated swelling (□). Glomeruli are more
898 prominent, typically swollen with eosinophilic fluid (→).

2.4.6. Linking molecular responses to apical outcomes

Exposure of fathead minnows to EE2 at early-life stages resulted in a series of key events ranging from molecular perturbations at the transcriptomic and proteomic level to apical outcomes (**Figure 2.4**). EE2 is a highly potent drug designed as an ER agonist, significantly upregulating *esr* gene coding for ER, indicating the onset of ER signaling activation. Transcriptomics-based PPI network and gene set enrichment analyses showed various linked gene-level perturbations, including significant enrichment in estrogen-associated gene sets. This cascade of transcriptional responses includes the induction of multiple forms of *vtg* gene, resulting in the overproduction of its Vtg protein products. Consequently, excess Vtg protein appeared to accumulate in liver, kidney, and body cavity, which has numerous downstream biochemical and physiological implications. While massive protein abundance was observed, exposure to EE2 did not translate to the onset of gonadal development in potential females. At the same time, it affected gonadal development in potential males or females, as indicated by the inhibition of developing gonads in the treated groups. This observation may be due to the organism channeling most energy towards adaptive mechanisms to counter further damage brought about by continuous EE2 exposure rather than normal development and/or the interactions of EE2 to the brain-pituitary-gonad axis, causing negative or positive feedback mechanisms on the secretion of pituitary gonadotropins, resulting in alterations and/or delay of growth and gonadal development (Fenske *et al*., 2005; Scholz and Klüver, 2009). The observed reduction in glycogen-type vacuolation of hepatocytes may be due to the continuous utilization of energy beyond what the organism can produce that is required to cope with the damage caused by EE2. The continuous demand for large amounts of energy for Vtg production and to maintain overall systemic homeostasis might have caused direct or indirect delays, or inhibition of gonad development, as well as smaller body size. Moreover, delayed

development of gonads, which is known to be involved with regulating overall growth in teleosts (Bhatta *et al*., 2012), may have led to shorter lengths and lower weights observed in FHM. It should be noted that somatic growth is also directly regulated by the GH/IGF-I system (Degani *et al*., 1996; Shved *et al*., 2007), although it was not significantly dysregulated in our molecular studies. Furthermore, the accumulation of Vtg protein in the kidneys altered renal histo-architecture, which is expected to cause renal function failure and may possibly lead to mortality (Folmar *et al*., 2001; Thorpe *et al*., 2007; Weber *et al*., 2004). It is noteworthy that wild FHM exposed to EE2 in a multi-year whole lake addition study showed VTG induction, kidney damage, liver and gonad effects, as well as near extinction of the population from the lake (Kidd *et al*., 2007; Palace *et al*., 2002). However, the population collapse was associated with year-class failure/lack of recruitment, and was not directly attributed to kidney or liver effects.

While most of the current legislation still mandates the use of adult animal models for the assessment of EDCs, recent developments in toxicity testing favor the use of alternative testing strategies, including embryonic bioassays as high throughput tools in toxicity testing and prioritization (Capela *et al*., 2020). Our study successfully demonstrated that the embryonic exposure approach identified disruptions of processes typically observed in adult fish models. Furthermore, molecular perturbations at the early-life stage resulted in apical outcomes typically observed at later life stages. Omics integration added a layer of biological complexity, which enhanced the understanding of the connectivity of molecular events to apical outcomes, providing support and evidence to better understand the mode of EE2 action across biological levels and providing information for a more robust extrapolation (Van Aggelen *et al*., 2010). Moreover, transcriptomic responses in this study showed relatively greater sensitivity compared to other alternative test systems such as the use of precision cut livers(Yadetie *et al*., 2018), rainbow trout

primary hepatocytes (Finne *et al*., 2007), and *in vitro* cultured rainbow trout hepatocytes (Hultman *et al*., 2015). Future studies should be directed towards assessing the sensitivity of the ELS test system in forecasting potential physiological or apical outcomes at later life stages, in addition to further validation of the utilization of this test system using other compounds which may act through different mechanisms. The findings of this study add to the increasing body of literature that successfully links gene expression changes to phenotypic responses to promote utilization of molecular fingerprints for its application in chemical risk assessment for regulatory purposes.

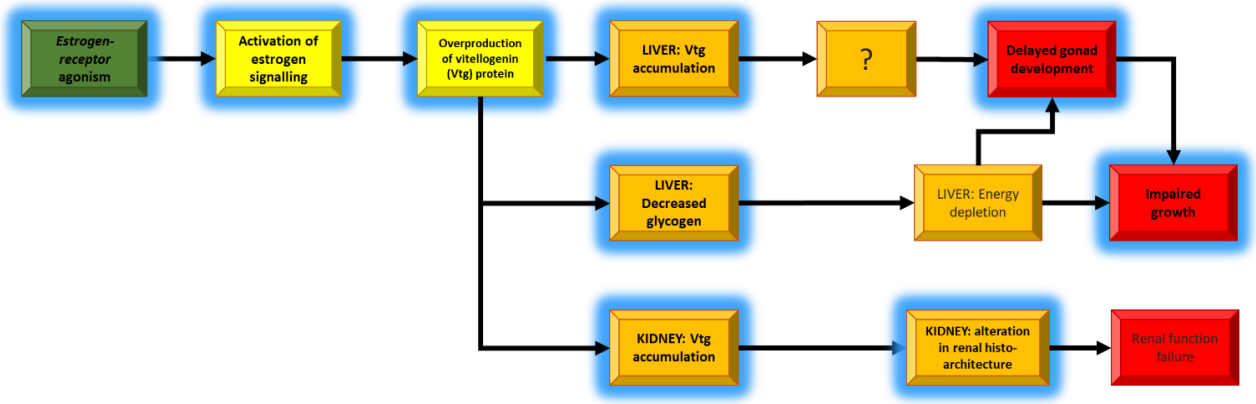

952

953 **Figure 2.4.** Putative toxicity pathway model for early-life stage FHM exposed to EE2 based on
954 the progression of responses across biological levels. Shadowed boxes are effects observed in this
955 study. (Note: Boxes without shadows are effects/processes likely to occur based on mined
956 literature.)

2.5. List of Supporting Information (Appendix B)

Appendix B1 - B4, Tables BS1 – BS4, and Figures BS1 – BS5.

The list of files below can be found as Supporting Information in

https://doi.org/10.1021/acs.est.0c05942

Figure File S1. Protein-protein interaction (PPI) network of significantly dysregulated genes from the high treatment group. Nodes represent the genes, edges represent interaction among genes, halo color is based on the rank of FC-sorted genes with red representing highest FC and blue are the lowest FCs. Spliced isoforms or post-translational modifications are collapsed in a single node.

Figure File S2. Protein-protein interaction (PPI) network of significantly abundant proteins from the high treatment group. Nodes represent the proteins, edges represent interaction among proteins, halo color is based on the rank of FC-sorted proteins with red representing highest FC and blue are the lowest FCs. Spliced isoforms or post-translational modifications are collapsed in a single node.

Figure File S3. Combined transcriptomics- and proteomics-based PPI network from the high treatment group. Nodes represent the genes/proteins, edges represent interaction among genes/proteins. Spliced isoforms or post-translational modifications are collapsed in a single node.

Dataset S1. List of dysregulated genes (DEG) and their respective degree of dysregulation relative to the solvent control group. (**S1.1**) List of dysregulated genes in the medium treatment group relative to the solvent control group. (**S1.2**) List of dysregulated genes in the high treatment group relative to the solvent control group. Cut-off threshold was set at FDR(Benjamini-Hochberg) ≤ 0.05 and a minimum effect size threshold fold-change $|FC| > 1.5$ relative to the solvent control group.

Some Sequence names (SeqName) don't have matched gene models (exemplar names) in the annotation database.

Dataset S2. Topological measurements in transcriptomics-based PPI network from high treatment group. Spliced isoforms or post-translational modifications were collapsed in a single term.

Dataset S3. List of differentially abundant proteins (DAP) in high treatment group and their respective degree of dysregulation relative to the solvent control group. Cut-off threshold was set at moderated p-value ≤ 0.05 and a minimum effect size threshold fold-change $|FC| > 1.5$ relative to the solvent control group. Some sequence names (SeqNames) don't have matched gene models (exemplar names) in the annotation database.

Dataset S4. Topological measurements in proteomics-based PPI network from high treatment group. Spliced isoforms or post-translational modifications were collapsed in a single term.

Dataset S5. Analysis of variance (ANOVA) of (**1**) survival rates and morphometric measurements ((**2a & 2b**) weight, (**3**) standard length, and (**4**) Fulton's condition factor, K) at 28dph. ANOVA was conducted followed by Tukey's multiple comparison post-hoc test.

Dataset S6. Regression analysis of survival rates and morphometric measurements (weight, standard length, and Fulton's condition factor, K) at 28dph.

Dataset S7. Statistical analyses (*t*-test) of histological measurements of the FHM eye (total cross-sectional area, total retinal thickness, and thickness of retinal layers (photoreceptor (PRL); outer plexiform (OPL), inner plexiform (IPL)), and eye index) at 28dph.

2.6. Acknowledgements

The authors acknowledge the support of key project managers (P. Poulin, A. Masse, J. Eng, E. Boulanger) and our various trainees. We thank Genome Canada, Genome Quebec, Genome Prairies, the Government of Canada, ECCC, Ministere de l'Economie, de la Science et de l'Innovation du Quebec, the University of Saskatchewan, and McGill University, as well as core project partners (US Environmental Protection Agency, US Army Corps of Engineers, Qiagen, SGS AXYS, and Shell USA) for their financial and other support. Access to the latest FHM genome assembly was permitted by the Molecular Indicators Branch, ORD, USEPA. Proteomics measurements were supported by the project CEITEC 2020 (LQ1601) and the CIISB research infrastructure project LM2018127 funded by MEYS CR. Computational resources for proteomics analyses were supplied by the project "e-Infrastruktura CZ" (e-INFRA LM2018140) provided within the program Projects of Large Research, Development and Innovations Infrastructures. MH and NB were supported by the CRC Program of NSERC. AJA was supported through the University of Saskatchewan Dean's Scholarship, Toxicology Devolved Scholarship, and the Mitacs Globalink Research Award. DG was supported through the University of Saskatchewan Dean's Scholarship and the NSERC-PGSD3 (#504753-2017). MB was supported through a Banting Postdoctoral Scholarship of NSERC. This project is part of the EcoToxChip project (ecotoxchip.ca).

CHAPTER 3: ASSESSING THE TOXICITY OF 17α-ETHINYLESTRADIOL IN RAINBOW TROUT USING A FOUR-DAY TRANSCRIPTOMICS BENCHMARK DOSE (BMD) EMBRYO ASSAY

PREFACE

Building upon the results of Chapter 2, this chapter leveraged the compelling evidence of the link of molecular toxicity pathways at ELS with apical outcomes at later life stages. In this chapter, a representative salmonid species, RBT, was used to estimate tPODs from transcriptomic datasets generated from whole embryos exposed to graded concentrations of EE2 from hatch to 4 dph. A molecular benchmark dose approach was used to calculate concentrations that would cause significant changes in gene expression relative to the control group. Estimated tPODs were then compared to observed physiological outcomes at 60 dph (length, weight, survival) and to those reported in the literature. Similar to Chapter 2, this chapter also attempted to link transcriptomic and proteomic changes at 4 dph to apical outcomes observed at later life stages.

The content of Chapter 3 was reprinted (adapted) from Alcaraz, A.J.G., Mikulášek, K., Potěšil, D., Park, B., Shekh, K., Ewald, J., Burbridge, C., Zdráhal, Z., Schneider, D., Xia, J., Crump, D., Basu, N., Hecker, M., 2021. Assessing the Toxicity of 17α-Ethinylestradiol in Rainbow Trout Using a 4-Day Transcriptomics Benchmark Dose (BMD) Embryo Assay. *Environ. Sci. Technol.* 55, 10608–10618. https://doi.org/10.1021/acs.est.1c02401. Copyright (2021), with permission from the American Chemical Society.

Author contributions:

Alper James G. Alcaraz (University of Saskatchewan) - Conceptualization, Methodology, Software, Validation, Formal Analysis, Investigation, Data Curation, Writing - Original Draft, Review and Editing, Visualization.

Dr. Kamil Mikulášek (Masaryk University) - Methodology, Formal Analysis, Investigation, Review and Editing.

Dr. David Potěšil (Masaryk University) - Methodology, Software, Formal Analysis, Investigation, Supervision, Review and Editing.

Dr. Kamran Shekh (University of Saskatchewan) – Methodology, Investigation, Review and Editing.

Bradley Park (University of Saskatchewan) - Methodology, Formal Analysis, Investigation, Review and Editing.

Jessica Ewald (McGill University) – Software, Review and Editing.

Connor Burbridge (University of Saskatchewan) - Methodology, Software, Review and Editing.

Dr. Jianguo Xia (McGill University) - Resources, Review and Editing, Supervision.

Dr. Zbyněk Zdráhal (Masaryk University) - Resources, Review and Editing, Supervision, Project Administration, Funding Acquisition.

David Schneider (University of Saskatchewan) - Resources, Supervision, Review and Editing.

Dr. Doug Crump (Environment and Climate Change Canada) - Conceptualization, Review and Editing, Project Administration, Funding Acquisition.

Dr. Niladri Basu (McGill University) - Conceptualization, Review and Editing, Project Administration, Funding Acquisition.

Dr. Markus Hecker (University of Saskatchewan) - Conceptualization, Resources, Writing – Original Draft, Review and Editing, Project Administration, Funding Acquisition.

3.1. Abstract

There is an urgent demand for more efficient and ethical approaches in ecological risk assessment. Using 17α-ethinylestradiol (EE2) as a model compound, this study established an embryo benchmark-dose (BMD) assay for rainbow trout (RBT; *Oncorhynchus mykiss*) to derive transcriptomic points-of-departure (tPODs) as an alternative to live-animal tests. Embryos were exposed to graded concentrations of EE2 (measured: 0, 1.13, 1.57, 6.22, 16.3, 55.1, and 169 ng/L) from hatch to 4 and up to 60 days post-hatch (dph) to assess molecular and apical responses, respectively. Whole proteome analyses of alevins did not show clear estrogenic effects. In contrast, transcriptomics revealed responses that were in agreement with apical effects, including excessive accumulation of intravascular and hepatic proteinaceous fluid and significant increases in mortality at 55.1 and 169 ng/L EE2 at later time points. Transcriptomic BMD analysis estimated the median of the 20th lowest geneBMD to be 0.18 ng/L, the most sensitive tPOD. Other estimates (0.78, 3.64, and 1.63 ng/L for the tenth percentile geneBMD, first peak geneBMD distribution, and median geneBMD of the most sensitive overrepresented pathway, respectively) were within the same order of magnitude as empirically derived apical PODs for EE2 in the literature. This 4-day alternative RBT embryonic assay was effective in deriving tPODs that are protective of chronic effects of EE2.

Keywords: estrogen; risk assessment; transcriptomic benchmark dose, endocrine disruption; alternative toxicity testing

3.2. Introduction

Societal demands and practices result in a steady increase in the production of chemical compounds and their release into aquatic environments where they can cause unintended adverse effects in non-target organisms. However, current regulatory frameworks for assessing the potential toxicological risks this ever-increasing number of chemicals poses are hampered because they are costly, time-consuming, and of significant ethical concern due to their reliance on live animal tests (Bernhardt *et al*., 2017; Hecker, 2018). For instance, tests with rainbow trout (RBT; *Oncorhynchus mykiss*), one of the key model test organisms extensively used in traditional ecological risk assessment (ERA) studies in freshwater ecosystems, are particularly time-consuming due to slow developmental times, and thus are prohibitively expensive. Furthermore, there are still significant uncertainties with regard to the use of traditional acute toxicity testing in predicting thresholds (points-of-departure; PODs) for chronic exposures as acute-to-chronic safety factors vary considerably (Ahlers *et al*., 2006). Consequently, there have been considerable efforts towards the development of new approach methodologies (NAM) to advance and improve current ERA strategies (Basu *et al*., 2019; Gwinn, 2020; Interagency Coordinating Committee on the Validation of Alternative Methods, 2018). Several NAMs have been developed for RBT, primarily *in vitro* and *in silico* approaches such as tissue explants (Beitel *et al*., 2015), stable cell lines (Fischer *et al*., 2019), and toxicokinetic and -dynamic models (Brinkmann *et al*., 2014). However, these approaches are limited with regards to reliably assessing potential hazards as they do not represent the complexity of whole organisms. Recently, short-term fish embryo assays have emerged as a promising alternative testing concept (reviewed in Lillicrap *et al*. (2016) and Sobanska *et al*. (2018)). Embryo-larval stages of oviparous animals such as fish (prior to independent feeding) are not considered live animals under current legislations in Europe and

North America (reviewed in Halder *et al*. (2010)). Furthermore, this life-stage is known to be the most sensitive to exposure to many chemicals, and toxicological insults incurred at this stage could result in chronic health impairments at later life-stages (Bhandari *et al*., 2015).

Another approach increasingly being considered to support ERAs is the use of mechanism-based testing strategies (Basu *et al*., 2019). Recent advancements in molecular biology and biotechnology have enabled the characterization of molecular responses, without *a priori* knowledge of specific mechanisms of toxicity, using next-generation omics technologies such as global transcriptomics. However, prospective toxicogenomic risk assessment approaches such as the use of transcriptomics-based benchmark-dose (BMD) strategies to predict the hazard of chemical contaminants have yet to be fully accepted for their use in regulatory risk assessment. Molecular perturbations generally occur rapidly after toxic insults, prior to phenotypic manifestations, and therefore provide early insights into the complex sublethal and/or chronic effects typically missed in standard acute toxicity testing (Ankley *et al*., 2010). In transcriptomics dose-response studies, toxicant-responsive genes are identified by means of BMD approaches, which are subsequently used to estimate transcriptome-wide PODs as discussed in a recent National Toxicology Program (NTP) report (National Toxicology Program, 2018) and in Farmahin *et al*. (2017). In particular, a recently developed transcriptomic BMD method showed promise in deriving transcriptomic PODs (tPODs) for estimating *in vivo* dose-responses that are protective of chronic effects (Farmahin *et al*., 2017; Pagé-Larivière *et al*., 2019; Yang *et al*., 2007). In fish, a reduced transcriptome approach was developed to estimate gene- and pathway-level effect concentration in embryonic zebrafish (Wang *et al*., 2018; Zhang *et al*., 2020). Regardless, the use of tPODs in quantitative risk assessment is still limited and much work is needed to establish such an approach for ecological species that can be reliably used in ERA and gain regulatory acceptance.

Given the promise fish embryo assays have shown for use in chemical hazard assessments, here we propose an embryo assay to derive tPODs using RBT. Specifically, considering that larval/alevin stages of fish express the full complement of genes that are also regulated in adults, we hypothesized that transcriptomic perturbations at this early stage may serve as an early indicator of possible later chronic and apical effects (reviewed in Ankley and Edwards, 2018). The main objective of this study was to establish a 4-day embryo-alevin assay for RBT to characterize the effects of chemicals using a transcriptomic BMD approach. This assay could then serve as an advanced tool in chemical testing prioritization as well as an alternative strategy to more extensive live-animal testing. 17α-ethinylestradiol (EE2), the active ingredient in many birth-control pills, was chosen as the model compound because it is a well-studied and potent emerging contaminant that has been thoroughly described with regards to its toxicity in fish. Furthermore, EE2 has been ubiquitously detected in surface waters globally, and represents a priority contaminant of concern (reviewed in Aris *et al*. (2014)). Together, these characteristics render it an ideal compound to establish a tPOD approach for embryonic fish. This study specifically aimed to: (1) characterize the trends in global transcriptome responses of RBT embryos/alevins exposed to EE2 for 96h, (2) assess downstream features after short (96h; proteomics) and sub-chronic (60d; histology, biometrics and survival) EE2 exposure, (3) link molecular responses to apical outcomes, and (4) derive tPODs and compare these with higher level physiological and apical response reported in our study and in the literature.

3.3. Materials and Methods

3.3.1. Fish maintenance and exposure conditions

Eyed-stage RBT embryos were acquired from Troutlodge, Inc (WA, USA) and were kept in McDonald-type hatching jars until the first signs of hatching were observed. Approximately 100 unhatched eggs were then transferred (Day 0) into hatching cups, which were kept in 9-liter tanks containing exposure solutions. Unhatched eggs were removed after 48 hrs. Embryos were exposed, in triplicate, to graded concentrations of EE2 (nominal: 1, 3, 10, 30, 100 and 300 ng/L; >98% purity, Sigma Aldrich, MO, USA) and controls (water control, 0.01% DMSO solvent control) under flow-through conditions (at least 50% v/v renewal per day) (**Figure C.S1; Appendix C.1**). Temperature was maintained at 15 ± 1 ^{o}C, under a 16:8 light:dark cycle, and conditions were monitored daily for temperature, and weekly for pH, conductivity, dissolved oxygen, ammonia, nitrates, nitrites, hardness, and alkalinity.

Three and five alevins were collected and pooled from each tank at 4 days post-hatch (dph) for transcriptomics and proteomics analyses, respectively. Samples were immediately flash frozen in liquid nitrogen and kept at -80^{o}C until further analyses. At 21 dph, fish were culled to 20 individuals per tank to avoid overcrowding. Surviving juveniles at 60 dph were euthanized and assessed for overt morphological abnormalities. Five randomly selected whole fish at 60 dph from each replicate were also fixed using HealthCare™ PROTOCOL™ SafeFix™ II All-Purpose Fixative (Fisher Scientific, MA, USA) for 48 hours, transferred to 70% ethanol, and then stored at room temperature until further processing for histological assessment. Lengths and weights were recorded at 4, 21, and 60 dph, and survival was recorded daily. The study was approved by the University of Saskatchewan Animal Research Ethics Board (Protocol# 20140079).

3.3.2. Chemical analyses

Concentrations of EE2 were measured in water samples collected from each tank at 4 and 21 dph (**Appendix C.2**). Collected samples were extracted by solid-phase extraction using 100 mg/6 ml Strata X polymeric cartridges (Phenomenex Inc, CA, USA). Concentrations of EE2 were measured using EE2-specific competitive enzyme-linked immunosorbent assay (ELISA) (Ecologiena®, Fukuoka, Japan, purchased from Eurofins Abraxis, PA, USA), following the manufacturer's protocol. The Ecologiena® EE2 ELISA kit is highly specific and has previously been used in measurements of EE2 in laboratory and environmental samples (Bailey *et al*., 2019; King *et al*., 2016).

3.3.3. Transcriptomics

Alevins from solvent control, 1, 3, 10, 30, and 100 ng/L treatment groups were used for transcriptomic analyses (**Appendix C.3**). Total RNA was extracted from each replicate using RNeasy Plus Universal Mini Kit (Qiagen, Germany). Samples with an RNA integrity number (RIN) $\geq$ 8 were sent for 200 base-pairs paired-end mRNA (100 x 2) sequencing using a NovaSeq 6000 S4 lane (Illumina, CA, USA) at Génome Québec Centre d'Expertise et de Services (Genome Quebec, QB, Canada).

Reads were assessed for quality, then trimmed to a minimum phred score of 20 and a minimum length of 35 bases using Trimmomatic (Bolger *et al*., 2014). The abundance of transcripts was estimated using Kallisto (Bray *et al*., 2016) with the reference RBT transcriptome (GenBank Acc# GCA_002163495.1). Significance of differentially expressed (DE) transcripts were assessed using DESeq2 (Love *et al*., 2014), with a minimum effect size threshold of the

absolute value of log2 fold-change (|log2FC|) ≥ 1 and a false discovery rate (FDR, Benjamini-Hochberg) ≤ 0.05. Raw fastq files are available through the NCBI GEO accession# GSE171788.

3.3.4. Proteomics

Alevins from the solvent control, 30, and 100 ng/L treatment groups were used for non-targeted proteomics analysis, as described by Alcaraz *et al*. (2021), with minor modifications (**Appendix C.4**). Briefly, whole body tissues were processed by filter-aided sample preparation (Wiśniewski *et al*., 2009; Wiśniewski and Rakus, 2014) using 30 kDa Microcon® filters (Merck Millipore, MA, USA). LC-MS/MS analyses of peptide mixtures were conducted using a Q Exactive™ HF-X Hybrid Quadrupole-Orbitrap™ mass spectrometer (Thermo Fisher Scientific, MA, USA) connected online to an Ultimate 3000 RSLCnano system (consisted of SRD-3400, NCS-3500RS CAP, WPS-3000 TPL RS; Thermo Fisher Scientific). Spectral characterization was carried out in MaxQuant v1.6.14(Tyanova *et al*., 2016) using default contaminant database (247 protein sequences) and the RBT reference proteome (GenBank Acc# GCA_002163495.1; 71,233 protein sequences). Significance of differentially abundant protein groups was assessed using *limma* with a cut-off moderated p-value ≤ 0.05 and a minimum effect size threshold |log2FC| ≥ 1 relative to the solvent control group. The MS proteomics data were deposited in the ProteomeXchange Consortium via the PRIDE (Perez-Riverol *et al*., 2019) partner repository with dataset identifier PXD025251.

3.3.5. Overrepresentation analyses

Significantly dysregulated transcripts and proteins were mapped to their respective RBT Entrez IDs. These IDs were then searched for their zebrafish orthologs using g:Profiler (Raudvere

et al., 2019). The mapping rate of RBT Entrez IDs to zebrafish was between 51 and 62%. Functional overrepresentation analyses were conducted using STRING v.11 (Szklarczyk *et al*., 2019) in Cytoscape (Shannon *et al*., 2003), with a cut-off FDR ≤ 0.05 and the whole zebrafish genome as the statistical domain.

3.3.6. Histological assessments

Liver histology was assessed in a subset of individuals from the solvent control and 100 ng/L treatment groups (3-4 individuals per replicate) (**Appendix C.5**). Briefly, fixed whole-body samples were embedded in paraffin, step-sectioned through the internal organs and stained with hematoxylin and eosin. Livers were assessed for changes in hepatocellular staining (i.e. basophilia) and vacuolation, and other changes were noted as well. Histological analyses were done qualitatively in support of molecular studies, and thus, only the highest concentration with transcriptomic data was assessed relative to the control group, and histological features were reported as presence/absence of phenotypes in individual fish examined. No statistical analysis was conducted on histological data.

3.3.7. Benchmark-dose analysis

Derivation of transcriptomic points-of-departure (tPOD) was conducted by means of the benchmark dose (BMD) approach using FastBMD (fastbmd.ca) (Ewald *et al*., 2020). DESeq2-normalized (relative log expression normalization) count estimates from Kallisto were filtered to remove 5% and 10% of the genes with lowest variance and abundance across treatment groups, respectively. This independent filtering step removes genes that are less likely to be informative; thus, it increases the statistical power of the differential expression analysis (Bourgon et al., 2010).

Then, DE ($|log2FC| \geq 1$; FDR ≤ 0.05) was conducted to reduce the number of computationally extensive curve-fittings and avoid modelling data with no statistical significance by removing features that are unlikely to exhibit concentration-response behaviour. A total of 1499 features were fitted using statistical models (Exp2, Exp3, Exp4, Exp5, Linear, Poly2, Hill, and Power), with a threshold lack-of-fit p-value > 0.1 and a benchmark-response (BMR) factor = 1. Control expression was set to the mean of control samples. Three tPOD estimates were derived based on the distribution of gene-level BMDs (geneBMD): (1) the median of the 20 lowest geneBMDs ($omicBMD_{20}$), (2) the tenth percentile geneBMD value ($omicBMD_{10th}$), and (3) the mode of the first peak geneBMD distribution ($omicBMD_{mode}$) (Pagé-Larivière *et al*., 2019). Lastly, a pathway-level BMD (pathBMD) was derived by bootstrapped median calculation of geneBMDs in a pathway and selecting the most sensitive (lowest value) pathBMD with a minimum of three geneBMDs (National Toxicology Program, 2018).

3.3.8. Statistical Analyses

Length, weight, condition factor (K), and survival rates were assessed at three time points (4, 21, 60 dph) for significant differences among treatment groups using one-way analysis of variance (ANOVA), followed by Tukey's multiple comparison post-hoc test, with a cut-off adjusted p-value < 0.05. In cases where assumptions of ANOVA were not met, the non-parametric ANOVA analogue, Kruskal-Wallis test, was performed, followed by Dunn's multiple comparison test with a cut-off p-value < 0.05. All non-omics statistical analyses were carried out in GraphPad Prism v.9.0.2 (**Appendix C.6**).

3.4. Results and Discussion

3.4.1. Chemical measurements and physicochemical characteristics of exposure solutions

Measured concentrations of EE2 were between 52 and 62% of nominal concentrations, except the lowest concentration which was 113% of the nominal concentration (**Table C.S1**). Water and solvent controls were below the detection sensitivity of the method. Physico-chemical characteristics of exposure solutions were within the acceptable range according to OECD 210 (OECD, 2013) (**Table C.S2**). From this point-forward, treatment groups are referred to as the measured concentrations.

3.4.2. General features of transcriptomic responses

Four-day exposure of RBT embryos/alevins to EE2 caused significant changes in global transcript expression. There were 930, 688, 210, 281, and 331 dysregulated transcripts in the 1.13, 1.57, 6.22, 16.3, and 55.1 ng/L treatment groups, respectively (**Figure 3.1A**). Of these, 48 overlapped across all treatment groups, all of which were upregulated. Downregulated transcripts were less consistent - none were common across all concentrations. Interestingly, the 1.13 ng/L and 6.22 ng/L treatments had the greatest and least number of dysregulated transcripts, respectively, which is in contrast to a previously reported dose-dependent increase in the number of significantly dysregulated genes in EE2-treated rats (Naciff *et al*., 2003). The number of dysregulated features is influenced by a multitude of factors, such as the number of replicates and set statistical thresholds, as well as the test concentrations used in a study. Considering their high biological activity and physiological role in many biological processes, low levels of estrogenic steroids may trigger a host of responses that are not necessarily indicative of toxic outcomes. At higher concentrations, the global response pattern may then shift to genes indicative of a toxic

response that may exhibit a classic concentration-dependent change (Pagé-Larivière *et al*., 2019). Here, we observed that the number of highly dysregulated transcripts (|log2FC| > 10) followed a concentration-dependent trend (1.13 ng/L = 67, 1.57 ng/L = 67, 6.22 ng/L = 69, 16.3 ng/L = 74, 55.1 ng/L = 90; slope = 0.428; R^2 = 99.92%). Common dysregulated transcripts included signature markers associated with exposure to estrogens such as transcripts coding for Vitelline envelope protein (Zona pellucida glycoprotein; Zp), as well as multiple variants of vitellogenin (Vtg), among others (**Dataset 1**, **Tab A1-A5** & **B**). Consistently among the highest upregulated transcripts were those associated with lipid metabolism, a biological process where estrogens are known to exert regulatory control (reviewed in Palmisano *et al*. (2017). Upregulation of these transcripts was previously observed in response to EE2-treatment in primary RBT hepatocytes (Hultman *et al*., 2015) and in other teleosts *in vivo* (Huff *et al*., 2018). Additionally, similarities between dysregulated transcripts at two successive concentrations tested were substantial, except between 1.57 and 6.22 ng/L, suggesting a possible shift in molecular response patterns between these two concentrations (**Table C.S3**). The differences in the general features of responses between 1.13 and 1.57 ng/L and between 6.22 and 55.10 ng/L also suggest hormetic effects at lower concentrations where transcripts involved in the maintenance of cytoskeletal architecture, metabolic homeostasis, scavenging, and tight junction interactions, among others, were observed, features which indicate general early cell responses. In hormesis, independent molecular functions necessary for cellular survival are activated to counter toxic insults and to survive in challenging environments through intrinsically generated multiple interacting signal transduction processes (Calabrese and Mattson, 2017). Furthermore, the overview heatmap profiles of differentially expressed transcripts in each treatment group showed distinct clustering of DE transcripts in the 1.13 and 1.57 ng/L treatment groups, while clear concentration-dependent responses of DE

transcripts occurred in the 6.22-55.1 ng/L treatment groups (**Figure C.S2**), supporting this hormesis hypothesis. At 6.22 ng/L, transcriptomic responses suggest that the biological system of exposed RBT had exceeded molecular response plasticity as most energy was expended towards specific responses, as evidenced by distinct concentration-associated increase or decrease in transcriptional expression of significantly dysregulated features. For instance, the common estrogenic biomarker *estrogen receptor 1* (*esr1*) only started showing significant dysregulation at 6.22 ng/L, although other biomarkers like *vtg* showed significant dysregulation at concentrations as low as 1.13 ng/L.

Functional enrichment analyses showed significant overrepresentation of 151, 135, 12, 65, and 83 terms and pathways in the 1.13, 1.57, 6.22, 16.3, and 55.1 ng/L treatment groups, respectively. None of these terms were consistently overrepresented across all treatment groups (**Figure C.S3**), further supporting the hypothesis that there could have been a shift in molecular responses between lower (1.57 ng/L) and higher (6.22 ng/L) EE2 concentrations. Most overrepresented terms and pathways in fish exposed to 1.13 and 1.57 ng/l were generally associated with cellular repair and maintenance pathways, while those at 6.22-55.1 ng/L were generally endocrine- and metabolism-associated processes (**Dataset 1, Tabs C1-C5**). Nine terms were overrepresented in at least four treatment groups, including chylomicron assembly, retinoid metabolism and transport, post-translational protein phosphorylation, regulation of insulin-like growth factor (IGF) transport and uptake by insulin-like growth factor binding proteins (IGFBPs), apolipoprotein A1/A4/E domain, and lipid transport, all of which have been previously associated with endocrine functions (Bravo et al., 2001; Kam et al., 2000). For instance, EE2 has been reported to interfere with the IGF system during development of bony fish (Shved *et al*., 2007), resulting in stunted growth (Shved *et al*., 2008), although this particular apical response was not

observed here. Similarly, apolipoproteins are important proteins responsible for lipid transport and were significantly dysregulated in estradiol-treated embryonic zebrafish (Hao *et al*., 2013). It has also been suggested that estrogens are possibly involved in post-translational modifications (Doyle *et al*., 2013), though very few studies investigated the role of estrogens in these processes.

3.4.3. Downstream responses in support of transcriptomic perturbations

3.4.3.1. Proteome-wide alterations

A total of 3200 protein groups were detected across all treatment groups, with the abundance of 243 and 300 having been significantly altered in 16.3 ng/L and 55.1 ng/L treatment groups, respectively (**Dataset 2, Tab A**). Of these differentially abundant protein groups, 123 were differentially abundant in both treatments (**Figure 3.1B; Dataset 2, Tab B**). Interestingly, all the distinctive estrogen-responsive Vtg protein variants were not significantly dysregulated in both treatment groups, which may be attributed to the high basal intensities of these proteins in alevins in all treatments, including controls, rendering any changes below detectable thresholds. Notably, the yolk sac is still prominent in RBT at 4 dph, and maternally transferred Vtg protein may still be present at high concentrations. Additionally, considerable fractions of proteins present in the yolk-sac may have diluted the detection of other EE2-responsive proteins in the main body of the yolk-sac alevin. In contrast, previously observed estrogen-responsive precursor glycoproteins Zp α, β and γ proteins were differentially abundant in both treatment groups, suggesting treatment-associated significant induction at the post-embryonic stage (Salinas *et al*., 2010). Then again, other estrogen-responsive proteins may not have been synthesized to detectable levels given the short 4 day exposure, and thus, may not be reflective of the initial gene expression (**Figure 3.1C**).

Overrepresentation analyses showed 108 and 153 significantly overrepresented terms and pathways for 16.3 ng/L and 55.1 ng/L treatment groups, respectively. Thirty-seven of these terms were common between the groups (**Dataset 2, Tab C** & **D**). However, most of these terms and pathways appear to be part of concerted immediate endogenous stress responses such as clathrin-mediated endocytosis, transport, metabolic signaling, activation of heat shock proteins, and oxidative phosphorylation, which protect the organism from toxicological insults. Results of overrepresentation analyses further support the idea that 4 days of exposure at the yolk-sac alevin stage may not have been long enough to elicit specific proteomic responses that are reflective of transcript expression particularly for a fish like RBT that has a relatively long life cycle. Future proteomics studies on RBT alevins should consider the removal of the yolk-sac prior to protein extraction to minimize detection of maternally transferred proteins, as well as longer exposure periods.

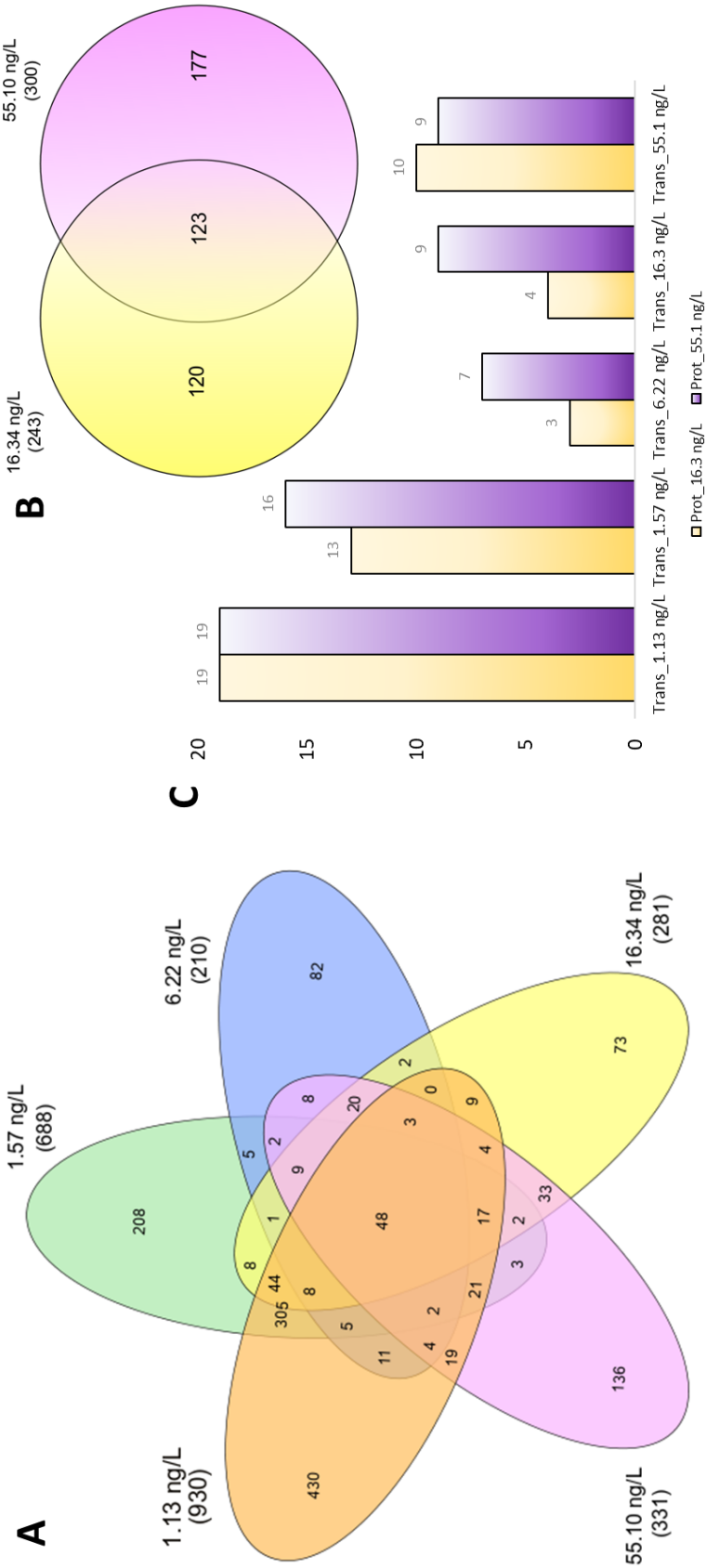
A
1.57 ng/L (688)
6.22 ng/L (210)
16.34 ng/L (281)
1.13 ng/L (930)
55.10 ng/L (331)
208
82
73
430
136
B
55.10 ng/L (300)
16.34 ng/L (243)
177
123
120
C
Trans_1.13 ng/L
Trans_1.57 ng/L
Trans_6.22 ng/L
Trans_16.3 ng/L
Trans_55.1 ng/L
Prot_16.3 ng/L
Prot_55.1 ng/L

Figure 3.1. Omics analyses. (**A**) Venn diagram of differentially expressed transcripts of 4 dph RBT exposed to EE2 (**Dataset 1, Tab A1-A5** & **Tab B**). (**B**) Venn diagram of DA proteins in 16.3 and 55.1 ng/L treatment groups. (**C**) Intersection of DE transcripts and differentially abundant proteins across all concentrations. Venn diagrams were constructed using InteractiVenn (Heberle et al., 2015).

3.4.3.2. Histological changes

EE2-exposed juvenile RBT exhibited histological characteristics typical of those observed in other early-life teleost species exposed to estrogenic compounds (Weber *et al*., 2003) (**Table C.S4**). Livers from solvent control fish showed normal histological appearance, with hepatocytes arranged into two cell-thick cords interspersed with sinusoids. Hepatocytes featured nuclei with prominent central nucleoli. Glycogen-type vacuolation was abundant, and lipid-type vacuolation was largely absent (**Figure 3.2A**). In contrast, livers of all individuals from the 55.1 ng/L treatment group exhibited greatly reduced glycogen-type vacuolation relative to the solvent control, and increased lipid-type vacuolation was observed in seven out of nine individuals examined. Furthermore, individuals from the treated group exhibited increased hepatocyte basophilia relative to the solvent control (**Figure 3.2B**), a common histological characteristic of estrogen-induced upregulation of Vtg protein (reviewed in Wolf and Wheeler, 2018). Similarly, signs of intravascular proteinaceous fluid were apparent in all livers from the treated group, which is presumed to be due to overproduction of proteins like coagulation factors, Vtgs, and other estrogen-responsive hormones and enzymes in the extracellular fluid (Van den Belt *et al*., 2002). Additionally, hepatocytes surrounding the sinusoids and bile canaliculi from the treated group were often tall columnar, and sinusoids were often dilated. Occasional hepatocyte cytomegaly and karyomegaly were also observed in EE2-exposed individuals, although not quantified.

Proteinaceous eosinophilic extracellular fluid was absent in the body cavities of individuals from the solvent control (**Figure 3.2C**) but was notably present in all individuals from the treated group (**Figure 3.2D**). The degree of fluid accumulation in individual fish from the treated group ranged from one to a few localized spots in a few sections, to extensive accumulation throughout most sections. This observation revealed a varied degree, but consistent occurrence of

proteinaceous fluid that leaked into the coelom. Similar histological observations have been previously reported in early-life stage fathead minnows (FHM) (Alcaraz *et al*., 2021b) and *Xenopus laevis* (Tompsett *et al*., 2012) exposed to the same or greater concentration of EE2, respectively. In fact, Tompsett *et al*. (2012) confirmed that this proteinaceous fluid contained Vtg protein.

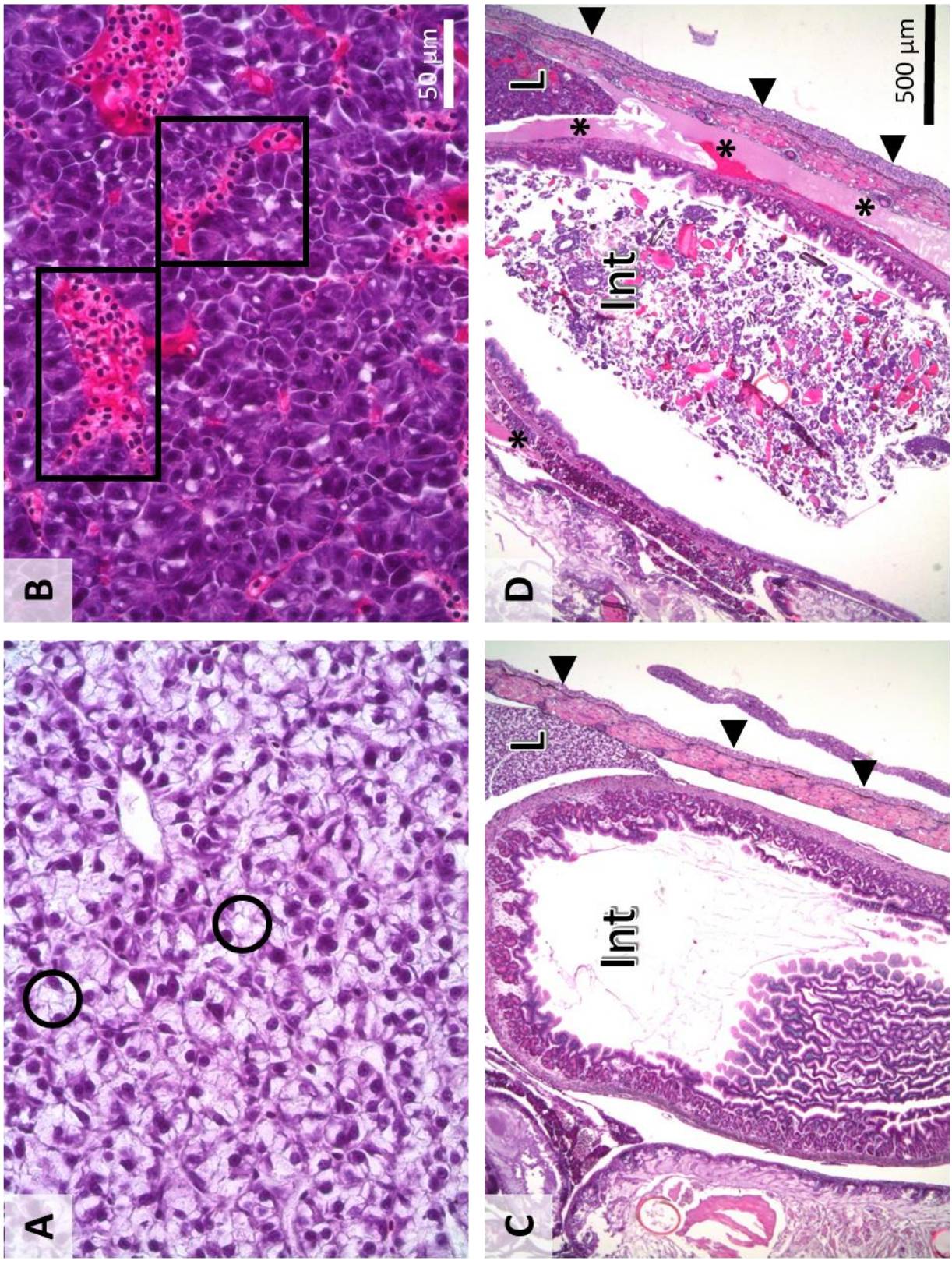
A
B
50 µm
C
L
Int
D
L
Int
500 µm

Figure 3.2. Photomicrographs of livers (A1&A2; Scale = 50µm) and coelom (A3&A4; Scale = 500µm) from EE2-exposed 60 dph RBT (hematoxylin and eosin stain). (**A**) solvent control, showing normal liver parenchyma, with abundant glycogen-type vacuolation (O); (**B**) 55.1 ng/L treatment group, showing increased hepatocyte basophilia (dark blue stain), reduced glycogen-type vacuolation, increased lipid-type vacuolation, and abundant eosinophilic (pink-staining) proteinaceous fluid within the sinusoids (□); (**C**) solvent control, showing clear space adjacent to internal organs; (**D**) 55.1 ng/L treatment group, showing eosinophilic proteinaceous fluid accumulation in the body cavity (*) near the body wall (arrowheads) adjacent to the intestine (Int) and liver (L).

3.4.3.3. Survival and morphometric measurements

Exposure to EE2 affected survival rates but not morphometric measurements in early-life RBT, with significant mortalities at very high concentrations during the early fry (55.1 and 169 ng/L) and swim-up stages (169 ng/L) (**Figure 3.3; Dataset C.S4**). Reports of mortalities due to acute and sub-chronic exposure to EE2 in fish are scarce, owing to its estrogenic but relatively low acute toxicity, with a previously reported LC50 of 1.7 mg EE2/L for adult zebrafish (Versonnen *et al*., 2003). This observation suggests that RBT alevins and fry are approximately one order of magnitude more sensitive than adult zebrafish. However, it should be noted that effects on survival in this study did not occur at environmentally relevant concentrations that were reported previously at sub-ng/L to single digit ng/L range (summarized in Aris *et al*., 2014). On the other hand, fish size and condition factor at 4 dph and 21dph were not significantly affected at any of the concentrations tested (**Figure C.S4**). These observations were in contrast to previously reported stunted growth in early-life stage FHM (Alcaraz *et al*., 2021b) and tilapia (Shved *et al*., 2008). The difference in these observations may be due to species-specific responses, particularly with regard to the length of exposure relative to the life-cycle of a given species of fish.

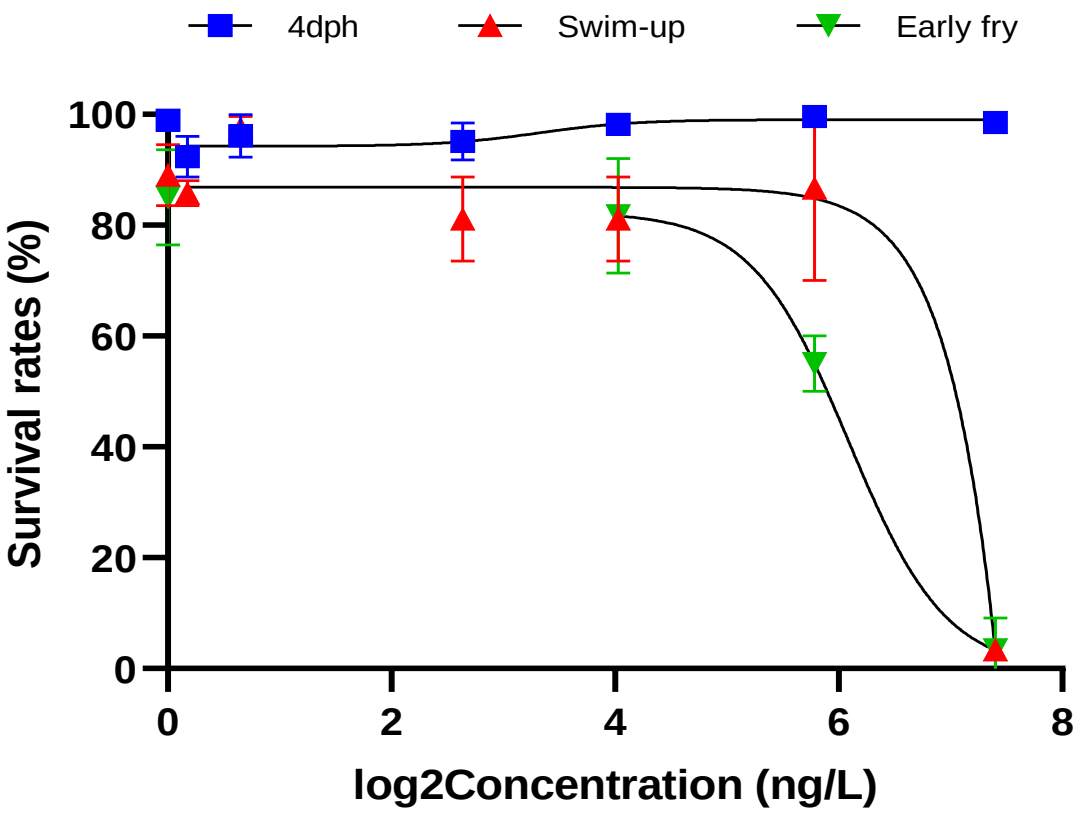

Figure 3.3. Survival rates (%) at early-life stages: 4 dph (all concentrations), swim-up (21 dph; all concentrations) and early fry (60 dph; solvent control, 16.3, 55.1, and 169 ng/L EE2). x-axis – survival rates in %; y-axis – log2 scale of concentration (in ng/L EE2). Datasets are presented as mean ± standard deviation.

3.4.3.4. From molecular responses to apical outcomes

Transcript-protein concordances of dysregulated features at 16.3 and 55.1 ng/L were weak, with only four and nine common features at the same concentration, respectively (**Figure 3.1C**). Zp α, β, and γ were the only transcript-protein pairs that were commonly dysregulated in the two treatment groups. While many protein-coding transcripts were highly dysregulated, particularly those associated with estrogenic responses, similar dysregulations were not reflected at the proteome level. Limited concordance between transcriptomic and proteomic responses was previously observed in EE2-exposed zebrafish (De Wit *et al*., 2010) and FHM (Alcaraz *et al*., 2021b). These observations were expected due to many post-translational factors influencing protein-product synthesis (Liu *et al*., 2016). Moreover, the limited direct projection of significant dysregulation of transcripts to proteins might also be ascribed to the short study duration, limiting the time to synthesize proteins. Furthermore, the coincident sampling for transcriptomic and proteomic analyses may be another reason for some of the low concordance, considering the delay of mRNA translation to proteins. Lastly, the presence of maternally transferred proteins in the yolk sac might have dominated measured proteins, as corroborated by very high spectral intensities of yolk proteins like Vtg. These very high levels of proteins could have masked changes in protein abundance brought about by EE2 exposure.

Observed histological features at 60 dph suggest excessive utilization of energy and the presence of large amounts of proteinaceous fluid within the liver and leaking into the coelom, which is hypothesized to be due to EE2-induced overproduction of estrogen-associated proteins (Alcaraz *et al*., 2021b; Palace *et al*., 2002; Van den Belt *et al*., 2002). These histological changes can be linked to observed perturbations at the transcriptome level. While gonads were not assessed in the current study, significant dysregulation of estrogen-associated transcripts suggests that

continuous exposure to EE2 would delay gonad development and shift gonadal sex ratio towards more females in exposed alevins, as previously observed in other fish species (Kidd *et al*., 2007; Weber *et al*., 2003). However, other expected apical responses, such as stunted growth, were not observed in this study. This may be due to the long life-cycle of RBT such that weight and length measurements at 4 dph and 21 dph did not result in any significant changes. Nonetheless, it can be concluded that transcriptional perturbations after 4 days of EE2 exposure were indicative of potential physiological or apical outcomes at a later life stage.

3.4.4. Transcriptomic dose-response

Benchmark-dose analysis showed that estimates of transcriptomic BMDs were effective predictors of empirically derived (apical) benchmark concentrations of EE2-associated toxicological responses reported in previous studies (**Table C.S5**). Of the 1499 features passing cut-off thresholds, 569 fitted the models, with most genes converging through the 2^{o} polynomial (Poly2) model based on the lowest Akaike information criterion (AIC) (**Figure C.S5**). There were 464 features with gene-level BMDs (geneBMDs) after filtering low confidence and geneBMDs greater than the highest concentration (**Figure 3.4A; DataSet S3, Tab A**) (National Toxicology Program, 2018) . It should be noted that the BMD modelling was conservative in that higher order polynomial models were not included since these models tend to fit data poorly and are prone to variability, and therefore, may add greater uncertainty with regard to predicting benchmark doses. Still, future analyses should specifically investigate the implications of and consider these models in BMD modelling.

Known estrogen-responsive genes exhibited robust concentration-response curves with narrow confidence intervals and notable minimal variations across replicates within a

concentration, particularly those that were highly expressed (**Figure 3.4B)**. These include genes coding for extracellular serine/threonine protein kinase FAM20C (*fam20c*), *esr1*, zona pellucida glycoprotein 2 (*zp2.3*), coagulation factor XIIIA (*f13a*), and multiple variants of *vtg*, among others. In contrast, concentration-response curves of many of the down-regulated genes exhibited higher variance (**Figure 3.4C**), owing to the intrinsic nature of data transformation (log-normalized) in modelling lowly expressed features. This observation implies that downregulated concentration-response trends may present greater challenges in transcriptome-wide dose-response analyses, especially when biological systems tend to diminish mRNA expression. Highly sensitive genes which are downregulated could result in low and below-detectable levels at higher treatment concentrations unless the abundance of transcripts was inherently high such that biological effects would still result in detectable mRNA levels. However, for genes that are expressed at lower levels (e.g. many nuclear receptors), deeper sequencing will be required. Optimal sequencing depth and number of replicates should be further evaluated for tPOD applications in the context of risk assessment, with considerations of the sensitivity, cost, and reasonable experimental design.

The recommended approach in deriving PODs at the transcriptomic level (Pagé-Larivière *et al*., 2019) yielded threshold concentrations of $omicBMD_{20}$ = 0.18 ng/L, $omicBMD_{10th}$ = 0.78 ng/L, and $omicBMD_{mode}$ = 3.64 ng/L (**Figure 3.4D; Figure C.S6**). The most sensitive KEGG pathway was cysteine and methionine metabolism, which is generally associated with amino acid synthesis, with a pathBMD of 1.63 ng/L (**DataSet S3, Tab B**). The pathway with the highest number of dysregulated genes was cholesterol metabolism (pathBMD = 3.65 ng/L) with 7 contributing genes. Estrogens are generally involved in lipid metabolic processes (Palmisano *et al*., 2017). Gene-set level BMDs have been shown to be highly correlated with apical BMDs (Thomas *et al*., 2013b) and NTP has recommended pathBMD in deriving tPODs, particularly when

using rats and human cell lines (National Toxicology Program, 2018). However, pathBMDs should be interpreted with caution as many ecologically relevant species that are important in ERA have poorly annotated reference genomes or transcriptomes, or were arbitrarily mapped against other species without extensive curation. For instance, RBT is not officially included in the KEGG database of organisms, and while users may perform functional annotation, these are loosely based on computationally inferred KEGG orthology. Accordingly, Pagé-Larivière *et al*. (2019) cautioned with regard to the use of pathBMD with non-model organisms lacking fully assembled genomes and well-curated annotations since the resulting estimates were largely variable and dependent on the annotation and pathway mapping.

To date, there have been no robust transcriptomic concentration-response studies that have been conducted for EE2. Metadata analyses for a 76-day RBT-fry exposure (Pagé-Larivière *et al*., 2019) and hepatic gene expression in zebrafish using microarrays (Yang *et al*., 2007) used concentrations that were too high (10 – 10000 ng/L EE2) to derive realistic omicBMDs. Consensus on apical EE2-associated lowest observed effective concentration (LOEC) values based on literature reports were generally between sub- to low-ng/L concentrations. For instance, Jobling *et al*. (2004) reported a LOEC for disruption of egg production of spawning pairs of FHM of 1 ng/L. Runnalls *et al*. (2015) observed inhibition of egg production in FHM at a LOEC of 0.5 ng/L, while Parrott and Blunt (2005) reported decreased egg fertilization and shift in sex ratio, as well as decreased male sex characteristics in FHM at a LOEC of 0.32 ng/L. In RBT, intersex was observed at 10 ng/L (Depiereux *et al*., 2014), while the number of eggs attaining the eyed stage of embryonic development was significantly affected at 16 ng/L (Schultz *et al*., 2003). The predicted no-effect concentration (PNEC) for EE2 was 0.35 ng/L based on available chronic toxicity data in 2008 (Caldwell *et al*., 2008) while a more conservative 0.10 ng/L was derived in 2012 based on

additional fish reproductive studies (Caldwell *et al*., 2012). Compared to all these cases, estimates of transcriptomic BMD in our study on short-term early-life stage RBT exposure were well within the range and are mostly protective with regards to apical LOECs, particularly $omicBMD_{20}$ and $omicBMD_{10th}$. While estimates for the $omicBMD_{20}$ and $omicBMD_{10th}$ were below the lowest measured concentration in this study and may have to be further validated experimentally using lower concentrations, these transcriptomic BMDs were within 10-fold of the lowest measured concentration and are good estimates of empirically derived apical BMDs. However, the main limitation of using $omicBMD_{20}$ and $omicBMD_{10th}$ is the lack of definitive biological interpretation typically inferred from gene sets (pathBMD). While still protective towards apical chronic effects of EE2, the estimate for $omicBMD_{mode}$ appeared to be the least sensitive. As this value typically suggests the primary onset of biological perturbations corresponding to specific biomolecular targets, therefore, it may be used to guide the elucidation of a particular mode of action. Nevertheless, it should be noted that the main purpose of the derivation of tPODs is to identify the concentration that would significantly perturb biology and would potentially result in a phenotypic outcome; mechanism or identification of this phenotypic outcome is secondary due to often limited information particularly when testing new compounds (National Toxicology Program, 2018). Still, establishing relationships between tPODs and apical outcomes add to the weight of evidence of the value of using tPODs in support of ERA of chemicals. Furthermore, current benchmark dose approaches do not allow for the calculation of confidence limits or variance of omicBMDs, and existing statistical tools should be optimized to include such estimates to increase confidence in derived threshold values.

Next-generation sequencing has enabled the integration of transcriptomic dose-response studies that can potentially advance ERA towards high throughput screening, particularly for

prioritization of chemical testing. Here, we have shown that the use of a transcriptomic BMD approach using short-term exposures with early embryonic/alevin life stages, which are not considered live animals under current legislations (Canadian Council on Animal Care, 2005; European Union, 2010; UK, 1993), can effectively estimate tPODs for EE2 that are as protective as those empirically derived using lengthy live-animal tests. Furthermore, we have also shown that relevant genes and pathways associated with EE2 in adult fish were significantly perturbed at the embryonic stage, confirming the hypothesis that embryo models can detect gene-level disturbances indicative of adult responses. More importantly, this study demonstrated that short-term whole embryo tPOD assays may have significant promise to replace adult fish tests, and as such may represent a powerful alternative testing strategy, especially when compared to *in vitro* NAMs that are prone to significant uncertainties. Future studies should be directed towards further validation of toxicogenomic benchmarking approaches using additional compounds and by including early life-stages of other species. In particular, there is an urgent need for curation of genome annotations for species relevant to ERA, as well as the development of strategies to derive tPODs for non-model organisms with incomplete genomes.

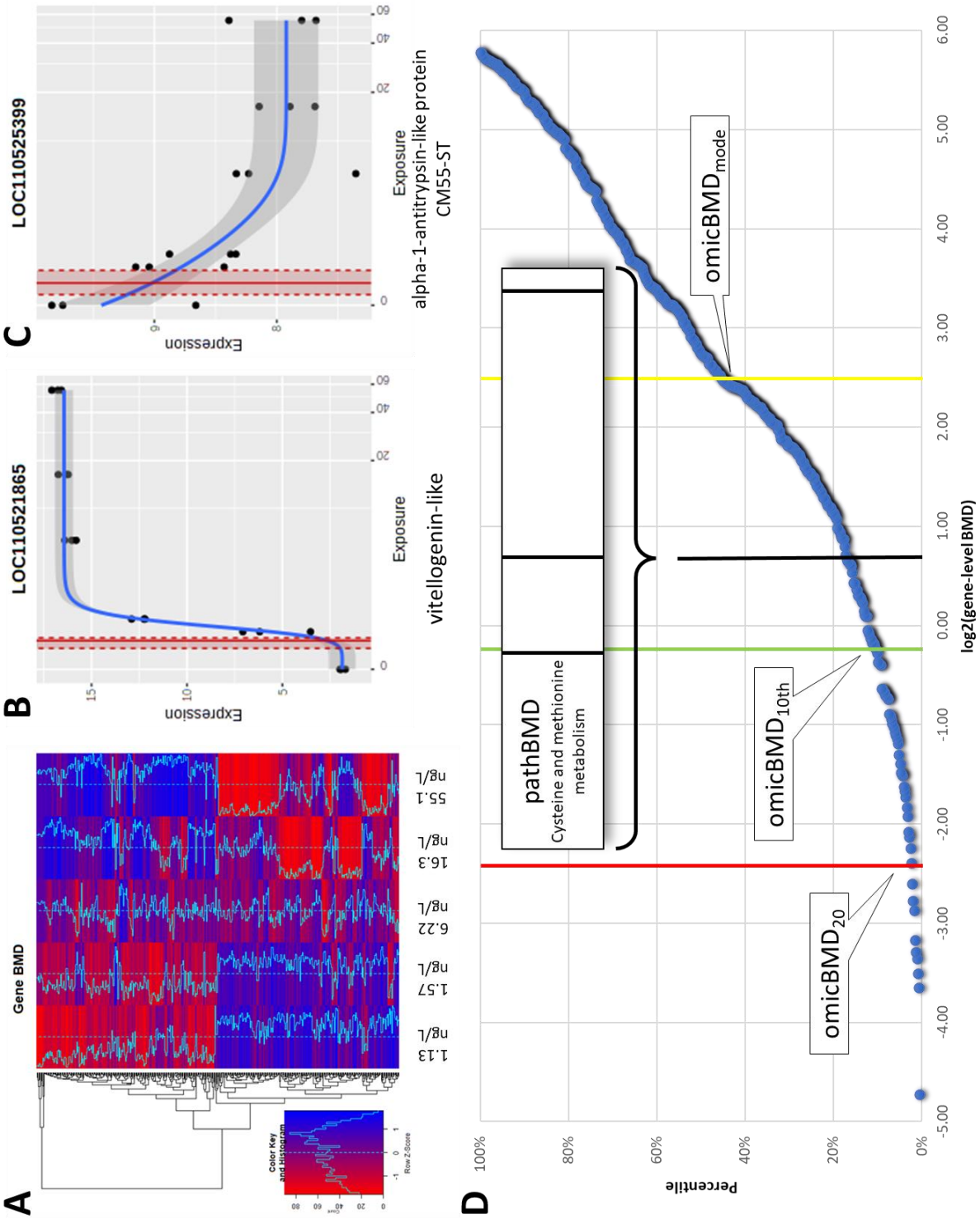
A
Gene BMD
1.13 ng/L
1.57 ng/L
6.22 ng/L
16.3 ng/L
55.1 ng/L
Color Key and Histogram
Row Z-Score
B
LOC110521865
Expression
Exposure
vitellogenin-like
C
LOC110525399
Expression
Exposure
alpha-1-antitrypsin-like protein CM55-ST
D
pathBMD
Cysteine and methionine metabolism
omicBMD20
omicBMD10th
omicBMDmode
Percentile
log2(gene-level BMD)

Figure 3.4. Transcriptomic points-of-departure (tPOD) based on benchmark response (BMR) factor = 1.0 for EE2-exposed RBT at 4 dph. (**A**) Differential expression heatmap of features with gene-level BMD (geneBMD). (**B**) Representative upregulated gene-level concentration-response curve (*vtg*-like). (**C**) Representative downregulated gene-level concentration-response curve (alpha-1-antitrypsin-like protein CM55-ST). For B and C, the intersection of the solid red line and blue line corresponds to the geneBMD; the red shaded area corresponds to the boundaries of the upper (BMD_u) and lower (BMD_l) limits of specific geneBMD at a 95% confidence interval. Shaded grey areas represent the 95% confidence interval. x-axis – EE2 concentration in ng/L (figure scaled at log2Concentration); y-axis – normalized expression (logCPM). (**D**) Transcriptomic PODs. Estimated concentrations at which the whole transcriptome responded to EE2 (omicBMD): ▮ median of the 20 most sensitive genes ($omicBMD_{20}$ = 0.18 ng/L), ▮ tenth percentile of all geneBMDs ($omicBMD_{10th}$ = 0.78 ng/L), and ▮ first mode of the geneBMD distribution ($omicBMD_{mode}$ = 3.64 ng/L) (**Figure S6**). ▮ Pathway-level BMD (pathBMD = 1.63 ng/L) based on the most sensitive (lowest value) bootstrapped median of constitutive geneBMDs in that specific pathway (with at least 3 genes, using KEGG annotation database). Inset bar: individual geneBMDs involved in the most sensitive pathBMD (cysteine and methionine metabolism).

3.5. List of Supporting Information (Appendix C)

Appendix C1 – C6, Tables CS1 – CS5, and Figures CS1 – CS6.

The list of files below can be found as Supporting Information in

https://doi.org/10.1021/acs.est.1c02401

Dataset S1. Transcriptomic datasets

Tab A1-A5. Differential expression results

Tab B. List of common dysregulated transcripts

Tab C1-C5. Transcriptomic overrepresentation results

Dataset S2. Proteomics datasets

Tab A1-A2. DAP for 30 and 100

Tab B. Overlap of DAPs

Tab C1-C2. Overrepresentation analyses results

Tab D. Overlap of overrepresentation results

Dataset S3. Results of benchmark-dose analyses

Tab A. Gene-level BMD

Tab B. Pathway-level BMD

Dataset S4. Statistical analyses of morphometrics and survival rates

Tab A1-A4. Statistical Analyses of Survival Rates

Tab B1-B3. Statistical Analyses of morphometric measurements at 4dph

Tab C1-C3. Statistical Analyses of morphometric measurements at swim-up

3.6. Acknowledgments

The authors acknowledge the support of key project managers (P. Poulin, A. Masse, J. Eng, E. Boulanger) and our various trainees. We thank Fisheries and Oceans Canada, Genome Canada, Genome Quebec, Genome Prairies, the Government of Canada, ECCC, Ministere de l'Economie, de la Science et de l'Innovation du Quebec, the University of Saskatchewan, and McGill University, as well as core project partners (US Environmental Protection Agency, US Army Corps of Engineers, Qiagen, SGS AXYS, and Shell USA) for their financial and other support. Proteomics measurements were supported by the project CEITEC 2020 (LQ1601) and the CIISB (LM2018127) funded by MEYS CR. Computational resources for proteomics analyses were supplied by the project "e-Infrastruktura CZ" (e-INFRA LM2018140) provided within the program Projects of Large Research, Development, and Innovations Infrastructures. MH and NB were supported by the CRC Program of NSERC. AGA was supported through the University of Saskatchewan Dean's Scholarship, Toxicology Devolved Scholarship, and the Mitacs Globalink Research Award. JE was supported through the NSERC CGS D fellowship. This project is part of the EcoToxChip project (ecotoxchip.ca).

CHAPTER4: COMPARATIVE ANALYSIS OF TRANSCRIPTOMIC POINTS-OF-DEPARTURE (tPODs) AND APICAL RESPONSES IN EMBRYO-LARVAL FATHEAD MINNOWS EXPOSED TO FLUOXETINE

PREFACE

In Chapter 2, results suggest that embryo-larval FHM exposed to EE2 showed conserved toxicity responses across levels of biological organization that are indicative of apical effects typically observed in more advanced life stages. In Chapter 3, transcriptional responses from short-term ELS exposure of RBT to EE2 effectively estimated tPODs that were protective of chronic apical effects at later life stages. Building upon these previous chapters, this chapter estimated tPODs for FLX using short-term embryo-larval exposure of FHM. Calculated tPODs were compared to behavioral bechmark concentrations at 4 dph and to physiological (standard length, weight, condition factor) and survival rates at 28 dph, as well as to other apical benchmark concentrations reported in the literature. This chapter also attempted to link significantly perturbed gene sets/pathways from global gene expression and non-target proteomics at 4 dph to apical responses.

Chapter 4 is currently under review (after revisions) for publication in *Environmental Pollution* as Alcaraz, A.J.G., Baraniuk, S., Mikulášek, K., Park, B., Lane, T. Burbridge, C., Ewald, J., Potěšil, D., Xia, J., Zdráhal, Z., Schneider, D., Crump, D., Basu, N., Hogan, N., Brinkmann., M., Hecker, M. Comparative analysis of transcriptomic points-of-departure (tPODs) and apical responses in embryo-larval fathead minnows exposed to fluoxetine.

Author contributions:

Alper James G. Alcaraz (University of Saskatchewan) - Conceptualization, Methodology, Software, Validation, Formal Analysis, Investigation, Data Curation, Writing - Original Draft, Review and Editing, Visualization

Shaina Baraniuk (University of Saskatchewan) - Methodology, Formal Analysis, Investigation, Review and Editing

Dr. Kamil Mikulášek (Masaryk University) - Methodology, Formal Analysis, Investigation, Review and Editing

Bradley Park (University of Saskatchewan) - Methodology, Formal Analysis, Investigation, Review and Editing

Taylor Lane (University of Saskatchewan; University of York)- Investigation, Review and Editing

Connor Burbridge (University of Saskatchewan) - Methodology, Software, Review and Editing

Jessica Ewald (McGill University) - Software, Review and Editing

Dr. David Potěšil (Masaryk University) - Methodology, Software, Formal Analysis, Investigation, Supervision, Review and Editing

Dr. Jianguo Xia (McGill University) - Resources, Review and Editing, Supervision

Dr. Zbyněk Zdráhal (Masaryk University) - Resources, Review and Editing, Supervision, Project Administration, Funding Acquisition

David Schneider (University of Saskatchewan) - Resources, Supervision, Review and Editing

Dr. Doug Crump (Environment and Climate Change Canada) - Conceptualization, Review and Editing, Project Administration, Funding Acquisition

Dr. Niladri Basu (McGill University) - Conceptualization, Review and Editing, Project Administration, Funding Acquisition

Dr. Natacha Hogan (University of Saskatchewan) - Conceptualization, Review and Editing, Project Administration

Dr. Markus Brinkmann (University of Saskatchewan) - Methodology, Validation, Formal Analysis, Investigation, Resources, Review and Editing, Visualization, Supervision, Project Administration

Dr. Markus Hecker (University of Saskatchewan) - Conceptualization, Methodology, Resources, Writing – Original Draft, Review and Editing, Supervision, Project Administration, Funding Acquisition

4.1. Abstract

Current approaches in chemical hazard assessment face significant challenges because they rely on live animal testing, which is time-consuming, expensive, and ethically questionable. These concerns serve as an impetus to develop new approach methodologies (NAMs) that do not rely on live animal tests. This study explored a molecular benchmark dose (BMD) approach using a 7-day embryo-larval fathead minnow (FHM) assay to derive transcriptomic points-of-departure (tPODs) to predict apical BMDs of fluoxetine (FLX), a highly prescribed and potent selective serotonin reuptake inhibitor frequently detected in surface waters. Fertilized FHM embryos were exposed to graded concentrations of FLX (confirmed at <LOD, 0.19, 0.74, 3.38, 10.2, 47.5 µg/L) for 32 days. Subsets of fish were subjected to omics and locomotor analyses at 7 days post-fertilization (dpf) and to histological and biometric measurements at 32 dpf. Enrichment analyses of transcriptomics and proteomics data revealed significant perturbations in gene sets associated with serotonergic and axonal functions. BMD analysis resulted in tPOD values of 0.56 µg/L (median of the 20 most sensitive gene-level BMDs), 5.0 µg/L (tenth percentile of all gene-level BMDs), 7.51 µg/L (mode of the first peak of all gene-level BMDs) , and 5.66 µg/L (pathway-level BMD). These tPODs were protective of locomotor and reduced body weight effects (LOEC of 10.2 µg/L) observed in this study and were reflective of chronic apical BMDs of FLX reported in the literature. Furthermore, the distribution of gene-level BMDs followed a bimodal pattern, revealing disruption of sensitive neurotoxic pathways at low concentrations and metabolic pathway perturbations at higher concentrations. This is one of the first studies to derive protective tPODs for FLX using a short-term embryo assay at a life stage not considered to be a live animal under current legislations.

Keywords: benchmark dose (BMD); selective serotonin reuptake inhibitor (SSRI); hazard assessment; live-animal alternatives; new approach methodology (NAM)

4.2. Introduction

Current testing frameworks supporting chemical and environmental risk assessment (ERA) are falling short of the global need to rapidly test the vast and ever-increasing numbers of chemicals that are of emerging concern (Bernhardt *et al*., 2017). This is particularly true for aquatic environments that serve as sinks for most environmental contaminants. Current toxicity testing approaches to support ERA rely heavily on the use of live organisms, which require extensive husbandry, are costly, and present significant ethical concerns. Thus, the development of new approach methodologies (NAMs) aimed at replacing, reducing and refining (3Rs) live animal testing while increasing throughput is imperative to improve hazard assessment strategies and regulatory decision-making. This has led to a paradigm shift towards the use of mechanistic data to identify molecular and cellular events indicative of phenotypic outcomes using alternative (i.e. *in vitro* and *in silico*) and short-term animal tests (Ankley and Edwards, 2018; Villeneuve *et al*., 2014). However, many mechanistic toxicity pathway models still need to be conclusively anchored to quantitative experimental data to fully realize the potential of these models in regulatory risk assessment. Additionally, most current models are based on *in vitro* and *ex vivo* studies, which are limited with regard to their ability to quantitatively predict empirical toxicity thresholds as they do not represent the complexity of whole organism.

A promising alternative toxicity testing approach is the use of embryonic assays combined with mechanism-based testing strategies, particularly for prioritizing chemicals for further testing (Basu *et al*., 2019). For instance, life stages of oviparous vertebrates, such as fish, prior to independent exogenous feeding are not considered live animals under current legislations (Canadian Council on Animal Care, 2005; European Union, 2010; Strähle *et al*., 2012; UK, 1993). However, they still express the majority of the complementary molecular features present in more

advanced life stages. Furthermore, the high sensitivity of the earliest life stages of fish render them an ideal model in toxicological studies (Wheeler *et al*., 2014). Thus, assessing changes in molecular response patterns at early life stages could potentially be used as an alternative testing strategy to support chemical hazard assessment. Indeed, it has been recently demonstrated that transcriptomics data from 96-hour rainbow trout embryo-alevin exposures can effectively estimate benchmark doses (transcriptomic points-of-departure, tPODs) that are well within the range (protective) of empirically derived chronic apical PODs from extensive live animal experiments (Alcaraz *et al*., 2021a).

A model fish species of interest in chemical hazard assessment and regulatory testing is the fathead minnow (FHM; *Pimephales promelas*). FHM is a temperate freshwater fish that is native to North America and is widely used as a model species in toxicological studies. A recent study exposing embryo-larval FHM to ethynylestradiol showed conserved toxicity responses across levels of biological organization that are indicative of apical effects typically observed in more advanced life stages (Alcaraz *et al*., 2021b). Therefore, transcriptomic benchmark dose (BMD) analysis based on early-life stage FHM could be used to estimate tPODs in support of hazard assessment.

The objective of the present study was to develop and validate the utility of a short-term embryo-larval FHM assay to estimate tPODs using fluoxetine (FLX) as the model chemical. FLX is among the most potent and commonly prescribed selective serotonin reuptake inhibitors (SSRI). FLX is commonly found at sub-therapeutic levels (<1 µg/L) in surface waters (Mole and Brooks, 2019) and is of significant concern in the aquatic environment due to its ability to induce inadvertent sub-lethal effects in aquatic organisms exposed at low concentrations (Martin *et al*., 2020). This neuroactive compound is known to affect reproduction, feeding, anxiety, and

cognitive behaviors in fish (Beulig and Fowler, 2008; Brooks, 2014; Mennigen *et al*., 2010a; Weinberger and Klaper, 2014). In this study, non-targeted whole transcriptome and proteome analyses were used to identify and characterize biological pathways that have conserved perturbations across levels of organization. Furthermore, morphometric, histological, and locomotor responses were assessed to anchor and link molecular perturbations to adverse apical outcomes. Finally, tPODs were estimated using a recently published transcriptomic BMD approach (Ewald *et al*., 2020; National Toxicology Program, 2018; Pagé-Larivière *et al*., 2019) and were compared to apical BMDs derived in this study and in the literature.

4.3. Materials and Methods

4.3.1. Fish culture and exposure conditions

All methods involving live animals reported here were approved by the Animal Research Ethics Board of the University of Saskatchewan (Protocol #20160090). Adult FHM (source of original brood stock: Aquatic Research Organisms Inc., NH, USA) were reared, maintained, and bred in-house. Fertilized eggs (<6 hours post-fertilization (hpf)) from multiple breeding pairs were pooled, then randomly assigned, and distributed to different treatment groups. The exposure experiment was initiated by placing embryos, between late cleavage and high blastula stage, in Petri dishes containing test solutions (**Figure 4.1**). Separate Petri dishes for each end point were established and maintained in a temperature-controlled environmental chamber and kept at 25 ± 1 ^{o}C and 16:8 light:dark cycle. Fish were exposed to 1.75, 7 and 28 µg/L fluoxetine (FLX; Certified reference material; Sigma-Aldrich, MO, USA) in quintuplicates for transcriptomics (20 embryos/replicate), proteomics (30 embryos/replicate) and histological/apical (30 embryos/replicate) assessments. Furthermore, three replicate Petri dishes were subjected to

behavioral analysis (15 embryos per replicate). To estimate transcriptomic points-of-departure (tPODs), FHM were exposed to two additional concentrations of FLX (0.44 and 112 µg/L), in triplicates, containing 20 embryos each, concurrently done and bracketing the above exposure regime for transcriptomics. For omics and behavioral analyses, embryos were reared to 7 days post-fertilization (dpf). For omics analyses, all larvae per replicate petri dish were pooled, flash-frozen in liquid nitrogen, and kept at -80°C. After 7 dpf, larvae for histological and biometric analyses were transferred to 9L glass aquaria, in a completely randomized design, containing the same test concentrations and maintained under flow-through conditions (~3x complete water exchanges per day) until 32 dpf, following OECD 210 (OECD, 2013). Larvae were fed daily *ad libitum* with *Artemia* nauplii starting 7 dpf. Each tank was monitored daily for temperature, pH, conductivity, and dissolved oxygen, and weekly for ammonia, nitrate, nitrite, hardness, and alkalinity. Surviving larvae at the end of the exposure (32 dpf) were euthanized using an overdose of buffered tricaine methanesulfonate (150 mg/L; MS222; Sigma-Aldrich). Whole larvae samples for histology from each replicate were placed individually in histocassettes and fixed whole in Cal-Ex™ II Fixative/Decalcifier (Fisher Chemical™, MA, USA) for 48 hours, and then transferred to 70% ethanol for storage until further processing. The body length and weight of each larva were measured, and overt morphological abnormalities were qualitatively recorded during takedown by a designated subjective observer. Fulton's condition factor (Froese, 2006) was calculated (Eq.1):

$$\text{Fulton`s condition factor, } k = \frac{w \times 100}{l^3} \qquad (1)$$

where: w = weight (mg) and l = length (mm)

Statistical analyses were carried out in Prism v.9.1 software (GraphPad Inc., LaJolla, USA). Biometric measurements and survival rates were assessed for significant differences across treatment groups using a one-way analysis of variance (ANOVA), followed by Tukey's multiple

comparison post-hoc test, with a cut-off p-value < 0.05. Outliers were removed (ROUT method, Q = 1%) and tests for assumptions of normality and homogeneity of variance were performed prior to ANOVA. In cases where assumptions of ANOVA were not met, the non-parametric ANOVA analogue, Kruskal-Wallis test, was performed, followed by Dunn's multiple comparison test with a cut-off p-value < 0.05.

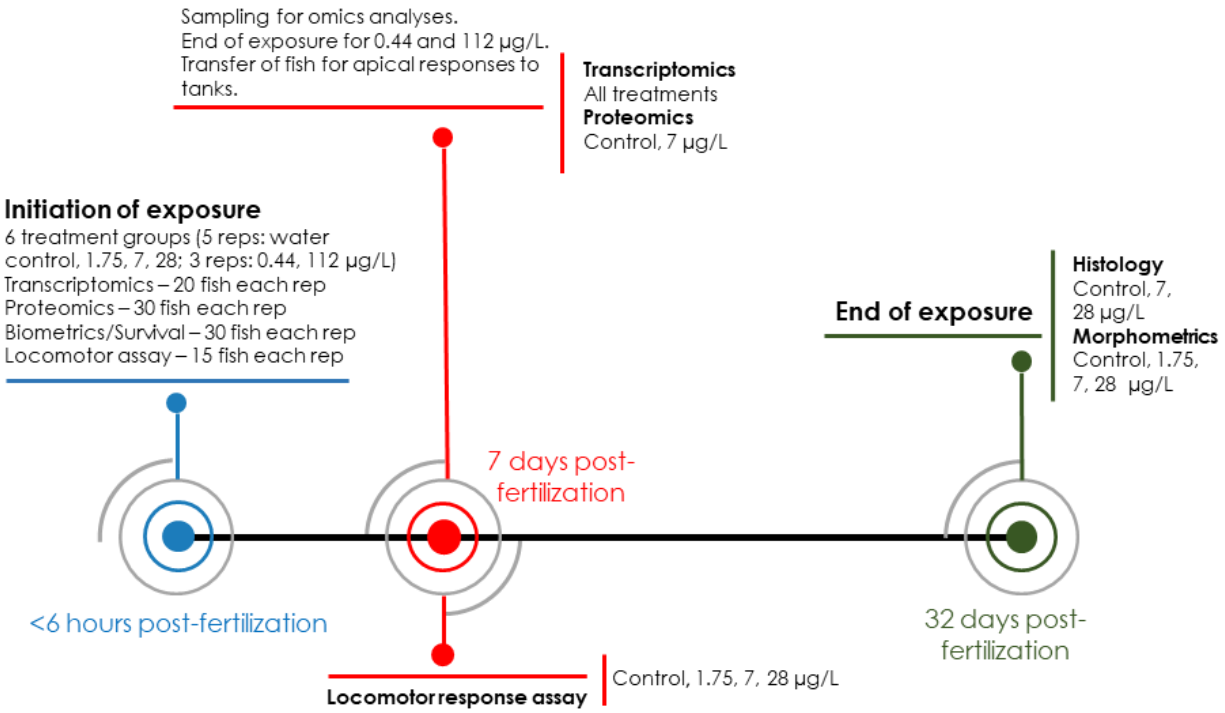

1784

1785 **Figure 4.1**. Study design. Exposures were initiated at <6 hours post-fertilization (hpf) by
1786 introducing the embryos to FLX-dosed solutions in Petri dishes. Transcriptomics and proteomics
1787 were conducted in pools of larvae sampled at 7 days post-fertilization (dpf). Histology and
1788 biometric measurements of whole larvae were done at 32 dpf. A separate study for the locomotor
1789 response assay was set up with the same exposure conditions. The locomotor assay was done at 7
1790 dpf. Treatment groups/concentrations are nominal. rep = replicate

4.3.2. Chemical analyses

Concentrations of FLX in test solutions were measured at SGS AXYS Analytical Services Ltd (BC, Canada). FLX was quantified following a previously described method (Long *et al*., 2013), with minor modifications (**Appendix D1**). Briefly, FLX from water samples was extracted by solid-phase extraction, then quantified using a Waters 2690 HPLC, equipped with Xterra MS C18 column (Waters; 10.0 cm, 2.1 mm i.d., 3.5 µm particle size), coupled with a Micromass Quattro Ultima MS/MS (Waters). For exposures in Petri dishes only (0.44 and 112 µg/L FLX), concentrations were based on the average % of nominal concentrations across all measured concentrations in tanks because the volumes used in petri dishes were too low for analytical testing. This was deemed an appropriate approximation of actual concentrations since the working solutions were from serially diluted stock solutions for all treatments.

4.3.3. Transcriptomics

Total RNA was extracted from pooled whole larvae using the RNeasy Plus Universal Mini Kit (Qiagen, Hilden, Germany) following the manufacturer`s protocol for whole tissue total RNA extraction. Samples with a RIN > 8 were sent to the McGill University and Génome Québec Innovation Centre for 200 cycles paired-end (100x2) sequencing on an Illumina NovaSeq S4 lane (Illumina Inc, San Diego CA, USA). RNASeq libraries were constructed following Alcaraz *et al*. (2021a).

Raw fastq files were assessed for quality using FastQC v0.11.9 (Andrews, n.d.). Adapters were trimmed and reads were filtered to a minimum Phred score of 20 and a minimum length of 35 bases using Trimmomatic v0.38 (Bolger *et al*., 2014). Reads were aligned to the latest fathead minnow transcriptome assembly (NCBI Acc# GCA_016745375.1; Martinson *et al*., n.d.) and

counts were estimated using Kallisto 0.46.0.4 (Bray *et al*., 2016). Features with less than five counts-per-million in at least 3 samples per treatment group were filtered out. The remaining features were normalized by use of the relative log expression (RLE) approach (Anders and Huber, 2010). Significance of differentially expressed (DE) transcripts were assessed using DESeq2 v1.31.18 (Love *et al*., 2014) and scored with a cut-off false discovery rate (FDR; Benjamini-Hochberg, BH) of ≤ 0.05 and a minimum effect size threshold fold-change $|FC| \geq 1.5$ relative to the water control group. Default software settings were used for analyses unless otherwise stated. Raw fastq files are available through the NCBI GEO accession# GSE179232.

Overrepresentation analyses were conducted using ClueGo v.2.5.7 (Bindea *et al*., 2009) in Cytoscape v.3.7.2 (Shannon *et al*., 2003). FHM gene symbols were mapped to *D. rerio* Gene Ontology (GO) databases (MF - Molecular function, BP - Biological process, and CC - Cellular component). Significantly dysregulated transcripts from all treatment groups were pooled and run through ClueGo functional analysis, identifying significantly overrepresented gene sets using two-sided hypergeometric test with BH corrected p-value ≤ 0.05.

4.3.4. Transcriptomic dose-response

Derivation of transcriptomic points-of-departure (tPOD) was conducted using FastBMD (fastbmd.ca; Ewald *et al*., 2020). Transcript count estimates were collapsed into gene-level features and normalized using RLE strategy. Normalized count estimates were filtered to remove 5% and 10% of all the genes with the lowest variance and abundance across treatment groups, respectively. Features that were unlikely to exhibit concentration-response were removed by filtering features without significant differences across treatment groups using the *limma* R package (Ritchie *et al*., 2015) with FDR ≤ 0.05 threshold cut-off. A total of 2343 features passed

the threshold and were fitted using statistical models (Exp2, Exp3, Exp4, Exp5, Linear, 2^{o} Polynomial (Poly2), Hill, and Power), with a threshold lack-of-fit p-value > 0.1 and a benchmark-response (BMR) factor = 1. The benchmark-dose (BMD) analysis was conservative such that higher-level models (Poly3 and Poly4) were not used as these models tend to overfit the datasets. The model with the lowest Akaike information criterion (AIC) was selected for each gene. Control expression was set to the mean of control samples. Individual gene-level (geneBMD), transcriptome-level (omicBMD) and pathway-level (pathBMD) tPODs were estimated based on previous recommendations (Ewald *et al*., 2020; National Toxicology Program, 2018; Pagé-Larivière *et al*., 2019). tPODs for the transcriptome-level include (1) the median of the 20 most sensitive geneBMDs ($omicBMD_{20}$), the tenth percentile of all geneBMDs ($omicBMD_{10th}$), and the mode of the first peak of all gene BMDs ($omicBMD_{mode}$). pathBMD was estimated as the most sensitive pathway based on bootstrapped median of constitutive geneBMDs of that specific pathway, which should have at least 3 geneBMDs.

4.3.5. Proteomics

An estimate from a separate study on early-life stage rainbow trout sub-chronic survival assay (data not shown) showed a NOEC of 7 µg/L FLX (nominal); hence, to assure that proteomic responses were not due to non-specific toxic responses, this concentration was selected for analysis in this study. Proteomics were conducted following Alcaraz *et al*. (2021a), with minor modifications (**Appendix D2**). Cell disruption and protein solubilization were done using SDT lysis buffer. The quality of protein extracts was assessed by use of 1-D SDS-PAGE (12% gels). Protein extracts were then processed by filter-aided sample preparation (FASP) (Wiśniewski *et al*., 2009; Wiśniewski and Rakus, 2014) in a 30 kDa membrane filter unit, using iodoacetamide

(Sigma-Aldrich) for alkylation and trypsin (Sequencing grade; Promega, WI, USA) for digestion. Cleaned and reconstituted FASP eluates were processed in an LC-MS/MS system consisting of a Q-Exactive™ HF-X Hybrid Quadrupole-Orbitrap™ mass spectrometer (Thermo Fisher Scientific, MA, USA) connected online to an Ultimate 3000 RSLCnano system (consisted of SRD-3400, NCS-3500RS CAP, WPS-3000 TPL RS; Thermo Fisher Scientific).

Raw mass spectrometric data files were analyzed using MaxQuant v.1.6.15 (Cox and Mann, 2008; Tyanova *et al*., 2016) with a built-in Andromeda search engine (Cox *et al*., 2011). Chromatograms were characterized using the FHM proteome assembly (NCBI Acc# GCA_016745375.1; 48,456 sequences; Martinson *et al*., n.d.), combined with the cRAP contaminant database (April 2021; 246 sequences). The first and main search were set with carbamidomethylation (C) as fixed modification, acetyl (protein N-term), oxidation (M), oxidation (P) and deamidation (N, Q) as optional modifications, and a maximum of two enzymes miss-cleavages. Peptides and proteins with an FDR (q-value) < 1% and at least one razor peptide were selected for differential abundance analyses. All downstream differential protein abundance analyses were done in KNIME (Berthold *et al*., 2008). Protein groups (PGs) with missing quantification values for all replicates within a treatment group were filtered out. Datasets were further filtered to keep PGs with 2 or more peptides, and at least two measured intensity values in both experimental groups. Log2-transformed PG intensities were quantile-normalized (**Figure D.S1**). The remaining missing values were imputed by the global minimum strategy. The significance of differentially abundant (DA) PGs was assessed using *limma* with a cut-off moderated p-value of ≤ 0.05 and a minimum effect size threshold of $|FC| > 1.5$ relative to the control group. Raw data were deposited in the ProteomeXchange Consortium via the Proteomics

Identifications (PRIDE) (Perez-Riverol *et al*., 2019) partner repository under accession# PXD027024.

All significant DA proteins with at least 2 peptides identified were used in the overrepresentation analyses as previously described (**Sec 4.3.3**).

4.3.6. Correlation analysis

Protein and transcript IDs were matched to their corresponding Entrez IDs. Since the number of proteins is limited by the instrument detection limit and chromatographic identification, the list of transcripts was filtered using Entrez IDs of the leading protein in each PG. The relative correspondence ratios of transcript-protein pairs were then analyzed by calculating Pearson's correlation of transcript expression ratios from each treatment group against their respective protein abundance ratios.

4.3.7. Histology

Ten individual fish were randomly selected from the control, five from 7 (*n*=1 per replicate), and ten from 28 µg/L FLX treatment groups (*n*=2 per replicate). Whole-body samples were dehydrated in graded alcohol concentrations, cleared in xylene, and infiltrated with molten paraffin using a Belair RVG/1 Vacuum Tissue Processor (Histology Core Facility, University of Saskatchewan). The samples were then embedded in paraffin blocks for longitudinal step-sectioning in the frontal plane (5 µm thick). Representative sections from each individual were taken at a minimum of five different levels through the body cavity at approximately 75 µm intervals, mounted on glass slides, and stained with Harris' hematoxylin and eosin.

Slides were analyzed using Axiostar Plus microscope (Carl Zeiss X-Ray Microscopy, LLC, CA, USA), interfaced with INFINITY1-1M digital camera and Infinity Analyze v7.0.2.930 software (Teledyne Lumenera, ON, Canada). Liver sections were assessed qualitatively for histological changes in the treated fish relative to the control group, including changes in hepatocyte size/structure, nuclear abnormalities, staining properties (i.e., the degree of the eosinophilic (pink) or basophilic (blue) staining of the hepatocyte parenchyma), cytoplasmic vacuolation, or any other notable differences. Histological features were reported as presence or absence for individual fish, and no statistical analyses were done for biological replicates.

4.3.8. Locomotor response assay

The locomotor response assay was conducted following a previously described protocol (Thompson and Vijayan, 2020), with minor modifications. Each replicate Petri dish (n=3), with fifteen larvae each, was introduced into a purpose-made temperature-controlled behaviour box that consisted of a visible light source, an infrared light source, and a camera, which allowed for the observation of the larvae during the dark phases. The dishes (one control plate and one treated plate) were placed in the behaviour box and the light was turned on for acclimatization of larvae. Video capture was initiated 6 minutes into the acclimatization period and continuously recorded for the assay duration of 16 minutes. Following 4 minutes recording under light conditions, the light was turned off for 4 minutes, turned on for 4 minutes and the experiment finished with another dark phase of 4 minutes. Individual fish were simultaneously tracked within each dish using Lolitrack 5 software (Loligo Systems, Viborg, Denmark). Larvae were then euthanized after the assay using an overdose (150 mg/L) of buffered MS-222.

The average distance moved over time was calculated for each plate per 1-min period of the experiment. Significant effects on the distance moved in light and dark phases were assessed using mixed-effects ANOVA (mixed-effects: lighting and concentration), followed by Dunnett‘s multiple comparisons test.

4.4. Results and Discussion

4.4.1. Chemical analyses and physico-chemical characteristics of exposure solutions

Measured concentrations of FLX in exposure solutions were 36 – 48% of nominal values, which is in accordance with observations in other studies (Hazelton *et al*., 2014) . It is speculated that the loss of FLX is due to adsorption of the chemical to the surfaces of the tanks, the possible degradation due to the slightly basic pH of the exposure solution, and/or uptake by fish. Treatment groups are subsequently referred to as the measured concentrations (**Table D.S1**). All physico-chemical parameters recommended by OECD 210 guidance document were met (**Table D.S2**), except temperature measurements of 22.43 ± 0.65^{o}C, which were slightly below the recommended 25 ± 1.5^{o}C. Nevertheless, this temperature is not expected to have affected the results of this study as optimal breeding of parent fish was attained at 23.5 ± 1^{o}C.

4.4.2. Survival, biometric measurements, and histology

Survival rates were not significantly affected at 32 dpf regardless of treatment (**Figure 4.2A; DataSet S1, Tab A**). This observation was expected as FLX typically causes chronic behavioral and physiological changes at lower concentrations than what was previously observed to cause acute toxicity (Brooks, 2014), with median lethal concentration (LC_{50}) of 196-212 µg/L (Stanley *et al*., 2007) and 705 µg/L (Brooks *et al*., 2003) in larval FHM. Biometric measurements revealed significant differences in body weight (**Figure 4.2B; DataSet S1, Tab B**), but not in body length or condition factor (**Figure 4.2C&D; DataSet S1, TabC&D**). Larval weight was affected at concentrations greater or equal to 10.2 µg/L relative to the control group, and a notable decreasing trend in body length and body weight occurred as the concentration of FLX increased, suggesting potential effects of FLX on long-term growth. Stanley *et al*. (2007) observed a similar

trend with a significant decrease in weight occurring at FLX concentrations greater or equal to 50 µg/L. Similarly, de Farias *et al*. (2020) reported a significant loss in weight gain in adult zebrafish exposed to 100 µg/L FLX for 30 days. FLX is known to have anorectic effects in fish (Dorelle *et al*., 2020; Weinberger and Klaper, 2014), leading to weight loss. This effect had been associated with the interaction of FLX with the serotonin target, disrupting metabolic processes (Mennigen *et al*., 2010b) and causing changes in the abundance of anorexigenic neuropeptides, resulting in reduced appetite and locomotion impairment, which could lead to reduced food intake and growth impairment (Groh *et al*., 2015).

Notable histological treatment-associated effects were absent in the liver tissues (**Figure D.S2**). This observation contrasts previously observed FLX-induced histological alterations (decreased hepatocyte vacuolation, blood vessel rupture, atypia, hyperemia, and hepatic cord disarrangement) in adult zebrafish at concentrations as low as 0.01 µg/L FLX (de Farias *et al*., 2020). However, normal hepatocyte proliferative activity was observed in livers of embryonic zebrafish exposed to 10 µg/L FLX for 96 hours, suggesting no significant changes in liver histo-structure (Nowakowska *et al*., 2020). These varied observations suggest that the histological effects of FLX may be life stage- and species-dependant.

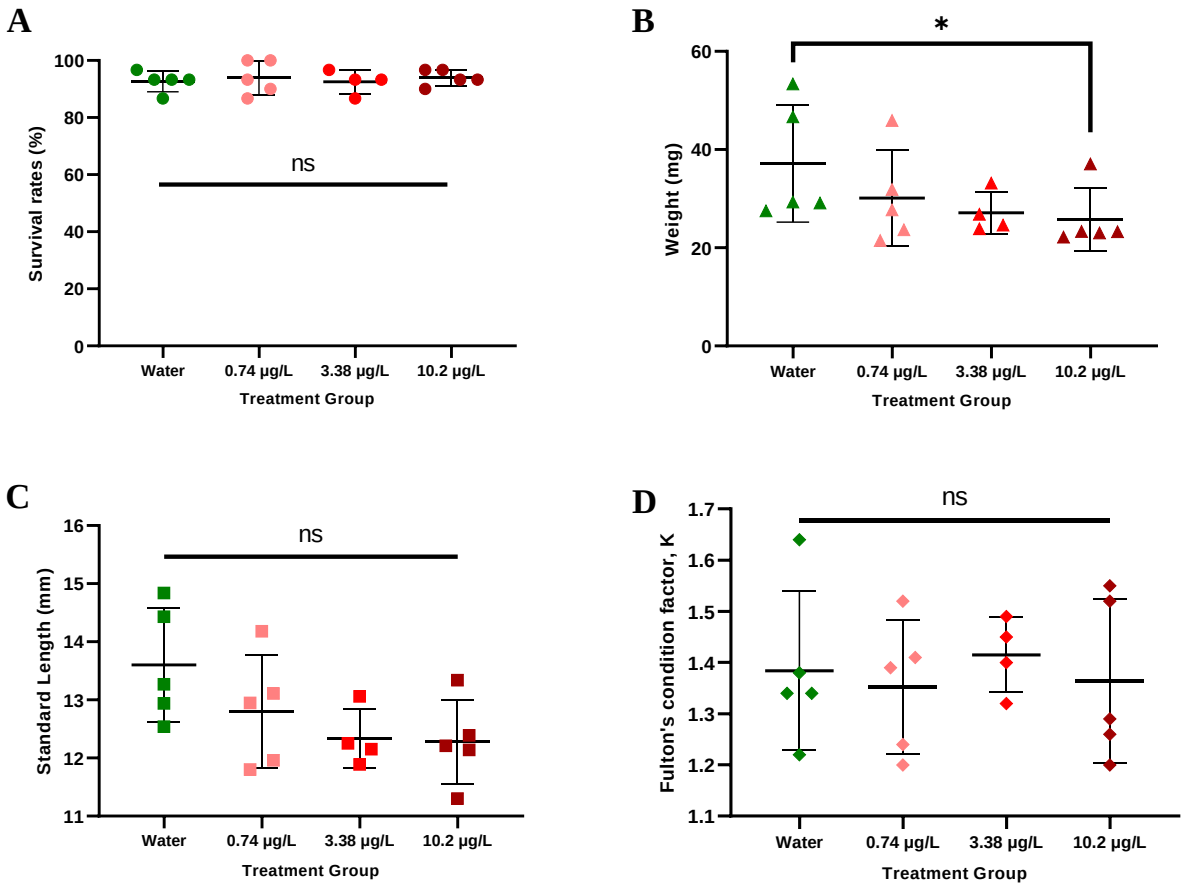

1969

1970 **Figure 4.2.** Biometric profiles and survival rates of FHM exposed to FLX at 32 dpf. (**A**) Survival
1971 rates, (**B**) body weight, (**C**) standard length, and (**D**) condition factor, K of control, 0.74, 3.38, and
1972 10.2 µg/L FLX treatment groups. These four treatment groups were reared to 32 dpf as these
1973 concentrations were expected to trigger biological effects but not mortality due to overall non-
1974 specific systemic effects. For B, C, and D, individual points correspond to average measurements
1975 within tank (biological replicate; ~30 surviving larvae per replicate). For all graphs, line and error
1976 bars represent mean ± standard deviation (of biological replicates).

4.4.3. Locomotor response

The locomotor response assay during the dark phase revealed distinct preference of FLX-exposed larvae towards the edges of the plate, in contrast to the preference of the control larvae to remain in the middle of the plate (**Figure 4.3A**). This observation disagrees with previously observed wall-seeking behaviour bias (thigmotaxis) of untreated zebrafish, regardless of age (Colwill and Creton, 2011). In another study, no effects of FLX treatment (control vs 200-2000 µg/L) was observed on zebrafish behaviour; however, all fish showed edge preference (Richendrfer *et al*., 2012) similar to the thigmotaxis behaviour of FLX-treated fish in this study.

Increased movements were observed during the first dark phase in all treatment groups, then gradually decreasing into a steady state in the subsequent light and dark phases (**Figure 4.3B**). The locomotor behaviour of untreated larvae was comparable with previously observed locomotor responses in untreated larval zebrafish where baseline activity was higher during the dark phase, but in contrast with untreated larval FHM where baseline activity was higher at light phase (Lovin *et al*., 2021; Steele *et al*., 2018). Moreover, average distance moved by larvae exposed to 0.74 µg/L appeared lower while 3.38 and 10.2 µg/L were higher relative to the control group, suggesting inhibitory locomotor effects of FLX at lower concentrations and stimulatory effects at higher concentrations. However, the variance was mainly due to lighting and not due to the interaction of lighting and treatment nor treatment alone (**Figure 4.3C; DataSet S2, Tab A**). When grouped per treatment, distance moved at 10.2 µg/L was significantly higher relative to control ($p = 0.03$; **Figure 4.3D; DataSet S2, Tab A**). In zebrafish, total swimming distance was significantly lower after exposure to ≥ 15.8 µg/L FLX (de Farias *et al*., 2019). While edge preference and the extent of (increased vs. decreased) distance moved might have been different compared to those previously described in the literature, significant changes in locomotor responses in this study

2000 nevertheless suggest anxiolytic effects of FLX at 10.2 µg/L confirming effects on behaviour that
2001 appear to follow complex and sometimes inconsistent patterns among studies and species.

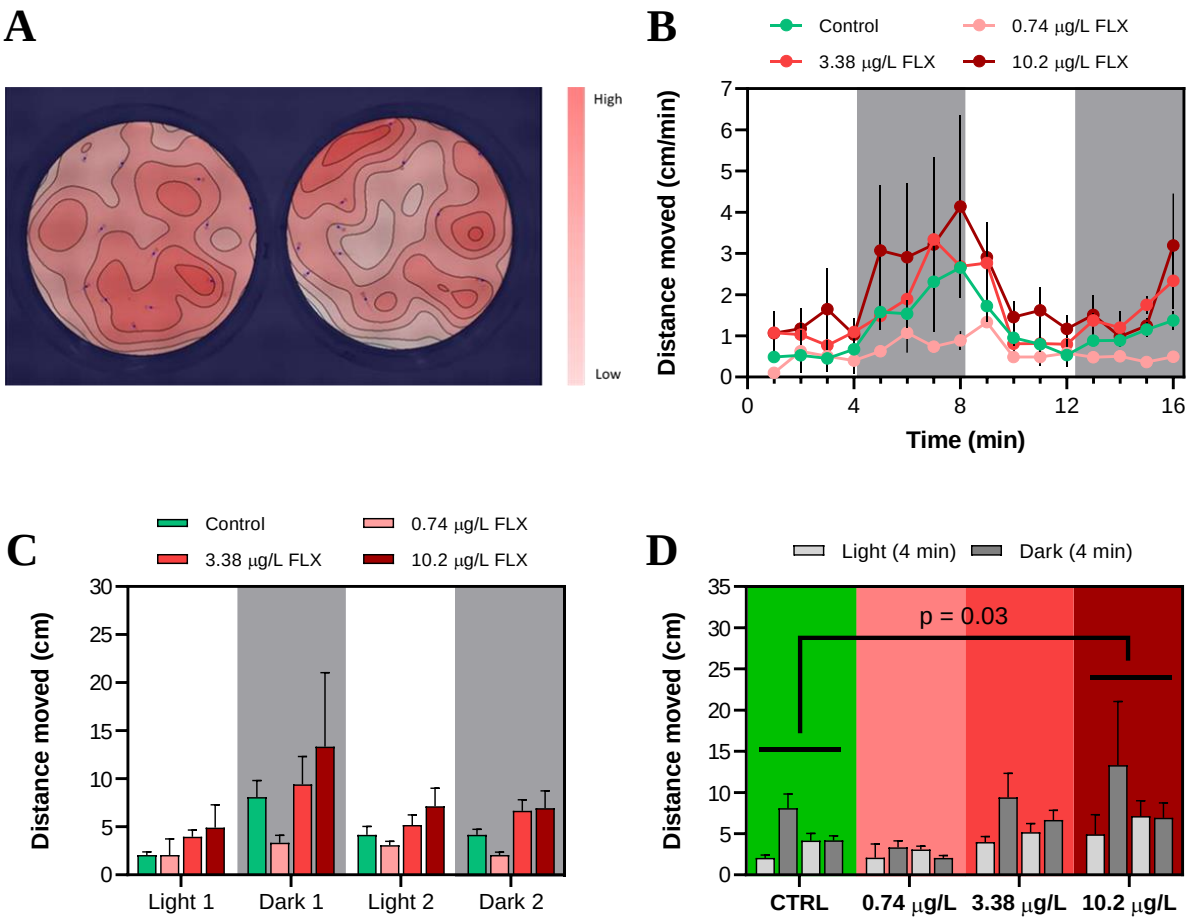

Figure 4.3. Locomotor responses at 7 dpf after exposure to FLX. (**A**) Heatmap of larval frequency detection in the exposure dish (water control and 10.2 µg/L FLX are shown in the left and right panel, respectively). The scale shows relative time spent of larvae in an area (Red – high frequency; white – low frequency). (**B**) Effects of fluoxetine on distance larvae moved throughout the light (white areas) and dark (shaded areas) phases in one-minute increments. (**C**) Distance moved throughout the light (white areas, 4-minute intervals) and dark (shaded areas, 4-minute intervals) phases (mixed-effects model with Dunnett`s post-hoc test, $p \leq 0.05$) (**D**) Distance moved throughout the light (white bars, 4-minute intervals) and dark (dark bars, 4-minute intervals) phases, grouped according to treatments. There were n = 3 replicate dishes per treatment group,

2012 with up to 15 larvae each. Symbols and error bars indicate mean and standard error of the mean,
2013 respectively.

4.4.6. Transcriptomics

Transcriptomics analyses showed 308, 159, 18, 22, and 370 DE transcripts after treatment of embryos with 0.19, 0.74, 3.38, 10.2, and 47.5 µg/L FLX (**Figure 4.4**). Only two DE transcripts were detected across all treatment groups (upregulated): an uncharacterized transcript (LOC120467989) and receptor-type tyrosine-protein phosphatase H-like transcript variant (LOC120475838; *ptprh* gene ortholog). In humans, *ptprh* is primarily expressed in brain and liver and is predicted to be involved in a multitude of cellular processes as a member of the protein-tyrosine phosphatase family, although there have been no reports directly associating *ptprh* to SSRIs. For LOC120467989, BLAST pairwise alignment revealed that this feature is an uncharacterized transcript variant in most phylogenetic relatives of FHM, with the closest predicted identity of RING (Really Interesting New Gene) finger protein 6-like in *T. trachurus*, which similarly has not been previously associated with SSRIs. Regardless, the consistently high expression of these transcripts following FLX exposure merits a closer investigation in future studies.

Larvae exposed to 3.38 and 47.5 µg/L FLX had the least and greatest number of dysregulated transcripts, respectively. The 47.5 µg/L and 0.19 µg/L treatment groups had the greatest number of common dysregulated transcripts (100 transcripts), the directions of which were relatively similar. GO terms of common transcripts included those associated with regulation of behaviour and molecular transport. It should be noted, however, that the number of dysregulated genes or transcripts does not necessarily translate into a more intense downstream perturbation. It could also mean that early systemic responses consisting of multiple cellular processes were activated to counter toxic insults; in fact, hormetic effects of FLX have been previously observed in fish and *Daphnia* (Campos *et al*., 2013; Lopes *et al*., 2020). Instead of the number of

dysregulated genes, the level of dysregulation of molecular features could indicate the severity of overall organismal responses. Interestingly, none of the expected transcripts coding for common FLX-targets were found dysregulated such as 5-hydroxytryptamine transporter (*slc6a4*), corticotropin-releasing hormone (*crh*), cocaine and amphetamine-regulated transcript (*cart*), and neuropeptide Y (*npy*), among others. Notably, these peptides are typically found in specific regions of the central nervous system (CNS); thus, their expression might have been significantly diluted by those of other genes expressed throughout other tissues present in whole body samples, given the relatively small proportion of CNS-associated gene expression in analyzing whole body tissue transcriptomics. Furthermore, CNS-related systems are more likely to be under rapid development in embryos, which may result in limitations with regard to the detection of possible affected genes in these regions. Nevertheless, while the differential expression of transcripts coding for common FLX-target neuropeptides might have been below detection, small perturbations in the CNS could trigger a cascade of reactions to other signalling processes, leading to amplified downstream responses that can be attributed to FLX, albeit indirectly. Transcripts coding for variants of synaptosome-associated and other synaptic proteins such as synapsin, synaptoporin, and synaptopodin, were significantly dysregulated in multiple treatment groups. Still, the limitations on the detection of tissue-specific or localized gene expression present challenges in the use of whole-body tissue transcriptomics in identifying specific molecular events, which can trigger downstream molecular responses.

ClueGo mapped 75.35% (486/645) of significantly dysregulated FHM transcripts to *D. rerio*, 94.86% (461) of which were functionally annotated in GO. There were 35 clusters composed of 130 significantly overrepresented GO terms (**Figure D.S3A**). A significant proportion of these overrepresented terms were associated with axonal and synaptic ontologies

(**Figure S3B**). These results agree with the fact that FLX acts by blocking the membrane transporter, which reduces the reuptake of serotonin from nerve synapses. FLX has also been shown to disrupt axonal growth and maturation in developing zebrafish, affecting the neural ontogeny of spontaneous swimming activity (Airhart *et al*., 2007). This is also in concordance with findings in rats, where perinatal exposure to FLX similarly disrupted chemoarchitectural and electrophysiological brain features, causing neurobiological and behavioral consequences (Simpson *et al*., 2011). In addition, there were significant perturbations in several gene sets associated with bone development. This may result in skeletal development impairment, similar to previously observed compromised embryonic bone development in SSRI-exposed zebrafish (Fraher *et al*., 2016). In general, while significant dysregulation of immediate FLX-target genes such as the serotonin receptor were not observed, significant dysregulation of other associated genes and gene sets indicated downstream serotonergic effects of FLX.

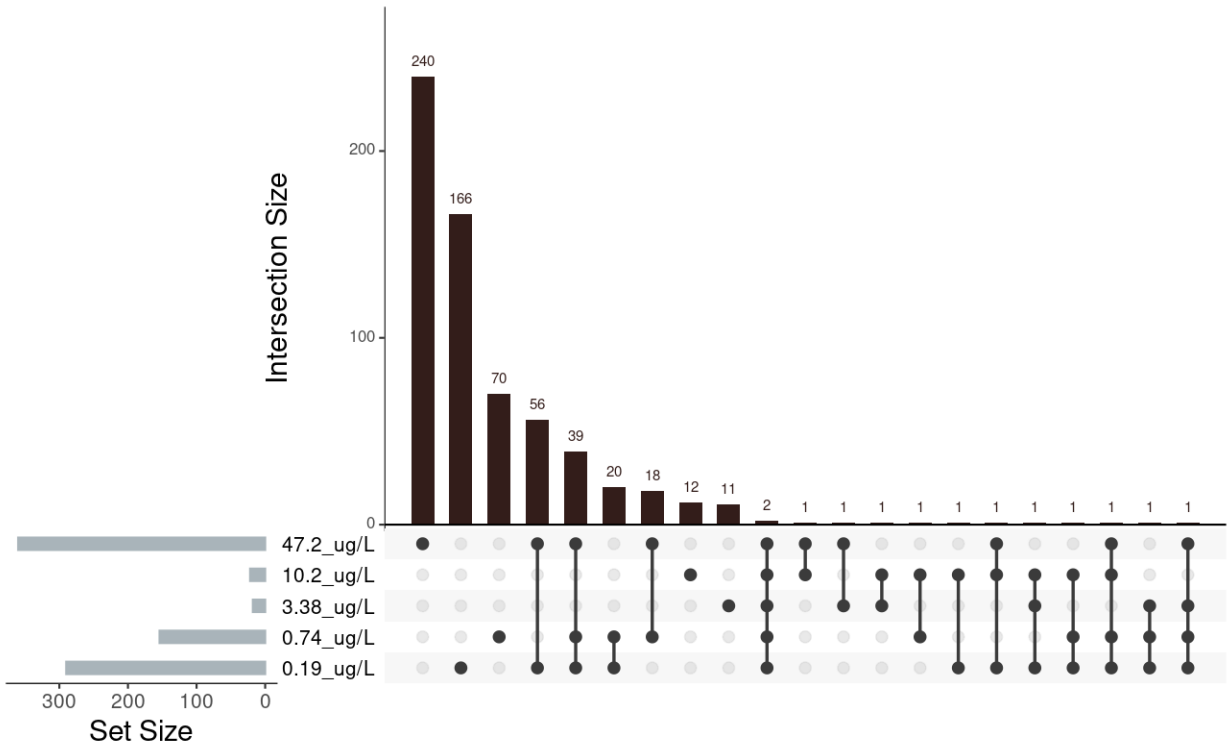

2072

2073 **Figure 4.4.** UpSet plot of significantly dysregulated transcripts from FLX-exposed FHM at 7 dpf.

4.4.5. Proteomics

Proteomics analysis detected 4116 PGs, 407 of which showed significant differences in abundance. Differentially abundant PGs were consisted of 982 protein IDs (identified with at least 2 peptides), corresponding to 481 unique protein products (**DataSet S4A**). This suggests that there were multiple protein isoforms/variants coming from the same gene. Similar to the results of the transcriptomic analysis, common FLX-target neuropeptides were not differentially abundant. Several synaptic proteins such as synaptotagmin, syntaxin, and calcium/calmodulin-dependent protein kinase were significantly dysregulated suggesting different responses among protein variants, which suggests that these protein variants have diverse functions. However, the direction of dysregulation of these proteins was not consistent. Of the 481 protein products, 372 were functionally annotated in GO, forming 40 clusters of 127 significantly overrepresented GO terms (**Figure D.S4; DataSet S4B**). These clusters include proteins associated with synaptic assembly, intra- and intercellular transport, metabolic processes, and structural differentiation/morphogenesis, among others, many of which have previously been observed to respond to FLX exposure. For instance, FLX disrupted synaptic assembly and activity due to suppression of growth of vertebrate and invertebrate neurons (Xu *et al*., 2010). In addition, a study on FLX-induced morphogenesis of mouse embryoid bodies revealed serotonin signaling-independent teratogenic effects of FLX (Warkus and Marikawa, 2018); instead, these effects were due to disruption of canonical Wnt signaling. Lastly, waterborne exposure to sub µg/L FLX has been observed to significantly affect metabolism in goldfish (Mennigen *et al*., 2010b), similar to disruptions in metabolic pathways from the results of proteomics in this study.

4.4.6. Correspondence of molecular features

There was no concordance ($r < |0.03|$, $p >>> 0.05$) between transcript expression ratios from any of the treatment groups and protein abundance ratios. There were 18 common features (based on gene symbols) between all dysregulated transcripts and proteins (**Figure 4.5A; Table D.S3**), although none of these had been previously associated specifically with FLX. This may suggest that these features may be involved in non-specific responses that were triggered in the presence of external challenges. For example, a number of these features are involved in inflammatory responses. Protein and mRNA abundance have been shown to have moderate similarity in certain cases such as sturgeons exposed to dioxin-like compounds (Doering *et al*., 2016) and disease-state in cancer studies (Tang *et al*., 2018). There is an implicit assumption that the biological implications of mRNA expression is mediated by its translation to its cognate proteins; however, genome-wide correlation between the abundances of mRNA and proteins is generally poor, owing to a variety of relevant regulatory mechanisms occurring between transcripts and protein products (Maier *et al*., 2009; Vogel and Marcotte, 2012). The study reported here provides further evidence of these generally weak concordance patterns. One of the objectives of looking into the relative concordances of mRNA and protein expression was to identify potentially robust features/biomarkers which were sensitive enough to be detected at both ‘omics levels. This would suggest a rapid and direct translation of mRNA to protein products given the short exposure duration. Interestingly, combined overrepresentation analysis showed that DE transcripts and DA proteins were complementary with regards to the characterization of overrepresented GO terms (**Figure 4.5B**) that could have been missed if analyzed separately, suggesting that there were interactions and feedback loops among these features at different molecular levels. This

observation highlights the value of comparing and integrating multiple molecular features in identifying relevant molecular processes associated with an external stimulus.

Proteins are considered the fundamental effectors of biological processes, but current sensitivities of methods and instrumentation in non-targeted proteomics limit its utilization in some applications, such as that in quantitative hazard characterization, in contrast to mRNA sequencing. The limited number of proteins identified also has implications in the statistical characterization of overrepresented terms and pathways where background domains are typically the whole reference proteome. In this study, less than 10% of proteins in the FHM proteome assembly were identified, which might have resulted in a lesser number of GO terms passing threshold. Currently, it appears that the sensitivity of non-target proteomics methods has limited applications in quantitative hazard assessment, but is nevertheless essential in supplementing the biological interpretation of molecular processes. Until the methods and sensitivity of non-target proteomics mature further and are more fully developed, quantitative molecular hazard assessment will have to rely on the assumption that differential mRNA expression translate into functional differences attributed to protein action.

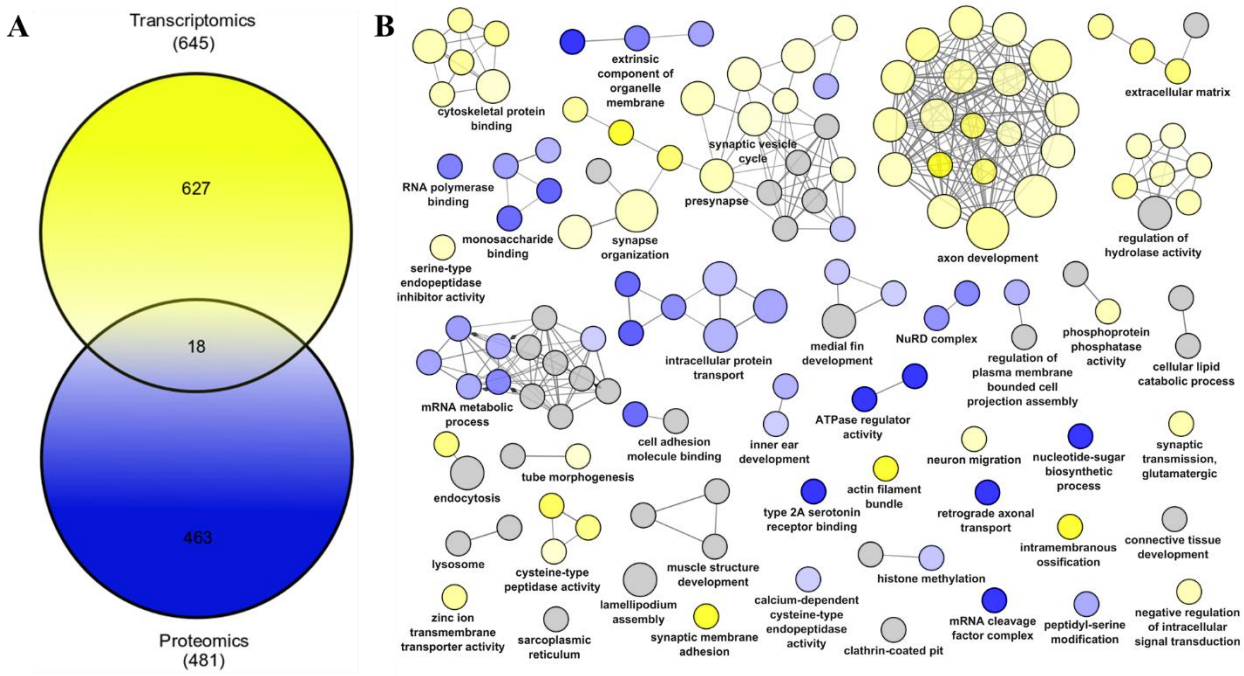

Figure 4.5. Combined transcriptomics and proteomics analyses. (**A**) Venn diagram of features from differentially expressed (DE) transcripts and differentially abundant (DA) proteins. (**B**) Overrepresentation analyses of combined significantly DE transcripts from all FLX treatment groups and DA proteins from 3.38 µg/L using gene ontologies (GO: molecular function, biological process, cellular component) from *D. rerio* as reference set. Statistical test was done using two-sided hypergeometric test with p-value cut off <0.05 followed by Benjamini-Hochberg correction for multiple testing (FDR < 0.05) and a kappa score = 0.04. Yellow nodes are based on DE transcript, blue nodes are based on DA proteins, while gray nodes are terms where DE transcripts and DA proteins both contribute. GO parent-child terms based on similar associated genes were fused (GO Fusion). Nodes were set with a minimum of 3 genes or 4% of genes in a term. Size of the nodes reflects the statistical significance of the terms. Clustering reflects the relationships between the terms based on the similarity of their associated genes. Group leading term is the most significant term of the cluster.

4.4.7. Transcriptomic points-of-departure and their implications to risk assessment

The transcriptomic BMD probability distribution curve exhibited a bimodal response (**Figure 4.6**). At lower concentrations, FLX-responsive genes appeared to be primarily involved in pathways associated with neurotoxic responses. Higher concentrations corresponded to metabolic pathways, although neurotoxic responses were still apparent (**DataSet S6A**). This bimodal response might explain the variability of reported potencies of FLX, with effective concentrations ranging from sub-µg/L to mg/L concentrations, depending on the measured endpoint. In this study, neurotoxic (locomotor response) and metabolism-associated (lower body weight in treated group) apical responses were significantly different relative to the control group, both at 10.2 µg/L FLX.

Benchmark dose analysis showed tPOD values that were more sensitive than observed apical LOECs in this study. Concentration-response patterns of most features converged following the Poly2 model (**Figure DS5**), resulting to a total of 2298 genes with a fitted model and 2153 genes with BMDs (**DataSet S6B**). Transcriptome-wide BMD analysis (**Figure 4.6**) estimated tPODs as (1) the median of the 20 most sensitive genes ($omicBMD_{20}$) = 0.56 µg/L FLX, (2) the tenth percentile of all geneBMDs ($omicBMD_{10th}$) = 5.0 µg/L FLX, and (3) the first mode of the geneBMD distribution ($omicBMD_{mode}$) = 7.51 µg/L FLX. While $omicBMD_{20}$ and $omicBMD_{10th}$ appeared to be the most sensitive tPODs, these values were based mainly on the most conservative and stable tPOD calculations and were independent of genome annotation (Pagé-Larivière *et al*., 2019), and therefore, should be interpreted with caution with regard to downstream biological implications. On the other hand, $omicBMD_{mode}$ was less sensitive than the other tPOD estimates; however, this value typically infers a specific mode of action (MOA) that is potentially biologically

relevant compared to omicBMD$_{20}$ and omicBMD$_{10th}$ and therefore, can be used to guide the elucidation of the compound's MOA.

The pathway-level BMD was 5.66 µg/L (pathBMD), calculated based on the bootstrapped median of constitutive geneBMDs of vasopressin-regulated water reabsorption pathway, the most sensitive (lowest pathBMD value) pathway with at least 3 geneBMDs altered by exposure to FLX. Vasopressins are neuropeptides influencing water reabsorption in the kidneys, suggesting possible modulation in renal processes, similar to those observed in the inner medullary collecting duct in kidneys of rats exposed to FLX (Moyses *et al*., 2008). The PI3K-Akt signaling pathway had the highest number of constitutive geneBMDs, with 44 features exhibiting concentration-dependent responses. FLX has been previously implicated in the regulation of glucolipid metabolism in rats through the PI3K-Akt signaling pathway. However, these pathways should be interpreted with caution with regard to predicting potential apical responses induced by FLX. While these pathways may be considered the most sensitive in the context of transcriptomic BMD, one should bear in mind that these are not necessarily statistically enriched, but merely based on a minimum of three genes, as recommended by NTP (National Toxicology Program, 2018). It should be noted that the purpose of estimating tPODs is to identify the dose or concentration that may potentially perturb biology; characterizing apical responses due to these molecular perturbations is secondary (National Toxicology Program, 2018; Pagé-Larivière *et al*., 2019), although this would be an important addition to support the weight-of-evidence for regulatory acceptability.

A limited literature search revealed that, to date, there have been very few alternative (e.g. *in vitro* or *ex vivo*) testing methodologies utilized successfully to quantitatively assess the potential hazards associated with FLX exposure in fish. For example, a fish hepatoma cell PLHC-1 cytotoxicity assay reported an EC50 of 6.34 mg/L for FLX (Caminada, 2008), which is several

orders of magnitude greater than previously reported threshold concentrations in *in vivo* studies. Although, it is acknowledged that several studies on early-life stage fish have been conducted to assess key responses to FLX, which may be used to estimate its apical POD, these studies were mechanistic in nature, needed prior knowledge of specific mechanism(s) of action, and would require more tedious methodology to quantitatively derive a POD (Bidel *et al*., 2016; Cunha *et al*., 2018; de Farias *et al*., 2019). Limited availability of alternative tests for objectively and reliably assessing the toxicity of FLX may be due to the fact that serotonergic signaling is best known for neural activity and is mainly localized in the CNS, although serotonin regulates numerous biological processes outside the nervous system (reviewed in Berger *et al*., 2009). A considerable range of effect-concentrations (EC) and hazard concentrations (HC_x) of FLX have been reported in the literature, from sub-ng/L to mg/L, corresponding to behavioral responses, biochemical endpoints, and biometric measurements (Beiras and Schönemann, 2021; de Farias *et al*., 2019; Kumar *et al*., 2016). This apparent variable potency of FLX is due to considerable limitations of existing studies, including "artifacts" of low dose effects, lack of proper replication, and non-standard endpoints, which all resulted in the current status of non-consensus for water quality guidelines for FLX (Sumpter *et al*., 2014). Nevertheless, estimated tPODs in this study appeared to be more sensitive than most apical PODs, and thus, we propose they can be considered protective towards chronic effects of FLX.

This study showed that while there are remaining challenges concerning the characterization of tissue-specific or localized gene targets and/or molecular initiating events using the short-term FHM embryo-larval assay, our approach could successfully characterize molecular pathways and mechanisms of action linked to apical outcomes. Furthermore, the strategy featured in our study represents one of the most sensitive alternative testing methods to date that has

successfully estimated tPODs comparable to the most sensitive empirically derived apical benchmark concentrations without the use of live animals beyond the stage of independent exogenous feeding. Thus, tPODs from the 7-day embryo-larval FHM assay present a significant promise to replace labor-intensive, time-consuming, and expensive adult fish tests. Accordingly, it appears to serve as a superior alternative to *in vitro* NAMs that would still require additional tiers of assessment factors to derive PODs that are protective of chronic apical responses. Future studies should be directed towards further development and validation of this testing strategy by using other compounds that project toxic insults by means of other mechanisms. Lastly, there is a need to evaluate the relative sensitivity of this approach across species to assess its utility in protecting environmentally relevant organisms, particularly those that cannot be used in routine ERA testing.

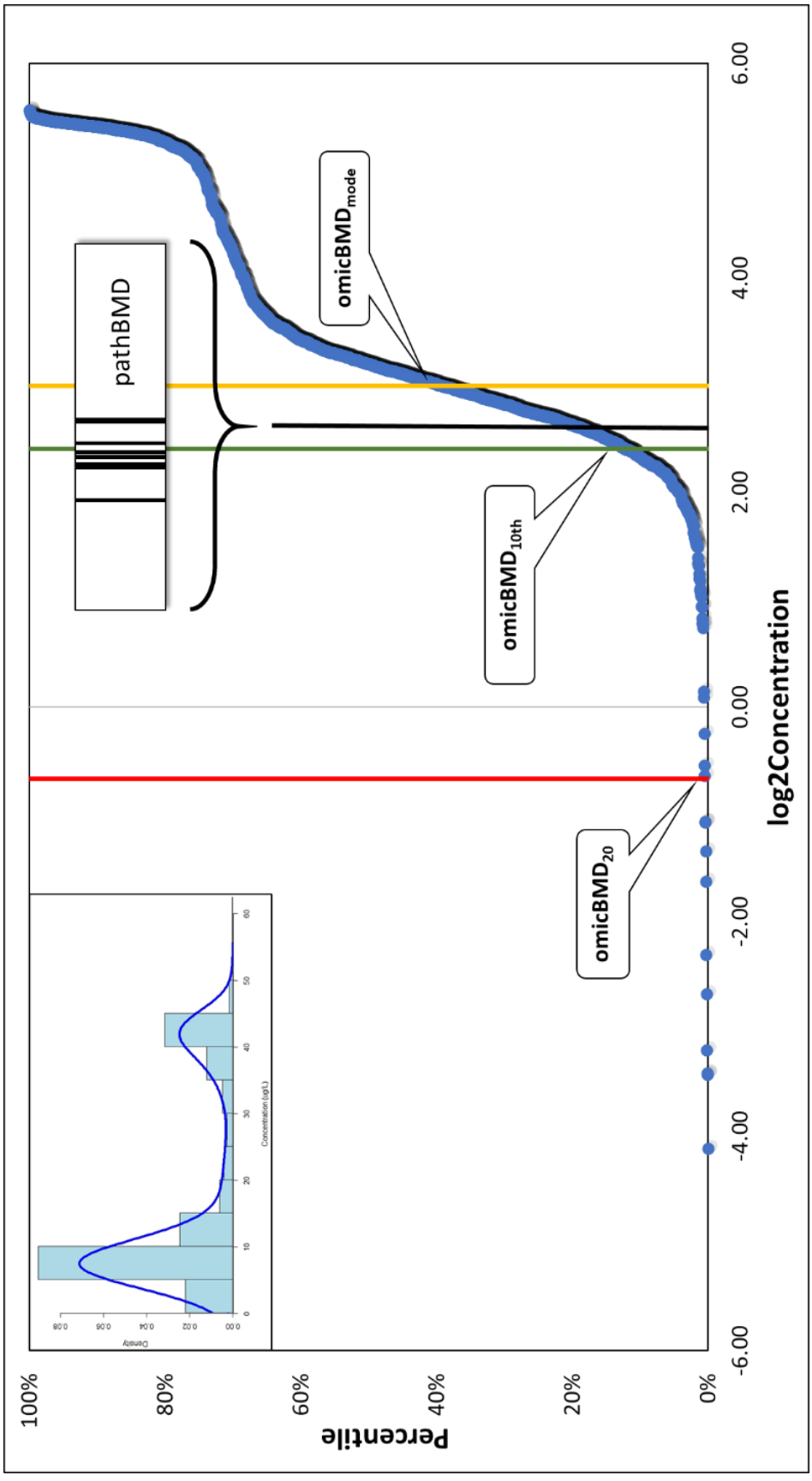
pathBMD
omicBMD$_{mode}$
omicBMD$_{10th}$
omicBMD$_{20}$
log2Concentration
Percentile
6.00
4.00
2.00
0.00
-2.00
-4.00
-6.00
100%
80%
60%
40%
20%
0%
Density
Concentration (log2)

2226

Figure 4.6. Transcriptome-wide points-of-departure (tPOD) in 7 dpf embryo-larval fathead minnows exposed to FLX (scaled at log2Concentration). ▮ median of the 20 most sensitive genes (omicBMD$_{20}$ = 0.56 µg/L), ▮ tenth percentile of all geneBMDs (omicBMD$_{10th}$ = 5.00 µg/L), and ▮ first mode of the geneBMD distribution (omicBMD$_{mode}$ = 7.51 µg/L). ▮ Pathway-level BMD (pathBMD = 5.66 µg/L) based on the lowest bootstrapped median of constitutive geneBMDs in that specific pathway (using KEGG annotation database). Inset bar: ▮ individual geneBMDs involved in the most sensitive pathBMD (vasopressin-regulated water reabsorption pathway). Inset figure: normal-scale histogram with probability density plot (blue line) showing bimodal curve. Bin-width is set to $h = 2\frac{\mathrm{IQR(x)}}{\sqrt[3]{n}}$, following the Freedman-Diaconis rule, where h = bin width, n = number of observations, and IQR(x) = interquartile range. Probability density plot was truncated at zero concentration.

4.5. List of Supporting Information (Appendix D)

Appendix D1 – D2, Figures D.S1 – D.S5, and Tables D.S1 – D.S3.

The list of files below can be found as Supporting Information in the submission in *Environmental Pollution*.

Dataset S1. Statistical analyses of survival and biometric measurements

Tab A. ANOVA and Tukey's multiple comparison test for 32 dpf survival rates

Tab B. Kruskal-Wallis and Dunn's multiple comparison test for weights at 32 dpf

Tab C. ANOVA and Tukey's multiple comparison test for standard length at 32 dpf

Tab D. ANOVA and Tukey's multiple comparison test for Fulton's condition factor at 32 dpf

Dataset S2. Statistical analyses of locomotor assay

Tab A. Mixed-effects analysis and Dunnett's multiple comparison test for Distance moved (light and concentration)

Tab B. ANOVA and Tukey's multiple comparison test for Total Distance moved

Dataset S3. Transcriptomics

Tab A1-A5. Results of differential expression analyses for each concentration at 7 dpf

Tab B. Overrepresentation analysis of all differentially expressed transcripts

Dataset S4. Proteomics

Tab A. Result of differential protein abundance analysis using *limma* with cut-off moderated p-value < 0.05

Tab B. Overrepresentation analysis of all differentially abundant proteins

Dataset S5. Overrepresentation analysis of combined differentially expressed transcripts (Cluster #1) and differentially abundant proteins (Cluster #2)

Dataset S6. Benchmark dose analyses

Tab A. pathBMD

Tab B. geneBMD

4.6. Acknowledgments

This study is part of the EcoToxChip project (ecotoxchip.ca), and the authors acknowledge the support of key project managers (P. Poulin, A. Masse, J. Eng, E. Boulanger) and various trainees. We thank Genome Canada, Genome Quebec, Genome Prairies, the Government of Canada, Environment and Climate Change Canada, Ministere de l`Economie, de la Science et de l`Innovation du Quebec, the University of Saskatchewan, and McGill University, as well as core project partners (US Environmental Protection Agency, US Army Corps of Engineers, Qiagen, SGS AXYS, and Shell USA) for their financial and other support. Proteomics measurements were supported by the project CEITEC 2020 (LQ1601) and the CIISB research infrastructure project LM2018127 funded by MEYS CR. Computational resources for proteomics analyses were supplied by the project "e-Infrastruktura CZ" (e-INFRA LM2018140) provided within the program Projects of Large Research, Development, and Innovations Infrastructures. MH and NB were supported by the CRC Program of NSERC. AGA was supported through the University of Saskatchewan Dean`s Scholarship, Toxicology Devolved Scholarship, and the Mitacs Globalink Research Award. MB is currently a faculty member of the Global Water Futures (GWF) program, which received funds from the Canada First Research Excellence Funds (CFREF). JE was supported through the NSERC CGS D fellowship. The authors also thank the Institute for Environmental Research, RWTH Aachen University for the camera and light source for the locomotor assay.

CHAPTER 5: TRANSCRIPTOMIC POINTS-OF-DEPARTURE (tPODs) IN THREE PHYLOGENETICALLY DISTANT FISHES: CASE STUDIES FOR 17α-ETHINYLESTRADIOL AND FLUOXETINE

PREFACE

This chapter concludes and synthesizes the research undertaken in this thesis for the derivation of protective tPODs using ELS exposure models of phylogenetically diverse fishes. Here, I expanded the work reported in Chapters 3 and 4 by deriving tPOD estimates for EE2 and FLX from ELS of the endangered WS, as well as from ELS of RBT exposed to FLX and FHM exposed to EE2. Hence, datasets used in this Chapter were comprised of original datasets and datasets previously used in Chapters 2 - 4. tPODs (the median of the benchmark concentrations (BMC) of the 20 most sensitive active genes, the BMC of the tenth percentile of all active genes, the BMC of the first mode of all active genes, and the median of the BMCs of constitutive active genes of the most sensitive pathway) were qualitatively compared to identify the most conservative estimation approach within and across species. Current limitations of these approaches were also discussed.

Chapter 5 is in preparation for submission to *Environmental Science & Technology* as Alcaraz, A.J.G., Shekh, K., Ankley, P.J., Challis, J.K., Lane, T.J., Malala Irugal Bandaralage, S., Hecker, M. Transcriptomic points-of-departure (tPODs) in three phylogenetically distant fishes: Case studies for 17α-ethinylestradiol and fluoxetine.

Author contribution:

Alper James G. Alcaraz (University of Saskatchewan) - Conceptualization, Methodology, Software, Validation, Formal Analysis, Investigation, Data Curation, Writing - Original Draft, Review and Editing, Visualization

Kamran Shekh (University of Saskatchewan) - Methodology, Investigation, Review and Editing

Phillip J. Ankley (University of Saskatchewan) - Validation, Formal Analysis, Investigation, Review and Editing

Jonathan K. Challis (University of Saskatchewan) - Methodology, Investigation, Review and Editing

Taylor J. Lane (University of Saskatchewan; University of York) - Investigation, Review and Editing

Susari Malala Irugal Bandaralage (University of Saskatchewan) - Investigation, Review and Editing

Markus Hecker (University of Saskatchewan) - Conceptualization, Methodology, Resources, Writing – Original Draft, Review and Editing, Supervision, Project Administration, Funding Acquisition

5.1. Abstract

There is urgent need for developing new approach methods (NAMs) to make chemical hazard assessment more efficient and reduce the use of live animals in toxicity testing. This study aimed to derive transcriptomic points-of-departure (tPODs) from short-term embryo-larval/alevin exposure studies with three phylogenetically distant ray-finned fishes to two contaminants of concern. tPODs were then compared to apical benchmark concentrations described in the literature. Embryos of white sturgeon (WS), rainbow trout (RBT), and fathead minnow (FHM) were exposed to graded concentrations of 17α-ethinylestradiol (EE2) and fluoxetine (FLX) until four days post-hatch and subjected to mRNA sequencing. Transcriptomic benchmark concentration (BMC) analyses yielded tPOD estimates that closely approximated apical PODs found in the literature. tPOD estimates for the median of the 20 most sensitive gene BMCs (omicBMC_{20}) were the most protective estimates across species and across chemicals, while annotation-dependent tPOD estimate derived from pathway enrichment analyses (pathBMC) appeared to be less sensitive. tPODs from RBT were the most protective for both EE2 and FLX, while FHM was the least sensitive species, but all estimates were within the range of reported apical PODs. This study highlighted that, despite some remaining uncertainties, tPODs derived from short-term embryo-larval/alevin exposures were protective of apical PODs and therefore show significant promise as a NAM to support chemical hazard assessment and regulatory decision making.

Keywords: white sturgeon; rainbow trout; fathead minnow; benchmark concentration (BMC); animal alternative; toxicogenomics

5.2. Introduction

Current approaches in chemical hazard assessment require extensive live animal testing, which is of significant ethical concern and relies on expensive and time-consuming methodologies. Such issues present major limitations in evaluating the hazards of the thousands of chemicals of emerging concern (CEC) that are generated, used, and released by society. CECs include pharmaceuticals and personal care products, brominated flame retardants, nanomaterials, and microplastics, among others. These chemicals are of particular concern as they are continuously discharged into surface waters through effluents of municipal wastewater treatment plants where they can impact non-target organisms (Patel *et al*., 2019; Sehonova *et al*., 2018). Thus, there is an urgent need to develop innovative approaches that would improve (reduce the use of live animals and decrease costs) and accelerate chemical testing strategies to support environmental risk assessment (ERA) of and regulatory decision-making for CECs.

Recent years have witnessed the onset of a paradigm shift and growing global efforts towards the use of new approach methodologies (NAMs) that aim to streamline chemical hazard assessment and reduce the use of live animals (Kavlock *et al*., 2018; Krewski *et al*., 2020). One of the featured approaches is the development of mechanistic toxicity models to identify molecular and cellular events that lead to adverse apical outcomes of regulatory relevance (Ankley *et al*., 2010; Villeneuve *et al*., 2014). Traditionally, the development of toxicity pathway models has relied on *in silico* (Brinkmann *et al*., 2014), *in vitro* (Doering *et al*., 2020), and *ex vivo* (Rahman *et al*., 2020) studies. Indeed, some of these models have proven successful in predicting downstream effects of specific molecular key events (Doering *et al*., 2018). However, many of these approaches are limited in estimating apical toxicity thresholds as they do not represent the complex interactions occurring within an organism after a toxic insult; hence, there are still gaps

2362 in the predictive capability of these models as they need to be anchored quantitatively to relevant
2363 apical outcomes to fully realize their translational capability in regulatory ecotoxicology.
2364 Recently, the use of molecular approaches involving embryonic life stages has shown great
2365 promise in estimating chronic apical threshold concentrations in fish (Alcaraz *et al*., 2021a,
2366 submitted). The approach utilized a toxicogenomic benchmark concentration (BMC) method for
2367 estimating transcriptomic points-of-departure (tPODs) from exposures at embryo/early alevin
2368 stages of fish. This approach has the advantages of (1) using the most sensitive stages in the fish
2369 life cycle that already express the majority of molecular features characteristic of adult fish, (2)
2370 utilizing a life stage prior to independent exogenous feeding, which is not considered a live animal
2371 under current legislations (Canadian Council on Animal Care, 2005; European Union, 2010;
2372 Strähle *et al*., 2012; UK, 1993), (3) featuring short-term (4-7 day) exposures being relatively less
2373 labor and resource-intensive, and (4) allowing the interrogation of the full suite of transcriptomic
2374 responses without *a priori* knowledge of a chemical's mechanism of action (MOA).

2375 While there is an increasing number of studies that apply toxicogenomics in support of
2376 chemical hazard assessment in fishes, most studies conducted so far utilized a few select model
2377 fish species such as zebrafish (*Danio rerio*), fathead minnow (*Pimephales promelas*) or medaka
2378 (*Oryzias latipes*/*O. melastigma*) (Caballero-Gallardo *et al*., 2016; Martyniuk *et al*., 2020).
2379 However, these species do not assure protection towards the plethora of native species of interest
2380 in natural ecosystems, and which represent the ultimate protection goal. Thus, there is a need to
2381 evaluate the utility of this approach across different fishes belonging to phylogentically distant
2382 families, particularly those that cannot be used in routine toxicity testing.

2383 The main objective of this study was to derive tPODs from three phylogenetically distant
2384 ray-finned fish species – a cyprinid, a salmonid, and an acipenserid (sturgeon) – at the embryo-

larval/alevin stages, using two CECs, 17α-ethinylestradiol (EE2) and fluoxetine (FLX). EE2 is a synthetic estrogenic compound frequently used as a contraceptive while FLX is one of the most highly prescribed selective serotonin reuptake inhibitors (SSRI). These compounds are found in surface waters and their toxicities are well described in the literature (reviewed in Brooks, 2014 and Laurenson *et al*., 2014), and therefore, there is a wealth of information on their respective MOAs and empirically derived apical PODs across several fish species are available to anchor and compare tPODs. Specifically, this study aimed to assess the potential of tPODs from embryo-larval/alevin fish exposure in estimating protective apical thresholds reported in the literature from CECs acting through distinct mechanisms and whether these estimates were protective across species. This study builds upon previous reports (Alcaraz *et al*., 2021a; Alcaraz *et al*., submitted; Chapters 2-4) on the use of the whole transcriptome BMC approach in estimating tPODs from short-term early life stage fish exposures.

5.3. Materials and Methods

This study used transcriptomic datasets that were generated using RNASeq from three phylogenetically distant fish species exposed to EE2 and FLX until four days post-hatch (dph). These datasets represent a combination of original studies and metadata from previously published work (**Table E.S1**) (Alcaraz *et al*., 2021a, 2021b, submitted; Chapters 2-4). All experiments were approved by the Animal Research Ethics Board of the University of Saskatchewan (Protocol No. 20070049 and 20140079) and the use of the endangered white sturgeon was permitted through the Species at Risk Act Permit No. 16-PPAC-00002).

5.3.1. Summary of experimental design and exposure conditions

Exposure experiments were performed according to the seasonal availability of fish embryos. FHM and RBT exposure experiments were conducted at the Aquatic Toxicology Research Facility while WS exposures took place at the Fish Quarantine Facility, Laboratory Animal Services Unit (all University of Saskatchewan). All fish were exposed to similar (nominal) ranges of five serially diluted concentrations of 17α-ethinylestradiol (EE2; >98% purity, Sigma Aldrich, MO, USA), with 0.01% DMSO as solvent control, and five serially diluted concentrations of fluoxetine (FLX; Certified reference material; Sigma Aldrich), with filtered facility water as control (**Table 5.1**). During the exposure experiments, test solutions were monitored for temperature, pH, conductivity, dissolved oxygen, ammonia, nitrates, nitrites, hardness, and alkalinity. The studies described here were parts of longer experiments (60 dph for RBT, 28 dph for FHM, 60 dph for WS), similar to those previously reported (Alcaraz *et al*., 2021a, submitted). General fish health status and other observations were noted daily, and survival rates were monitored throughout the duration of the individual studies.

Table 5.1. Summary of test concentrations for EE2 (in ng/L) and FLX (in µg/L) studies. All working solutions for the EE2 study were prepared with a final concentration of 0.01% DMSO. All working solutions for the FLX study were prepared using filtered facility water. Measured concentrations were expressed as the mean of measurements from multiple timepoints across all replicates.

17α-ethinylestradiol (ng/L) †					
white sturgeon		**rainbow trout‡**		**fathead minnow**	
nominal	*measured*	*nominal*	*measured*	*nominal*	*measured*
0	< 0.01	0	< 0.01	0	< 0.01Δ
1	0.36	1	1.13	1	1.07
3	1.47	3	1.57	4	4.27
10	8.85	10	6.22	10	10.67
30	24.99	30	16.34	20	23.46Δ
100	73.95	100	55.10	100	95.99Δ
Fluoxetine (µg/L) *					
white sturgeon		**rainbow trout**		**fathead minnow⁋**	
nominal	*measured*	*nominal*	*measured*	*nominal*	*measured*
0	0	0	0	0	0
0.44	0.09	0.44	0.09	0.44	0.19
1.75	0.37	1.75	0.37	1.75	0.74
7	1.83	7	1.83	7	3.38
28	11.56	28	11.56	28	10.2
112	107.51	112	107.51	112	47.5

† 0.01% DMSO as solvent control

* facility water/ no solvent used

‡ from Alcaraz *et al*., 2021a

Δ from Alcaraz *et al*., 2021b

⁋ from Alcaraz *et al*. (submitted)

5.3.1.1. White sturgeon

WS eggs were sourced from the Nechako White Sturgeon Conservation Centre (Vanderhoof BC, Canada). Gametes were obtained from five males and five female wild-caught WS, and fertilized *ex vivo*. Fertilized eggs were then reared in McDonald-type jars and brought to the University of Saskatchewan fish quarantine facility for exposure experiments. Exposures commenced after first signs of hatching by transferring 40 unhatched eggs into aerated 1-L jars with exposure solution, in triplicates per treatment group. Exposures were maintained at 14 ± 1 ^{o}C and a 16:8 light:dark cycle, under static-renewal condition (at least 75% v/v renewal twice per day to maintain water quality) for 4 days. After 4 days post-hatch (dph), pools of three yolk-sac larvae were collected from each tank, flash-frozen in liquid nitrogen, and kept at -80^{o}C until further processing for transcriptomic analysis.

5.3.1.2. Rainbow trout

RBT exposure experiments were previously described in Alcaraz *et al*. (2021a). Briefly, eyed-stage RBT embryos were acquired from Troutlodge, Inc (WA, USA) and were reared in McDonald-type hatching jars until first signs of hatching were observed. One hundred unhatched eggs were then transferred into 9-L tanks containing exposure solutions, in triplicates per treatment group. Temperature was maintained at 15 ± 1 ^{o}C, under a 16:8 light:dark cycle, under flow-through conditions (at least 50% v/v renewal per day) for four days. Pools of three yolk-sac alevins were collected from each tank at 4 dph. Tissues were flash-frozen in liquid nitrogen and kept at -80^{o}C until further processing for transcriptomic analysis.

5.3.1.3. Fathead minnow

FHM exposure experiments were conducted as previously described (Alcaraz *et al*., 2021b). Briefly, 20 embryos (between late cleavage and high blastula stage) from an in-house breeding colony (original source: Aquatic Research Organisms Inc., Hampton, USA) were placed each into 3-5 replicate petri dishes per treatment group with exposure solutions. All Petri dishes were maintained under static renewal conditions (> 50% v/v renewal per day), a 16:8 light:dark cycle, and at a temperature of 24 ± 1^{o}C. At 4 dph, all larvae within a replicate petri dish were pooled, flash-frozen in liquid nitrogen, and kept at -80^{o}C until further processing for transcriptomic analysis.

5.3.2. Chemical analyses

Concentrations reported here represent means of measured FLX and EE2 from water samples collected throughout longer exposure durations (from fertilization/hatch to early fry stages) the studies described here were a part of, with exception of the sturgeon FLX experiment. Due to potential risks of pathogenic contamination from wild-caught sources, WS experiments had to be conducted in a quarantine facility with limited space, which resulted in not being able to collect sufficient water samples for FLX analyses. Hence, measured concentrations for FLX from RBT was used for WS since these experiments shared stock solutions. Because the analysis of EE2 required much lower volumes of water, we were able to confirm EE2 exposure concentrations during the WS experiment.

Analyses of EE2 in water samples were previously described in Alcaraz *et al*. (2021b) for FHM and in Alcaraz *et al*. (2021a) for RBT and WS. Water samples were extracted by solid-phase extraction prior to analysis. For FHM, EE2 was quantified by spiking extracted samples with

deuterated EE2 and measuring the concentrations using high performance liquid chromatography-tandem mass spectrometry (LC-MS; Waters, MA, USA). For RBT and WS, concentrations of EE2 were measured using EE2-specific competitive enzyme-linked immunosorbent assay (ELISA; Ecologiena®, Fukuoka, Japan).

The analysis of FLX in the FHM study was previously described (Alcaraz *et al*., submitted). For RBT and WS, concentrations of FLX were measured through quantification by isotope dilution. Briefly, sample aliquots were spiked with fluoxetine-d5 (d_5-FLX; CDN Isotopes, QB, Canada). FLX in samples was then quantified using a Vanquish UHPLC, coupled to a Q-Exactive™ HF Quadrupole-Orbitrap™ mass spectrometer (Thermo Fisher Scientific, MA, USA).

5.3.3. Sample preparation, sequencing, and data pre-processing

Total RNA was extracted from each replicate using RNeasy Plus Universal Mini Kit (Qiagen, Germany). Samples with an RNA integrity number (RIN) ≥ 8 were used for RNA sequencing. Library preparation and sequencing for FHM and RBT were previously described in Alcaraz *et al*. (2021b) and in Alcaraz *et al*. (2021a), respectively, and were done at Génome Québec Centre d'Expertise et de Services (Genome Quebec, QB, Canada). For WS, libraries were prepared in-house using NEBNext Ultra Directional kit with poly(A) magnetic isolation module (New England Biolabs Ltd, ON, Canada). Total RNA was poly(A)-enriched prior to the synthesis of double-stranded DNA. Size fragments of dsDNA libraries were assessed using the high-sensitivity DNA analysis kit in the 2100 Bioanalyzer instrument (Agilent Technologies, Waldbronn, Germany) and were quantified in a Qubit 4 fluorometer (Thermo Fisher Scientific). High quality dsDNA libraries were sequenced in-house using a 150-cycles (75 x 2) paired-end sequencing cartridge in a NextSeq 500 instrument (Illumina Inc, San Diego CA, USA).

Reads were assessed using FastQC (Andrews, n.d.) and trimmed in pairs to a minimum Phred score of 20 and a minimum length of 35 bases per paired read using Trimmomatic (Bolger *et al*., 2014). Cleaned reads were aligned to their respective transcriptome assembly (WS: NCBI GEO Acc# GSE79624; RBT: GCA_002163495.1; FHM: GCA_016745375.1) to estimate the abundance of transcripts using Kallisto (Bray *et al*., 2016). Reads that have not been previously reported were submitted to the NCBI GEO repository with accession number XXXXXX. Other raw files were accessed using the GEO accession numbers GSE156916, GSE171788, and GSE179232.

5.3.4. Transcriptomic benchmark concentration analyses

Transcriptomic points-of-departure (tPODs) are concentrations corresponding to whole transcriptome effect level based on pre-set benchmark response (BMR) that is considered adverse or significant. The most protective and stable tPODs are those focused on active genes – molecular features (gene or transcript) that fit into statistical models and have valid benchmark concentration (BMC) values as per the National Toxicology Program (NTP) Approach to Genomic Dose-Response Modeling recommendations (i.e., BMCs not exceeding the highest tested concentration, acceptable confidence intervals, etc.)(National Toxicology Program, 2018). These tPOD estimates include (1) the median of the 20 most sensitive geneBMCs ($omicBMC_{20}$), the tenth percentile of all geneBMCs ($omicBMC_{10th}$), and the mode of the first peak of all gene BMCs ($omicBMC_{mode}$) (Pagé-Larivière *et al*., 2019).

Transcriptomic BMC analyses were conducted separately on each study using FastBMD (Ewald *et al*., 2020). FastBMD follows the recommended methods by the NTP. Modules for FHM and RBT were used for datasets in the respective species. Transcript counts were collapsed to

genes prior to downstream analyses. Since no WS module is available in FastBMD, annotation-free mode was used in the BMC analysis. Count estimates were normalized using the relative log expression (RLE) normalization (Anders and Huber, 2010). Normalized datasets were filtered to remove 5% and 10% of the features with lowest variance and abundance across treatment groups, respectively. Features that were unlikely to exhibit concentration-response behaviour were removed by calculating differential gene expression relative to the control group using *limma* (Ritchie *et al*., 2015), with a threshold cut-off false discovery rate (FDR) ≤ 0.05. The remaining features were fitted using statistical models (Exp2, Exp3, Exp4, Exp5, Linear, 2^o Polynomial (Poly2), Hill, and Power), with a threshold lack-of-fit p-value > 0.1 and a BMR factor = 1. Curve fittings were conservative such that higher order polynomials (Poly3 and Poly4) were not used due to the tendency of these models to overfit datasets, given the small number of datapoints. Control expression was set to the mean of control samples. Gene/transcript-level BMC (geneBMC) values from the model with the lowest Akaike information criterion (AIC) were selected for use in the estimation of transcriptome-level (omicBMC) tPOD. Pathway-level (pathBMC) tPODs were also calculated for RBT and FHM and defined as the most sensitive pathway (lowest pathBMC) based on bootstrapped median of constitutive geneBMCs of that specific pathway, with at least 3 geneBMCs in the pathway. PathBMCs were not calculated for WS as there is currently no established genome/transcriptome, and therefore, gene set annotation for this species.

5.4. Results and Discussion

5.4.1. Survival rates at 4 dph, physico-chemical characteristics of exposure solutions, and chemical analyses

No significant mortalities were observed at 4 dph across all studies, which was expected as EE2 and FLX are not known to cause acute toxicity at the tested concentrations, with previously reported LC50s in the mg/L and high ug/L ranges, respectively (Alcaraz *et al*., 2021a; Henry and Black, 2008; Versonnen *et al*., 2003). All physico-chemical characteristics of exposure solutions were within the recommended parameters of OECD 210 (OECD, 2013), with a few minor deviations (± 2 ^{o}C) from exact temperature recommendations**,** although these were not expected to affect the results as the test species are known to thrive in habitats with considerable temperature ranges. Measured concentrations were 36 – 117% of nominal for EE2 and 20 – 96% for FLX (**Table E.S2**).

5.4.2. tPODs of EE2 across species

Features with BMCs after early-life exposure to EE2 represented 75, 84, and 53% of all features with fitted models for WS, RBT, and FHM, respectively (**Table 5.2**). These relatively low ratios may have been due to the wide confidence intervals of some geneBMC estimates, estimates greater than the highest dose, and expression values that did not exceed the BMR (National Toxicology Program, 2018). Indeed, FHM had over 600 features with geneBMCs higher than the highest tested concentration, which were excluded in downstream analyses, and which were likely to have moved the second mode further to the right of the *x*-axis if higher concentrations were tested, suggesting lesser transcriptional sensitivity of FHM to EE2, overall. Nonetheless, the bimodal distribution patterns of geneBMCs for EE2 across the three species were comparable,

with two peaks each. A notable similarity between the distribution patterns of RBT and WS can be observed (**Figure 5.1**), characterized by a high first peak at low concentrations and a relatively flatter second peak. The similarity across response patterns may be rooted in the largely conserved immunological and endocrine functions in ray-finned fish (Bury, 2017), which are the primary targets of EE2. Downstream biochemical and physiological bimodal responses have also been observed by other authors in response to exposure of fishes to xenoestrogens (Anderson *et al*., 2020; Pawlowski *et al*., 2004), which could have been driven by a variety of molecular perturbations occurring across concentrations. RBT geneBMCs formed a narrow peak at very low concentrations, with an $omicBMC_{mode}$ of 4.38 ng/L, compared to 16.51 and 24.93 ng/L for WS and FHM, respectively, both of which have relatively broader and lower first peaks, suggesting a relatively simultaneous transcriptional perturbations in a smaller window of concentrations. A second and wider mode above 80 ng/L can be observed for FHM, suggesting that most of the active genes deviated from the control treatment responses at higher concentrations compared to RBT and a lesser extent to WS. The second mode is interpreted as the secondary onset of cellular processes, which represents general stress response and disruption of molecular machinery. Nevertheless, the values for $omicBMC_{mode}$ derived across the three species in this study were within the same range of some less sensitive apical BMCs for EE2 reported previously; for instance, GSI, condition factor, the number of batches of eggs, and fertilization rates in FHM significantly decreased when exposed to 10-100 ng/L EE2 (Pawlowski *et al*., 2004). Similarly, reduction in testis mass, number of eggs attaining the eyed stage of embryonic development, and plasma 11-ketotestosterone were observed in RBT exposed to 10-100 ng/L EE2 (Schultz *et al*., 2003).

OmicBMC$_{10th}$ were 7.98, 1.44, and 27.82 ng/L for WS, RBT, and FHM, respectively, all of which were within the tested concentrations for all species. On the other hand, omicBMC$_{20}$ were 0.06, 0.12, and 2.39 ng/L for WS, RBT and FHM, respectively, which were the most sensitive tPOD estimate in all species. Only the estimate for FHM fell within the tested concentrations, although estimates for RBT and WS were still within 10% of the lowest tested concentrations. Pathway-level BMC for RBT was 1.68 ng/L with 5 genes contributing to fatty acid biosynthesis pathway, while carbon metabolism pathway had the greatest number of genes, with 46, and a pathBMC of 4.64. PathBMC for FHM was 45.61 ng/L for olfactory transduction, with 3 active genes, while neuroactive ligand interaction pathway had the greatest number of active genes of 17. Most, if not all geneBMCs contributing to the most sensitive pathBMC of RBT were within the first mode, while that of the FHM were in the second mode, suggesting a more relevant first mode for RBT but second mode for FHM, in terms of estimating pathBMC.

There have been no studies that directly compared the apical effects of EE2 among WS, RBT, and FHM. A previous report showed that a distant relative of WS, the Siberian sturgeon, appeared to be more sensitive *in vivo* against the phytoestrogen genistein in terms of hepatocyte Vitellogenin (Vtg) protein abundance, relative to RBT (Latonnelle *et al*., 2002). Vtg is the classic biomarker for the exposure of fish to estrogens, such as EE2 (Jones *et al*., 2000). Similarly, there have been no direct comparisons of the apical effects of EE2 between FHM and RBT, but previous reports suggest a relatively greater sensitivity of FHM compared to RBT based on a range of apical outcomes such as plasma Vtg and other reproductive parameters (Caldwell *et al*., 2012), although endpoints and experimental parameters were not necessarily identical, and therefore, should be interpreted with caution. In the literature, the consensus apical EE2 lowest observed effect concentration (LOEC) was between sub- to low- ng/L concentrations, such as those that caused

disruption of egg production and quality in FHM (Jobling *et al*., 2004; Parrott and Blunt, 2005; Runnalls *et al*., 2015), and a predicted no-effect concentration (PNEC) of 0.10 and 0.35 ng/L, respectively (Caldwell *et al*., 2012, 2008). The estimate for omicBMC_{20} for RBT and WS closely approximated the PNEC and were well protective of the apical thresholds that caused adverse effects. In contrast, the omicBMC_{20} for FHM differed by approximately one order of magnitude.

Table 5.2. Summary of tPODs across species. Datasets were fitted using the models Exp2, Exp3, Exp4, Exp5, Linear, Poly2, Hill, and Power, with a threshold lack-of-fit p-value > 0.1 and a benchmark-response (BMR) factor = 1.

	FLX (µg/L)			EE2 (ng/L)		
	WS	**RBT**	**FHM**	**WS**	**RBT**	**FHM**
Features with fitted model	1715	1378	2300	2957	2326	1367
Features with BMC	1222	1110	2154	2219	1957	724
omicBMC$_{20}$	0.02	0.02	0.56	0.06	0.12	2.39
omicBMC$_{10th}$	0.64	0.32	5.0	7.98	1.44	27.82
omicBMC$_{mode}$	2.08	5.01	7.43	16.51	4.38	24.93
pathBMC	-	0.19	5.66	-	1.68	45.61

omicBMC$_{20}$ = median of the 20 most sensitive geneBMCs

omicBMC$_{10th}$ = tenth percentile of all geneBMCs

omicBMC$_{mode}$ = mode of the first peak of all gene BMCs

pathBMC = most sensitive pathway BMC, with at least 3 geneBMCs, based on bootstrapped median of constitutive geneBMCs of that specific pathway

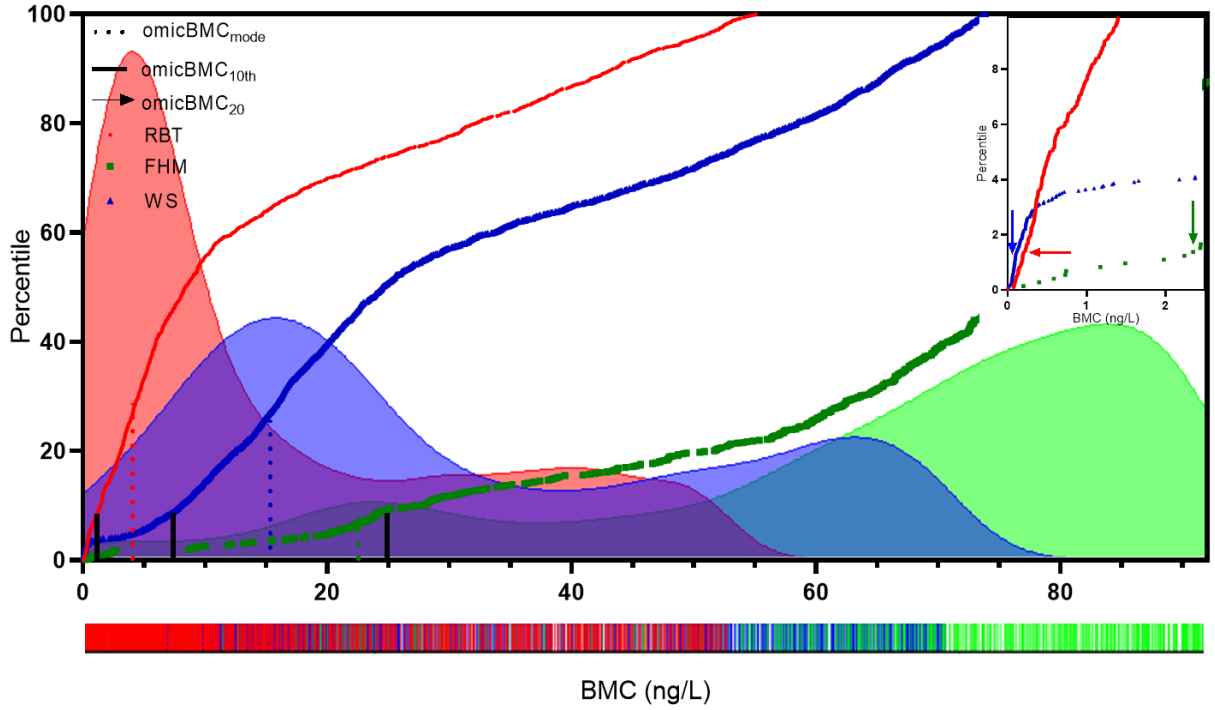

Figure 5.1. Transcriptome-wide points-of-departure derived from embryonic exposures to EE2 across three freshwater fish species. Distribution patterns of geneBMCs were depicted with the density plots; broken lines showing the mode of the first peak of all geneBMCs within a species (omicBMC$_{mode}$); solid black lines show the 10th percentile of all geneBMCs (omicBMC$_{10th}$); straight line showing the 10th percentile. ◯ RBT; □ FHM; Δ WS. *X*-axis – EE2 benchmark response (BMC; in ng/L); *Y*-axis – cumulative percentile of geneBMCs. Rug – individual geneBMCs. Inset: Scaled figure highlighting (arrows) omicBMC$_{20}$. RBT – rainbow trout; FHM – fathead minnow; WS – white sturgeon; omicBMC$_{10th}$ – the 10th percentile of all geneBMCs; omicBMC$_{20}$ – median of the 20 most sensitive geneBMCs; omicBMC$_{mode}$ – mode of the first peak of all geneBMCs. Note: Density plots were used to assess distribution patterns/modes and were not scaled to the *Y*-axis.

5.4.3. tPODs of FLX across species

Features with BMCs represented 71, 81, and 94% of features with fitted models for WS, RBT, and FHM, respectively (**Table 5.2**). Distribution patterns showed WS geneBMCs with a prominent single peak at very low concentrations, FHM with two well defined peaks, and RBT with two low peaks at the lower and upper end of the tested concentrations with geneBMCs well distributed across the tested concentration range (**Figure 5.2A**). The bimodal tPOD response patterns observed in the two teleosts may be one of the causes of a wide range of measured biological potencies of FLX that have been reported in the literature (Bidel *et al*., 2016; Cunha *et al*., 2018; de Farias *et al*., 2019). On the other hand, there have been no reports on the apical responses of WS to FLX; hence, there were no information to validate or explain the single peak/mode of geneBMC distribution observed. Perhaps the difference in response patterns between the teleosts and the sturgeon may be one of the evolutionary implications that could be attributed to the teleost-specific whole genome duplication events, which occurred after the phylogenetic divergence of the Acipenseriformes lineage from the actinopterygian stem (Glasauer and Neuhauss, 2014). However, it is yet to be investigated how the conservation of molecular targets of FLX in ray-finned fishes were affected by these evolutionary events, although serotonergic mechanisms and FLX metabolism were reported to be relatively conserved across vertebrates (Beulig and Fowler, 2008; Margiotta-Casaluci et al., 2014b). A dose-dependent rapid development and hyperactive behaviour were qualitatively observed in WS relative to controls, although this observation must be validated with an experiment specifically designed to evaluate this endpoint. In contrast, accelerated development (degree days to swim up; **Figure E.S1**), concentration-dependent mortalities (**Figure E.S2**), and concentration-dependent hyperactivity (qualitatively observed; data not shown) were observed in RBT at later life stages. These

observations were not apparent at all in FHM even at 28 dph. These observations may suggest greater potency of FLX in WS, which may be due to coincident perturbations in multiple genes and pathways at low concentrations as it appeared in the geneBMC distribution, although these observations have to be further validated. $OmicBMC_{mode}$ were 2.08, 5.01, and 7.43 µg/L for WS, RBT, and FHM, respectively. These tight estimates across species were within the range of concentrations reported to cause adverse apical effects in FHM (Weinberger and Klaper, 2014), although extremely high and extremely low concentrations (sub-µg/L to mg/L) of FLX have also been reported to cause changes in behaviour and locomotor response in other fish (Kohlert *et al*., 2012; Martin *et al*., 2019). $OmicBMC_{10th}$ were 0.64, 0.32, and 5.0 µg/L for WS, RBT, and FHM, respectively (**Figure 5.2B**), and were within the tested concentrations. $OmicBMC_{20}$ were 0.02, 0.02, and 0.56 µg/L for WS, RBT, and FHM, respectively (**Figure 5.2C & 5.2D**), and although only the estimate for FHM was within the tested concentrations, both estimates for WS and RBT were within 10% of the lowest tested concentrations. These sub- to low-µg/L $omicBMC_{10th}$ and $omicBMC_{20}$ tPOD estimates for FLX were protective of some of the most sensitive responses observed in the literature such as that of multigenerational hypocortisolism and behavioral disruption in zebrafish exposed to 0.54 µg/L FLX (Vera-Chang *et al*., 2018).

The pathBMC of the most sensitive pathway for RBT was 0.19 µg/L for hippo signaling pathway with 3 constitutive geneBMCs while the pathway with the greatest number (28) of constitutive geneBMC was lysosome pathway with pathBMC of 89.9 ug/L. For FHM, the pathBMC of 5.66 ug/L for vasopressin-regulated water reabsorption was the most sensitive pathBMC with 9 geneBMCs and PI3K-Akt signaling pathway had the greatest number of constitutive geneBMCs (43) with pathBMC of 8.98 µg/L. These pathways are generally involved in the regulation of cellular homeostasis, cell proliferation, and homeostasis, but a deeper dive into

specific functions would be necessary to elucidate the specific MOA of the compounds tested. No pathBMD could be calculated for WS for the reasons specified above.

There have been no studies directly comparing the apical responses of the three tested species towards FLX. Observed apical responses such as histological, behavioral, and physiological responses in fish occurred at a wide range of concentrations, ranging from sub-µg/L to mg/L (Brooks, 2014; Stanley *et al*., 2007). All estimated tPODs in this study were within the lower spectrum of concentrations that have been reported to result to these apical responses, with omicBMD$_{20}$ from WS and RBT being the most protective and within the same range of the most sensitive apical endpoints.

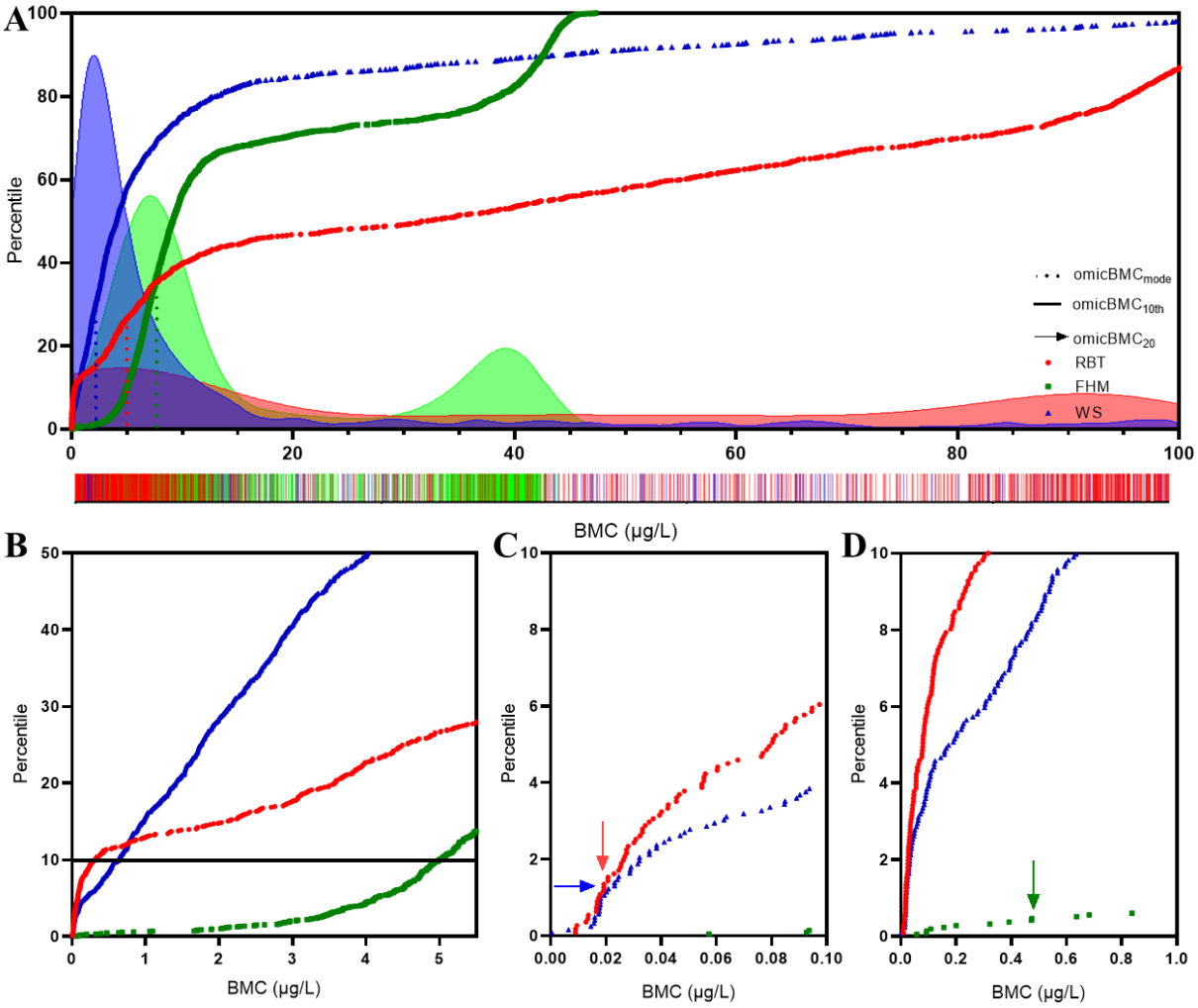

Figure 5.2. Transcriptome-wide points-of-departure after embryonic exposures to FLX across three fish species. (**A**) Distribution patterns of geneBMCs with density plots showing the mode of the first peak of all geneBMCs within a species (omicBMC$_{mode}$); Rug – individual geneBMCs. (**B**) the 10th percentile of all geneBMCs (omicBMC$_{10th}$); straight line showing the 10th percentile. (**C**) and (**D**) median of the 20 most sensitive geneBMCs (omicBMC$_{20}$). ◯ RBT; □ FHM; Δ WS. RBT – rainbow trout; FHM – fathead minnow; WS – white sturgeon. *X*-axis – FLX benchmark concentration (in µg/L). *Y*-axis – cumulative percentile of geneBMCs. *X*- and *Y*-axes were scaled

to highlight tPODs. Note: Density plots were used to assess distribution patterns/modes and were not scaled to the *Y*-axis

5.4.4. Insights from EE2 and FLX tPODs in embryonic fish

This study demonstrated that whole embryo-alevin/larval tPOD estimates were comparable to empirically derived apical PODs in the literature, with omicBMC$_{20}$ and omicBMC$_{10th}$ exhibiting sensitive and reasonable estimates that were protective of even some of the most sensitive apical PODs reported in the literature (de Farias *et al*., 2020; Parrott and Blunt, 2005). The omicBMC$_{mode}$ were relatively less sensitive. As this estimate reflects changes in specific molecular targets (Judson *et al*., 2016), the modes of the geneBMC distribution can potentially be used as a guide to elucidate the modes-of-action of the compound given that it is formed by a collective set of genes with expression values departing from the control-level expression (Chauhan *et al*., 2016). However, the elucidation of specific mechanisms of toxic action of chemicals based on geneBMC distribution modes was beyond the scope of this study but is an important theme in future research.

Generally, RBT embryos were the most sensitive in terms of all tPOD estimates and that derived tPODs were protective across species both for FLX and EE2, whereas FHM appeared to be the least sensitive despite the longer exposure duration of FHM (from ~6 hrs post-fertilization (hpf) to 4 dph; approximately 7 days total). The tPOD estimates of WS and RBT were more comparable to each other than those obtained for FHM. Furthermore, BMC distribution patterns, specifically for EE2, were more similar between RBT and WS than between either of these species and FHM. This observation is interesting because cyprinids are phylogenetically closer to salmonids than sturgeons, and therefore, the responses were expected to be more similar between the two teleost species. One explanation for these differences may be the length of exposure and developmental times. FHM were exposed earlier and for a longer time than the other two fishes (from 6hpf); hence, compensatory and downstream physiological responses may have taken place and manifested feedback responses to the toxic insults; the shorter exposure time for WS and RBT

(from hatch to 4 dph) may not have been sufficient time for these compensatory feedbacks to manifest yet. A time-course study on transcriptional responses may help elucidate this hypothesis. Typically, cyprinids such as FHM and zebrafish are the choices for many ecotoxicological studies due their relatively ease of husbandry, small size, and short breeding cycle, among others (Ankley and Villeneuve, 2006; Dai *et al*., 2014). However, salmonids, including RBT, have been reported to be among the most sensitive commonly tested freshwater fish, while cyprinids appeared to be the least sensitive, and which was demonstrated in a study that evaluated a suite of 190 chemicals (Teather and Parrott, 2006). In contrast, apical PODs for WS were not available for comparison due to limitations in its use in toxicological studies because of the conservation status of several of its populations in North America, as well as its long life-cycle. It should be noted that the WS dataset may not necessarily be directly comparable to those of the two teleosts at it was analyzed at the transcript level using a *de novo* assembled transcriptome, while RBT and FHM were summarized into gene-level responses. This means that there are possible redundancies in the reference transcriptome of WS that could result in a shift of the distribution peak when summarized into gene levels. However, this may not be ascertained unless a fully assembled genome or transcriptome is available for WS. Nevertheless, estimated tPODs from WS were within the range of those of the two teleost species assessed in this study, and therefore, we argue that tPODs from teleosts, specifically from RBT, could be protective towards adverse apical effects to WS. Of course, additional studies with a wider range of diverse chemical contaminants are needed to confirm this hypothesis.

A fundamental limitation of estimated protective tPODs in this study, specifically $omicBMC_{20}$ and $omicBMC_{10th}$, was the lack of definitive biological interpretation typically inferred from the identity of the active genes and gene sets. PathBMC is typically the choice for

tPOD estimation as it can be anchored to biological inference from gene set information, and therefore, aid in informing possible mechanisms of action and characterization of plausible links to the etiology of biological responses (Dean *et al*., 2017; Farmahin *et al*., 2017; National Toxicology Program, 2018); however, this strategy is highly influenced by the annotation of the genome or transcriptome of the species under study, which is a significant limitation in nonstandard organisms. It is notable that pathway-based tPODs (pathBMC) were not the most protective estimates in this study, which has also been observed previously (Pagé-Larivière *et al*., 2019). In fact, only ~35-45% of the active genes of the three tested species were annotated with KEGG orthologs, and therefore, limited the downstream gene set enrichment analyses. Annotations are typically biased towards more studied biomolecular processes that are relevant especially for human health, and thus, may not be a robust representation of environmentally relevant concerns. Until functional databases improve and develop focused annotations for non-human/non-mammalian species, it remains difficult to reliably conduct such analyses. Currently, the implications of the results would be limited to those associated with human functions, unless the mechanisms are conserved across vertebrates.

Another limitation may be the use of embryo-larval/alevin stage that could affect the identification of gene targets specific to certain tissues or organs as these may get diluted in the analyses of whole embryo transcriptomes, which adds to the difficulty of MOA characterization. Also, artifacts of molecular processes related to an organism's active development at this life stage might interfere in the mechanistic characterization of the MOA of a chemical at later life stages. On the other hand, effects on developmental processes may represent unique and highly sensitive endpoints indicative of apical effects at this often most sensitive life stage. Nevertheless, it should be noted that the primary purpose of deriving tPODs is to quickly and cost-effectively identify the

concentration or dose that would closely approximate toxicity thresholds and that mechanistic hazard identification is secondary; thus, direct mechanistic linkage to adverse effects is not critical at this point. Still, it is acknowledged that mechanistic linkage of molecular perturbations to adverse outcomes will be necessary for regulatory acceptance in chemical hazard assessment.

This study clearly demonstrated the potential for embryonic stage-derived tPODs to aid in chemical hazard assessment; however, much work is needed for the regulatory acceptance of this strategy in deriving toxicity thresholds. In particular, there is a need to establish a more robust non-mammalian databases for the interpretation and linkage of molecular perturbations with biological functions and processes. In particular, more extensive genome assemblies and curation of annotations of species of interest are needed, as well as improvement of databases such as KEGG to include molecular interactions and processes for species other than humans to reflect biological processes that are unique to oviparous (e.g. reproduction) or aquatic vertebrates. Specific studies addressing reproducibility of results are also crucial, such as the number of reasonable replications, exposure windows and timing, sequencing depth, the number and range of concentrations to test, and curve fitting strategies, among others. Recommendations from the NTP genomic dose-response modelling may serve as a guide in establishing guidelines in the standardization of procedures in deriving tPODs from embryonic fish studies. Lastly, studies utilizing other fish species and compounds acting on diverse mechanisms should be conducted to validate the effectivity of this strategy in deriving robust tPODs that are protective of apical PODs across species.

5.5. List of Supporting Information (Appendix E)

Tables ES1-ES2 and Figures ES1-ES2.

The list of files below can be found as Supporting Information in the submission to *Environmental Science and Technology*

DataSet S1. Raw Counts (abundances) for WS, RBT, and FHM after alignment to their respective reference transcriptomes

Tab A. RBT_EE2. Raw counts of RBT exposed to EE2

Tab B. FHM_EE2. Raw counts of FHM exposed to EE2

Tab C. WS_EE2. Raw counts of WS exposed to EE2

Tab D. RBT_FLX. Raw counts of RBT exposed to FLX

Tab E. FHM_FLX. Raw counts of FHM exposed to FLX

Tab F. WS_FLX. Raw counts of WS exposed to FLX

DataSet S2. Calculated geneBMC for WS, RBT, and FHM

Tab A. RBT_EE2. Detailed geneBMC parameters and values for RBT exposed to EE2

Tab B. FHM_EE2. Detailed geneBMC parameters and values for FHM exposed to EE2

Tab C. WS_EE2. Detailed geneBMC parameters and values for WS exposed to EE2

Tab D. RBT_FLX. Detailed geneBMC parameters and values for RBT exposed to FLX

Tab E. FHM_FLX. Detailed geneBMC parameters and values for FHM exposed to FLX

Tab F. WS_FLX. Detailed geneBMC parameters and values for WS exposed to FLX

DataSet S3. Calculated pathBMC for RBT and FHM

Tab A. RBT_EE2. pathBMC for RBT exposed to EE2

Tab B. FHM_EE2. pathBMC for FHM exposed to EE2

Tab C. RBT_FLX. pathBMC for RBT exposed to FLX

5.6. Acknowledgments

The authors acknowledge the support of the EcoToxChip project. We thank Fisheries and Oceans Canada, Genome Canada, Genome Quebec, Genome Prairies, the Government of Canada, ECCC, Ministere de l'Economie, de la Science et de l'Innovation du Quebec, the University of Saskatchewan, and McGill University, as well as the project partners (US Environmental Protection Agency, US Army Corps of Engineers, Qiagen, SGS AXYS, and Shell USA) for their financial and other support. MH was supported by the CRC Program of NSERC. AJA and KS were supported through the University of Saskatchewan Dean's Scholarship. AJA, KS, PJA, and TL were supported through the Toxicology Devolved Scholarship. JKC was supported through a Banting Postdoctoral Scholarship of NSERC. The authors acknowledge D. Schneider, C. Burbridge, and J. Ewald for their valuable advise and the discussions on data analyses. The authors are also grateful to the Nechako White Sturgeon Recovery Initiative Facility in Vanderhoof, BC that donated white sturgeon embryos to this study.

CHAPTER 6: GENERAL DISCUSSION

6.1. Introduction

The increasing number of chemicals that require toxicity testing, which is hampered by high costs, low throughput, and significant ethical concerns, prompted a growing interest in the development of new approach methodologies (NAMs) that can replace, reduce, and refine (3R) the use of live animals (Kavlock *et al*., 2018; Krewski *et al*., 2020). While *in vitro* and computational methods hold promise as alternatives to live animal tests, many of these models are limited with regards to quantitatively predicting adverse outcomes and their corresponding toxicity thresholds as these models do not represent the entirety of an organism. Recent developments suggest that early-life stages (ELS) of fish are sensitive surrogates of adult fish (Wheeler *et al*., 2014) while not being considered as live animals in many jurisdictions (Canadian Council on Animal Care, 2005; European Union, 2010; UK, 1993). Similarly, advancements in omics technologies now allow the interrogation of full suites of molecular families without *a priori* knowledge of the modes of action (MOA) of a compound, and can provide a snapshot of molecular perturbations before long-term apical effects are observed (Garcia-Reyero and Perkins, 2011; Schirmer *et al*., 2010; Zhang *et al*., 2018). Together, (molecular) mechanistic information in ELS assays present a compelling strategy for the development of NAMs that may aid in regulatory decision-making as they are more likely to gain regulatory acceptance than tissue-/cell-based *in vitro* assay and *in silico* models (Basu *et al*., 2019). Thus, this dissertation aimed to develop short-term ELS assays for evolutionary diverse species of fish for the derivation of transcriptomic points-of-departure (tPODs), particularly for chemical testing prioritization, in support of environmental risk assessment (ERA). Specifically, fathead minnow (FHM), rainbow trout (RBT), and white sturgeon (WS) were exposed at the embryonic stage to graded concentrations of two contaminants of concern (CECs), 17α-ethinylestradiol (EE2) and fluoxetine (FLX). Whole body tissues were

collected for transcriptomic and proteomic analyses at 4-days post-hatch (dph). The remaining larvae/alevins were continuously exposed to CECs until 28 dph (FHM) and 60 dph (RBT) for histological investigations, biometric measurements, and survival analysis. Construction of toxicity pathway models was attempted to link molecular pathways with downstream effects and apical outcomes. Transcriptomic points-of-departure (tPODs) were calculated and compared to concentrations that caused apical chronic effects in studies conducted here and in the literature. Lastly, tPODs of EE2 and FLX were compared across species.

6.2. Toxicity pathway models at early-life stages of fish

It is commonly accepted that establishing a toxicity pathway model is a tedious and comprehensive process and requires a suite of studies including those that interrogate molecular, physiological, histological and apical responses (Andersen *et al*., 2015). Perhaps the most compelling result in this dissertation with regards to deriving mechanistic toxicity pathways using fish ELS are those from Chapter 2, which demonstrated that molecular analyses of EE2-exposed embryo-larval FHM at 4 dph revealed core responses that are indicative of apical outcomes (Alcaraz *et al*., 2021b). Genes coding for specific biomarkers associated with EE2 were highly dysregulated in a concentration-dependent manner, such as *vitellogenin* (*vtg*), *aromatase* (*cyp19a1b*), and *estrogen receptor 1* (*esr1*) with their corresponding protein products showing similar dysregulation patterns. Likewise, overrepresented gene sets from both omic levels showed significant perturbations along the estrogen signalling pathway. Histological observations, as well as length and weight analyses, showed responses that were in accordance with these molecular responses. Similarly, Chapter 3 demonstrated that apical responses at 60 dph in EE2-exposed RBT were linked to transcriptomic responses at 4 dph (Alcaraz *et al*., 2021a). However, in certain cases

the assembly of toxicity pathway models may require examination of specific molecular signals from target organs and tissues (e.g. selective serotonin reuptake inhibitors (SSRIs) specifically affect particular regions of the brain; low molecular weight hydrocarbons (LMWHCs) affect cardiovascular functions), among others. This may be one of the main limitations of whole-body omics analyses with ELS as certain tissue-specific signals may be diluted and lost, and it may be challenging to attribute certain signals to specific tissues/cells where the greatest toxicological insults occurred. For instance, Chapter 4 revealed that most of the common FLX-target genes and/or proteins were not significantly dysregulated in 4 dph FHM, which could be an artifact of signal dilution in whole body tissue analyses given that these features are known to be specifically expressed in certain regions of the central nervous system (CNS). Even so, functional analyses integrating whole-body transcriptomics and proteomics with downstream results and information from the literature may provide additional evidence that can be used to build informed putative toxicity pathway models. In Chapter 3, proteomic profiles at 4 dph provided limited mechanistic evidence with regards to the classic estrogenic endpoints such as overproduction of Vtg protein, which could have been due to several factors, including the presence of prominent yolk sac biasing assessment, among others. Nevertheless, histological observations and previous studies (Alcaraz *et al*., 2021a; Tompsett *et al*., 2012) presented overwhelming evidence of the presence of this protein in fish and frogs exposed to EE2. In Chapter 4, FLX-induced transcriptomic and proteomic perturbations at 4 dph in FHM were complementary, providing more comprehensive and informative insights into the mechanism of toxicity of this chemical than when analyzed independently, and offered information that can be linked to apical outcomes. Overall, while the putative models developed here were not complete, they provided support and weight-of-evidence regarding the link between molecular signals and apical outcomes.

In general, concordances of transcript-protein pairs were weak in all the studies conducted as part of this thesis (Chapters 2-4), observations that were not unexpected as similar observations were made in many other studies. It was hypothesized that these inconsistencies are primarily due to the many post-translational factors influencing the synthesis of the resulting protein products (Liu *et al*., 2016; Maier *et al*., 2009; Vogel and Marcotte, 2012; Wu *et al*., 2013). In fish, very limited concordance between transcriptomic and proteomic responses was previously observed in EE2-exposed zebrafish (De Wit *et al*., 2010), which was in accordance with the limited concordance observed in FHM and RBT in this thesis (Alcaraz *et al*., 2021b, 2021a; Chapters 2-4). For instance, in Chapter 2, 22 features were significantly dysregulated in both the transcriptome and proteome level of EE2-exposed FHM, including multiple variants of the estrogenicity biomarker *vtg*, but the overall concordance of transcript abundance ratios and protein abundance ratios was very weak (Pearson's $\rho = 0.130$). Regardless, important signalling pathways were typically present at both omic levels. In Chapters 2 and 4, combined network analyses of differentially expressed transcripts and differentially abundant proteins were complementary with regards to the characterization of overrepresented terms and pathways that could have been missed if analyzed separately, suggesting that there were interactions and feedback loops among these features at different molecular levels. This observation highlights the value of comparing and integrating multiple molecular features from different omics streams in identifying relevant molecular processes associated with an external stimulus.

Notable inconsistencies were observed in the proteomic profiles across the conducted experiments, and how these profiles could inform the toxicity pathway models developed. In Chapter 2, proteomics showed direct translation of several important transcripts to protein products when FHM was exposed to EE2. In contrast, exposure to FLX showed proteomics results that were

not the products of immediate translation from significantly dysregulated transcripts but were complementary to the transcriptomic profiles at a functional level (Chapter 4). In RBT, proteomic profiles had a less clear link with the transcriptomic profiles. In addition to the intrinsic properties of genomic translation noted above, several extrinsic factors may have also contributed to these inconsistent observations:

(1) *Co-incident sampling for transcriptomics and proteomics.* Much remains to be resolved regarding the dynamics (how much and how quickly) of gene product formation and the interactions of biomolecules at different biological levels, which drives their abundances and activities (Liu *et al*., 2016; Maier *et al*., 2009). mRNA molecules can be simultaneously transcribed and translated, and post-transcriptional regulation plays an important role in the control of the abundances of gene products. Despite increased transcriptional activities of CEC-responsive genes, the level of synthesized gene products may not necessarily be observed at the proteome level at the same instant as at the transcriptome level. In Chapter 3, multiple variants of *vtg* were significantly dysregulated at the transcriptomic level, but were not differentially abundant at the proteome level, both of which were processed from samples at 4 dph. However, histological observations at later life stages showed overwhelming evidence of the presence of this protein (Alcaraz *et al*., 2021a).

(2) *Localization of target proteins in certain regions of the organ/tissue.* Proteins exhibit spatial localization among tissues, which is tightly linked to protein functions (Digre and Lindskog, 2021). For instance, tissue-elevated expression of glial fibrillary acidic protein is observed in the brain, follicle stimulating hormone beta subunit in the endocrine tissues, insulin in the pancreas, and fatty acid binding protein 4 in the adipose and soft tissues (www.proteinatlas.org). Thus, the abundance of proteins in small tissues or in specific regions of an organ may become diluted

relative to the summation of the whole-body protein, rendering its presence below detectable levels. In Chapter 4, common FLX-target neuropeptides were not differentially abundant which could be because these peptides are typically found in specific regions of the CNS; thus, their abundance might have been significantly diluted by those of other proteins expressed throughout other tissues present in whole body samples.

(3) *Short exposure times limiting the synthesis of protein products and associated detectable abundance differences.* Estrogen-responsive proteins exhibited high spectral intensities in Chapters 2 and 3; however, detectable protein abundance differences were only observed in FHM exposed to EE2 for 7 days to EE2 (Chapter 2) and not in RBT exposed to EE2 for 4 days (Chapter 3), even though exposure concentrations were similar. The reason for this difference may be due to FHM having been exposed for 3 additional days, and hence may have had enough time to synthesize gene products in response to the toxic insult, as well as manifestation of feedback responses. In addition to exposure times, these observations may have been affected by differences in developmental time between the two species and (4).

(4) *Presence of significant concentrations of maternally transferred proteins in RBT that may have masked changes in protein abundance ratios.* At the time of sampling (4 dph) rainbow trout had still prominent yolk sacks compared to FHM that were approaching swim-up and independent feeding. As yolk consists predominantly of Vtg and closely related proteins, any potential differences in yolk protein production in these fish may have been diluted as corroborated by very high spectral intensities of yolk proteins in RBT in treated and untreated groups (Chapter 3).

Despite these shortcomings of the proteomics studies conducted as part of this dissertation, good concordance between downstream responses and transcriptomics was observed, which

supports the construction of a toxicity pathway model. For instance, histological observations in EE2-exposed FHM and RBT showed evidences of proteinaceous fluids in the liver, kidneys, and coelom (Alcaraz *et al*., 2021a, 2021b; Chapters 2 & 3), suggesting EE2-induced overproduction of estrogen-associated proteins such as Vtg and coagulation factors, among others (Tompsett *et al*., 2012; Weber *et al*., 2003; Wolf and Wheeler, 2018). Behavioral responses were altered in FLX-exposed FHM, which were corroborated by combined transcriptomics and proteomics overrepresentation analyses (Chapter 4) and by reports in the literature (Brooks, 2014; Mole and Brooks, 2019). Thus, downstream responses observed in the studies done here and those found in the literature tend to supplement/complement the linkage across biological levels. More importantly in the context of chemical hazard assessment, evidence of the transcriptomics-apical response linkages instilled confidence in the connection between changes in gene expression and apical outcomes, which paved the way for exploring derivation of tPODs discussed in the next section. tPODs are based on the hypothesis that genomic dose response studies (GDRS) provide a good approximation of the toxicological potencies of chemicals observed under apical chronic scenarios (Thomas *et al*., 2013a).

6.3. tPODs from ELS exposures

tPODs are concentrations corresponding to whole transcriptome effect levels based on pre-set benchmark responses (BMRs) that are considered adverse or significant (Ewald *et al*., 2020; National Toxicology Program, 2018; Pagé-Larivière *et al*., 2019). The National Toxicology Program (NTP) recommended the use of a pathway-level benchmark concentration (pathBMC) to estimate the tPOD as this approach is based on biologically interpretable sets of genes that may produce biological effects such that it may provide indication/evidence of the possible mechanism

of action (National Toxicology Program, 2018). However, derivation of pathBMCs is dependent on the level of annotation of the genome/transcriptome of the species of interest. This is problematic because many ecologically relevant species that are important for ERA lack fully assembled and/or have poorly annotated genomes. In recent years, studies have explored other statistical approaches to calculate tPODs (Chauhan *et al*., 2016; Farmahin *et al*., 2017; Thomas *et al*., 2013b; Webster *et al*., 2015), but statistical tPODs based on the distribution of gene-level benchmark concentrations (geneBMCs) seem to produce the most stable and protective estimates (Pagé-Larivière *et al*., 2019). These tPODs are based on the statistical estimates from benchmark concentrations (BMCs) of active features – genes or transcripts that have BMCs - which include (1) the median of BMCs of the 20 most sensitive active genes ($omicBMC_{20}$), (2) the value of the BMC of the tenth percentile of all active genes ($omicBMC_{10th}$), and (3) the mode of the first peak of all geneBMCs ($omicBMC_{mode}$).

A comprehensive and detailed discussion of cross-species tPODs comparison can be found in Chapter 5 of this dissertation. In brief, tPODs across species derived from 4 dph alevins/larvae were generally within the range of empirically derived apical PODs reported in this study and in the literature (**Table 6.1**). Overall, $omicBMC_{20}$s were the most sensitive and protective (lowest tPOD value) among all tPOD estimates across species for both EE2 and FLX (Chapter 5). The estimated $omicBMC_{20}$s for EE2 across species were at par with the consensus apical POD of 1 ng/L, while $omicBMC_{20}$s for FLX were within the more sensitive/protective range of concentrations relative to those reported in the literature (Alcaraz *et al*., 2021a; Chapters 2-5). While protective and sensitive, a major critique with $omicBMC_{20}$ is that they are purely based on statistical and not necessarily biological outcomes. It is acknowledged that the main purpose of the derivation of tPODs is to identify the concentration that would significantly perturb biology

and would potentially result in a phenotypic outcome (National Toxicology Program, 2018). However, the mechanisms associated with or the identification of specific phenotypic outcomes may be necessary as weight-of-evidence for regulatory acceptability in chemical hazard identification. While the omicBMC$_{20}$ estimates in this study may be limited to 2 CECs and 3 fish species, the high sensitivities and protectiveness of the derived values towards apical chronic PODs show significant promise and should be expanded to a broader range of chemical contaminants of concern and species of interest in future studies.

One possible strategy to characterize the link between omicBMC$_{20}$ and apical outcomes could be by manual curation of the annotations of the 20 most sensitive features and placing them into gene sets or pathways. Then, interaction networks these genes are involved in can be established and used to explain biological and molecular processes that may lead to (an) apical outcome(s). This strategy may be a more attractive approach than using pathBMC since operating with the 20 most sensitive features with high confidence through manual curation is less tedious and relatively more accurate than computationally inferred annotation of the whole genome/transcriptome without manual curation for the estimation of pathBMC. This strategy can also be extended, at a certain extent, to omicBMC$_{10th}$, although this is less practical due to possibly greater number of genes that need to be curated but at the same time, may yield more information. However, it should be noted that the approach that was developed in this dissertation used whole body ELS fish, which is limited with regards to characterizing key events and key event relationships in toxicity pathways. Specifically, the approach may not be able to discriminate tissue-/organ-specific responses or may lack sensitivity for some lowly expressed genes due to tissue dilution. Nevertheless, the concept of tPODs was developed as a tool for chemical

prioritization to inform more in-depth testing (National Toxicology Program, 2018). It is not yet a mature science that can independently characterize MOAs or set toxicological thresholds.

Overall, RBT appeared to be the most sensitive species based on the derived tPODs closely followed by WS, relative to estimates obtained from FHM, both for EE2 and FLX. This observation is interesting since RBT and FHM are much closer phylogenetically, although it is acknowledged that phylogenetic distance should not be a default basis and explanation for similarities and differences in species responses. One possible explanation for these differences may be the length of exposure and developmental times. FHM were exposed earlier and for a longer time than the other two fishes (summarized in Chapter 5); hence, compensatory and downstream physiological responses may have taken place and manifested feedback responses to the toxic insults; the shorter exposure time for WS and RBT (from hatch to 4 dph) may not have been sufficient time for these compensatory feedbacks to manifest. A time-course study on transcriptional responses may help elucidate this hypothesis. In addition, RBT and FHM were analyzed (summarized) at gene-level while datasets from WS were analyzed at the transcriptome-level due to the absence of a fully assembled genome. These differences would render the results not directly comparable, but regardless, tPOD estimates across species were within a tight range of concentrations despite these 2 major differences in exposure experiments and data analyses. Estimates were relatively comparable across species and compared well to empirically-derived apical PODs, suggesting that the use of short-term ELS of fish assays in deriving tPODs, even with minor variations in the process, hold promise as an effective surrogate for long-term/chronic adult exposures. In addition, tPODs derived here were significantly more sensitive relative to cell-based assays in deriving PODs/BMCs (Caminada, 2008; Pagé-Larivière *et al*., 2019) and are

directly comparable to apical PODs without a need for additional safety factors, further highlighting the advantage of the approach being developed in this study.

Table 6.1. Summary of tPODs across species. Datasets were fitted using the models Exp2, Exp3, Exp4, Exp5, Linear, Poly2, Hill, and Power, with a threshold lack-of-fit p-value > 0.1 and a benchmark-response (BMR) factor = 1.

	FLX (µg/L)			EE2 (ng/L)		
tPOD	**WS**	**RBT**	**FHM**	**WS**	**RBT**	**FHM**
omicBMC$_{20}$	0.02	0.02	0.56	0.06	0.12	2.39
omicBMC$_{10th}$	0.64	0.32	5.0	7.98	1.44	27.82
omicBMC$_{mode}$	2.08	5.01	7.43	16.51	4.38	24.93
pathBMC	-	0.19	5.66	-	1.68	45.61

omicBMC$_{20}$ = median of BMCs of the 20 most sensitive active genes

omicBMC$_{10th}$ = value of the BMC of the tenth percentile of all active genes

omicBMC$_{mode}$ = mode of the first peak of all geneBMCs

pathBMC = most sensitive pathway BMC, with at least 3 geneBMCs, based on bootstrapped median of constitutive geneBMCs of that specific pathway

6.4. Future work

The application of tPODs in chemical and environmental risk assessment is a growing concept, particularly for chemical testing prioritization. Most often, strategies on deriving tPODs were based on rats/mice (Farmahin *et al*., 2017; Johnson *et al*., 2014; Thomas *et al*., 2013b) and cell lines (Black *et al*., 2012; Chauhan *et al*., 2016). However, these strategies face either significant animal ethics issues for the use of live animals or derived threshold concentrations require *in-vitro*-to-*in-vivo* extrapolation. In this dissertation, we proposed short-term ELS (prior to independent exogenous feeding) fish exposures for use in the derivation of tPODs that were protective of chronic apical effects while using fish life-stages that are not considered live animals under current legislations. Unlike *in vitro* and *in silico* NAMs, the approach proposed here is lower in throughput and relatively more expensive and tedious, but the estimated tPODs were more robust in estimating apical PODs. These aspects have significantly improved relative to current chemical hazard testing approaches where live animals are being used, but the methods could still be further advanced by streamlining and optimizing several steps. Regardless of its promise, this strategy is still at its infancy and much work is needed to gain confidence in the use of ELS-derived tPODs in chemical hazard assessment. The following recommendations are based on the experience and conduct of this dissertation:

1. Identify the optimal number of replication with considerations on reasonable experimental set-up and cost, as well as the minimum number of dose/concentration/treatment groups for the effective derivation of tPODs;
2. Test and optimize higher-throughput methods in ELS exposures such as petri-dishes and/or micro-well plates;

3. Determine the ideal sequencing depth such that important molecular responses are within detectable levels while reducing sequencing costs;
4. Assess current statistical strategies in tPOD estimation and identify the best strategies to estimate tPODs that are protective of apical POD;
5. Identify strategies to link statistical tPOD estimates to biological context. The adverse outcome pathway (AOP) framework could be a key tool in this exercise;
6. Conduct similar studies using other species of fish belonging to phylogenetically diverse families;
7. Identify fish species which may potentially serve as an overall standard species for the derivation of tPODs;
8. Use other compounds/mixtures and assess how derived tPODs compare to their corresponding apical PODs;
9. Standardize and develop guidance documents for tPOD derivation from ELS fish. To date, the use of omics technologies in ERA and chemical hazard assessment remains to be sufficiently validated and trusted by the regulatory community (Sauer *et al*., 2017). A guidance document would allow direct cross-comparison of datasets and standardization of dataset generation, processing, and interpretation for regulatory acceptability.

Moreover, additional case studies are needed in establishing the link between tPODs and apical effects to gain further confidence in its use in regulatory ecotoxicology. Efforts should also be directed towards genome assembly and curation of functional annotations particularly for species important to ERA for more accurate prediction of the mechanisms of toxicity. In addition, with the vast numbers of compounds that need to be tested, the derivation of tPODs should advance

further than simply for the purposes of chemical testing prioritization and should mature such that one can derive reference doses and margin of exposure values that are anchored to a biological context that is useful for evaluating human and environmental risks. Finally, once proteomics techniques and instrumentation mature such that the majority of the proteins in the proteome are detected so that a truly global proteomic profile is achieved, it may be of interest to develop proteomics-based PODs since proteins are the fundamental effectors of cellular processes and therefore are more relevant in downstream biological processes.

6.5. Conclusion

In conclusion, this study demonstrated that omics responses can be linked to downstream and apical outcomes in diverse fish species. These connections serve as foundations for the use of tPODs in estimating apical PODs. Fish ELS-derived tPODs were effective in estimating chronic apical PODs, and that tPODs derived using this strategy fall within a tight range of concentrations across phylogenetically distant fish species. Therefore, fish ELS-derived tPODs hold promise in replacing, reducing, and refinement of the use of live animals in chemical hazard assessment. After additional careful calibration and validation, the here proposed ELS tPOD-based hazard assessment strategy holds significant promise to replace or minimize current live animal-based regulatory testing requirements by enabling accurate prediction of protective toxicity thresholds that are biologically sound, high-throughput, low cost, and with minimal ethical concerns.

REFERENCES

Afgan, E., Baker, D., Batut, B., van den Beek, M., Bouvier, D., Čech, M., Chilton, J., Clements, D., Coraor, N., Grüning, B.A., Guerler, A., Hillman-Jackson, J., Hiltemann, S., Jalili, V., Rasche, H., Soranzo, N., Goecks, J., Taylor, J., Nekrutenko, A., Blankenberg, D., 2018. The Galaxy platform for accessible, reproducible and collaborative biomedical analyses: 2018 update. Nucleic Acids Res. 46, W537–W544. https://doi.org/10.1093/nar/gky379

Ahlers, J., Riedhammer, C., Vogliano, M., Ebert, R.U., Kühne, R., Schüürmann, G., 2006. Acute to chronic ratios in aquatic toxicity - Variation across trophic levels and relationship with chemical structure. Environ. Toxicol. Chem. 25, 2937–2945. https://doi.org/10.1897/05-701R.1

Airhart, M.J., Lee, D.H., Wilson, T.D., Miller, B.E., Miller, M.N., Skalko, R.G., 2007. Movement disorders and neurochemical changes in zebrafish larvae after bath exposure to fluoxetine (PROZAC). Neurotoxicol. Teratol. 29, 652–664. https://doi.org/10.1016/j.ntt.2007.07.005

Alcaraz, A.J.G., Mikulášek, K., Potěšil, D., Park, B., Shekh, K., Ewald, J., Burbridge, C., Zdráhal, Z., Schneider, D., Xia, J., Crump, D., Basu, N., Hecker, M., 2021a. Assessing the Toxicity of 17α-Ethinylestradiol in Rainbow Trout Using a 4-Day Transcriptomics Benchmark Dose (BMD) Embryo Assay. Environ. Sci. Technol. 55, 10608–10618. https://doi.org/10.1021/acs.est.1c02401

Alcaraz, A.J.G., Potěšil, D., Mikulášek, K., Green, D., Park, B., Burbridge, C., Bluhm, K., Soufan, O., Lane, T., Pipal, M., Brinkmann, M., Xia, J., Zdráhal, Z., Schneider, D., Crump, D., Basu, N., Hogan, N., Hecker, M., 2021b. Development of a Comprehensive Toxicity Pathway Model for 17α-Ethinylestradiol in Early Life Stage Fathead Minnows (Pimephales

promelas). Environ. Sci. Technol. 55, 5024–5036. https://doi.org/10.1021/acs.est.0c05942

Allen, L., O'Connell, A., Kiermer, V., 2019. How can we ensure visibility and diversity in research contributions? How the Contributor Role Taxonomy (CRediT) is helping the shift from authorship to contributorship. Learn. Publ. 32, 71–74. https://doi.org/10.1002/LEAP.1210

Anders, S., Huber, W., 2010. Differential expression analysis for sequence count data. Genome Biol. 11, 1–12. https://doi.org/10.1186/gb-2010-11-10-r106

Andersen, L., Holbech, H., Gessbo, Å., Norrgren, L., Petersen, G.I., 2003. Effects of exposure to 17α-ethinylestradiol during early development on sexual differentiation and induction of vitellogenin in zebrafish (Danio rerio). Comp. Biochem. Physiol. - C Toxicol. Pharmacol. 134, 365–374. https://doi.org/10.1016/S1532-0456(03)00006-1

Andersen, M.E., McMullen, P.D., Krewski, D., 2015. Developing tools for defining and establishing pathways of toxicity. Arch. Toxicol. 89, 809. https://doi.org/10.1007/S00204-015-1512-Y

Anderson, J.C., Beyger, L., Guchardi, J., Holdway, D.A., 2020. The Effects of 17α-Ethinylestradiol on the Heart Rate of Embryonic Japanese Medaka (Oryzias latipes). Environ. Toxicol. Chem. 39, 904–912. https://doi.org/10.1002/ETC.4691

Anderson, J.C., Carlson, J.C., Low, J.E., Challis, J.K., Wong, C.S., Knapp, C.W., Hanson, M.L., 2013. Performance of a constructed wetland in Grand Marais, Manitoba, Canada: Removal of nutrients, pharmaceuticals, and antibiotic resistance genes from municipal wastewater. Chem. Cent. J. 7, 54–69. https://doi.org/10.1186/1752-153X-7-54

Andersson, C., Katsiadaki, I., Lundstedt-Enkel, K., Örberg, J., 2007. Effects of 17α-ethynylestradiol on EROD activity, spiggin and vitellogenin in three-spined stickleback

(Gasterosteus aculeatus). Aquat. Toxicol. 83, 33–42. https://doi.org/10.1016/j.aquatox.2007.03.008

Andrews, S., n.d. FastQC A Quality Control tool for High Throughput Sequence Data [WWW Document]. URL https://www.bioinformatics.babraham.ac.uk/projects/fastqc/ (accessed 12.1.19).

Ankley, G.T., Bennett, R.S., Erickson, R.J., Hoff, D.J., Hornung, M.W., Johnson, R.D., Mount, D.R., Nichols, J.W., Russom, C.L., Schmieder, P.K., Serrrano, J.A., Tietge, J.E., Villeneuve, D.L., 2010. Adverse outcome pathways: A conceptual framework to support ecotoxicology research and risk assessment. Environ. Toxicol. Chem. 29, 730–741. https://doi.org/10.1002/etc.34

Ankley, G.T., Edwards, S.W., 2018. The adverse outcome pathway: A multifaceted framework supporting 21st century toxicology. Curr. Opin. Toxicol. 9, 1–7. https://doi.org/10.1016/j.cotox.2018.03.004

Ankley, G.T., Villeneuve, D.L., 2006. The fathead minnow in aquatic toxicology: Past, present and future. Aquat. Toxicol. 78, 91–102. https://doi.org/10.1016/j.aquatox.2006.01.018

Aris, A.Z., Shamsuddin, A.S., Praveena, S.M., 2014. Occurrence of 17α-ethynylestradiol (EE2) in the environment and effect on exposed biota: a review. Environ. Int. 69, 104–119. https://doi.org/10.1016/j.envint.2014.04.011

Armstrong, B.M., Lazorchak, J.M., Jensen, K.M., Haring, H.J., Smith, M.E., Flick, R.W., Bencic, D.C., Biales, A.D., 2016. Reproductive effects in fathead minnows (Pimphales promelas) following a 21 d exposure to 17α-ethinylestradiol. Chemosphere 144, 366–373. https://doi.org/10.1016/j.chemosphere.2015.08.078

Assenov, Y., Ramírez, F., Schelhorn, S.-E., Lengauer, T., Albrecht, M., 2008. Computing

topological parameters of biological networks. Bioinformatics 24, 282–4. https://doi.org/10.1093/bioinformatics/btm554

Auerbach, S.S., Paules, R.S., 2018. Genomic dose response: Successes, challenges, and next steps. Curr. Opin. Toxicol. 11–12, 84–92. https://doi.org/10.1016/J.COTOX.2019.04.002

Ayobahan, S.U., Eilebrecht, E., Kotthoff, M., Baumann, L., Eilebrecht, S., Teigeler, M., Hollert, H., Kalkhof, S., Schäfers, C., 2019. A combined FSTRA-shotgun proteomics approach to identify molecular changes in zebrafish upon chemical exposure. Sci. Rep. 9, 1–12. https://doi.org/10.1038/s41598-019-43089-7

Bailey, C., von Siebenthal, E.W., Rehberger, K., Segner, H., 2019. Transcriptomic analysis of the impacts of ethinylestradiol (EE2) and its consequences for proliferative kidney disease outcome in rainbow trout (Oncorhynchus mykiss). Comp. Biochem. Physiol. Part C Toxicol. Pharmacol. 222, 31–48. https://doi.org/10.1016/j.cbpc.2019.04.009

Basu, N., Crump, D., Head, J., Hickey, G., Hogan, N., Maguire, S., Xia, J., Hecker, M., 2019. EcoToxChip: A next-generation toxicogenomics tool for chemical prioritization and environmental management. Environ. Toxicol. Chem. 38, 279–288. https://doi.org/10.1002/etc.4309

Beiras, R., Schönemann, A.M., 2021. Water quality criteria for selected pharmaceuticals and personal care products for the protection of marine ecosystems. Sci. Total Environ. 758, 143589. https://doi.org/10.1016/j.scitotenv.2020.143589

Beitel, S.C., Doering, J.A., Eisner, B.K., Hecker, M., 2015. Comparison of the sensitivity of four native Canadian fish species to 17-α ethinylestradiol, using an in vitro liver explant assay. Environ. Sci. Pollut. Res. 22, 20186–20197. https://doi.org/10.1007/s11356-015-5101-7

Beitel, S.C., Doering, J.A., Patterson, S.E., Hecker, M., 2014. Assessment of the sensitivity of

three North American fish species to disruptors of steroidogenesis using in vitro tissue explants. Aquat. Toxicol. 152, 273–283. https://doi.org/10.1016/j.aquatox.2014.04.013

Berger, M., Gray, J.A., Roth, B.L., 2009. The expanded biology of serotonin. Annu. Rev. Med. https://doi.org/10.1146/annurev.med.60.042307.110802

Bernhardt, E.S., Rosi, E.J., Gessner, M.O., 2017. Synthetic chemicals as agents of global change. Front. Ecol. Environ. 15, 84–90. https://doi.org/10.1002/fee.1450

Berthold, M.R., Cebron, N., Dill, F., Gabriel, T.R., Kötter, T., Meinl, T., Ohl, P., Sieb, C., Thiel, K., Wiswedel, B., 2008. KNIME: The Konstanz Information Miner, in: Preisach, C., Burkhardt, H., Schmidt-Thieme, L., R., D. (Eds.), Data Analysis, Machine Learning and Applications. Studies in Classification, Data Analysis, and Knowledge Organization. Springer, Berlin, Heidelberg, pp. 319–326. https://doi.org/10.1007/978-3-540-78246-9_38

Beulig, A., Fowler, J., 2008. Fish on prozac: Effect of serotonin reuptake inhibitors on cognition in goldfish. Behav. Neurosci. 122, 426–432. https://doi.org/10.1037/0735-7044.122.2.426

Bhandari, R.K., Vom Saal, F.S., Tillitt, D.E., 2015. Transgenerational effects from early developmental exposures to bisphenol A or 17α-ethinylestradiol in medaka, Oryzias latipes. Sci. Rep. 5, 1–5. https://doi.org/10.1038/srep09303

Bhatta, S., Iwai, T., Miura, C., Higuchi, M., Shimizu-Yamaguchi, S., Fukada, H., Miura, T., 2012. Gonads directly regulate growth in teleosts. Proc. Natl. Acad. Sci. U. S. A. 109, 11408–11412. https://doi.org/10.1073/pnas.1118704109

Biales, A.D., Bencic, D.C., Flick, R.W., Lazorchak, J., Lattier, D.L., 2007. Quantification and associated variability of induced vitellogenin gene transcripts in fathead minnow (Pimephales promelas) by quantitative real-time polymerase chain reaction assay. Environ. Toxicol. Chem. 26, 287–296. https://doi.org/10.1897/06-213R.1

Bidel, F., Di Poi, C., Imarazene, B., Koueta, N., Budzinski, H., Van Delft, P., Bellanger, C., Jozet-Alves, C., 2016. Pre-hatching fluoxetine-induced neurochemical, neurodevelopmental, and immunological changes in newly hatched cuttlefish. Environ. Sci. Pollut. Res. 23, 5030–5045. https://doi.org/10.1007/s11356-015-4591-7

Bindea, G., Mlecnik, B., Hackl, H., Charoentong, P., Tosolini, M., Kirilovsky, A., Fridman, W.-H., Pagès, F., Trajanoski, Z., Galon, J., 2009. ClueGO: a Cytoscape plug-in to decipher functionally grouped gene ontology and pathway annotation networks. Bioinformatics 25, 1091–3. https://doi.org/10.1093/bioinformatics/btp101

Black, M., Armbrust, K., 2007. The Environmental Occurrence, Fate, and Ecotoxicity of Selective Serotonin Reuptake Inhibitors (SSRIs) in Aquatic Environments| Research Project Database | Grantee Research Project | ORD | US EPA.

Black, M.B., Budinsky, R.A., Dombkowski, A., Cukovic, D., LeCluyse, E.L., Ferguson, S.S., Thomas, R.S., Rowlands, J.C., 2012. Cross-species Comparisons of Transcriptomic Alterations in Human and Rat Primary Hepatocytes Exposed to 2,3,7,8-Tetrachlorodibenzo-p-dioxin. Toxicol. Sci. 127, 199–215. https://doi.org/10.1093/toxsci/kfs069

Bogers, R., De Vries-Buitenweg, S., Van Gils, M., Baltussen, E., Hargreaves, A., van de Waart, B., De Roode, D., Legler, J., Murk, A., 2006. Development of chronic tests for endocrine active chemicals. Part 2: An extended fish early-life stage test with an androgenic chemical in the fathead minnow (Pimephales promelas). Aquat. Toxicol. 80, 119–130. https://doi.org/10.1016/j.aquatox.2006.07.020

Bolger, A.M., Lohse, M., Usadel, B., 2014. Trimmomatic: a flexible trimmer for Illumina sequence data. Bioinformatics 30, 2114–20. https://doi.org/10.1093/bioinformatics/btu170

Bosker, T., Munkittrick, K.R., Lister, A., MacLatchy, D.L., 2016. Mummichog (*Fundulus*

heteroclitus) continue to successfully produce eggs after exposure to high levels of 17α-ethinylestradiol. Environ. Toxicol. Chem. 35, 1107–1112. https://doi.org/10.1002/etc.3239

Bourgon, R., Gentleman, R., Huber, W., 2010. Independent filtering increases detection power for high-throughput experiments. Proc. Natl. Acad. Sci. 107, 9546–9551. https://doi.org/10.1073/pnas.0914005107

Bravo, E., Cantafora, A., Avella, M., Botham, K.M., 2001. Metabolism of Chylomicron Cholesterol is Delayed by Estrogen. An In Vivo Study in the Rat. Exp. Biol. Med. 226, 112–118. https://doi.org/10.1177/153537020122600208

Bray, N.L., Pimentel, H., Melsted, P., Pachter, L., 2016. Near-optimal probabilistic RNA-seq quantification. Nat. Biotechnol. 34, 525–527. https://doi.org/10.1038/nbt.3519

Bringolf, R.B., Heltsley, R.M., Newton, T.J., Eads, C.B., Fraley, S.J., Shea, D., Cope, W.G., 2010. Environmental occurrence and reproductive effects of the pharmaceutical fluoxetine in native freshwater mussels. Environ. Toxicol. Chem. 29, n/a-n/a. https://doi.org/10.1002/etc.157

Brinkmann, M., Eichbaum, K., Buchinger, S., Reifferscheid, G., Bui, T., Schäffer, A., Hollert, H., Preuss, T.G., 2014. Understanding receptor-mediated effects in rainbow trout: In vitro - In vivo extrapolation using physiologically based toxicokinetic models. Environ. Sci. Technol. 48, 3303–3309. https://doi.org/10.1021/es4053208

Brockmeier, E.K., Hodges, G., Hutchinson, T.H., Butler, E., Hecker, M., Tollefsen, K.E., Garcia-Reyero, N., Kille, P., Becker, D., Chipman, K., Colbourne, J., Collette, T.W., Cossins, A., Cronin, M., Graystock, P., Gutsell, S., Knapen, D., Katsiadaki, I., Lange, A., Marshall, S., Owen, S.F., Perkins, E.J., Plaistow, S., Schroeder, A., Taylor, D., Viant, M., Ankley, G., Falciani, F., 2017. The role of omics in the application of adverse outcome

pathways for chemical risk assessment. Toxicol. Sci. 158, 252–262. https://doi.org/10.1093/toxsci/kfx097

Brooks, B.W., 2014. Fish on Prozac (and Zoloft): Ten years later. Aquat. Toxicol. 151, 61–67. https://doi.org/10.1016/j.aquatox.2014.01.007

Brooks, B.W., Turner, P.K., Stanley, J.K., Weston, J.J., Glidewell, E.A., Foran, C.M., Slattery, M., La Point, T.W., Huggett, D.B., 2003. Waterborne and sediment toxicity of fluoxetine to select organisms. Chemosphere 52, 135–142. https://doi.org/10.1016/S0045-6535(03)00103-6

Bury, N.R., 2017. The evolution, structure and function of the ray finned fish (Actinopterygii) glucocorticoid receptors. Gen. Comp. Endocrinol. 251, 4–11. https://doi.org/10.1016/j.ygcen.2016.06.030

Caballero-Gallardo, K., Olivero-Verbel, J., L. Freeman, J., 2016. Toxicogenomics to Evaluate Endocrine Disrupting Effects of Environmental Chemicals Using the Zebrafish Model. Curr. Genomics 17, 515–527. https://doi.org/10.2174/1389202917666160513105959

Calabrese, E.J., Mattson, M.P., 2017. How does hormesis impact biology, toxicology, and medicine? npj Aging Mech. Dis. 3, 13. https://doi.org/10.1038/s41514-017-0013-z

Caldwell, D.J., Mastrocco, F., Anderson, P.D., Länge, R., Sumpter, J.P., 2012. Predicted-no-effect concentrations for the steroid estrogens estrone, 17β-estradiol, estriol, and 17α-ethinylestradiol. Environ. Toxicol. Chem. 31, 1396–1406. https://doi.org/10.1002/etc.1825

Caldwell, D.J., Mastrocco, F., Hutchinson, T.H., Länge, R., Heijerick, D., Janssen, C., Anderson, P.D., Sumpter, J.P., 2008. Derivation of an aquatic predicted no-effect concentration for the synthetic hormone, 17α-ethinyl estradiol. Environ. Sci. Technol. 42, 7046–7054. https://doi.org/10.1021/es800633q

Caminada, D., 2008. Pharmaceuticals as environmental pollutants : cytotoxicity and biochemical effects in an in vitro model system for aquatic organism. University of Zurich, Zurich. https://doi.org/10.5167/uzh-163769

Campos, B., Garcia-Reyero, N., Rivetti, C., Escalon, L., Habib, T., Tauler, R., Tsakovski, S., Piña, B., Barata, C., 2013. Identification of metabolic pathways in daphnia magna explaining hormetic effects of selective serotonin reuptake inhibitors and 4-nonylphenol using transcriptomic and phenotypic responses. Environ. Sci. Technol. 47, 9434–9443. https://doi.org/10.1021/es4012299

Canadian Council on Animal Care, 2005. Canadian Council on Animal Care guidelines on: the care and use of fish in research, teaching and testing. Ottawa.

Capela, R., Garric, J., Castro, L.F.C., Santos, M.M., 2020. Embryo bioassays with aquatic animals for toxicity testing and hazard assessment of emerging pollutants: A review. Sci. Total Environ. https://doi.org/10.1016/j.scitotenv.2019.135740

Chan, H.S., Chang, S.J., Wang, T.Y., Ko, H.J., Lin, Y.C., Lin, K.T., Chang, K.M., Chuang, Y.J., 2012. Serine protease PRSS23 is upregulated by estrogen receptor α and associated with proliferation of breast cancer cells. PLoS One 7. https://doi.org/10.1371/journal.pone.0030397

Chauhan, V., Kuo, B., McNamee, J.P., Wilkins, R.C., Yauk, C.L., 2016. Transcriptional benchmark dose modeling: Exploring how advances in chemical risk assessment may be applied to the radiation field. Environ. Mol. Mutagen. 57, 589–604.

Chen, F.P., Wang, K.C., Huang, J.D., 2009. Effect of Estrogen on the Activity and Growth of Human Osteoclasts In Vitro. Taiwan. J. Obstet. Gynecol. 48, 350–355. https://doi.org/10.1016/S1028-4559(09)60323-5

Chen, Y., Lun, A.T.L., Smyth, G.K., 2016. From reads to genes to pathways: differential expression analysis of RNA-Seq experiments using Rsubread and the edgeR quasi-likelihood pipeline. F1000Research 5, 1438. https://doi.org/10.12688/f1000research.8987.2

Colli-Dula, R.C., Martyniuk, C.J., Kroll, K.J., Prucha, M.S., Kozuch, M., Barber, D.S., Denslow, N.D., 2014. Dietary exposure of 17-alpha ethinylestradiol modulates physiological endpoints and gene signaling pathways in female largemouth bass (Micropterus salmoides). Aquat. Toxicol. 156, 148–160. https://doi.org/10.1016/j.aquatox.2014.08.008

Colwill, R.M., Creton, R., 2011. Locomotor behaviors in zebrafish (Danio rerio) larvae. Behav. Processes 86, 222–229. https://doi.org/10.1016/j.beproc.2010.12.003

Comerton, A.M., Andrews, R.C., Bagley, D.M., Baugros, J.B., Giroud, B., Dessalces, G., Grenier-Loustalot, M.F., Cren-Olivé, C., Benijts, T., Dams, R., Lambert, W., Leenheer, A. De, Brody, J.G., Rudel, R.A., Chen, J., Pawliszyn, J.B., Colborn, T., vom, S.S., Soto, A.M., Costa, L.G., Giordano, G., Guizzetti, M., Vitalone, A., Díaz-Cruz, M.S., Barceló, D., Doerr-MacEwen, N.A., Haight, M.E., Farré, M., Fatta, D., Nikolaou, A., Achilleos, A., Meriç, S., Gabet, V., Miège, C., Bados, P., Coquery, M., Giger, W., Gómez, M.J., Agüera, A., Mezcua, M., Hurtado, J., Mocholí, F., Fernández-Alba, A.R., Gros, M., Petrović, M., Barceló, D., Gros, M., Petrović, M., Barceló, D., Hua, W., Bennett, E.R., Letcher, R.J., Jahnke, A., Gandrass, J., Ruck, W., Jobling, S., Nolan, M., Tyler, C.R., Brighty, G., Sumpter, J.P., Kampioti, A.A., Cunha, A.C.B. da, Alda, M.L. de, Barceló, D., Kim, K.S., Oh, B.S., Kang, J.W., Chung, D.M., Cho, W.H., Choi, Y.K., Kolpin, D.W., Furlon, E.T., Meyer, M.T., Thurman, E.M., Zaugg, S.D., Barber, L.B., Buxton, H.T., Larsson, D.J., Adolfsson-Erici, M., Parkkonen, J., Pettersson, M., Berg, A.H., Olsson, P.-E., Förlin, L., Leatherland, J.F., Lin, W.C., Chen, H.C., Ding, W.H., Lindqvist, N., Tuhkanen, T.,

Kronberg, L., Lishman, L., Loraine, G.A., Pettigrove, M.E., Monzón, A.L., Moreno, D. V., Padrón, M.T., Ferrera, Z.S., Rodríguez, J.J.S., Pavlović, D.M., Babić, S., Horvat, A.M., Kaštelan-Macan, M., Pérez, S., Barceló, D., Pichon, V., Pietrogrande, M.C., Basaglia, G., Purdom, C.E., Hardiman, P.A., Bye, V.J., Eno, N.C., Tyler, C.R., Sumpter, J.P., Radjenović, J., Petrović, M., Barceló, D., Reddersen, K., Heberer, T., Renew, J.E., Huang, C.H., Richardson, S.D., Rossi, D.T., Zhang, N., Safe, S., Safe, S., Schultz, M., Lëffler, D., Wagner, M., Ternes, T.A., Schwab, B.W., Hayes, E.P., Fiori, J.M., Mastrocco, F.J., Roden, N.M., Cragin, D., Meyerhoff, R.D., D'Aco, V.J., Anderson, P.D., Servos, M.R., Smith, M., McInnis, R., Burnison, B.K., Lee, B.H., Backus, S., Solomon, G.M., Schettler, T., Stackelberg, P.E., Furlong, E.T., Meyer, M.T., Zaugg, S.D., Henderson, A.K., Reissman, D.B., Steen, R.A., Hogenboom, A.C., Leonards, P.G., Peerboom, R.L., Cofino, W.P., Brinkmasn, U.T., Suchara, E.A., Budziak, D., Martendal, E., Costa, L.F., Carasek, E., Ternes, T.A., Weber, R.A., Pierik, F.H., Dohle, G.R., Burdorf, A., Wennmalm, A., Gunnarsson, B., Westerhoff, P., Yoon, Y., Snyder, S., Wert, E., Zhang, S., Zhang, Q., Darisaw, S., Ehie, O., Wang, G., Zrostlíková, J., Hajšlová, J., Poustka, J., Begany, P., Zuehlke, S., Duennbier, U., Heberer, T., 2009. Practical overview of analytical methods for endocrine-disrupting compounds, pharmaceuticals and personal care products in water and wastewater. Philos. Trans. A. Math. Phys. Eng. Sci. 367, 3923–39. https://doi.org/10.1098/rsta.2009.0111

Cox, J., Mann, M., 2008. MaxQuant enables high peptide identification rates, individualized p.p.b.-range mass accuracies and proteome-wide protein quantification. Nat. Biotechnol. 26, 1367–72. https://doi.org/10.1038/nbt.1511

Cox, J., Matic, I., Hilger, M., Nagaraj, N., Selbach, M., Olsen, J. V., Mann, M., 2009. A practical

guide to the maxquant computational platform for silac-based quantitative proteomics. Nat. Protoc. 4, 698–705. https://doi.org/10.1038/nprot.2009.36

Cox, J., Neuhauser, N., Michalski, A., Scheltema, R.A., Olsen, J. V., Mann, M., 2011. Andromeda: A Peptide Search Engine Integrated into the MaxQuant Environment. J. Proteome Res. 10, 1794–1805. https://doi.org/10.1021/pr101065j

Cunha, V., Rodrigues, P., Santos, M.M., Moradas-Ferreira, P., Ferreira, M., 2018. Fluoxetine modulates the transcription of genes involved in serotonin, dopamine and adrenergic signalling in zebrafish embryos. Chemosphere 191, 954–961. https://doi.org/10.1016/j.chemosphere.2017.10.100

Dai, Y.-J., Jia, Y.-F., Chen, N., Bian, W.-P., Li, Q.-K., Ma, Y.-B., Chen, Y.-L., Pei, D.-S., 2014. Zebrafish as a model system to study toxicology. Environ. Toxicol. Chem. 33, 11–17. https://doi.org/10.1002/ETC.2406

Daughton, C.G., 2003. Cradle-to-cradle stewardship of drugs for minimizing their environmental disposition while promoting human health. II. Drug disposal, waste reduction, and future directions. Environ. Health Perspect. 111, 775–785. https://doi.org/10.1289/ehp.5948

de Farias, N.O., Oliveira, R., Moretti, P.N.S., e Pinto, J.M., Oliveira, A.C., Santos, V.L., Rocha, P.S., Andrade, T.S., Grisolia, C.K., 2020. Fluoxetine chronic exposure affects growth, behavior and tissue structure of zebrafish. Comp. Biochem. Physiol. Part C Toxicol. Pharmacol. 237, 108836. https://doi.org/10.1016/j.cbpc.2020.108836

de Farias, N.O., Oliveira, R., Sousa-Moura, D., de Oliveira, R.C.S., Rodrigues, M.A.C., Andrade, T.S., Domingues, I., Camargo, N.S., Muehlmann, L.A., Grisolia, C.K., 2019. Exposure to low concentration of fluoxetine affects development, behaviour and acetylcholinesterase activity of zebrafish embryos. Comp. Biochem. Physiol. Part - C

Toxicol. Pharmacol. 215, 1–8. https://doi.org/10.1016/j.cbpc.2018.08.009

De Wit, M., Keil, D., Ven, K. van der, Vandamme, S., Witters, E., Coen, W. De, 2010. An integrated transcriptomic and proteomic approach characterizing estrogenic and metabolic effects of 17 α-ethinylestradiol in zebrafish (Danio rerio). Gen. Comp. Endocrinol. 167, 190–201. https://doi.org/10.1016/j.ygcen.2010.03.003

Dean, J.L., Jay Zhao, Q., Lambert, J.C., Hawkins, B.S., Thomas, R.S., Wesselkamper, S.C., 2017. Application of Gene Set Enrichment Analysis for Identification of Chemically-Induced, Biologically Relevant Transcriptomic Networks and Potential Utilization in Human Health Risk Assessment. Toxicol. Sci. 157, kfx021. https://doi.org/10.1093/toxsci/kfx021

Degani, G., Boker, R., Jackson, K., 1996. Growth hormone, gonad development, and steroid levels in female carp. Comp. Biochem. Physiol. - C Pharmacol. Toxicol. Endocrinol. 115, 133–140. https://doi.org/10.1016/S0742-8413(96)00079-5

Denslow, N.D., Chow, M.C., Kroll, K.J., Green, L., 1999. Vitellogenin as a biomarker of exposure for estrogen or estrogen mimics. Ecotoxicology 8, 385–398. https://doi.org/10.1023/A:1008986522208

Depiereux, S., Liagre, M., Danis, L., De Meulder, B., Depiereux, E., Segner, H., Kestemont, P., 2014. Intersex Occurrence in Rainbow Trout (Oncorhynchus mykiss) Male Fry Chronically Exposed to Ethynylestradiol. PLoS One 9, e98531. https://doi.org/10.1371/journal.pone.0098531

Digre, A., Lindskog, C., 2021. The Human Protein Atlas—Spatial localization of the human proteome in health and disease. Protein Sci. 30, 218–233. https://doi.org/10.1002/pro.3987

Doering, J.A., Dubiel, J., Wiseman, S., 2020. Predicting Early Life Stage Mortality in Birds and

Fishes from Exposure to Low-Potency Agonists of the Aryl Hydrocarbon Receptor: A Cross-Species Quantitative Adverse Outcome Pathway Approach. Environ. Toxicol. Chem. 39, 2055–2064. https://doi.org/10.1002/etc.4816

Doering, J.A., Tang, S., Peng, H., Eisner, B.K., Sun, J., Giesy, J.P., Wiseman, S., Hecker, M., 2016. High Conservation in Transcriptomic and Proteomic Response of White Sturgeon to Equipotent Concentrations of 2,3,7,8-TCDD, PCB 77, and Benzo[a]pyrene. Environ. Sci. Technol. 50, 4826–4835. https://doi.org/10.1021/acs.est.6b00490

Doering, J.A., Wiseman, S., Giesy, J.P., Hecker, M., 2018. A Cross-species Quantitative Adverse Outcome Pathway for Activation of the Aryl Hydrocarbon Receptor Leading to Early Life Stage Mortality in Birds and Fishes. Environ. Sci. Technol. 52, 7524–7533. https://doi.org/10.1021/acs.est.8b01438

Dorelle, L.S., Da Cuña, R.H., Sganga, D.E., Rey Vázquez, G., López Greco, L., Lo Nostro, F.L., 2020. Fluoxetine exposure disrupts food intake and energy storage in the cichlid fish Cichlasoma dimerus (Teleostei, Cichliformes). Chemosphere 238, 124609. https://doi.org/10.1016/j.chemosphere.2019.124609

Doyle, M.A., Bosker, T., Martyniuk, C.J., MacLatchy, D.L., Munkittrick, K.R., 2013. The effects of 17-α-ethinylestradiol (EE2) on molecular signaling cascades in mummichog (Fundulus heteroclitus). Aquat. Toxicol. 134–135, 34–46. https://doi.org/10.1016/j.aquatox.2013.03.001

Ebele, A.J., Abou-Elwafa Abdallah, M., Harrad, S., 2017. Pharmaceuticals and personal care products (PPCPs) in the freshwater aquatic environment. Emerg. Contam. 3, 1–16. https://doi.org/10.1016/j.emcon.2016.12.004

European Union, 2010. Directive 2010/63/EU of the European Parliament and of the Council of

22 September 2010 on the protection of animals used for scientific purposes. Off. J. Eur. Union 53, 33–79. https://doi.org/10.3000/17252555.L_2010.276.eng

Ewald, J., Soufan, O., Xia, J., Basu, N., 2020. FastBMD: an online tool for rapid benchmark dose-response analysis of transcriptomics data. Bioinformatics. https://doi.org/10.1093/bioinformatics/btaa700

Farmahin, R., Williams, A., Kuo, B., Chepelev, N.L., Thomas, R.S., Barton-Maclaren, T.S., Curran, I.H., Nong, A., Wade, M.G., Yauk, C.L., 2017. Recommended approaches in the application of toxicogenomics to derive points of departure for chemical risk assessment. Arch. Toxicol. 91, 2045–2065. https://doi.org/10.1007/s00204-016-1886-5

Fenske, M., Maack, G., Schäfers, C., Segner, H., 2005. An environmentally relevant concentration of estrogen induces arrest of male gonad development in zebrafish, Danio rerio. Environ. Toxicol. Chem. 24, 1088–1098. https://doi.org/10.1897/04-096R1.1

Feswick, A., Loughery, J.R., Isaacs, M.A., Munkittrick, K.R., Martyniuk, C.J., 2016. Molecular initiating events of the intersex phenotype: Low-dose exposure to 17α-ethinylestradiol rapidly regulates molecular networks associated with gonad differentiation in the adult fathead minnow testis. Aquat. Toxicol. 181, 46–56. https://doi.org/10.1016/j.aquatox.2016.10.021

Finne, E.F., Cooper, G.A., Koop, B.F., Hylland, K., Tollefsen, K.E., 2007. Toxicogenomic responses in rainbow trout (Oncorhynchus mykiss) hepatocytes exposed to model chemicals and a synthetic mixture. Aquat. Toxicol. 81, 293–303. https://doi.org/10.1016/j.aquatox.2006.12.010

Fischer, M., Belanger, S.E., Berckmans, P., Bernhard, M.J., Bl aha, L., Coman Schmid, D.E., Dyer, S.D., Haupt, T., Hermens, J.L., Maria Hultman, kj T., Heike Laue, K., Lillicrap, A.,

Marie Mlna ıkov, K., Natsch, A., ı Nov ak, J., Sinnige, T.L., Knut Erik Tollefsen, K., Valentin von Niederh, K., Witters, H., Zupani, A., Schirmer, K., 2019. Repeatability and Reproducibility of the RTgill-W1 Cell Line Assay for Predicting Fish Acute Toxicity. Toxicol. Sci. 169, 353–364. https://doi.org/10.1093/toxsci/kfz057

Folmar, L.C., Gardner, G.R., Schreibman, M.P., Magliulo-Cepriano, L., Mills, L.J., Zaroogian, G., Gutjahr-Gobell, R., Haebler, R., Horowitz, D.B., Denslow, N.D., 2001. Vitellogenin-induced pathology in male summer flounder (Paralichthys dentatus). Aquat. Toxicol. 51, 431–441. https://doi.org/10.1016/S0166-445X(00)00121-1

Fraher, D., Hodge, J.M., Collier, F.M., McMillan, J.S., Kennedy, R.L., Ellis, M., Nicholson, G.C., Walder, K., Dodd, S., Berk, M., Pasco, J.A., Williams, L.J., Gibert, Y., 2016. Citalopram and sertraline exposure compromises embryonic bone development. Mol. Psychiatry 21, 656–664. https://doi.org/10.1038/mp.2015.135

Froehner, S., Machado, K.S., Stefan, E., Bleninger, T., da Rosa, E.C., de Castro Martins, C., 2012. Occurrence of selected estrogens in mangrove sediments. Mar. Pollut. Bull. 64, 75–79. https://doi.org/10.1016/j.marpolbul.2011.10.021

Froehner, S., Piccioni, W., Machado, K.S., Aisse, M.M., 2011. Removal Capacity of Caffeine, Hormones, and Bisphenol by Aerobic and Anaerobic Sewage Treatment. Water, Air, Soil Pollut. 216, 463–471. https://doi.org/10.1007/s11270-010-0545-3

Froese, R., 2006. Cube law, condition factor and weight-length relationships: History, meta-analysis and recommendations. J. Appl. Ichthyol. 22, 241–253. https://doi.org/10.1111/j.1439-0426.2006.00805.x

Garcia-Reyero, N., Perkins, E.J., 2011. Systems biology: Leading the revolution in ecotoxicology. Environ. Toxicol. Chem. 30, 265–273. https://doi.org/10.1002/etc.401

Glasauer, S.M.K., Neuhauss, S.C.F., 2014. Whole-genome duplication in teleost fishes and its evolutionary consequences. Mol. Genet. Genomics 289, 1045–1060. https://doi.org/10.1007/s00438-014-0889-2

Gracia, R., 2005. Fluoxetine, in: Encyclopedia of Toxicology. Elsevier, pp. 347–348. https://doi.org/10.1016/B0-12-369400-0/00421-X

Groh, K.J., Carvalho, R.N., Chipman, J.K., Denslow, N.D., Halder, M., Murphy, C.A., Roelofs, D., Rolaki, A., Schirmer, K., Watanabe, K.H., 2015. Development and application of the adverse outcome pathway framework for understanding and predicting chronic toxicity: I. Challenges and research needs in ecotoxicology. Chemosphere 120, 764–777. https://doi.org/10.1016/j.chemosphere.2014.09.068

Guest, P.C., Knowles, M.R., Molon-Noblot, S., Salim, K., Smith, D., Murray, F., Laroque, P., Hunt, S.P., de Felipe, C., Rupniak, N.M., McAllister, G., 2004. Mechanisms of action of the antidepressants fluoxetine and the substance P antagonist L-000760735 are associated with altered neurofilaments and synaptic remodeling. Brain Res. 1002, 1–10. https://doi.org/10.1016/j.brainres.2003.11.064

Gwinn, M.R., 2020. New Approach Methodologies (NAMs) and Chemical Risk Assessment. The United States Environmental Protection Agency's Center for Computational Toxicology and Exposure. https://doi.org/10.23645/EPACOMPTOX.12837488.V1

Halder, M., Léonard, M., Iguchi, T., Oris, J.T., Ryder, K., Belanger, S.E., Braunbeck, T.A., Embry, M.R., Whale, G., Norberg-King, T., Lillicrap, A., 2010. Regulatory aspects on the use of fish embryos in environmental toxicology. Integr. Environ. Assess. Manag. 6, 484–491. https://doi.org/10.1002/ieam.48

Hamad, A., Kluk, M., Fox, J., Park, M., Turner, J.E., 2007. The effects of aromatase inhibitors

and selective estrogen receptor modulators on eye development in the Zebrafish (Danio rerio). Curr. Eye Res. 32, 819–827. https://doi.org/10.1080/02713680701573712

Hao, R., Bondesson, M., Singh, A. V., Riu, A., McCollum, C.W., Knudsen, T.B., Gorelick, D.A., Gustafsson, J.Å., 2013. Identification of estrogen target genes during zebrafish embryonic development through transcriptomic analysis. PLoS One 8, 79020. https://doi.org/10.1371/journal.pone.0079020

Hazelton, P.D., Du, B., Haddad, S.P., Fritts, A.K., Chambliss, C.K., Brooks, B.W., Bringolf, R.B., 2014. Chronic fluoxetine exposure alters movement and burrowing in adult freshwater mussels. Aquat. Toxicol. 151, 27–35. https://doi.org/10.1016/j.aquatox.2013.12.019

Health Canada, 2018. Evaluation of the use of toxicogenomics in risk assessment at Health Canada : an exploratory document on current Health Canada practices for the use of toxicogenomics in risk assessment. Ottawa, Ontario.

Heberle, H., Meirelles, G.V., da Silva, F.R., Telles, G.P., Minghim, R., 2015. InteractiVenn: a web-based tool for the analysis of sets through Venn diagrams. BMC Bioinformatics 16, 169. https://doi.org/10.1186/s12859-015-0611-3

Hecker, M., 2018. Non-model Species in Ecological Risk Assessment, in: Garcia-Reyero, N., Murphy, C.A. (Eds.), A Systems Biology Approach to Advancing Adverse Outcome Pathways for Risk Assessment. Springer International Publishing, Cham, pp. 107–132. https://doi.org/10.1007/978-3-319-66084-4_6

Hecker, M., Hollert, H., 2011. Endocrine disruptor screening: regulatory perspectives and needs. Environ. Sci. Eur. 23, 15. https://doi.org/10.1186/2190-4715-23-15

Henry, T.B., Black, M.C., 2008. Acute and chronic toxicity of fluoxetine (selective serotonin reuptake inhibitor) in western Mosquitofish. Arch. Environ. Contam. Toxicol. 54, 325–330.

https://doi.org/10.1007/s00244-007-9018-0

Hill, R.L., Janz, D.M., 2003. Developmental estrogenic exposure in zebrafish (Danio rerio): I. Effects on sex ratio and breeding success. Aquat. Toxicol. 63, 417–29. https://doi.org/10.1016/s0166-445x(02)00207-2

Hiramatsu, N., Matsubara, T., Weber, G.M., Sullivan, C. V., Hara, A., 2002. Vitellogenesis in Aquatic Animals. Fish. Sci. 68, 694–699. https://doi.org/10.2331/fishsci.68.sup1_694

Huff, M., Da Silveira, W.A., Carnevali, O., Renaud, L., Hardiman, G., 2018. Systems analysis of the liver transcriptome in adult male zebrafish exposed to the plasticizer (2-ethylhexyl) phthalate (DEHP). Sci. Rep. 8, 1–17. https://doi.org/10.1038/s41598-018-20266-8

Hughes, S.R., Kay, P., Brown, L.E., 2013. Global Synthesis and Critical Evaluation of Pharmaceutical Data Sets Collected from River Systems. Environ. Sci. Technol. 47, 661–677. https://doi.org/10.1021/es3030148

Hultman, M.T., Song, Y., Tollefsen, K.E., 2015. 17α-Ethinylestradiol (EE2) effect on global gene expression in primary rainbow trout (Oncorhynchus mykiss) hepatocytes. Aquat. Toxicol. 169, 90–104. https://doi.org/10.1016/j.aquatox.2015.10.004

Hyeon, J.-Y., Hur, S.-P., Kim, B.-H., Byun, J.-H., Kim, E.-S., Lim, B.-S., Lee, B.-I., Kim, S.-K., Takemura, A., Kim, S.-J., 2019. Involvement of Estrogen and Its Receptors in Morphological Changes in the Eyes of the Japanese Eel, Anguilla japonica, in the Process of Artificially-Induced Maturation. Cells 8, 310. https://doi.org/10.3390/cells8040310

Interagency Coordinating Committee on the Validation of Alternative Methods, 2018. A strategic roadmap for establishing new approaches to evaluate the safety of chemicals and medical products in the United States. https://doi.org/10.22427/NTP-ICCVAM-ROADMAP2018

Jeffries, M.K.S., Stultz, A.E., Smith, A.W., Rawlings, J.M., Belanger, S.E., Oris, J.T., 2014. Alternative methods for toxicity assessments in fish: Comparison of the fish embryo toxicity and the larval growth and survival tests in zebrafish and fathead minnows. Environ. Toxicol. Chem. 33, 2584–2594. https://doi.org/10.1002/etc.2718

Jeffries, M.K.S., Stultz, A.E., Smith, A.W., Stephens, D.A., Rawlings, J.M., Belanger, S.E., Oris, J.T., 2015. The fish embryo toxicity test as a replacement for the larval growth and survival test: A comparison of test sensitivity and identification of alternative endpoints in zebrafish and fathead minnows. Environ. Toxicol. Chem. 34, 1369–1381. https://doi.org/10.1002/etc.2932

Jobling, S., Casey, D., Rogers-Gray, T., Oehlmann, J., Schulte-Oehlmann, U., Pawlowski, S., Baunbeck, T., Turner, A.P., Tyler, C.R., 2004. Comparative responses of molluscs and fish to environmental estrogens and an estrogenic effluent. Aquat. Toxicol. 66, 207–222. https://doi.org/10.1016/j.aquatox.2004.01.002

Johnson, G.E., Soeteman-Hernández, L.G., Gollapudi, B.B., Bodger, O.G., Dearfield, K.L., Heflich, R.H., Hixon, J.G., Lovell, D.P., MacGregor, J.T., Pottenger, L.H., Thompson, C.M., Abraham, L., Thybaud, V., Tanir, J.Y., Zeiger, E., van Benthem, J., White, P.A., 2014. Derivation of point of departure (PoD) estimates in genetic toxicology studies and their potential applications in risk assessment. Environ. Mol. Mutagen. 55, 609–623. https://doi.org/10.1002/em.21870

Jones, P.D., De Coen, W.M., Tremblay, L., Giesy, J.P., 2000. Vitellogenin as a biomarker for environmental estrogens. Water Sci. Technol. 42, 1–14. https://doi.org/10.2166/wst.2000.0546

Judson, R., Houck, K., Martin, M., Richard, A.M., Knudsen, T.B., Shah, I., Little, S.,

Wambaugh, J., Setzer, R.W., Kothya, P., Phuong, J., Filer, D., Smith, D., Reif, D., Rotroff, D., Kleinstreuer, N., Sipes, N., Xia, M., Huang, R., Crofton, K., Thomas, R.S., 2016. Analysis of the effects of cell stress and cytotoxicity on in vitro assay activity across a diverse chemical and assay space. Toxicol. Sci. 152, 323–339. https://doi.org/10.1093/toxsci/kfw092

Kam, G.Y.W., Leung, K.-C., Baxter, R.C., Ho, K.K.Y., 2000. Estrogens Exert Route- and Dose-Dependent Effects on Insulin-Like Growth Factor (IGF)-Binding Protein-3 and the Acid-Labile Subunit of the IGF Ternary Complex*. J. Clin. Endocrinol. Metab. 85, 1918–1922. https://doi.org/10.1210/jcem.85.5.6527

Kammers, K., Cole, R.N., Tiengwe, C., Ruczinski, I., 2015. Detecting significant changes in protein abundance. EuPA Open Proteomics 7, 11–19. https://doi.org/10.1016/j.euprot.2015.02.002

Kavlock, R.J., Bahadori, T., Barton-Maclaren, T.S., Gwinn, M.R., Rasenberg, M., Thomas, R.S., 2018. Accelerating the Pace of Chemical Risk Assessment. Chem. Res. Toxicol. 31, 287–290. https://doi.org/10.1021/acs.chemrestox.7b00339

Khan, A., Mathelier, A., 2017. Intervene: A tool for intersection and visualization of multiple gene or genomic region sets. BMC Bioinformatics 18, 287. https://doi.org/10.1186/s12859-017-1708-7

Kidd, K.A., Blanchfield, P.J., Mills, K.H., Palace, V.P., Evans, R.E., Lazorchak, J.M., Flick, R.W., 2007. Collapse of a fish population after exposure to a synthetic estrogen. Proc. Natl. Acad. Sci. 104, 8897–8901. https://doi.org/10.1073/pnas.0609568104

Kidd, K.A., Paterson, M.J., Rennie, M.D., Podemski, C.L., Findlay, D.L., Blanchfield, P.J., Liber, K., 2014. Direct and indirect responses of a freshwater food web to a potent synthetic

oestrogen. Philos. Trans. R. Soc. B Biol. Sci. 369, 20130578. https://doi.org/10.1098/rstb.2013.0578

Kim, D., Langmead, B., Salzberg, S.L., 2015. HISAT: a fast spliced aligner with low memory requirements. Nat. Methods 12, 357–60. https://doi.org/10.1038/nmeth.3317

King, O.C., van de Merwe, J.P., McDonald, J.A., Leusch, F.D.L., 2016. Concentrations of levonorgestrel and ethinylestradiol in wastewater effluents: Is the progestin also cause for concern? Environ. Toxicol. Chem. 35, 1378–1385. https://doi.org/10.1002/etc.3304

Kitagawa, E., Kishi, K., Ippongi, T., Kawauchi, H., Nakazono, K., Suzuki, K., Ohba, H., Hayashi, Y., Iwahashi, H., Masuo, Y., 2009. Effects of endocrine disruptors on nervous system related gene expression: Comprehensive analysis of Medaka fish, in: Atmospheric and Biological Environmental Monitoring. Springer Netherlands, pp. 229–239. https://doi.org/10.1007/978-1-4020-9674-7_15

Kohlert, J.G., Mangan, B.P., Kodra, C., Drako, L., Long, E., Simpson, H., 2012. Decreased Aggressive and Locomotor Behaviors in Betta Splendens after Exposure to Fluoxetine. Psychol. Rep. 110, 51–62. https://doi.org/10.2466/02.13.PR0.110.1.51-62

Koschützki, D., Schreiber, F., 2008. Centrality analysis methods for biological networks and their application to gene regulatory networks. Gene Regul. Syst. Bio. 2008, 193–201. https://doi.org/10.4137/grsb.s702

Krewski, D., Andersen, M.E., Tyshenko, M.G., Krishnan, K., Hartung, T., Boekelheide, K., Wambaugh, J.F., Jones, D., Whelan, M., Thomas, R., Yauk, C., Barton-Maclaren, T., Cote, I., 2020. Toxicity testing in the 21st century: progress in the past decade and future perspectives. Arch. Toxicol. 94, 1–58. https://doi.org/10.1007/s00204-019-02613-4

Kumar, A., Batley, G.E., Nidumolu, B., Hutchinson, T.H., 2016. Derivation of water quality

guidelines for priority pharmaceuticals. Environ. Toxicol. Chem. 35, 1815–1824. https://doi.org/10.1002/etc.3336

Kumar, P., Panigrahi, P., Johnson, J., Weber, W.J., Mehta, S., Sajulga, R., Easterly, C., Crooker, B.A., Heydarian, M., Anamika, K., Griffin, T.J., Jagtap, P.D., 2019. QuanTP: A Software Resource for Quantitative Proteo-Transcriptomic Comparative Data Analysis and Informatics. J. Proteome Res. 18, 782–790. https://doi.org/10.1021/acs.jproteome.8b00727

Kwon, J.-W., Armbrust, K.L., 2006. Laboratory persistence and fate of fluoxetine in aquatic environments. Environ. Toxicol. Chem. 25, 2561–2568. https://doi.org/10.1897/05-613R.1

Lane, T., Green, D., Bluhm, K., Raes, K., Janz, D.M., Liber, K., Hecker, M., 2019. In ovo exposure of fathead minnow (Pimephales promelas) to selenomethionine via maternal transfer and embryo microinjection: A comparative study. Aquat. Toxicol. 216. https://doi.org/10.1016/j.aquatox.2019.105299

Latonnelle, K., Le Menn, F., Kaushik, S.J., Bennetau-Pelissero, C., 2002. Effects of Dietary Phytoestrogens in Vivo and in Vitro in Rainbow Trout and Siberian Sturgeon: Interests and Limits of the in Vitro Studies of Interspecies Differences. Gen. Comp. Endocrinol. 126, 39–51. https://doi.org/10.1006/gcen.2001.7773

Laurenson, J.P., Bloom, R.A., Page, S., Sadrieh, N., 2014. Ethinyl Estradiol and Other Human Pharmaceutical Estrogens in the Aquatic Environment: A Review of Recent Risk Assessment Data. AAPS J. 16, 299–310. https://doi.org/10.1208/s12248-014-9561-3

Lillicrap, A., Belanger, S., Burden, N., Pasquier, D. Du, Embry, M.R., Halder, M., Lampi, M.A., Lee, L., Norberg-King, T., Rattner, B.A., Schirmer, K., Thomas, P., 2016. Alternative approaches to vertebrate ecotoxicity tests in the 21st century: A review of developments over the last 2 decades and current status. Environ. Toxicol. Chem. 35, 2637–2646.

https://doi.org/10.1002/etc.3603

Liney, K.E., Hagger, J.A., Tyler, C.R., Depledge, M.H., Galloway, T.S., Jobling, S., 2006. Health Effects in Fish of Long-Term Exposure to Effluents from Wastewater Treatment Works. Environ. Health Perspect. 114, 81–89. https://doi.org/10.1289/ehp.8058

Liu, Y., Beyer, A., Aebersold, R., 2016. On the Dependency of Cellular Protein Levels on mRNA Abundance. Cell 165, 535–550. https://doi.org/10.1016/j.cell.2016.03.014

Liu, Z., Huang, R., Roberts, R., Tong, W., 2019. Toxicogenomics: A 2020 Vision. Trends Pharmacol. Sci. 40, 92–103. https://doi.org/10.1016/j.tips.2018.12.001

Long, E.R., Dutch, M., Weakland, S., Chandramouli, B., Benskin, J.P., 2013. Quantification of pharmaceuticals, personal care products, and perfluoroalkyl substances in the marine sediments of Puget Sound, Washington, USA. Environ. Toxicol. Chem. 32, 1701–1710. https://doi.org/10.1002/etc.2281

Lopes, D.G., Duarte, I.A., Antunes, M., Fonseca, V.F., 2020. Effects of antidepressants in the reproduction of aquatic organisms: a meta-analysis. Aquat. Toxicol. 227, 105569. https://doi.org/10.1016/j.aquatox.2020.105569

Love, M.I., Huber, W., Anders, S., 2014. Moderated estimation of fold change and dispersion for RNA-seq data with DESeq2. Genome Biol. 15, 550. https://doi.org/10.1186/s13059-014-0550-8

Lovin, L.M., Kim, S., Taylor, R.B., Scarlett, K.R., Langan, L.M., Chambliss, C.K., Chatterjee, S., Scott, J.T., Brooks, B.W., 2021. Differential influences of (±) anatoxin-a on photolocomotor behavior and gene transcription in larval zebrafish and fathead minnows. Environ. Sci. Eur. 33, 40. https://doi.org/10.1186/s12302-021-00479-x

Maier, T., Güell, M., Serrano, L., 2009. Correlation of mRNA and protein in complex biological

samples. FEBS Lett. https://doi.org/10.1016/j.febslet.2009.10.036

Margiotta-Casaluci, L., Owen, S.F., Cumming, R.I., Polo, A. de, Winter, M.J., Panter, G.H., Rand-Weaver, M., Sumpter, J.P., 2014b. Quantitative Cross-Species Extrapolation between Humans and Fish: The Case of the Anti-Depressant Fluoxetine. PLoS One 9, e110467. https://doi.org/10.1371/JOURNAL.PONE.0110467

Margiotta-Casaluci, Luigi, Owen, S.F., Cumming, R.I., de Polo, A., Winter, M.J., Panter, G.H., Rand-Weaver, Mariann, Sumpter, J.P., LaLone, C., Villeneuve, D., Cavallin, J., Kahl, M., Durhan, E., Perkins, E., Ankley, G., Crofton, K., Garcia-Reyero, N., LaLone, C., Celander, M., Goldstone, J., Denslow, N., Iguchi, T., Kille, P., Lipsky, M., Sharp, L., Ibrahim, L., Preuss, T., Ratte, H., Hommen, U., Boxall, A., Rudd, M., Brooks, B., Caldwell, D., Choi, K., Kuemmerer, K., Runnalls, T., Margiotta-Casaluci, L, Kugathas, S., Sumpter, J., Rand-Weaver, M, Margiotta-Casaluci, L, Patel, A., Panter, G., Owen, S., Gunnarsson, L., Jauhiainen, A., Kristiansson, E., Nerman, O., Larsson, D., Winter, M., Owen, S., Murray-Smith, R., Panter, G., Hetheridge, M., Berninger, J., Brooks, B., Seiler, J., Caldwell, D., Mastrocco, F., Margiotta-Casaluci, L, Brooks, B., Margiotta-Casaluci, L, Hannah, RE, Sumpter, J., Huggett, D., Cook, J., Ericson, J., Williams, RT, Oakes, K., Coors, A., Escher, B., Fenner, K., Garric, J., Mennigen, J., Stroud, P., Zamora, J., Moon, T., Trudeau, V., Maximino, C., Brito, T. de, Batista, A. da S., Herculano, A., Morato, S., Baldwin, D, Baldwin, DS, Waldman, S., Allgulander, C., Cachat, J, Stewart, A., Grossman, L., Gaikwad, S., Kadri, F., Egan, R., Bergner, C., Hart, P., Cachat, JM, Canavello, P., Jr, T.V., Perez-Hurtado, P., Chambliss, C., Brooks, B., Kristensen, J., Ilett, K., Hackett, L., Yapp, P., Paech, M., Levin, E., Bencan, Z., Cerutti, D., Schulz, M., Schmoldt, A., Gould, G., Brooks, B., Frazer, A., Owens, M., Morgan, W., Plott, S., Nemeroff, C., Kim, Y., Nam, R., Yoo, Y.,

Lee, C., Klooster, J., Yazulla, S., Kamermans, M., Lillesaar, C., Smeets, W., Gonzalez, A., Sundvik, M., Panula, P., Baraban, S., Ellis, L., Soanes, K., Kokel, D., Bryan, J., Laggner, C., White, R., Cheung, C., Rihel, J., Prober, D., Arvanites, A., Lam, K., Zimmerman, S., Rihel, J., Schier, A., Wolman, M., Granato, M., Bencan, Z., Sledge, D., Levin, E., Lopez-Patino, M., Yu, L., Cabral, H., Zhdanova, I., Dulawa, S., Hollick, K., Gundersen, B., Hen, R., Zhang, Y., Raap, D., Garcia, F., Serres, F., Ma, Q., Wong, R., Perrin, F., Oxendine, S., Kezios, Z., Sawyer, S., Amsterdam, J., Fawcett, J., Quitkin, F., Reimherr, F., Rosenbaum, J., Kelly, M., Perry, P., Holstad, S., Garvey, M., Norman, T., Gupta, R., Burrows, G., Parker, G., Judd, F., Bjerkenstedt, L., Flyckt, L., Overo, K., Lingjaerde, O., Preskorn, S., Harvey, A., Scordo, M., Spina, E., Dahl, M., Gatti, G., Perucca, E., McRobb, F., Sahagun, V., Kufareva, I., Abagyan, R., Goldstone, J., McArthur, A., Kubota, A., Zanette, J., Parente, T., Hiemke, C., Hartter, S., Ring, B., Eckstein, J., Gillespie, J., Binkley, S., Vandenbranden, M., Bergstrom, R., Lemberger, L., Farid, N., Wolen, R., Preskorn, S., Alderman, J., Chung, M., Harrison, W., Messig, M., Altamura, A., Moro, A., Percudani, M., Jannuzzi, G., Gatti, G., Magni, P., Spina, E., Pacifici, R., Lundmark, J., Reis, M., Bengtsson, F., Charlier, C., Broly, F., Lhermitte, M., Pinto, E., Ansseau, M., Eap, C., Bondolfi, G., Zullino, D., Savary-Cosendai, L., Powell-Golay, K., Fjordside, L., Jeppesen, U., Eap, C., Powell, K., Baumann, P., Jr, T.V., Gould, G., Berninger, J., Connors, K., Keele, N., Sumpter, J., Donnachie, R., Johnson, A., Pittman, J., Ichikawa, K., Airhart, M., Lee, D., Wilson, T., Miller, B., Miller, M., Kohlert, J., Mangan, B., Kodra, C., Drako, L., Long, E., Anderson, P., Johnson, A., Pfeiffer, D., Caldwell, D., Hannah, R, Johnson, A., Keller, V., Williams, RJ, Young, A., Sumpter, J., Johnson, A., Williams, RJ, Kortenkamp, A., Scholze, M., Ankley, G., Bennett, R., Erickson, R., Hoff, D., Hornung, M., 2014a. Quantitative Cross-Species Extrapolation

between Humans and Fish: The Case of the Anti-Depressant Fluoxetine. PLoS One 9, e110467. https://doi.org/10.1371/journal.pone.0110467

Martín-Pozo, L., de Alarcón-Gómez, B., Rodríguez-Gómez, R., García-Córcoles, M.T., Çipa, M., Zafra-Gómez, A., 2019. Analytical methods for the determination of emerging contaminants in sewage sludge samples. A review. Talanta 192, 508–533. https://doi.org/10.1016/J.TALANTA.2018.09.056

Martin, J.M., Bertram, M.G., Saaristo, M., Ecker, T.E., Hannington, S.L., Tanner, J.L., Michelangeli, M., O'Bryan, M.K., Wong, B.B.M., 2019. Impact of the widespread pharmaceutical pollutant fluoxetine on behaviour and sperm traits in a freshwater fish. Sci. Total Environ. 650, 1771–1778. https://doi.org/10.1016/j.scitotenv.2018.09.294

Martin, J.M., Nagarajan-Radha, V., Tan, H., Bertram, M.G., Brand, J.A., Saaristo, M., Dowling, D.K., Wong, B.B.M., 2020. Antidepressant exposure causes a nonmonotonic reduction in anxiety-related behaviour in female mosquitofish. J. Hazard. Mater. Lett. 1, 100004. https://doi.org/10.1016/j.hazl.2020.100004

Martínez, R., Esteve-Codina, A., Herrero-Nogareda, L., Ortiz-Villanueva, E., Barata, C., Tauler, R., Raldúa, D., Piña, B., Navarro-Martín, L., 2018. Dose-dependent transcriptomic responses of zebrafish eleutheroembryos to Bisphenol A. Environ. Pollut. 243, 988–997. https://doi.org/10.1016/j.envpol.2018.09.043

Martinson, J., Bencic, D.C., Toth, G.P., Kostich, M.S., Flick, R.W., See, M.J., Lattier, D., Biales, A.D., Huang, W., n.d. De novo assembly and annotation of a highly contiguous reference genome of the fathead minnow (Pimephales promelas) reveals an AT-rich repetitive genome with compact gene structure. https://doi.org/10.1101/2021.02.24.432777

Martyniuk, C.J., Feswick, A., Munkittrick, K.R., Dreier, D.A., Denslow, N.D., 2020. Twenty

years of transcriptomics, 17alpha-ethinylestradiol, and fish. Gen. Comp. Endocrinol. 286. https://doi.org/10.1016/j.ygcen.2019.113325

Matozzo, V., Gagné, F., Marin, M.G., Ricciardi, F., Blaise, C., 2008. Vitellogenin as a biomarker of exposure to estrogenic compounds in aquatic invertebrates: A review. Environ. Int. 34, 531–545. https://doi.org/10.1016/j.envint.2007.09.008

Matthiessen, P., Wheeler, J.R., Weltje, L., 2018. A review of the evidence for endocrine disrupting effects of current-use chemicals on wildlife populations. Crit. Rev. Toxicol. 48, 195–216. https://doi.org/10.1080/10408444.2017.1397099

McCarthy, D.J., Chen, Y., Smyth, G.K., 2012. Differential expression analysis of multifactor RNA-Seq experiments with respect to biological variation. Nucleic Acids Res. 40, 4288–4297. https://doi.org/10.1093/nar/gks042

Mennigen, J.A., Lado, W.E., Zamora, J.M., Duarte-Guterman, P., Langlois, V.S., Metcalfe, C.D., Chang, J.P., Moon, T.W., Trudeau, V.L., 2010a. Waterborne fluoxetine disrupts the reproductive axis in sexually mature male goldfish, Carassius auratus. Aquat. Toxicol. 100, 354–364. https://doi.org/10.1016/j.aquatox.2010.08.016

Mennigen, J.A., Sassine, J., Trudeau, V.L., Moon, T.W., 2010b. Waterborne fluoxetine disrupts feeding and energy metabolism in the goldfish Carassius auratus. Aquat. Toxicol. 100, 128–137. https://doi.org/10.1016/j.aquatox.2010.07.022

Mercier, G., Lennon, A.M., Renouf, B., Dessouroux, A., Ramaugé, M., Courtin, F., Pierre, M., 2004. MAP Kinase Activation by Fluoxetine and Its Relation to Gene Expression in Cultured Rat Astrocytes. J. Mol. Neurosci. 24, 207–216. https://doi.org/10.1385/JMN:24:2:207

Mohamed, A.R., King, H., Evans, B., Reverter, A., Kijas, J.W., 2018. Multi-tissue transcriptome

profiling of north American derived Atlantic salmon. Front. Genet. 9. https://doi.org/10.3389/fgene.2018.00369

Mole, R.A., Brooks, B.W., 2019. Global scanning of selective serotonin reuptake inhibitors: occurrence, wastewater treatment and hazards in aquatic systems. Environ. Pollut. 250, 1019–1031. https://doi.org/10.1016/j.envpol.2019.04.118

Morando, M.B., Medeiros, L.R., McDonald, M.D., 2009. Fluoxetine treatment affects nitrogen waste excretion and osmoregulation in a marine teleost fish. Aquat. Toxicol. 95, 164–71.

Moyses, Z.P., Nakandakari, F.K., Magaldi, A.J., 2008. Fluoxetine effect on kidney water reabsorption. Nephrol. Dial. Transplant. 23, 1173–1178. https://doi.org/10.1093/ndt/gfm714

Naciff, J.M., Overmann, G.J., Torontali, S.M., Carr, G.J., Tiesman, J.P., Richardson, B.D., Daston, G.P., 2003. Gene expression profile induced by 17α-ethynyl estradiol in the prepubertal female reproductive system of the rat. Toxicol. Sci. 72, 314–330. https://doi.org/10.1093/toxsci/kfg037

National Research Council, 2007. Toxicity testing in the 21st century: A vision and a strategy. The National Academies Press, Washington, DC. https://doi.org/10.17226/11970

National Toxicology Program, 2018. NTP Research Report on National Toxicology Program Approach to Genomic Dose-Response Modeling. 111 TW Alexander Dr, Durham, NC 27709, USA. https://doi.org/10.22427/NTP-RR-5

Nilsen, E., Smalling, K.L., Ahrens, L., Gros, M., Miglioranza, K.S.B., Picó, Y., Schoenfuss, H.L., 2019. Critical review: Grand challenges in assessing the adverse effects of contaminants of emerging concern on aquatic food webs. Environ. Toxicol. Chem. 38, 46–60. https://doi.org/10.1002/etc.4290

Nowakowska, K., Giebułtowicz, J., Kamaszewski, M., Adamski, A., Szudrowicz, H.,

Ostaszewska, T., Solarska-Dzięciołowska, U., Nałęcz-Jawecki, G., Wroczyński, P., Drobniewska, A., 2020. Acute exposure of zebrafish (Danio rerio) larvae to environmental concentrations of selected antidepressants: Bioaccumulation, physiological and histological changes. Comp. Biochem. Physiol. Part - C Toxicol. Pharmacol. 229, 108670. https://doi.org/10.1016/j.cbpc.2019.108670

Nuzzi, R., Scalabrin, S., Becco, A., Panzica, G., 2019. Sex hormones and optic nerve disorders: A review. Front. Neurosci. 13, 57. https://doi.org/10.3389/fnins.2019.00057

OECD, 2013. Test No. 210: Fish, Early-life Stage Toxicity Test, OECD Guidelines for the Testing of Chemicals, Section 2, OECD Guidelines for the Testing of Chemicals, Section 2. OECD, Paris. https://doi.org/10.1787/9789264203785-en

Overturf, M.D., Anderson, J.C., Pandelides, Z., Beyger, L., Holdway, D. a, 2015. Pharmaceuticals and personal care products: A critical review of the impacts on fish reproduction. Crit. Rev. Toxicol. 8444, 1–23. https://doi.org/10.3109/10408444.2015.1038499

Pagé-Larivière, F., Crump, D., O'Brien, J.M., 2019. Transcriptomic points-of-departure from short-term exposure studies are protective of chronic effects for fish exposed to estrogenic chemicals. Toxicol. Appl. Pharmacol. 378, 114634. https://doi.org/10.1016/j.taap.2019.114634

Painter, M.M., Buerkley, M.A., Julius, M.L., Vajda, A.M., Norris, D.O., Barber, L.B., Furlong, E.T., Schultz, M.M., Schoenfuss, H.L., 2009. Antidepressants at environmentally relevant concentrations affect predator avoidance behavior of larval fathead minnows (Pimephales promelas). Environ. Toxicol. Chem. 28, 2677–2684. https://doi.org/10.1897/08-556.1

Palace, V.P., Evans, R.E., Wautier, K., Baron, C., Vandenbyllardt, L., Vandersteen, W., Kidd,

K., 2002. Induction of vitellogenin and histological effects in wild fathead minnows from a lake experimentally treated with the synthetic estrogen, ethynylestradiol. Water Qual. Res. J. Canada 37, 637–650. https://doi.org/10.2166/wqrj.2002.042

Palmisano, B.T., Zhu, L., Stafford, J.M., 2017. Role of estrogens in the regulation of liver lipid metabolism, in: Advances in Experimental Medicine and Biology. Springer New York LLC, pp. 227–256. https://doi.org/10.1007/978-3-319-70178-3_12

Papoulias, D.M., Noltie, D.B., Tillitt, D.E., 2000. An in vivo model fish system to test chemical effects on sexual differentiation and development: exposure to ethinyl estradiol. Aquat. Toxicol. 48, 37–50. https://doi.org/10.1016/S0166-445X(99)00026-0

Parrott, J.L., Blunt, B.R., 2005. Life-cycle exposure of fathead minnows (Pimephales promelas) to an ethinylestradiol concentration below 1 ng/L reduces egg fertilization success and demasculinizes males. Environ. Toxicol. 20, 131–141. https://doi.org/10.1002/tox.20087

Partridge, C., Boettcher, A., Jones, A.G., 2010. Short-term exposure to a synthetic estrogen disrupts mating dynamics in a pipefish. Horm. Behav. 58, 800–807. https://doi.org/10.1016/j.yhbeh.2010.08.002

Pascovici, D., Handler, D.C.L., Wu, J.X., Haynes, P.A., 2016. Multiple testing corrections in quantitative proteomics: A useful but blunt tool. Proteomics 16, 2448–2453. https://doi.org/10.1002/pmic.201600044

Patel, M., Kumar, R., Kishor, K., Mlsna, T., Pittman, C.U., Mohan, D., 2019. Pharmaceuticals of emerging concern in aquatic systems: Chemistry, occurrence, effects, and removal methods. Chem. Rev. 119, 3510–3673. https://doi.org/10.1021/acs.chemrev.8b00299

Pawlowski, S., Van Aerle, R., Tyler, C.R., Braunbeck, T., 2004. Effects of 17α-ethinylestradiol in a fathead minnow (Pimephales promelas) gonadal recrudescence assay. Ecotoxicol.

Environ. Saf. 57, 330–345. https://doi.org/10.1016/J.ECOENV.2003.07.019

Perez-Riverol, Y., Csordas, A., Bai, J., Bernal-Llinares, M., Hewapathirana, S., Kundu, D.J., Inuganti, A., Griss, J., Mayer, G., Eisenacher, M., Pérez, E., Uszkoreit, J., Pfeuffer, J., Sachsenberg, T., Yilmaz, Ş., Tiwary, S., Cox, J., Audain, E., Walzer, M., Jarnuczak, A.F., Ternent, T., Brazma, A., Vizcaíno, J.A., 2019. The PRIDE database and related tools and resources in 2019: Improving support for quantification data. Nucleic Acids Res. 47, D442–D450. https://doi.org/10.1093/nar/gky1106

Pertea, M., Pertea, G.M., Antonescu, C.M., Chang, T.-C., Mendell, J.T., Salzberg, S.L., 2015. StringTie enables improved reconstruction of a transcriptome from RNA-seq reads. Nat. Biotechnol. 33, 290–295. https://doi.org/10.1038/nbt.3122

Petrie, B., Barden, R., Kasprzyk-Hordern, B., 2015. A review on emerging contaminants in wastewaters and the environment: Current knowledge, understudied areas and recommendations for future monitoring. Water Res. 72, 3–27. https://doi.org/10.1016/j.watres.2014.08.053

Rahman, L., Williams, A., Gelda, K., Nikota, J., Wu, D., Vogel, U., Halappanavar, S., 2020. 21st Century Tools for Nanotoxicology: Transcriptomic Biomarker Panel and Precision-Cut Lung Slice Organ Mimic System for the Assessment of Nanomaterial-Induced Lung Fibrosis. Small 16, 2000272. https://doi.org/10.1002/smll.202000272

Rand-Weaver, M., Margiotta-Casaluci, L., Patel, A., Panter, G.H., Owen, S.F., Sumpter, J.P., 2013. The read-across hypothesis and environmental risk assessment of pharmaceuticals. Environ. Sci. Technol. 47, 11384–11395. https://doi.org/10.1021/es402065a

Raudvere, U., Kolberg, L., Kuzmin, I., Arak, T., Adler, P., Peterson, H., Vilo, J., 2019. g:Profiler: a web server for functional enrichment analysis and conversions of gene lists

(2019 update). Nucleic Acids Res. 47, W191–W198. https://doi.org/10.1093/nar/gkz369

Reiner, A.P., Heckbert, S.R., Vos, H.L., Ariëns, R.A.S., Lemaitre, R.N., Smith, N.L., Lumley, T., Rea, T.D., Hindorff, L.A., Schellenbaum, G.D., Rosendaal, F.R., Siscovick, D.S., Psaty, B.M., 2003. Genetic variants of coagulation factor XIII, postmenopausal estrogen therapy, and risk of nonfatal myocardial infarction. Blood 102, 25–30. https://doi.org/10.1182/blood-2002-07-2308

Ren, B., Liu, M., Ni, J., Tian, J., 2018. Role of Selenoprotein F in Protein Folding and Secretion: Potential Involvement in Human Disease. Nutrients 10, 1619. https://doi.org/10.3390/nu10111619

Richendrfer, H., Pelkowski, S.D., Colwill, R.M., Creton, R., 2012. On the edge: Pharmacological evidence for anxiety-related behavior in zebrafish larvae. Behav. Brain Res. 228, 99–106. https://doi.org/10.1016/j.bbr.2011.11.041

Ritchie, M.E., Phipson, B., Wu, D., Hu, Y., Law, C.W., Shi, W., Smyth, G.K., 2015. Limma powers differential expression analyses for RNA-sequencing and microarray studies. Nucleic Acids Res. 43, e47. https://doi.org/10.1093/nar/gkv007

Robinson, M.D., McCarthy, D.J., Smyth, G.K., 2010. edgeR: a Bioconductor package for differential expression analysis of digital gene expression data. Bioinformatics 26, 139–140. https://doi.org/10.1093/bioinformatics/btp616

Robinson, M.D., Oshlack, A., 2010. A scaling normalization method for differential expression analysis of RNA-seq data. Genome Biol. 11, R25. https://doi.org/10.1186/gb-2010-11-3-r25

Rose, E., Paczolt, K.A., Jones, A.G., 2013. The effects of synthetic estrogen exposure on premating and postmating episodes of selection in sex-role-reversed Gulf pipefish. Evol. Appl. 6, 1160–70. https://doi.org/10.1111/eva.12093

Roush, K.S., Krzykwa, J.C., Malmquist, J.A., Stephens, D.A., Sellin Jeffries, M.K., 2018. Enhancing the fathead minnow fish embryo toxicity test: Optimizing embryo production and assessing the utility of additional test endpoints. Ecotoxicol. Environ. Saf. 153, 45–53. https://doi.org/10.1016/j.ecoenv.2018.01.042

Runnalls, T.J., Beresford, N., Kugathas, S., Margiotta-Casaluci, L., Scholze, M., Scott, A.P., Sumpter, J.P., 2015. From single chemicals to mixtures-Reproductive effects of levonorgestrel and ethinylestradiol on the fathead minnow. Aquat. Toxicol. 169, 152–167. https://doi.org/10.1016/j.aquatox.2015.10.009

Salinas, K., Hemmer, M.J., Serrano, J., Higgins, L., Anderson, L.B., Benninghoff, A.D., Williams, D.E., Walker, C., 2010. Identification of estrogen-responsive vitelline envelope protein fragments from rainbow trout (Oncorhynchus mykiss) plasma using mass spectrometry. Mol. Reprod. Dev. 77, 963–970. https://doi.org/10.1002/mrd.21244

Sampayo, R.G., Toscani, A.M., Rubashkin, M.G., Thi, K., Masullo, L.A., Violi, I.L., Lakins, J.N., Cáceres, A., Hines, W.C., Leskow, F.C., Stefani, F.D., Chialvo, D.R., Bissell, M.J., Weaver, V.M., Simian, M., 2018. Fibronectin rescues estrogen receptor α from lysosomal degradation in breast cancer cells. J. Cell Biol. 217, 2777–2798. https://doi.org/10.1083/jcb.201703037

Sauer, U.G., Deferme, L., Gribaldo, L., Hackermüller, J., Tralau, T., van Ravenzwaay, B., Yauk, C., Poole, A., Tong, W., Gant, T.W., 2017. The challenge of the application of 'omics technologies in chemicals risk assessment: Background and outlook. Regul. Toxicol. Pharmacol. 91, S14–S26. https://doi.org/10.1016/j.yrtph.2017.09.020

Sauvé, S., Desrosiers, M., 2014. A review of what is an emerging contaminant. Chem. Cent. J. 8, 15. https://doi.org/10.1186/1752-153X-8-15

Schäfers, C., Teigeler, M., Wenzel, A., Maack, G., Fenske, M., Segner, H., 2007. Concentration- and time-dependent effects of the synthetic estrogen, 17α-ethinylestradiol, on reproductive capabilities of the zebrafish, Danio rerio. J. Toxicol. Environ. Heal. - Part A Curr. Issues 70, 768–779. https://doi.org/10.1080/15287390701236470

Schirmer, K., Fischer, B.B., Madureira, D.J., Pillai, S., 2010. Transcriptomics in ecotoxicology. Anal. Bioanal. Chem. 397, 917–923. https://doi.org/10.1007/s00216-010-3662-3

Scholz, S., Klüver, N., 2009. Effects of Endocrine Disrupters on Sexual, Gonadal Development in Fish. Sex. Dev. 3, 136–151. https://doi.org/10.1159/000223078

Schultz, D.R., Tang, S., Miller, C., Gagnon, D., Shekh, K., Alcaraz, A.J.G., Janz, D.M., Hecker, M., 2021. A Multi-Life Stage Comparison of Silver Nanoparticles Toxicity on the Early Development of Three Canadian Fish Species. Environ. Toxicol. Chem. etc.5210. https://doi.org/10.1002/etc.5210

Schultz, I.R., Skillman, A., Nicolas, J.-M., Cyr, D.G., Nagler, J.J., 2003. Short-term exposure to 17α-ethynylestradiol decreases the fertility of sexually maturing male rainbow trout (*Oncorhynchus mykiss*). Environ. Toxicol. Chem. 22, 1272–1280. https://doi.org/10.1002/etc.5620220613

Schultz, M.M., Painter, M.M., Bartell, S.E., Logue, A., Furlong, E.T., Werner, S.L., Schoenfuss, H.L., 2011. Selective uptake and biological consequences of environmentally relevant antidepressant pharmaceutical exposures on male fathead minnows. Aquat. Toxicol. 104, 38–47. https://doi.org/10.1016/J.AQUATOX.2011.03.011

Schwindt, A.R., Winkelman, D.L., Keteles, K., Murphy, M., Vajda, A.M., 2014. An environmental oestrogen disrupts fish population dynamics through direct and transgenerational effects on survival and fecundity. J. Appl. Ecol. 51, 582–591.

https://doi.org/10.1111/1365-2664.12237

Sehonova, P., Svobodova, Z., Dolezelova, P., Vosmerova, P., Faggio, C., 2018. Effects of waterborne antidepressants on non-target animals living in the aquatic environment: A review. Sci. Total Environ. https://doi.org/10.1016/j.scitotenv.2018.03.076

Shannon, P., Markiel, A., Ozier, O., Baliga, N.S., Wang, J.T., Ramage, D., Amin, N., Schwikowski, B., Ideker, T., 2003. Cytoscape: a software environment for integrated models of biomolecular interaction networks. Genome Res. 13, 2498–504. https://doi.org/10.1101/gr.1239303

Shved, N., Berishvili, G., Baroiller, J.F., Segner, H., Reinecke, M., 2008. Environmentally relevant concentrations of 17α-ethinylestradiol (EE2) interfere with the growth hormone (gh)/insulin-like growth factor (IGF)-I system in developing bony fish. Toxicol. Sci. 106, 93–102. https://doi.org/10.1093/toxsci/kfn150

Shved, N., Berishvili, G., D'Cotta, H., Baroiller, J.F., Segner, H., Eppler, E., Reinecke, M., 2007. Ethinylestradiol differentially interferes with IGF-I in liver and extrahepatic sites during development of male and female bony fish. J. Endocrinol. 195, 513–523. https://doi.org/10.1677/JOE-07-0295

Simpson, K.L., Weaver, K.J., De Villers-Sidani, E., Lu, J.Y.F., Cai, Z., Pang, Y., Rodriguez-Porcel, F., Paul, I.A., Merzenich, M., Lin, R.C.S., 2011. Perinatal antidepressant exposure alters cortical network function in rodents. Proc. Natl. Acad. Sci. U. S. A. 108, 18465–18470. https://doi.org/10.1073/pnas.1109353108

Sobanska, M., Scholz, S., Nyman, A.-M., Cesnaitis, R., Gutierrez Alonso, S., Klüver, N., Kühne, R., Tyle, H., de Knecht, J., Dang, Z., Lundbergh, I., Carlon, C., De Coen, W., 2018. Applicability of the fish embryo acute toxicity (FET) test (OECD 236) in the regulatory

context of Registration, Evaluation, Authorisation, and Restriction of Chemicals (REACH). Environ. Toxicol. Chem. 37, 657–670. https://doi.org/10.1002/etc.4055

Stanley, J.K., Ramirez, A.J., Chambliss, C.K., Brooks, B.W., 2007. Enantiospecific sublethal effects of the antidepressant fluoxetine to a model aquatic vertebrate and invertebrate. Chemosphere 69, 9–16. https://doi.org/10.1016/j.chemosphere.2007.04.080

Steele, W.B., Kristofco, L.A., Corrales, J., Saari, G.N., Haddad, S.P., Gallagher, E.P., Kavanagh, T.J., Kostal, J., Zimmerman, J.B., Voutchkova-Kostal, A., Anastas, P., Brooks, B.W., 2018. Comparative behavioral toxicology with two common larval fish models: Exploring relationships among modes of action and locomotor responses. Sci. Total Environ. 640–641, 1587–1600. https://doi.org/10.1016/j.scitotenv.2018.05.402

Strähle, U., Scholz, S., Geisler, R., Greiner, P., Hollert, H., Rastegar, S., Schumacher, A., Selderslaghs, I., Weiss, C., Witters, H., Braunbeck, T., 2012. Zebrafish embryos as an alternative to animal experiments-A commentary on the definition of the onset of protected life stages in animal welfare regulations. Reprod. Toxicol. 33, 128–132. https://doi.org/10.1016/j.reprotox.2011.06.121

Sumpter, J.P., Donnachie, R.L., Johnson, A.C., 2014. The apparently very variable potency of the anti-depressant fluoxetine. Aquat. Toxicol. 151, 57–60. https://doi.org/10.1016/j.aquatox.2013.12.010

Sun, J., Tang, S., Peng, H., Saunders, D.M.V., Doering, J.A., Hecker, M., Jones, P.D., Giesy, J.P., Wiseman, S., 2016. Combined Transcriptomic and Proteomic Approach to Identify Toxicity Pathways in Early Life Stages of Japanese Medaka (*Oryzias latipes*) Exposed to 1,2,5,6-Tetrabromocyclooctane (TBCO). Environ. Sci. Technol. 50, 7781–7790. https://doi.org/10.1021/acs.est.6b01249

Szklarczyk, D., Gable, A.L., Lyon, D., Junge, A., Wyder, S., Huerta-Cepas, J., Simonovic, M., Doncheva, N.T., Morris, J.H., Bork, P., Jensen, L.J., Von Mering, C., 2019. STRING v11: Protein-protein association networks with increased coverage, supporting functional discovery in genome-wide experimental datasets. Nucleic Acids Res. 47, D607–D613. https://doi.org/10.1093/nar/gky1131

Tang, W., Zhou, M., Dorsey, T.H., Prieto, D.A., Wang, X.W., Ruppin, E., Veenstra, T.D., Ambs, S., 2018. Integrated proteotranscriptomics of breast cancer reveals globally increased protein-mRNA concordance associated with subtypes and survival. Genome Med. 10, 1–14. https://doi.org/10.1186/s13073-018-0602-x

Teather, K., Parrott, J., 2006. Assessing the Chemical Sensitivity of Freshwater Fish Commonly Used in Toxicological Studies. Water Qual. Res. J. 41, 100–105. https://doi.org/10.2166/wqrj.2006.011

Templeton, M.R., Graham, N., Voulvoulis, N., 2009. Emerging chemical contaminants in water and wastewater. Philos. Trans. A. Math. Phys. Eng. Sci. 367, 3873–5. https://doi.org/10.1098/rsta.2009.0144

Thomas, R.S., Philbert, M.A., Auerbach, S.S., Wetmore, B.A., Devito, M.J., Cote, I., Rowlands, J.C., Whelan, M.P., Hays, S.M., Andersen, M.E., Meek, M.E. (Bette), Reiter, L.W., Lambert, J.C., Clewell, H.J., Stephens, M.L., Zhao, Q.J., Wesselkamper, S.C., Flowers, L., Carney, E.W., Pastoor, T.P., Petersen, D.D., Yauk, C.L., Nong, A., 2013a. Incorporating New Technologies Into Toxicity Testing and Risk Assessment: Moving From 21st Century Vision to a Data-Driven Framework. Toxicol. Sci. 136, 4–18. https://doi.org/10.1093/toxsci/kft178

Thomas, R.S., Wesselkamper, S.C., Wang, N.C.Y., Zhao, Q.J., Petersen, D.D., Lambert, J.C.,

Cote, I., Yang, L., Healy, E., Black, M.B., Clewell, H.J., Allen, B.C., Andersen, M.E., 2013b. Temporal Concordance Between Apical and Transcriptional Points of Departure for Chemical Risk Assessment. Toxicol. Sci. 134, 180–194. https://doi.org/10.1093/toxsci/kft094

Thompson, W.A., Vijayan, M.M., 2020. Environmental levels of venlafaxine impact larval behavioural performance in fathead minnows. Chemosphere 259, 127437. https://doi.org/10.1016/j.chemosphere.2020.127437

Thorpe, K.L., Benstead, R., Hutchinson, T.H., Tyler, C.R., 2007. Associations between altered vitellogenin concentrations and adverse health effects in fathead minnow (Pimephales promelas). Aquat. Toxicol. 85, 176–183. https://doi.org/10.1016/j.aquatox.2007.08.012

Tompsett, A.R., Wiseman, S., Higley, E., Pryce, S., Chang, H., Giesy, J.P., Hecker, M., 2012. Effects of 17α-ethynylestradiol on sexual differentiation and development of the African clawed frog (Xenopus laevis). Comp. Biochem. Physiol. - C Toxicol. Pharmacol. 156, 202–210. https://doi.org/10.1016/j.cbpc.2012.06.002

Tyanova, S., Temu, T., Cox, J., 2016. The MaxQuant computational platform for mass spectrometry-based shotgun proteomics. Nat. Protoc. 11, 2301–2319. https://doi.org/10.1038/nprot.2016.136

UK, 1993. The Animals (Scientific Procedures) Act(Amendment) Order 1993. Queen's Printer of Acts of Parliament, United Kingdom.

Uren Webster, T.M., Shears, J.A., Moore, K., Santos, E.M., 2015. Identification of conserved hepatic transcriptomic responses to 17β-estradiol using high-throughput sequencing in brown trout. Physiol. Genomics 47, 420–431. https://doi.org/10.1152/physiolgenomics.00123.2014

USEPA OW/ORD Emerging Contaminants Workgroup, 2008. White Paper on Aquatic life criteria for contaminants of emerging concern Part 1. General challenges and recommendations Draft Document.

van Aerle, R., Pounds, N., Hutchinson, T.H., Maddix, S., Tyler, C.R., 2002. Window of sensitivity for the estrogenic effects of ethinylestradiol in early life-stages of fathead minnow, Pimephales promelas. Ecotoxicology 11, 423–434. https://doi.org/10.1023/A:1021053217513

Van Aerle, R., Runnalls, T.J., Tyler, C.R., 2004. Ontogeny of gonadal sex development relative to growth in fathead minnow. J. Fish Biol. 64, 355–369. https://doi.org/10.1111/j.0022-1112.2004.00296.x

Van Aggelen, G., Ankley, G.T., Baldwin, W.S., Bearden, D.W., Benson, W.H., Chipman, J.K., Collette, T.W., Craft, J.A., Denslow, N.D., Embry, M.R., Falciani, F., George, S.G., Helbing, C.C., Hoekstra, P.F., Iguchi, T., Kagami, Y., Katsiadaki, I., Kille, P., Liu, L., Lord, P.G., McIntyre, T., O'Neill, A., Osachoff, H., Perkins, E.J., Santos, E.M., Skirrow, R.C., Snape, J.R., Tyler, C.R., Versteeg, D., Viant, M.R., Volz, D.C., Williams, T.D., Yu, L., 2010. Integrating omic technologies into aquatic ecological risk assessment and environmental monitoring: Hurdles, achievements, and future outlook. Environ. Health Perspect. 118, 1–5. https://doi.org/10.1289/ehp.0900985

Van den Belt, K., Wester, P.W., van der Ven, L.T.M., Verheyen, R., Witters, H., 2002. Effects of ethynylestradiol on the reproductive physiology in zebrafish (*Danio rerio*): Time dependency and reversibility. Environ. Toxicol. Chem. 21, 767–775. https://doi.org/10.1002/etc.5620210412

Vera-Chang, M.N., St-Jacques, A.D., Gagné, R., Martyniuk, C.J., Yauk, C.L., Moon, T.W.,

Trudeau, V.L., 2018. Transgenerational hypocortisolism and behavioral disruption are induced by the antidepressant fluoxetine in male zebrafish Danio rerio. Proc. Natl. Acad. Sci. 115, E12435–E12442. https://doi.org/10.1073/pnas.1811695115

Versonnen, B.J., Arijs, K., Verslycke, T., Lema, W., Janssen, C.R., 2003. In vitro and in vivo estrogenicity and toxicity of o-, m-, and p-dichlorobenzene. Environ. Toxicol. Chem. 22, 329–335.

Vidal-Dorsch, D.E., Bay, S.M., Maruya, K., Snyder, S.A., Trenholm, R.A., Vanderford, B.J., 2012. Contaminants of emerging concern in municipal wastewater effluents and marine receiving water. Environ. Toxicol. Chem. 31, 2674–2682. https://doi.org/10.1002/ETC.2004

Villeneuve, D.L., Crump, D., Garcia-Reyero, N., Hecker, M., Hutchinson, T.H., LaLone, C.A., Landesmann, B., Lettieri, T., Munn, S., Nepelska, M., Ottinger, M.A., Vergauwen, L., Whelan, M., 2014. Adverse outcome pathway (AOP) development I: Strategies and principles. Toxicol. Sci. 142, 312–320. https://doi.org/10.1093/toxsci/kfu199

Villeneuve, D.L., Garcia-Reyero, N., 2011. Vision & strategy: Predictive ecotoxicology in the 21st century. Environ. Toxicol. Chem. 30, 1–8. https://doi.org/10.1002/etc.396

Villeneuve, D.L., Knoebl, I., Kahl, M.D., Jensen, K.M., Hammermeister, D.E., Greene, K.J., Blake, L.S., Ankley, G.T., 2006. Relationship between brain and ovary aromatase activity and isoform-specific aromatase mRNA expression in the fathead minnow (Pimephales promelas). Aquat. Toxicol. 76, 353–368. https://doi.org/10.1016/j.aquatox.2005.10.016

Vogel, C., Marcotte, E.M., 2012. Insights into the regulation of protein abundance from proteomic and transcriptomic analyses. Nat. Rev. Genet. 13, 227–232. https://doi.org/10.1038/nrg3185

Voisin, A.-S., Kültz, D., Silvestre, F., 2019. Early-life exposure to the endocrine disruptor 17-α-

ethinylestradiol induces delayed effects in adult brain, liver and ovotestis proteomes of a self-fertilizing fish. J. Proteomics 194, 112–124. https://doi.org/10.1016/j.jprot.2018.12.008

Wang, P., Xia, P., Yang, J., Wang, Z., Peng, Y., Shi, W., Villeneuve, D.L., Yu, H., Zhang, X., 2018. A Reduced Transcriptome Approach to Assess Environmental Toxicants Using Zebrafish Embryo Test. Environ. Sci. Technol. 52, 821–830. https://doi.org/10.1021/acs.est.7b04073

Warkus, E.L.L., Marikawa, Y., 2018. Fluoxetine Inhibits Canonical Wnt Signaling to Impair Embryoid Body Morphogenesis: Potential Teratogenic Mechanisms of a Commonly Used Antidepressant. Toxicol. Sci. 165, 372–388. https://doi.org/10.1093/toxsci/kfy143

Weber, L.P., Balch, G.C., Metcalfe, C.D., Janz, D.M., 2004. Increased kidney, liver, and testicular cell death after chronic exposure to 17α-ethinylestradiol in medaka (Oryzias latipes). Environ. Toxicol. Chem. 23, 792. https://doi.org/10.1897/02-570

Weber, L.P., Hill, R.L., Janz, D.M., 2003. Developmental estrogenic exposure in zebrafish (Danio rerio): II. Histological evaluation of gametogenesis and organ toxicity. Aquat. Toxicol. 63, 431–446. https://doi.org/10.1016/S0166-445X(02)00208-4

Webster, A.F., Zumbo, P., Fostel, J., Gandara, J., Hester, S.D., Recio, L., Williams, A., Wood, C.E., Yauk, C.L., Mason, C.E., 2015. Mining the Archives: A Cross-Platform Analysis of Gene Expression Profiles in Archival Formalin-Fixed Paraffin-Embedded Tissues. Toxicol. Sci. 148, 460–472. https://doi.org/10.1093/toxsci/kfv195

Weil, M., Scholz, S., Zimmer, M., Sacher, F., Duis, K., 2009. Gene expression analysis in zebrafish embryos: A potential approach to predict effect concentrations in the fish early life stage test. Environ. Toxicol. Chem. 28, 1970. https://doi.org/10.1897/08-627.1

Weinberger, J., Klaper, R., 2014. Environmental concentrations of the selective serotonin

reuptake inhibitor fluoxetine impact specific behaviors involved in reproduction, feeding and predator avoidance in the fish Pimephales promelas (fathead minnow). Aquat. Toxicol. 151, 77–83. https://doi.org/10.1016/j.aquatox.2013.10.012

Wheeler, J.R., Maynard, S.K., Crane, M., 2014. An evaluation of fish early life stage tests for predicting reproductive and longer-term toxicity from plant protection product active substances. Environ. Toxicol. Chem. 33, 1874–1878. https://doi.org/10.1002/etc.2630

Winder, V.L., Sapozhnikova, Y., Pennington, P.L., Wirth, E.F., 2009. Effects of fluoxetine exposure on serotonin-related activity in the sheepshead minnow (Cyprinodon variegatus) using LC/MS/MS detection and quantitation. Comp. Biochem. Physiol. Part C Toxicol. Pharmacol. 149, 559–565. https://doi.org/10.1016/j.cbpc.2008.12.008

Wiśniewski, J.R., Rakus, D., 2014. Multi-enzyme digestion FASP and the 'Total Protein Approach'-based absolute quantification of the Escherichia coli proteome. J. Proteomics 109, 322–331. https://doi.org/10.1016/J.JPROT.2014.07.012

Wiśniewski, J.R., Zougman, A., Nagaraj, N., Mann, M., 2009. Universal sample preparation method for proteome analysis. Nat. Methods 6, 359–362. https://doi.org/10.1038/nmeth.1322

Wolf, J.C., Wheeler, J.R., 2018. A critical review of histopathological findings associated with endocrine and non-endocrine hepatic toxicity in fish models. Aquat. Toxicol. 197, 60–78. https://doi.org/10.1016/j.aquatox.2018.01.013

Wong, D.T., Hornq, J.S., Bymaster, F.P., Hauser, K.L., Molloy, H.B., 1974. A selective inhibitor of serotonin uptake: Lilly 110140, 3-(p-trifluromethylphenoxy)-n-methyl-3-phenylpropylamine. Lifs Sci. 15, 471–479.

Wong, R.Y., Oxendine, S.E., Godwin, John, Cryan, J., Sweeney, F., Durant, C., Christmas, D.,

Nutt, D., Jacobson, L., Cryan, J., Westenberg, H., Pinna, G., Costa, E., Guidotti, A., Wong, D., Bymaster, F., Engleman, E., Wong, D., Bymaster, F., Reid, L., Fuller, R., Perry, K., Koch, S., Perry, K., Nelson, D., Conway, R., Threlkeld, P., Bymaster, F., Robertson, D., Krushinski, J., Fuller, R., Leander, J., Egan, R., Bergner, C., Hart, P., Cachat, J., Canavello, P., Elegante, M., Elkhayat, S., Bartels, B., Tien, A., Tien, D., Dulawa, S., Holick, K., Gundersen, B., Hen, R., Pinna, G., Costa, E., Guidotti, A., Pinna, G., Costa, E., Guidotti, A., Longone, P., Michele, F. Di, D'Agati, E., Romeo, E., Pasini, A., Rupprecht, R., Barbaccia, M., Reddy, D., O'Malley, B., Rogawski, M., Pinna, G., Rasmusson, AM, Schule, C., Eser, D., Baghai, T., Nothdurfter, C., Kessler, J., Rupprecht, R., Guidotti, A., Dong, E., Matsumoto, K., Pinna, G., Rasmusson, AM, Costa, E., Pinna, G., Dong, E., Matsumoto, K., Costa, E., Guidotti, A., Jain, N., Hirani, K., Chopde, C., Bitran, D., Foley, M., Audette, D., Leslie, N., Frye, C., Landgraf, R., Semsar, K., Perreault, H., Godwin, J, Cryan, J., Holmes, A., Overli, O., Pottinger, T., Carrick, T., Overli, E., Winberg, S., Landgraf, R., Wigger, A., Wong, R., Perrin, F., Oxendine, S., Kezios, Z., Sawyer, S., Zhou, L., Dereje, S., Godwin, J, Maximino, C., Brito, T. de, Batista, A. da S., Herculano, A., Morato, S., Gouveia, A., Stewart, A., Gaikwad, S., Kyzar, E., Green, J., Roth, A., Kalueff, A., Clark, K., Boczek, N., Ekker, S., Steenbergen, P., Richardson, M., Champagne, D., Champagne, D., Hoefnagels, C., Kloet, R. de, Richardson, M., Howe, K., Clark, M., Torroja, C., Torrance, J., Berthelot, C., Muffato, M., Collins, J., Humphray, S., McLaren, K., Matthews, L., Griebel, G., Belzung, C., Perrault, G., Sanger, D., Miller, B., Schultz, L., Gulati, A., Su, A., Pletcher, M., Panula, P., Chen, Y., Priyadarshini, M., Kudo, H., Semenova, S., Sundvik, M., Sallinen, V., Lillesaar, C., Wang, Y., Takai, R., Yoshioka, H., Shirabe, K., Gould, G., Brooks, B., Park, J., Heah, T., Gouffon, J., Henry, T., Sayler, G., Zon, L., Peterson, R., Rihel, J., Schier,

A., Grunwald, D., Eisen, J., Brooks, B., Chambliss, C., Stanley, J., Ramirez, A., Banks, K., Johnson, R., Lewis, R., Gaworecki, K., Klaine, S., Paterson, G., Metcalfe, C., Auer, P., Doerge, R., Wu, T., Nacu, S., Trapnell, C., Roberts, A., Goff, L., Pertea, G., Kim, D., Kelley, D., Pimentel, H., Salzberg, S., Rinn, J., Pachter, L., Trapnell, C., Williams, B., Pertea, G., Mortazavi, A., Kwan, G., Baren, M. van, Salzberg, S., Wold, B., Pachter, L., Trapnell, C., Hendrickson, D., Sauvageau, M., Goff, L., Rinn, J., Pachter, L., Reimand, J., Arak, T., Vilo, J. g, Reimand, J., Kull, M., Peterson, H., Hansen, J., Vilo, J. g, Cummings, M., Larkins-Ford, J., Reilly, C., Wong, R., Ramsey, M, Hofmann, H., Lynch, K., Ramsey, ME, Cummings, M., Ramsey, ME, Maginnis, T., Wong, R., Brock, C., Cummings, M., Pfaffl, M., Horgan, G., Dempfle, L., McCurley, A., Callard, G., Sousa, N., Almeida, O., Wotjak, C., Uzunova, V., Sheline, Y., Davis, J., Rasmusson, A, Uzunov, D., Costa, E., Guidotti, A., Godwin, J, Thompson, R., Braida, D., Donzelli, A., Martucci, R., Capurro, V., Busnelli, M., Chini, B., Sala, M., Thorsell, A., Neumann, I., Landgraf, R., Karlsson, R., Holmes, A., Heilig, M., Crawley, J., Slattery, D., Neumann, I., Kask, A., Harro, J., Horsten, S. von, Redrobe, J., Dumont, Y., Quirion, R., Missig, G., Ayers, L., Schulkin, J., Rosen, J., Trent, N., Menard, J., Onaka, T., Takayanagi, Y., Yoshida, M., Meyer-Lindenberg, A., Domes, G., Kirsch, P., Heinrichs, M., Labuschagne, I., Phan, K., Wood, A., Angstadt, M., Chua, P., Heinrichs, M., Stout, J., Nathan, P., Petrovic, P., Kalisch, R., Singer, T., Dolan, R., Donner, J., Sipila, T., Ripatti, S., Kananen, L., Chen, X., Kendler, K., Lonnqvist, J., Pirkola, S., Hettema, J., Hovatta, I., Bonga, S.W., Barton, B., Alsop, D., Vijayan, M., Fekete, E., Zorrilla, E., Pan, W., Kastin, A., Gysling, K., Forray, M., Haeger, P., Daza, C., Rojas, R., Neufeld-Cohen, A., Tsoory, M., Evans, A., Getselter, D., Gil, S., Lowry, C., Vale, WW, Chen, A., Spina, M., Merlo-Pich, E., Akwa, Y., Balducci, C., Basso, A.,

Zorrilla, E., Britton, K., Rivier, J, Vale, WW, Koob, G., Gehlert, D., Shekhar, A., Morin, S., Hipskind, P., Zink, C., Gackenheimer, S., Shaw, J., Fitz, S., Sajdyk, T., Moreau, J., Kilpatrick, G., Jenck, F., Slawecki, C., Somes, C., Rivier, JE, Ehlers, C., Sajdyk, T., Schober, D., Gehlert, D., Shekhar, A., Venihaki, M., Sakihara, S., Subramanian, S., Dikkes, P., Weninger, S., Liapakis, G., Graf, T., Majzoub, J., Jamieson, P., Li, C., Kukura, C., Vaughan, J., Vale, W, Deussing, J., Breu, J., Kuhne, C., Kallnik, M., Bunck, M., Glasl, L., Yen, Y., Schmidt, M., Zurmuhlen, R., Vogl, A., Lennartsson, A., Jonsdottir, I., Diaz-Moran, S., Palencia, M., Mont-Cardona, C., Canete, T., Blazquez, G., Martinez-Membrives, E., Lopez-Aumatell, R., Tobena, A., Fernandez-Teruel, A., Torner, L., Neumann, I., Pottinger, T., Prunet, P., Pickering, A., Avella, M., Schreck, C., Prunet, P., Liu, G., Cai, G., Cai, Y., Sheng, Z., Jiang, J., Mei, Z., Wang, Z., Guo, L., Fei, J., Mennigen, J., Martyniuk, C., Crump, K., Xiong, H., Zhao, E., Popesku, J., Anisman, H., Cossins, A., Xia, X., Trudeau, V., Benton, C., Miller, B., Skwerer, S., Suzuki, O., Schultz, L., Cameron, M., Marron, J., Pletcher, M., Wiltshire, T., Huang, G., Ben-David, E., Piella, A.T., Edwards, A., Flint, J., Shifman, S., Lee, J., Ko, E., Kim, YE, Min, J., Liu, J., Kim, Y, Shin, M., Hong, M., Bae, H., Griffith, M., Griffith, O., Mwenifumbo, J., Goya, R., Morrissy, A., Morin, R., Corbett, R., Tang, M., Hou, Y., Pugh, T., Morey, J., Ryan, J., Dolah, F. Van, Hawlena, D., Schmitz, O., Lima, S., MÃ¸ller, M.A.P., Peter, J., Santos, E., Kille, P., Workman, V., Paull, G., Tyler, C., Toth, A., Varala, K., Newman, T., Miguez, F., Hutchison, S., Willoughby, D., Simons, J., Egholm, M., Hunt, J., Hudson, M., Robinson, G., Sarma, M. Sen, Whitfield, C., Robinson, G., Whitfield, C., Cziko, A.-M., Robinson, G., Aubin-Horth, N., Landry, C., Letcher, B., Hofmann, H., Renn, S., Aubin-Horth, N., Hofmann, H., Sanogo, Y., Hankison, S., Band, M., Obregon, A., Bell, A., Catalan, A., Hutter, S., Parsch, J., Drew, R., Settles, M.,

Churchill, E., Williams, S., Balli, S., Robison, B., Wong, R., Ramsey, ME, Cummings, M., Fitzpatrick, M., Ben-Shahar, Y., Smid, H., Vet, L., Robinson, G., Sokolowski, M., Wada, K., Howard, J., McConnell, P., Whitney, O., Lints, T., Rivas, M., Horita, H., Patterson, M., White, S., Scharff, C., Kanehisa, M., Goto, S., Sato, Y., Furumichi, M., Tanabe, M., Kanehisa, M., Goto, S., Mennigen, J., Lado, W., Zamora, J., Duarte-Guterman, P., Langlois, V., Metcalfe, C., Chang, J., Moon, T., Trudeau, V., Gunn, B., Brown, A., Lambert, J., Belelli, D., Zimmerberg, B., Brunelli, S., Hofer, M., Akwa, Y., Purdy, R., Koob, G., Britton, K., Evans, J., Sun, Y., McGregor, A., Connor, B., Engin, E., Treit, D., Homberg, J., Olivier, J., Blom, T., Arentsen, T., Brunschot, C. van, Schipper, P., Korte-Bouws, G., Luijtelaar, G. van, Reneman, L., Bouet, V., Klomp, A., Freret, T., Wylezinska-Arridge, M., Lopez-Tremoleda, J., Dauphin, F., Boulouard, M., Booij, J., Gsell, W., Reneman, L., Olivier, J., Blom, T., Arentsen, T., Homberg, J., 2013. Behavioral and neurogenomic transcriptome changes in wild-derived zebrafish with fluoxetine treatment. BMC Genomics 14, 348. https://doi.org/10.1186/1471-2164-14-348

Wu, Fengchang, Fang, Y., Li, Yushuang, Cui, X., Zhang, R., Guo, G., Giesy, J.P., Wu, F, Fang, @bullet Y, Li, Y, Whitacre, D.M., 2014. Predicted No-Effect Concentration and Risk Assessment for 17-[Beta]-Estradiol in Waters of China, in: Whitacre, D.M. (Ed.), Reviews of Environmental Contamination and Toxicology. Springer International Publishing, Switzerland. https://doi.org/10.1007/978-3-319-01619-1_2

Wu, L., Candille, S.I., Choi, Y., Xie, D., Jiang, L., Li-Pook-Than, J., Tang, H., Snyder, M., 2013. Variation and genetic control of protein abundance in humans. Nature 499, 79–82. https://doi.org/10.1038/nature12223

Xu, F., Luk, C., Richard, M.P., Zaidi, W., Farkas, S., Getz, A., Lee, A., Van Minnen, J., Syed,

N.I., 2010. Antidepressant fluoxetine suppresses neuronal growth from both vertebrate and invertebrate neurons and perturbs synapse formation between Lymnaea neurons. Eur. J. Neurosci. 31, 994–1005. https://doi.org/10.1111/j.1460-9568.2010.07129.x

Yadetie, F., Zhang, X., Hanna, E.M., Aranguren-Abadía, L., Eide, M., Blaser, N., Brun, M., Jonassen, I., Goksøyr, A., Karlsen, O.A., 2018. RNA-Seq analysis of transcriptome responses in Atlantic cod (Gadus morhua) precision-cut liver slices exposed to benzo[a]pyrene and 17α-ethynylestradiol. Aquat. Toxicol. 201, 174–186. https://doi.org/10.1016/j.aquatox.2018.06.003

Yang, L., Allen, B.C., Thomas, R.S., 2007. BMDExpress: A software tool for the benchmark dose analyses of genomic data. BMC Genomics 8, 387. https://doi.org/10.1186/1471-2164-8-387

Yeung, Y., Stanley, E.R., 2010. Rapid Detergent Removal from Peptide Samples with Ethyl Acetate for Mass Spectrometry Analysis. Curr. Protoc. Protein Sci. 59, 16.12.1-16.12.5. https://doi.org/10.1002/0471140864.ps1612s59

Yim, S.H., Everley, R.A., Schildberg, F.A., Lee, S.G., Orsi, A., Barbati, Z.R., Karatepe, K., Fomenko, D.E., Tsuji, P.A., Luo, H.R., Gygi, S.P., Sitia, R., Sharpe, A.H., Hatfield, D.L., Gladyshev, V.N., 2018. Role of Selenof as a Gatekeeper of Secreted Disulfide-Rich Glycoproteins. Cell Rep. 23, 1387–1398. https://doi.org/10.1016/j.celrep.2018.04.009

Zhang, X., Hecker, M., Park, J.-W., Tompsett, A.R., Newsted, J., Nakayama, K., Jones, P.D., Au, D., Kong, R., Wu, R.S.S., Giesy, J.P., 2008. Real-time PCR array to study effects of chemicals on the Hypothalamic–Pituitary–Gonadal axis of the Japanese medaka. Aquat. Toxicol. 88, 173–182. https://doi.org/10.1016/j.aquatox.2008.04.009

Zhang, X., Wang, P., Xia, P., 2020. Dose-Dependent Transcriptomic Approach for Mechanistic

Screening in Chemical Risk Assessment, in: Jiang, G., Li, X. (Eds.), A New Paradigm for Environmental Chemistry and Toxicology. Springer Singapore, Singapore, pp. 33–56. https://doi.org/10.1007/978-981-13-9447-8_4

Zhang, X., Xia, P., Wang, P., Yang, J., Baird, D.J., 2018. Omics Advances in Ecotoxicology. Environ. Sci. Technol. 52, 3842–3851. https://doi.org/10.1021/acs.est.7b06494

Zong, X., Yang, H., Yu, Y., Zou, D., Ling, Z., He, X., Meng, X., 2011. Possible role of pax-6 in promoting breast cancer cell proliferation and tumorigenesis. BMB Rep. 44, 595–600. https://doi.org/10.5483/BMBRep.2011.44.9.595

APPENDICES

APPENDIX A

Table A.S1. CRediT author statement

Term	Definition
Conceptualization	Ideas; formulation or evolution of overarching research goals and aims
Methodology	Development or design of methodology; creation of models
Software	Programming, software development; designing computer programs; implementation of the computer code and supporting algorithms; testing of existing code components
Validation	Verification, whether as a part of the activity or separate, of the overall replication/ reproducibility of results/experiments and other research outputs
Formal analysis	Application of statistical, mathematical, computational, or other formal techniques to analyze or synthesize study data
Investigation	Conducting a research and investigation process, specifically performing the experiments, or data/evidence collection
Resources	Provision of study materials, reagents, materials, patients, laboratory samples, animals, instrumentation, computing resources, or other analysis tools
Data Curation	Management activities to annotate (produce metadata), scrub data and maintain research data (including software code, where it is necessary for interpreting the data itself) for initial use and later reuse
Writing - Original Draft	Preparation, creation and/or presentation of the published work, specifically writing the initial draft (including substantive translation)
Writing - Review & Editing	Preparation, creation and/or presentation of the published work by those from the original research group, specifically critical review, commentary or revision – including pre-or postpublication stages
Visualization	Preparation, creation and/or presentation of the published work, specifically visualization/ data presentation
Supervision	Oversight and leadership responsibility for the research activity planning and execution, including mentorship external to the core team
Project administration	Management and coordination responsibility for the research activity planning and execution
Funding acquisition	Acquisition of the financial support for the project leading to this publication

This table is reprinted from Allen *et al.*, (2019). Copyright (2019), with permission from the Association of Learned & Professional Society Publishers (Learned Publishing).

APPENDIX B

B.1. Chemical analyses

Water samples from exposure tanks were collected at three time points during the flow-through exposure experiment (4, 14 and 28dph). Water samples were collected from each replicate tank and pooled for analyses at each time point. Concentrations of EE2 in exposure solutions were measured at SGS AXYS Analytical Services Ltd, Sidney BC, Canada using a protocol published previously (Long *et al*., 2013). Briefly, water samples were extracted by solid-phase extraction and were spiked with d4-17α-ethinylestradiol (d4-EE2; CDN Isotopes, Pointe-Claire QC, Canada; Prod# D-4319) for quantification by isotope dilution using a Waters 2690 HPLC or Waters 2795 HPLC (Waters, Milford MA, USA), equipped with a Waters Xterra MS C18 (10.0 cm length, 2.1 mm i.d., 3.5 μm particle size; Waters), coupled with a Micromass Quattro Ultima MS/MS (Waters) operating in negative ion electrospray mode at unit resolution. A gradient elution using (A) water at pH = 10 (adjusted using NH_4OH) and (B) 1:1 acetonitrile:methanol was used. A seven-point calibration curve ranging from 1.25-780 ng/mL was used for quantitation using 1/x weighted linear calibration and response relative to d4-EE2. Measured concentrations were corrected for % recovery of d4-EE2. The limit of detection was 6.46 ng/L.

B.2. Transcriptomics

Since the concentration of EE2 in the low treatment group was below detection limits, only the samples from the solvent control, medium, and high treatment groups were used to assess transcriptional responses. Total RNA was extracted from pooled whole embryos for each replicate using RNEasy Plus Universal Mini Kit (Qiagen, Hilden, Germany; Cat# 73404) following the manufacturer's protocol for whole tissue total RNA extraction. Total RNA concentrations were

measured using the QIAxpert (Qiagen) and the RNA Integrity Number (RIN) was assessed with an Agilent RNA 6000 Nano kit (Agilent Technologies, Waldbronn, Germany; Part#5067-1511) in an Agilent 2100 Bioanalyzer (Agilent Technologies). Samples with RIN > 8 were sent to the McGill University and Génome Québec Innovation Centre for 200 base-pairs paired-end (100x2) sequencing using a HiSeq 4000 instrument (Illumina Inc, San Diego CA, USA).

Raw fastq files were assessed using FastQC(Andrews, n.d.) and trimmed, in pairs, to a minimum phred score of 20 and a minimum length of 35 bases per paired read using Trimmomatic (Bolger *et al*., 2014). Reads were aligned against the latest FHM reference genome build (NCBI Acc# WIOS00000000) using HISAT2 (Kim *et al*., 2015). StringTie was used to reconstruct the transcriptome and to estimate expression levels of transcripts and genes (Pertea *et al*., 2015). Raw counts were filtered to remove features with less than five counts per million in at least five samples and were normalized by use of the trimmed mean of M values (TMM) approach (Robinson and Oshlack, 2010) using edgeR (McCarthy *et al*., 2012; Robinson *et al*., 2010). Replicate1 of the solvent control group did not cluster with other replicates within the treatment group (**Figure B.S5**); thus, it was not included in the differential expression analysis. Significance of differentially expressed genes (DEG) were assessed using the quasi-likelihood pipeline (Chen *et al*., 2016), and scored with a cut-off false discovery rate (FDR; Benjamini-Hochberg) of ≤ 0.05 and a minimum effect size threshold fold-change $|FC| > 1.5$ relative to the solvent control group. Default software settings were used for analyses, unless otherwise stated. Raw fastq files are available through the NCBI GEO accession# GSE156916.

B.3. Proteomics

The transcriptomic analyses showed more pronounced transcriptional perturbations in the high treatment group; thus, only the samples from the solvent and high treatment groups were selected for non-targeted proteomics analysis. Cell disruption and protein solubilization were done using SDT buffer (4% Sodium dodecyl sulfate (SDS; Sigma-Aldrich, St. Louis MO, USA; Cat# 436143), 0.1 M Dithiothreitol (DTT; Thermo Fisher Scientific, Waltham MA, USA, Cat# R0862), 0.1 M Tris/HCl (Sigma-Aldrich, Cat# 10812846001; pH = 7.6) lysis buffer in a Thermomixer® (Eppendorf, Hamburg, Germany) at 95ºC, for 2 hours. Quality of protein extracts was assessed by use of 1D SDS-PAGE (12% gels). Protein extracts were then processed following standard protocol for filter-aided sample preparation (FASP) (Wiśniewski *et al*., 2009; Wiśniewski and Rakus, 2014). Briefly, proteins were alkylated using 50 mM iodoacetamide (Sigma-Aldrich, Cat# I1149) for 20 mins at RT and digested using trypsin (Sequencing grade; Promega, Madison WI, USA, Cat# V5111) in 50 mM ammonium bicarbonate at 37ºC for 18 hrs, on a 30 kDa membrane filter unit. Resulting peptides were eluted with ammonium bicarbonate (AB) buffer and the FASP eluates were kept at -80ºC until further LC-MS/MS analysis.

FASP eluates were cleaned using 3 iterations (Yeung and Stanley, 2010) of ethylacetate extraction to remove SDS contamination and then were completely dried in a SpeedVac vacuum concentrator (Thermo Fisher Scientific, Waltham MA, USA). Cleaned peptides were reconstituted by acid extraction using 50 µl of (1:1) 5% formic acid (LC-MS grade, >99% purity; Fisher Scientific Cat# A11750) and 100% acetonitrile (HPLC grade, >99.9%; Sigma-Aldrich, Cat# 34851), with 1.5 µl of 0.01% poly(ethylene glycol) (PEG; Millipore-Sigma, Cat# 95172) to reduce sample loses. The final solution was transferred to a TPX (polymethylpentane) vial and vacuum concentrated using SpeedVac vacuum concentrator to a final volume of 15 µl.

LC-MS/MS analyses were conducted using an Orbitrap Fusion™ Lumos™ Tribrid Mass Spectrometer system (Thermo Fisher Scientific) connected online to an Ultimate 3000 RSLCnano system (consisted of SRD-3400, NCS-3500RS CAP, WPS-3000 TPL RS; Thermo Fisher Scientific). Prior to LC separation, tryptic digests were online concentrated and desalted on a cartridge trapping column (300 µm × 5 mm, C18 PepMap100, 5µm particles, 100 A; Thermo Fisher Scientific, Cat#160454) using 0.1% formic acid (FA) in water. The peptides were eluted from the trapping column onto an Acclaim Pepmap100 C18 analytical column (3 µm particles, 75 µm × 500 mm; Thermo Fisher Scientific, Cat# 164570) by non-linear gradient (2-35% of mobile phase B; mobile phase A: 0.1% FA in water; mobile phase B: 0.1% FA in 80% acetonitrile). The analytical column was directly connected to the Digital PicoView® 550 (New Objective, Woburn MA, USA) ion source with sheath gas option and SilicaTip emitter (New Objective; P/N: FS360-20-15-N-20-C12) utilization. Active Background Ion Reduction Device (ABIRD; ESI Source Solutions, Woburn MA, USA) was installed to the LC-MS/MS system to isolate the experiment from variable background ion interferences. MS data were acquired in a data-dependent acquisition strategy, selecting up to top 20 precursors based on precursor abundance in the survey scan (350 - 2000 m/z). The resolution of the survey scan was 120,000 (at 200 m/z) with a target value of 4×10^5 ions and maximum injection time of 100 ms. Higher-energy collisional dissociation (HCD) MS/MS spectra were acquired with a target value of 5×10^4 and resolution of 15,000 (at 200 m/z). The maximum injection time for MS/MS was 22 ms.

Raw mass spectrometric data files were analyzed using MaxQuant (Cox and Mann, 2008; Tyanova *et al*., 2016) with built-in Andromeda search engine (Cox *et al*., 2011). Samples were mapped against the FHM proteome assembly (NCBI Acc# WIOS00000000), combined with the cRAP contaminant database (January 2020; 246 sequences). The reference proteome was cleaned

for duplicated and highly similar sequences (>95% similarity; minimum of 35 amino acids; a total of 35,108 proteins) prior to analysis. Oxidation (M) and deamidation (N, Q) as optional modifications, carbamidomethylation (C) as fixed modification and two enzymes miss-cleavages were set for the first and main search. Peptides and proteins with an FDR (q-value) < 1% and at least one razor peptide (peptide that has been assigned to the Protein Group with the largest number of total identified) (Cox *et al.,* 2009) were selected for downstream analyses. Raw data were deposited in the ProteomeXchange Consortium via the Proteomics Identifications (PRIDE) partner repository (Accession# PXD021155).

All downstream differential protein abundance analyses were done in KNIME (Berthold *et al*., 2008) using the OmicsWorkflow pipeline found at the repository https://github.com/OmicsWorkflows. Protein groups with missing quantification values on all replicates within a treatment group were filtered out. Median normalization strategy was applied to all protein group intensities across samples (**Figure B.S2**). Significance of differentially abundant protein (DAP) groups was assessed using *limma* (Ritchie *et al*., 2015), with a cut-off moderated p-value of ≤ 0.05 and a minimum effect size threshold of |FC| > 1.5 relative to the solvent control group. *limma* estimates moderated p-values by using the whole dataset to shrink sample variances towards pooled estimate, which have been shown to be a practical approach in detecting DAP with minimal loss from false negatives (Kammers *et al*., 2015; Pascovici *et al*., 2016). Default software settings were used for analyses, unless otherwise stated.

B.4. Statistical Analyses

Survival rates of replicate 2 at 28dph showed extreme deviation (high mortality) from the rest of the dataset, resulting to relatively higher length and weight due to lesser competition within

a tank; thus, this replicate was not included in the statistical analyses of survival rates and morphometrics.

Fulton's condition factor (Froese, 2006) was calculated using the following equation:

$$\text{Fulton's condition factor, } k = \frac{w \times 100}{l^3}$$

where: w = weight in mg and l = length in mm.

Data on growth, condition factor, and survival rates were assessed for significant differences across treatment groups using a one-way analysis of variance (ANOVA), followed by Tukey's multiple comparison post-hoc test, with a cut-off p-value < 0.05. Tests for assumptions were performed prior to ANOVA. In cases where assumptions of ANOVA were not met, the non-parametric ANOVA analogue, Kruskal-Wallis test, was performed, followed by Dunn's multiple comparison test with a cut-off p-value < 0.05. Regression analyses were done on all treatment groups, excluding the water control group, using ordinary least-squares (OLS) linear regression.

Opportunistic eye histology was conducted on a randomly selected subset of fish across all replicates (solvent control, n=5; high treatment group, n=7). Assessments were made on one eye per fish at the widest cross-sectional area. The total cross section area of the eye was measured, as well as the total retina thickness and thickness of 3 individual retina layers: the photoreceptor layer (PRL), outer plexiform layer (OPL), and inner plexiform layer (IPL). Eye Index (EI) was calculated as: EI = [eye area (mm2)/fish length (mm)]*100 (modified from Hyeon *et al*., 2019)).

All non-omics statistical analyses were carried out in GraphPad Prism.

Table B.S1. List of software used in Chapter 2.

Software	Versions	Use
FastQC	v0.11.9	Quality control of raw reads
Trimmomatic	v0.38	Trimming of low quality and short reads (< 35 bp)
HISAT2	v2.1.0	Alignment of reads to the reference genome
StringTie	v1.3.4d	Counting mapped reads
edgeR	v3.26.5	Differential expression analysis
Samtools	v1.9	Data manipulation of aligned reads
Cytoscape	v3.7.1	Platform for downstream network analysis
g:Profiler	Ensembl 98, Ensembl Genomes 45 (rev 4d9abf6, database built on 2020-03-07)	Enrichment analyses
STRING	v11	Construction of PPI network
NetworkAnalyzer	v4.4.5	Docked in Cytoscape; Assessment of topological

		parameters of the PPI network
Galaxy Europe		Analysis platform for QuanTP
QuanTP	v1.0.0	Evaluation of transcript-protein pair concordance
MaxQuant	v.1.6.10.43	Quantitative proteomics software to identify proteins from mass spectra
KNIME	v3.7.2	Downstream (differential abundance analysis) quantitative proteomics analysis
GraphPad Prism	v8.4.2	Statistical analyses of survival and morphometrics

4382

4383

Table B.S2. Nominal and measured concentrations of EE2 in exposure tanks. Concentrations were based on percent (%) recovery of standard d4-EE2 spiked to the samples. Water samples were collected prior to (t = 4dph), during (t = 14 dph), and immediately after (t = 28dph) flow-through exposure. (t = time; dph = days post hatch; ND = not detectable/below detection limit).

Treatment Group	Nominal Concentration (ng/L)	Measured concentration @ t = 4dph	Measured concentration @ t = 14dph	Measured concentration @ t = 28dph	Average Concentration (ng/L)
Water Control	0	ND	ND	ND	ND
Solvent Control	0	ND	ND	ND	ND
Low dose	4	ND	ND	ND	ND
Medium dose	20	30.69	25.05	14.65	23.46 ± 8.13
High dose	100	118.51	86.33	83.11	95.99 ± 19.58

Table B.S3. Average physico-chemical characteristics of exposure solutions measured daily (temperature, pH, conductivity and dissolved oxygen) and weekly (ammonia, nitrates, nitrite, hardness and alkalinity).

Parameters	Values
Temperature	23.12 ± 0.77 ^{o}C
pH	8.28 ± 0.09
Conductivity	486.6 ± 12.5 µS/cm
Dissolved oxygen (DO)	104.4 ± 2.6 %
Ammonia	≤ 0.25 mg/L
Nitrates	0.68 ± 0.35 mg/L
Nitrite	≤ 0.05 mg/L
Hardness	175.43 ± 15.53 mg $CaCO_3$/L
Alkalinity	143.79 ± 7.22 mg $CaCO_3$/L

Table B.S4. Incidence of pathological features in control and exposed larval FHM.

FHM ELS				
TISSUE	**PATHOLOGIC FEATURE**	**INCIDENCE**		
		Solvent Control n=15	**Medium n=15**	**High n=15**
Gonad	Differentiation (ovaries vs. testes)	6M : 9F	14 ?* : 1 F	14 ?* : 1 F
Kidney	Tubules distorted / enlarged	0	6	15
	Tubule lumens dilated	0	1	13
	Tubule lumens contain eosinophilic fluid	0	1	13
	Epithelial cells hypertrophied / vacuolated / swollen	0	6	15
	Glomeruli - increased # and size	0	9	14
Liver	Hepatocyte basophilia	0	15	15
	Hepatocyte glycogen accumulation	12	4	0
	Hepatocyte lipid accumulation	0	0	0
	Eosinophilic intravascular fluid accumulation	0	15	15
Coelom	Eosinophilic fluid accumulation	0	6	14

*Gonad was either not detected, or was undifferentiated/poorly developed.

M – male

F – female

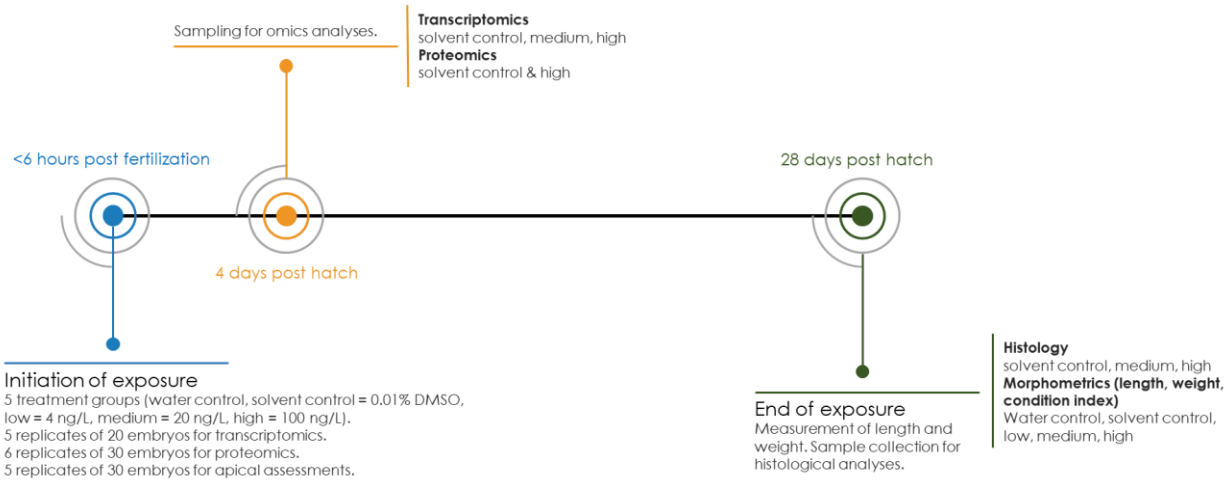

Figure B.S.1. Study design. Exposures were initiated at <6 hpf, between late cleavage and high blastula developmental stages. Samples for omics analyses were collected at 4dph. Exposure was terminated at 28dph, when measurements for lengths and weights of individual fish were taken and samples for histological analyses were preserved. Survival was monitored throughout the experiment.

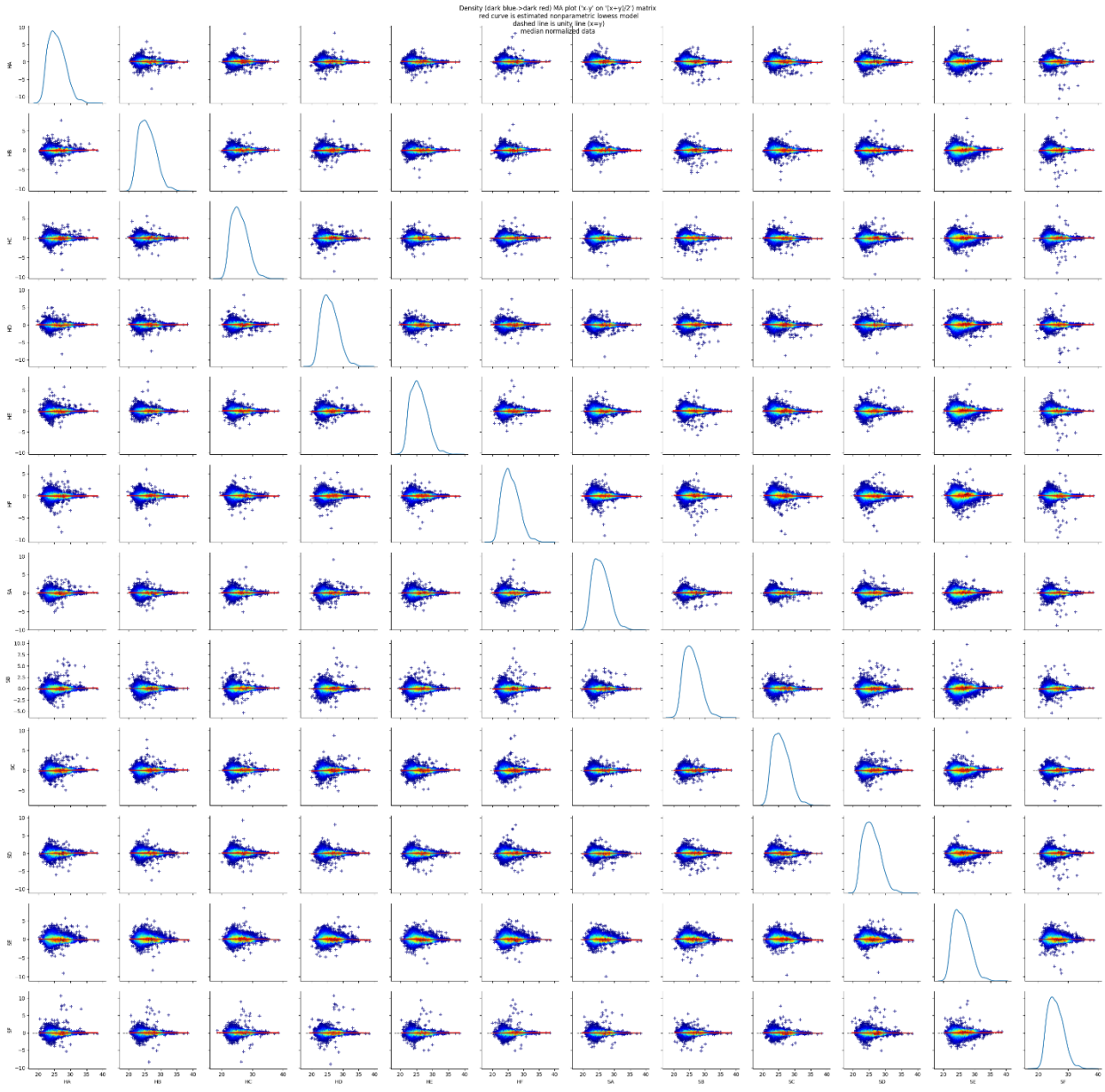

Figure B.S2. Median-normalized MA plot of proteomics samples.

1

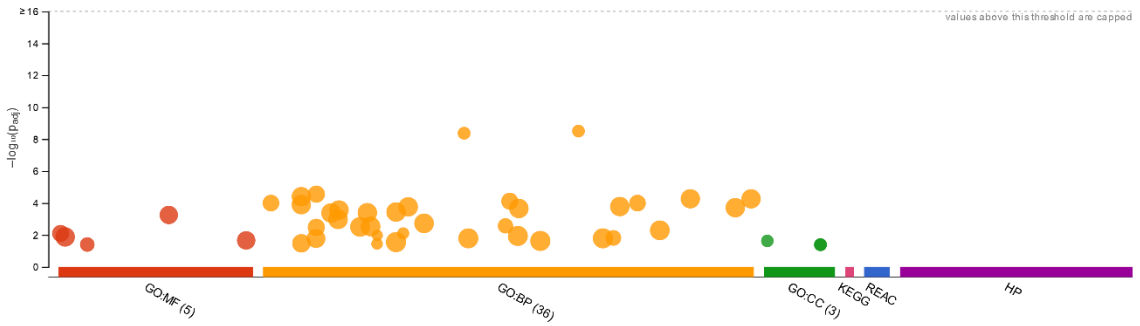

4407

Source	Term Name	Term ID	Term Size	Effective Domain Size	Adjusted p-value	Query Size	Intersection Size
GO:MF	sequence-specific DNA binding	GO:0043565	1400	23956	0.0005628	61	15
GO:MF	DNA-binding transcription factor activity, RNA polymerase II-specific	GO:0000981	612	23956	0.008051161	61	9
GO:MF	DNA binding	GO:0003677	2532	23956	0.013323067	61	18
GO:MF	transcription regulator activity	GO:0140110	1459	23956	0.021982549	61	13
GO:MF	lipid transporter activity	GO:0005319	149	23956	0.039864457	3	2
GO:BP	cellular response to estrogen stimulus	GO:0071391	49	21726	3.14E-09	8	5
GO:BP	response to estrogen	GO:0043627	52	21726	4.27E-09	8	5
GO:BP	sensory organ development	GO:0007423	673	21726	2.79751E-05	59	13
GO:BP	regulation of transcription, DNA-templated	GO:0006355	2348	21726	4.0026E-05	61	23
GO:BP	regulation of nucleic acid-templated transcription	GO:1903506	2387	21726	5.44804E-05	61	23
GO:BP	regulation of RNA biosynthetic process	GO:2001141	2388	21726	5.49082E-05	61	23
GO:BP	sensory system development	GO:0048880	604	21726	7.72972E-05	59	12
GO:BP	visual system development	GO:0150063	498	21726	0.000101471	59	11
GO:BP	eye development	GO:0001654	498	21726	0.000101471	59	11
GO:BP	transcription, DNA-templated	GO:0006351	2499	21726	0.000127586	61	23
GO:BP	nucleic acid-templated transcription	GO:0097659	2536	21726	0.000167206	61	23
GO:BP	RNA biosynthetic process	GO:0032774	2542	21726	0.000174618	61	23
GO:BP	regulation of cellular macromolecule biosynthetic process	GO:2000112	2559	21726	0.000197311	61	23
GO:BP	regulation of RNA metabolic process	GO:0051252	2575	21726	0.000221145	61	23
GO:BP	regulation of macromolecule biosynthetic process	GO:0010556	2607	21726	0.000277038	61	23
GO:BP	regulation of cellular biosynthetic process	GO:0031326	2648	21726	0.000367839	61	23
GO:BP	regulation of nucleobase-containing compound metabolic process	GO:0019219	2663	21726	0.000407454	61	23
GO:BP	regulation of biosynthetic process	GO:0009889	2668	21726	0.000421515	61	23
GO:BP	regulation of gene expression	GO:0010468	2809	21726	0.001061362	61	23
GO:BP	nucleobase-containing compound biosynthetic process	GO:0034654	2902	21726	0.00188774	61	23
GO:BP	eye morphogenesis	GO:0048592	221	21726	0.002656164	59	7
GO:BP	aromatic compound biosynthetic process	GO:0019438	2978	21726	0.002967349	61	23
GO:BP	heterocycle biosynthetic process	GO:0018130	2988	21726	0.0031456	61	23
GO:BP	central nervous system development	GO:0007417	685	21726	0.003348307	61	11
GO:BP	organic cyclic compound biosynthetic process	GO:1901362	3074	21726	0.00513877	61	23
GO:BP	response to estradiol	GO:0032355	33	21726	0.007982758	3	2

GO:BP	optic nerve development	GO:0021554	19	21726	0.010682539	47	3
GO:BP	regulation of nitrogen compound metabolic process	GO:0051171	3726	21726	0.011569677	61	25
GO:BP	sensory organ morphogenesis	GO:0090596	289	21726	0.015404875	59	7
GO:BP	regulation of primary metabolic process	GO:0080090	3798	21726	0.016327081	61	25
GO:BP	cellular nitrogen compound biosynthetic process	GO:0044271	3542	21726	0.016367354	61	24
GO:BP	nervous system development	GO:0007399	1716	21726	0.016918852	61	16
GO:BP	regulation of macromolecule metabolic process	GO:0060255	3878	21726	0.02367494	61	25
GO:BP	regulation of cellular metabolic process	GO:0031323	3917	21726	0.028260292	61	25
GO:BP	regulation of transcription by RNA polymerase II	GO:0006357	1426	21726	0.033534025	53	13
GO:BP	epithalamus development	GO:0021538	25	21726	0.036134688	53	3
GO:CC	photoreceptor outer segment	GO:0001750	45	21269	0.023710041	48	3
GO:CC	photoreceptor cell cilium	GO:0097733	54	21269	0.040858593	48	3
GO:CC	9+0 non-motile cilium	GO:0097731	54	21269	0.040858593	48	3

2

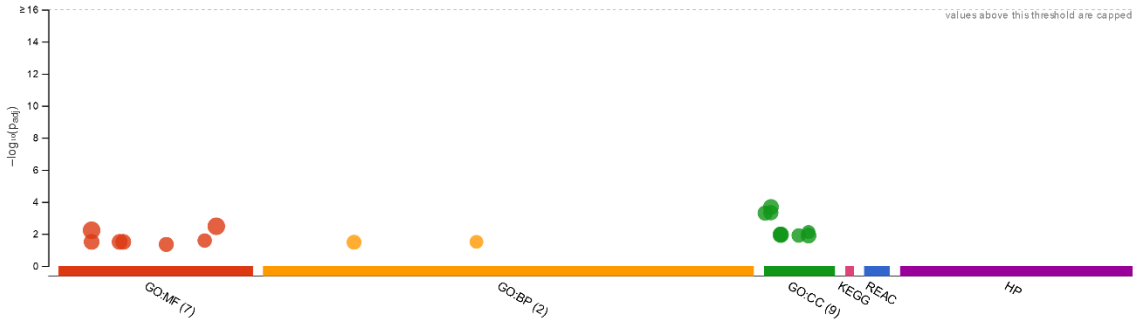

4408

Source	Term Name	Term ID	Term Size	Effective Domain Size	Adjusted p-value	Query Size	Intersection Size
GO:MF	peptidase activity, acting on L-amino acid peptides	GO:0070011	821	23956	0.003372	252	24
GO:MF	peptidase activity	GO:0008233	850	23956	0.005988	252	24
GO:MF	cell adhesion molecule binding	GO:0050839	129	23956	0.026204	75	5
GO:MF	hydrolase activity, acting on acid phosphorus-nitrogen bonds	GO:0016825	291	23956	0.031913	252	12
GO:MF	serine hydrolase activity	GO:0017171	291	23956	0.031913	252	12
GO:MF	serine-type peptidase activity	GO:0008236	291	23956	0.031913	252	12
GO:MF	identical protein binding	GO:0042802	191	23956	0.04578	132	7
GO:BP	cell-cell junction organization	GO:0045216	86	21726	0.031689	90	5
GO:BP	lipid catabolic process	GO:0016042	170	21726	0.033548	252	10
GO:CC	vacuole	GO:0005773	288	21269	0.000211	270	16
GO:CC	lysosome	GO:0005764	204	21269	0.000479	269	13
GO:CC	lytic vacuole	GO:0000323	205	21269	0.000506	269	13
GO:CC	tight junction	GO:0070160	87	21269	0.007644	90	5
GO:CC	sarcomere	GO:0030017	133	21269	0.010018	150	7
GO:CC	cell junction	GO:0030054	411	21269	0.011365	35	6
GO:CC	myofibril	GO:0030016	137	21269	0.0121	150	7
GO:CC	contractile fiber	GO:0043292	138	21269	0.012672	150	7
GO:CC	anchoring junction	GO:0070161	271	21269	0.012861	33	5

3

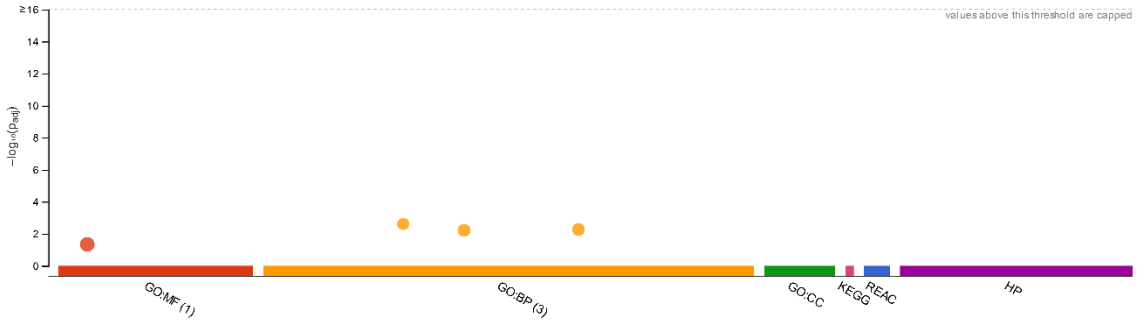

Source	Term Name	Term ID	Term Size	Effective Domain Size	Adjusted p-value	Query Size	Intersection Size
GO:MF	lipid transporter activity	GO:0005319	149	23956	0.045559	3	2
GO:BP	response to estradiol	GO:0032355	33	21726	0.002412	3	2
GO:BP	cellular response to estrogen stimulus	GO:0071391	49	21726	0.00537	3	2
GO:BP	response to estrogen	GO:0043627	52	21726	0.006054	3	2

Figure B.S3. Manhattan plots of significantly enriched pathways from (**1**) significantly upregulated genes from high treatment group, (**2**) significantly downregulated genes from high treatment group, and (**3**) all significantly dysregulated genes from medium treatment group. Enrichment analyses were conducted using g:Profiler with cut-off threshold enrichment p-value < 0.05. (MF – molecular function; BP – biological process; CC – cellular component; KEGG – Kyoto Encyclopedia of Genes and Genomes; REAC – Reactome; HP – Human Phenotype Ontology).

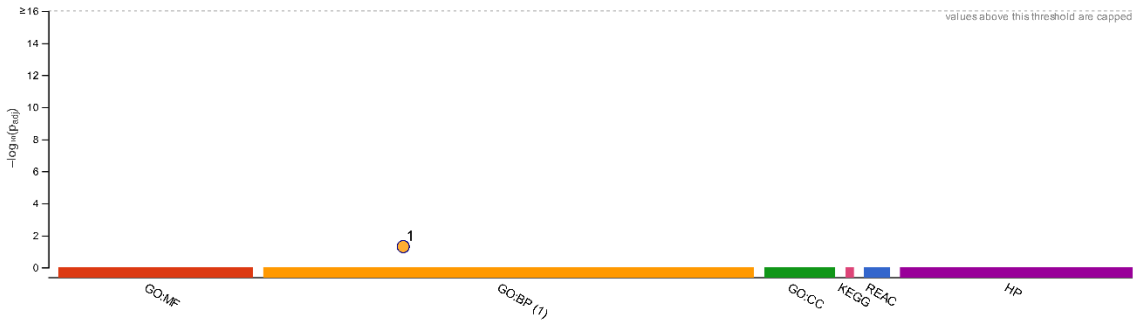

Source	Term Name	Term ID	Term Size	Effective Domain Size	Adjusted p-value	Query Size	Intersection Size
GO:BP	response to estradiol	GO:0032355	33	21726	0.049745	7	2

Figure B.S4. Manhattan plot of significantly enriched pathways from all significantly differentially abundant Enrichment analyses were conducted using g:Profiler with cut-off threshold enrichment p-value < 0.05. (MF – molecular function; BP – biological process; CC – cellular component; KEGG – Kyoto Encyclopedia of Genes and Genomes; REAC – Reactome; HP – Human Phenotype Ontology).

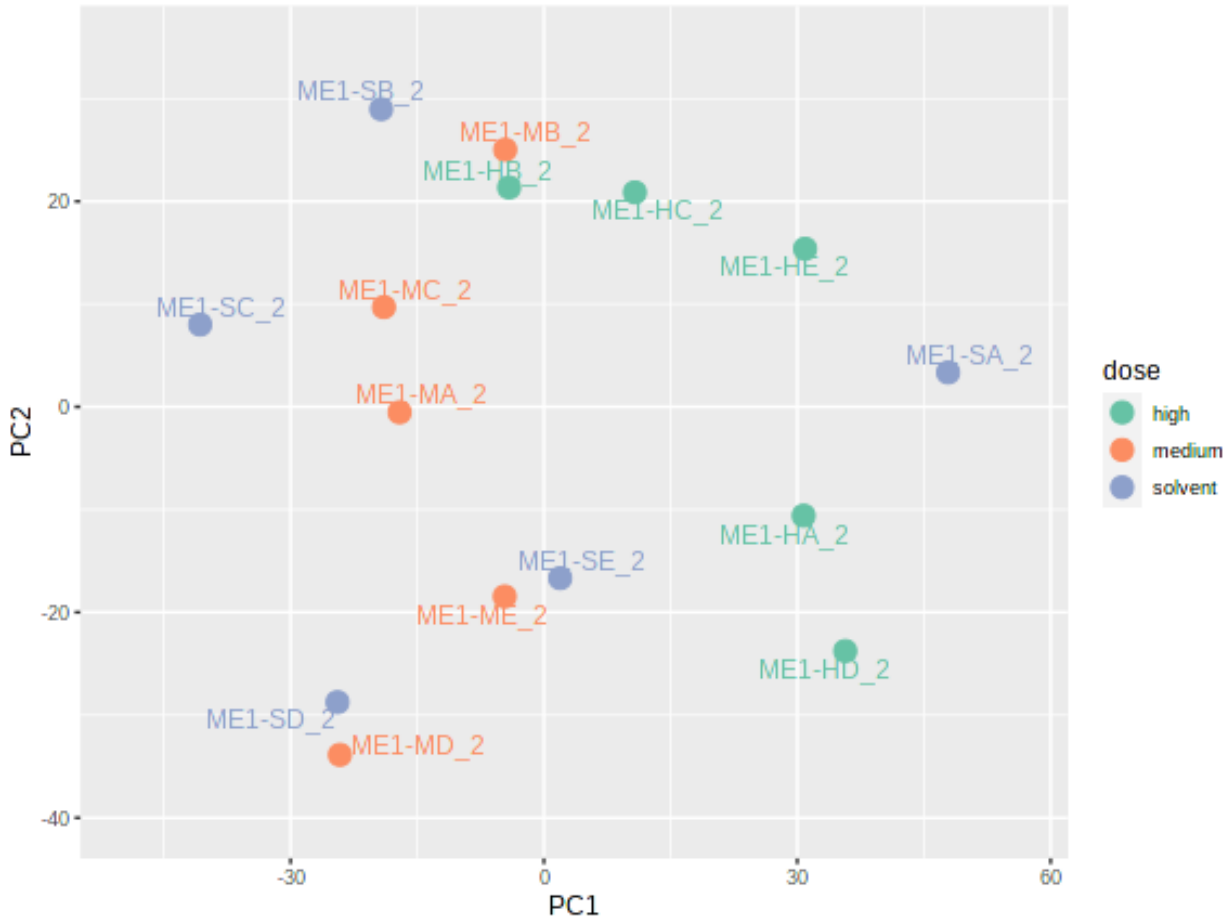

4427

4428 **Figure B.S5.** PCA plot of RNA-seq samples. Solvent1 was removed in downstream analyses as

4429 it failed to cluster with other solvent control replicates.

APPENDIX C

C.1. Fish maintenance and exposure conditions

Eyed-stage RBT embryos (2N) were purchased from Troutlodge, Inc (WA, USA) and were kept in McDonald-type hatching jars until first signs of hatchings were observed. Approximately 100 unhatched eggs were then transferred (Day 0) into each of the hatching cups, which were kept in 9-liter tanks containing exposure solutions (3 tanks x 8 treatments). Unhatched eggs were removed after 48 hrs.

Embryos were exposed, in triplicate, to graded concentrations (nominal: water control, 0.01% DMSO solvent control, 1, 3, 10, 30, 100 and 300 ng/L) of EE2 (>98% purity, Sigma Aldrich, MO, USA) under flow-through conditions (at least 50% v/v renewal per day) (**Figure C.S1**). The final concentration of DMSO in all treatment groups was 0.01% v/v, except for the water control. These concentrations were selected based on chronic apical endpoints previously reported in the literature (Aris *et al*., 2014). Temperature was maintained at 15 ± 1 ^{o}C, under a 16:8 light:dark cycle. Tanks were monitored daily for temperature, and weekly for pH, conductivity, dissolved oxygen, ammonia, nitrates, nitrites, hardness, and alkalinity. *Artemia* nauplii were introduced to alevins at 14 days post hatch (dph), and fish were then transitioned to a diet of frozen bloodworms starting 30 dph.

Three and five alevins were collected and pooled from each tank after 4 dph for transcriptomics and proteomics analyses, respectively. These samples were then immediately flash frozen in liquid nitrogen and kept at -80^{o}C until further analyses. Swim-up fry were released into the tanks outside the hatching cups. At the end of the swim-up stage (~100% swim up in control group, 21 dph), fish were culled to 20 individuals per tank to avoid overcrowding, and the rest were euthanized using 450 mg/L buffered MS 222 (Sigma Aldrich). In addition, only the water

control, solvent control, 30, 100, and 300 ng/L treatment groups were maintained after swim-up as mortalities were not expected to occur at lower concentrations. Surviving juveniles were euthanized at 60 dph and assessed qualitatively for overt morphological abnormalities. Whenever abnormalities were identified, a second person was consulted to confirm the observation. Five randomly selected whole fish from each replicate at 60 dph were also fixed in an all-purpose fixative for 48 hours, transferred to 70% ethanol, then stored at room temperature until further processing for histological assessment. Lastly, length and weight measurements were taken at 4, 21, and 60 dph by the same person throughout the experiment so as to minimize multiple experimenter biases. However, since significant mortalities occurred at the highest concentrations, fish density in the tanks was affected which is therefore not treatment-associated; hence, length, weight, and condition factor at 60 dph were not presented here. Survival was also recorded daily. The study was approved by the University of Saskatchewan Animal Research Ethics Board (Protocol# 20140079).

C.2. Chemical analyses

Water samples were collected from each tank at 4 and 21 dph. EE2 was captured via hydrophobic retention on optimized reverse-phase solid-phase extraction (SPE) sorbent using 100 mg/6 ml Strata X polymeric cartridges (Phenomenex Inc, CA, USA) under gentle vacuum. Cartridges were dried on the manifold, then EE2 was eluted with 100% Methanol (Optima™ for HPLC, Fisher Chemical, Hampton NH, USA), followed by solvent evaporation to dryness under constant flow of Nitrogen stream. Samples were reconstituted and pre-diluted with 10% Methanol to suitable dilutions within the dynamic range of detection of the enzyme-linked immunosorbent assay (ELISA) kit (50 – 3000 ng/L). Concentrations of EE2 were measured using EE2-specific

competitive ELISA (Ecologiena®, Fukuoka, Japan, purchased from Eurofins Abraxis, PA, USA), following the manufacturer's protocol. The Ecologiena® EE2 ELISA kit is highly specific and has previously been used in measurement of EE2 in environmental samples (King *et al*., 2016). Absorbance was read at λ = 450 nm on a Tecan Spark® multimode microplate reader and EE2 concentrations were quantified against a standard curve using Assayfit Pro v1.3 software (Assay Cloud, Nijmegen, The Netherlands).

C.3. Transcriptomics

Solvent control, 1, 3, 10, 30, and 100 ng/L treatment groups were used for transcriptomics analyses. Fish from 300 ng/L treatment group were not used for transcriptomics due to significant mortalities as early as swim-up stage, which could have skewed transcriptomic effects towards responses associated with non-specific causes of mortality. Total RNA was extracted from each replicate of pooled alevins using RNeasy Plus Universal Mini Kit (Qiagen, Germany). Samples with RNA integrity number (RIN) ≥8 were sent to Génome Québec Centre d'Expertise et de Services for mRNA sequencing (Genome Quebec, Montreal, QB, Canada). Libraries were prepared from 250 ng total RNA using NEBNext Ultra Directional kit with poly(A) magnetic isolation module (New England Biolabs Ltd, ON, Canada). Total RNA was poly(A)-enriched prior to the synthesis of double-stranded DNA. Libraries were quantified using the KAPA Library Quantification kit with Revised Primers-SYBR Fast Universal kit (Kapa Biosystems). Average size fragment was determined using a LabChip GX (Perkin Elmer, ON, Canada) instrument. A 1% PhiX library was spiked into a pool of 225 pM dsDNA, and was loaded onto a NovaSeq 6000 S4 lane (Illumina, CA, USA) for a 200 cycles (100 x 2) paired-end mode sequencing.

Base calling was performed using RTA v3.4.4 (Illumina). Base calls were then demultiplexed and fastq files were generated for each sample using the bcl2fastq2 v2.20 (Illumina) software. Reads were assessed for quality using FastQC v 0.72 (Andrews, n.d.), then trimmed to a minimum Phred score of 20 and a minimum length of 35 bases using Trimmomatic v.0.38.1 (Bolger *et al*., 2014). The abundance of transcripts was estimated using Kallisto (Bray *et al*., 2016), mapped against the reference RBT transcriptome (GenBank Acc# GCA_002163495.1). Only features with 5 counts-per-million in at least 3 samples were kept for differential expression analysis. Significance of differentially expressed (DE) transcripts was assessed using DESeq2 (Love *et al*., 2014), with a minimum effect size threshold of the absolute value of log2 fold-change ($|\log2FC| \geq 1$ and a false discovery rate (FDR, Benjamini-Hochberg) ≤ 0.05. Default software settings were used unless stated otherwise. Raw fastq files are available through the NCBI GEO accession# GSE171788.

C.4. Proteomics

Since the exposure duration was short, only the highest concentrations which may rapidly induce responses were analyzed for proteomic alterations. Alevins from the solvent control, 30, and 100 ng/L treatment groups were used for non-targeted proteomics analysis, as described in Alcaraz *et al*. (2021) with minor revisions. Briefly, whole body tissues were processed by filter-aided sample preparation (Wiśniewski *et al*., 2009; Wiśniewski and Rakus, 2014) using 30 kDa Microcon® filters (Merck Millipore, MA, USA), where alkylation was done using iodoacetamide and digestion using trypsin. LC-MS/MS analyses of peptide mixtures were conducted using a Q Exactive™ HF-X Hybrid Quadrupole-Orbitrap™ mass spectrometer (Thermo Fisher Scientific, MA, USA) connected online to an Ultimate 3000 RSLCnano system (consisted of SRD-3400,

NCS-3500RS CAP, WPS-3000 TPL RS; Thermo Fisher Scientific). Prior to LC separation, tryptic digests were online concentrated and desalted on a cartridge trapping column (300 µm × 5 mm, C18 PepMap100, 5µm particles, 100 A; Thermo Fisher Scientific) using 0.1% formic acid (FA) in water. The peptides were eluted from the trapping column onto an Acclaim Pepmap100 C18 analytical column (3 µm particles, 75 µm × 500 mm; Thermo Fisher Scientific) by linear gradient (3-35% of mobile phase B; mobile phase A: 0.1% FA in water; mobile phase B: 0.1% FA in 80% acetonitrile) over 130 minutes of active gradient and subsequent increase of mobile phase B to 80% in 5 minutes and 5 minutes column wash with 80% of mobile phase B. The analytical column was directly connected to the Digital PicoView® 550 (New Objective, Woburn MA, USA) ion source with sheath gas option and SilicaTip emitter (New Objective; P/N: FS360-20-15-N-20-C12) utilization.

Analysis of mass spectrometric data was carried out using MaxQuant v1.6.14 (Tyanova *et al*., 2016). MS/MS ion searches were done using the MaxQuant contaminant database (247 protein sequences) and the RBT reference proteome (GenBank Acc# GCA_002163495.1; 71,233 protein sequences). Carbamidomethyl (C) was set for fixed modification while Oxidation (M), Deamidation (NQ), Oxidation (P), and Acetyl (Protein N-term) were set as variable modifications, with a maximum of 2 missed cleavages allowed for first and main search. Peptides and proteins with an FDR (q-value) < 1% and at least one razor peptide were selected for downstream analyses. Changes in the abundance of proteins were assessed in KNIME v.4.2.3 (Berthold *et al*., 2008). Data were filtered to keep protein groups with 2 or more peptides, and at least two measured intensity values in both experimental groups being compared. Log2-transformed protein group intensities were loess-normalized. Significance of differentially abundant protein (DAP) groups was assessed using *limma* with a cut-off moderated p-value ≤ 0.05 and a minimum effect size

threshold |log2FC| ≥ 1 relative to the solvent control group. Limma estimates moderated p-values by using the whole dataset to shrink sample variances towards pooled estimate, which have been shown to be a practical approach in detecting DAP with minimal loss from false negatives (Kammers *et al*., 2015; Pascovici *et al*., 2016). Proteomic spectral datasets were deposited in the ProteomeXchange Consortium via the PRIDE (Perez-Riverol *et al*., 2019) partner repository with dataset identifier PXD025251. DAP analysis workflow template can be found in https://github.com/OmicsWorkflows.

C.5. Histological assessments

At 60 dph, 5 fish per replicate from each treatment were randomly selected for histology. Individuals were fixed whole in HealthCare™ PROTOCOL™ SafeFix™ II All-Purpose Fixative (Fisher Scientific, MA, USA) for 48 hours, and then transferred to 70% ethanol for storage. The ethanol was decanted and replaced twice to remove excess fixative from the tissues prior to further processing. A subset of individuals from the solvent control and 100 ng/L treatment groups (3-4 individuals per replicate) were selected for processing. The samples were trimmed (i.e., head and tail removed) and then dehydrated in graded alcohols, cleared in xylene, and infiltrated with molten paraffin using a Belair RVG/1 Vacuum Tissue Processor (University of Saskatchewan, Histology Core Facility). The samples were then embedded in paraffin blocks for longitudinal step-sectioning in frontal plane (5 mm thick). For each individual, representative sections were taken at a minimum of nine different levels through the body cavity at approximately 100 mm intervals, mounted on glass slides, and stained with Harris' hematoxylin and eosin.

Liver sections were assessed for the presence/absence of glycogen-type and lipid-type vacuolation and the overall staining (eosinophilic or basophilic) of the hepatocyte parenchyma

(Wolf and Wheeler, 2018). All tissue sections were also assessed for the presence of proteinaceous fluid within the body cavity. Histological analyses were done qualitatively in support of molecular studies, and thus, only the highest concentration with transcriptomic data was assessed and histological features were reported as presence/absence in individual fish examined. No statistical analysis was done.

C.6. Statistical Analyses

Apical outcomes (length, weight, condition factor, and survival rates) at 4, 21, and 60 dph were assessed for significant differences between treatment groups using one-way analysis of variance (ANOVA), followed by Tukey's multiple comparison post-hoc test, with a cut-off adjusted p-value < 0.05. Prior to ANOVA, outliers were identified using ROUT method (Q = 1%) and assumptions of ANOVA were tested (normality, homoscedasticity). In cases where assumptions of ANOVA were not met, the non-parametric ANOVA analogue, Kruskal-Wallis test, was performed, followed by Dunn's multiple comparison test with a cut-off p-value < 0.05. All non-omics statistical analyses were carried out in GraphPad Prism v.9.0.2.

Table C.S1. Nominal and measured concentrations of EE2 in exposure tanks based on EE2-specific competitive ELISA measurements.

Treatment Group (Nominal concentration in ng/L)	Measured Concentration (ng/L) (mean ± standard deviation)	% Nominal
Water Control	< 0.01	
Solvent Control (0.01% DMSO)	< 0.01	
1 ng/L	1.13 ± 0.10	113
3 ng/L	1.57 ± 0.33	52
10 ng/L	6.22 ± 1.16	62
30 ng/L	16.34 ± 2.45	54
100 ng/L	55.10 ± 9.46	55
300 ng/L	168.93 ± 21.74	56

Table C.S2. Average physico-chemical characteristics of exposure solutions measured daily (temperature) and weekly (pH, conductivity and dissolved oxygen, ammonia, nitrates, nitrite, hardness and alkalinity). Values are expressed as mean ± standard deviation.

Parameters	Values
Temperature	14.96 ± 0.52 ^{o}C
pH	7.99 ± 0.19
Conductivity	247.51 ± 34.26 µS/cm
Dissolved oxygen (DO)	97.83 ± 5.73 %
Ammonia	≤ 0.25 mg/L*
Nitrates	≤ 0.5 mg/L*
Nitrite	≤ 0.05 mg/L*
Hardness	110.86 ± 16.85 mg $CaCO_3$/L
Alkalinity	84.58 ± 13.65 mg $CaCO_3$/L

*during rare occasions of detectable levels of ammonia, nitrates, and/or nitrites during random testing throughout the week, all exposure solutions were immediately renewed by up to 75%.

Table C.S3. Percent overlap of dysregulated transcripts. Left columns are the number of overlapping transcripts. Right columns highlighted in yellow are the percent overlap between the two groups being compared, where percent overlap equals the number of overlapping transcripts over the number of dysregulated transcripts in a given concentration (#dysreg; column values).

# dysreg	930		688		210		281		331
	1.13 ng/L		**1.57 ng/L**		**6.22 ng/L**		**16.3 ng/L**		**55.1 ng/L**
1.13 ng/L	X								
1.57 ng/L	450	48.39	X						
6.22 ng/L	81	8.71	80	11.63	X				
16.3 ng/L	133	14.30	137	19.91	91	43.33	X		
55.1 ng/L	118	12.69	104	15.12	96	45.71	136	48.40	X

Table C.S4. Summary of incidences of pathologic features observed in 60 dph RBT exposed to EE2.

Tissue	Pathologic Feature	Incidence	
		Solvent Control n=10	**55.1 ng/L n=9**
Liver	Hepatocyte basophilia	0	9
	Hepatocyte glycogen vacuolation	10	0
	Hepatocyte lipid vacuolation	0	7
	Eosinophilic intravascular fluid accumulation	1	9
Coelom	Eosinophilic fluid accumulation	0	9

*where n is the number of individual fish examined and does not correspond to biological replicates. At least 3 fish per replicate tank were examined for pathological features.

Table C.S5. Selected literature of apical chronic responses to EE2.

Species	Life-stage	Length of exposure	Endpoint	Concentration (ng/L)	Reference
P. Promelas	Adult breeding pairs	21 days	Decreased egg production	1	(Jobling *et al*., 2004)
P. Promelas	Adult breeding pairs	21 days	Inhibition of egg production	0.5	(Runnalls *et al*., 2015)
P. Promelas	Life cycle (from 48 hpf to F1 generation)		Decreased egg fertilization	0.32	(Parrott and Blunt, 2005)
			Skewed sex ratio to females	0.32	(Parrott and Blunt, 2005)
			Decreased male sex characteristics	0.32	(Parrott and Blunt, 2005)
O. mykiss	All male fry	60-136 dpf	Intersex gonads	10	(Depiereux *et al*., 2014)
O. mykiss	Adult male	62 days	Reduction in the number of eggs attaining the eyed stage	10	(Schultz *et al*., 2003)

*dpf – days post fertilization

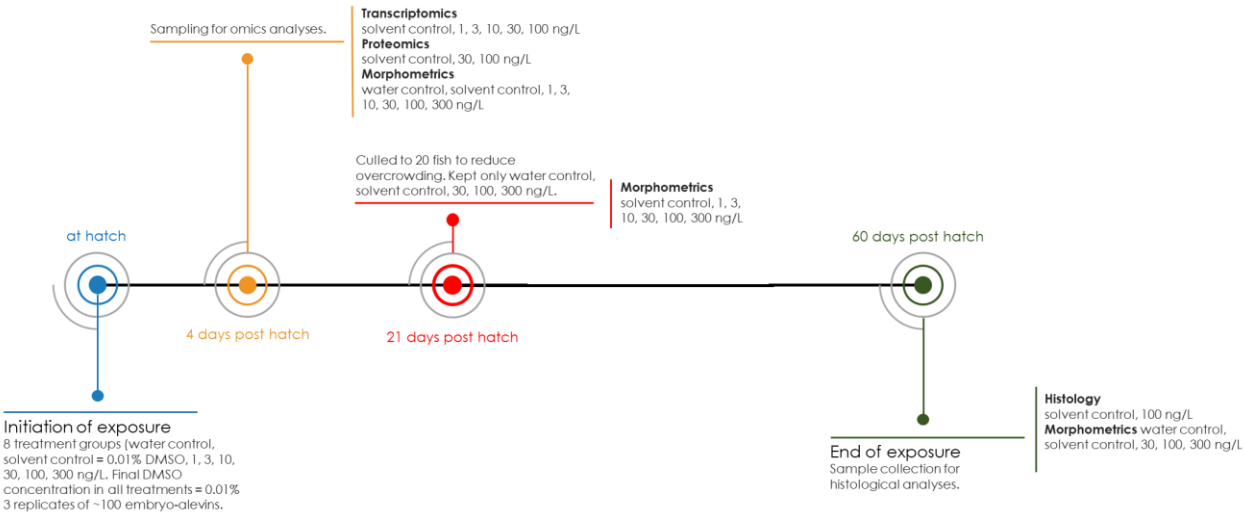

Figure C.S1. Study design. Exposures were initiated at hatch (Day 0). Three replicates each of ~100 embryos were exposed to water, solvent control (0.01% DMSO), 1, 3, 10, 30, 100, and 300 ng/L nominal concentrations of EE2. Samples for omics analyses were collected at 4 dph. Fish were culled to 20 individuals at swim-up (21 dph) to prevent overcrowding. Exposure was terminated at 60 dph where samples for histology were collected. Weight and length measurements were taken at 4, 21, and 60 dph. Survival was monitored throughout the experiment.

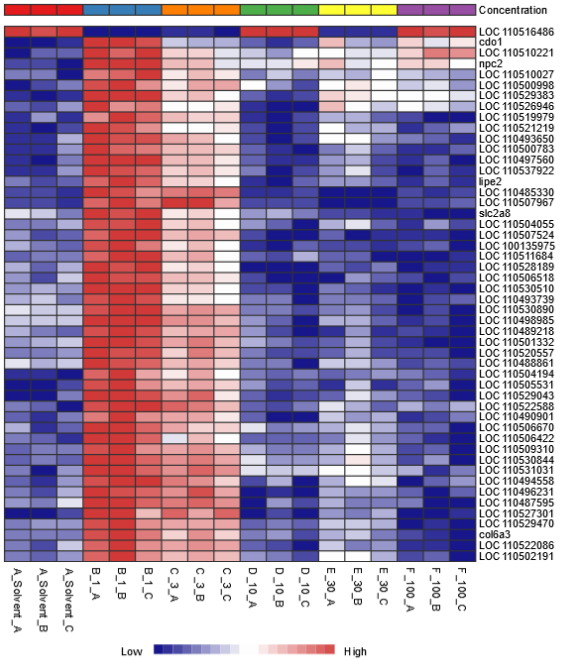

1.13 ng/L

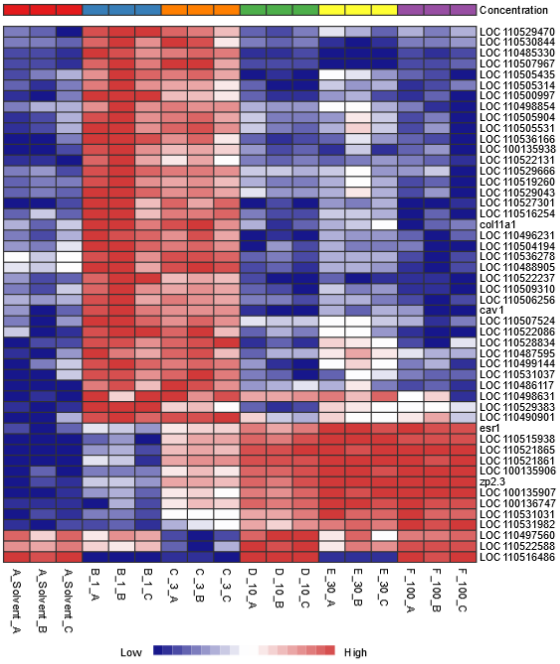

1.57 ng/L

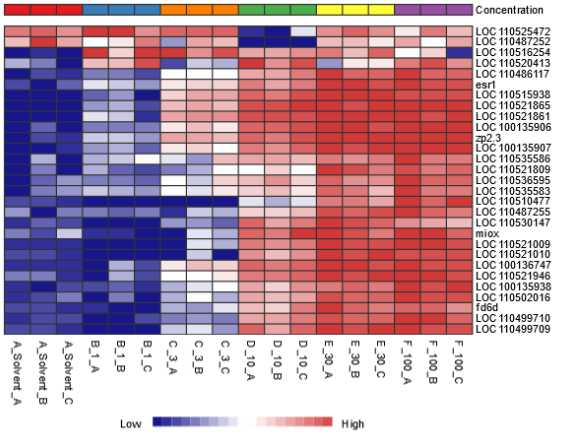

6.22 ng/L

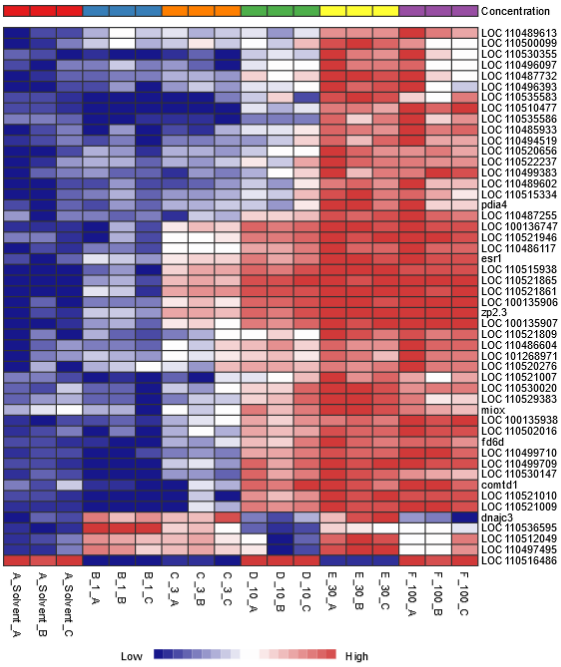

16.3 ng/L

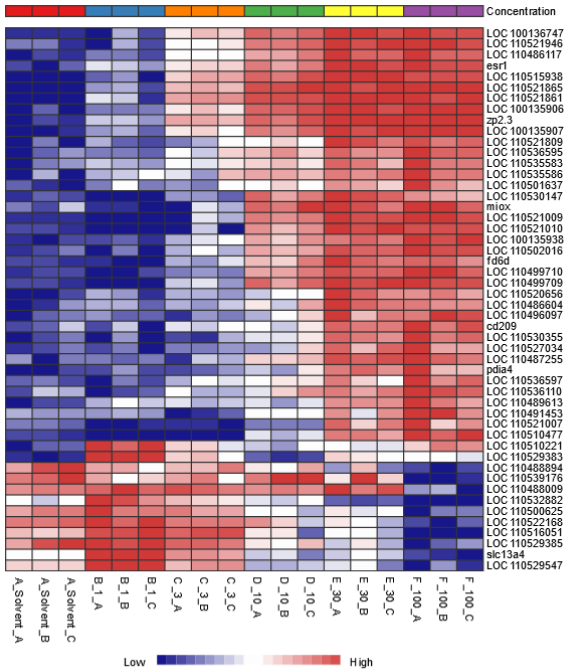

55.1 ng/L

4613 **Figure C.S2.** Truncated overview heatmap profiles across concentrations based on DE transcripts

4614 in the respective concentration.

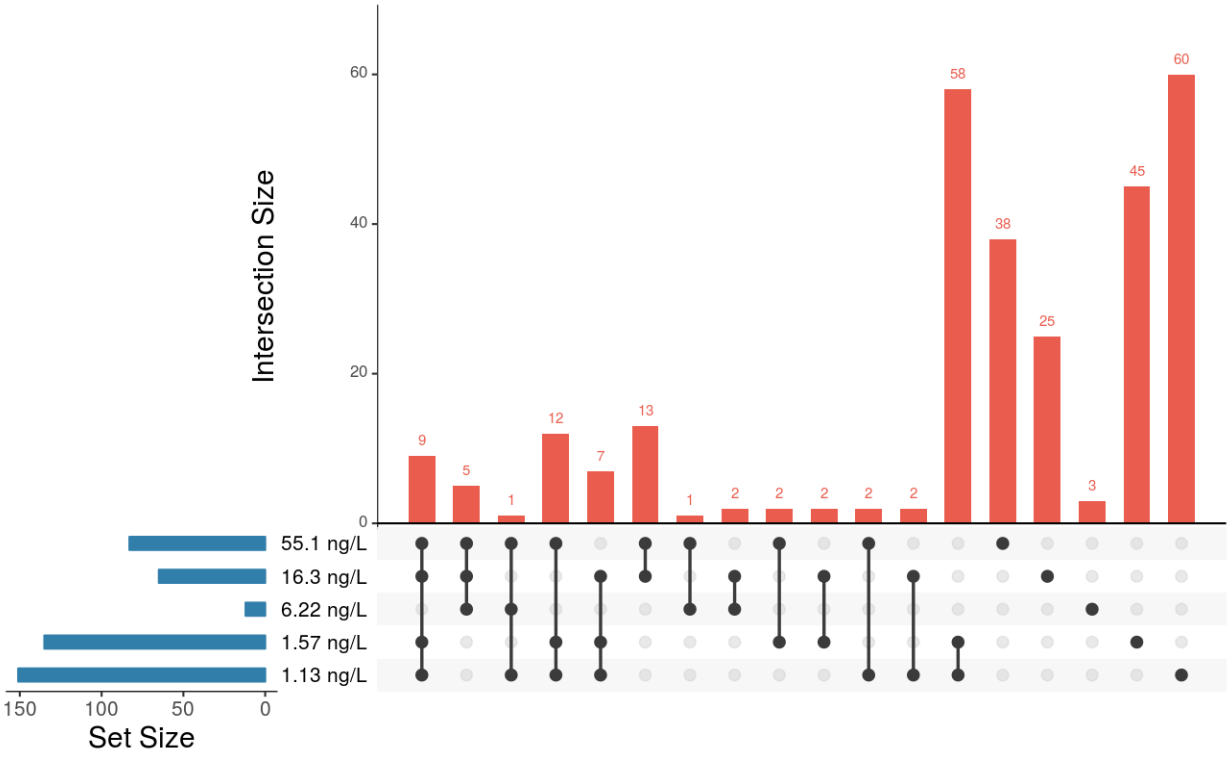

4615

4616 **Figure C.S3.** UpSetR plot of intersecting overrepresented terms and pathways based on

4617 significantly dysregulated transcripts. Plot was constructed using Intervene (Khan and Mathelier,

4618 2017).

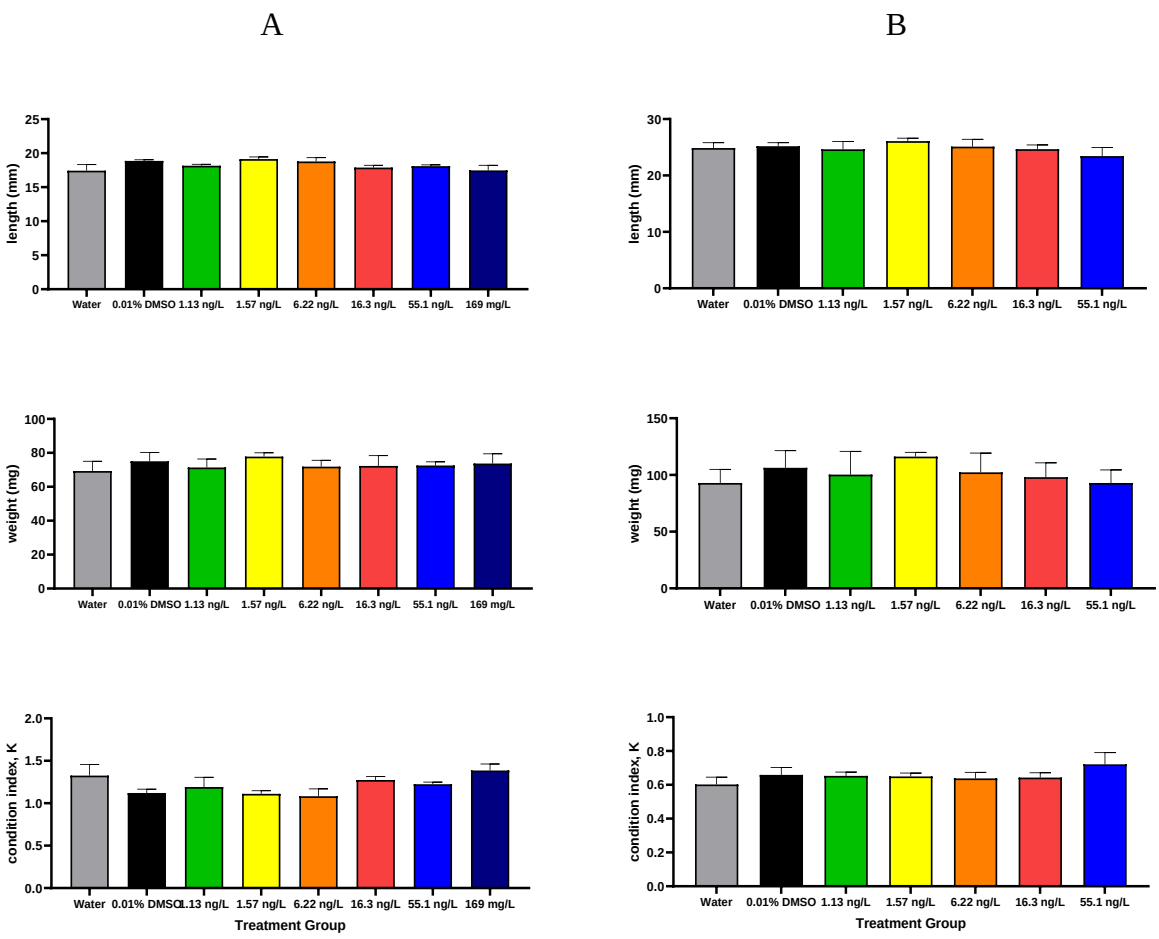

Figure C.S4. Morphometric measurements at (A) 4 dph and (B) swim-up stage (21 dph) (**DataSet 4, Tabs B1-B3 and C1-C3**). Top = length (mm); Middle = weight (mg), Bottom = condition factor, K. Datasets represent mean ± standard deviation.

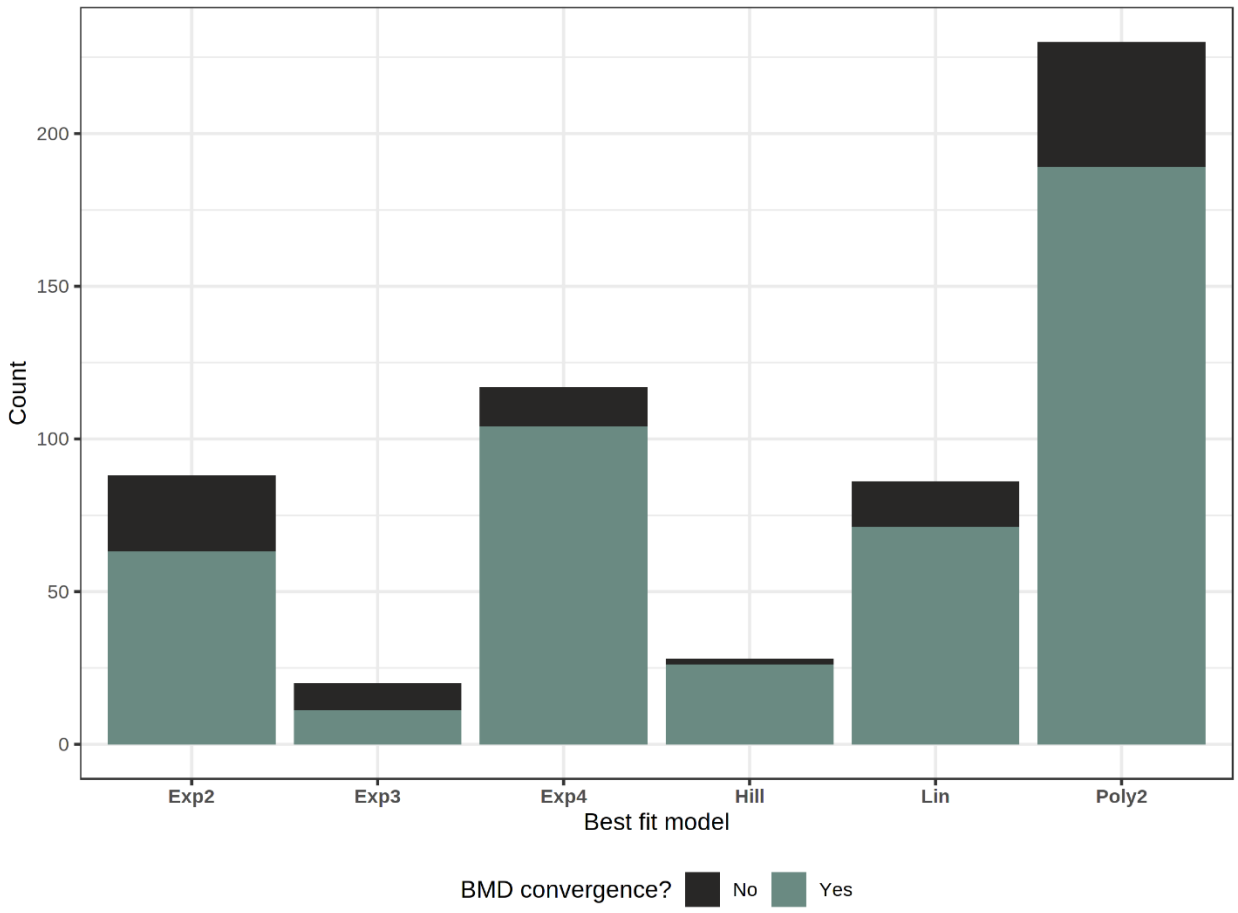

4622

4623 **Figure C.S5.** Frequency of statistical models among best fit curves based on the lowest AIC.

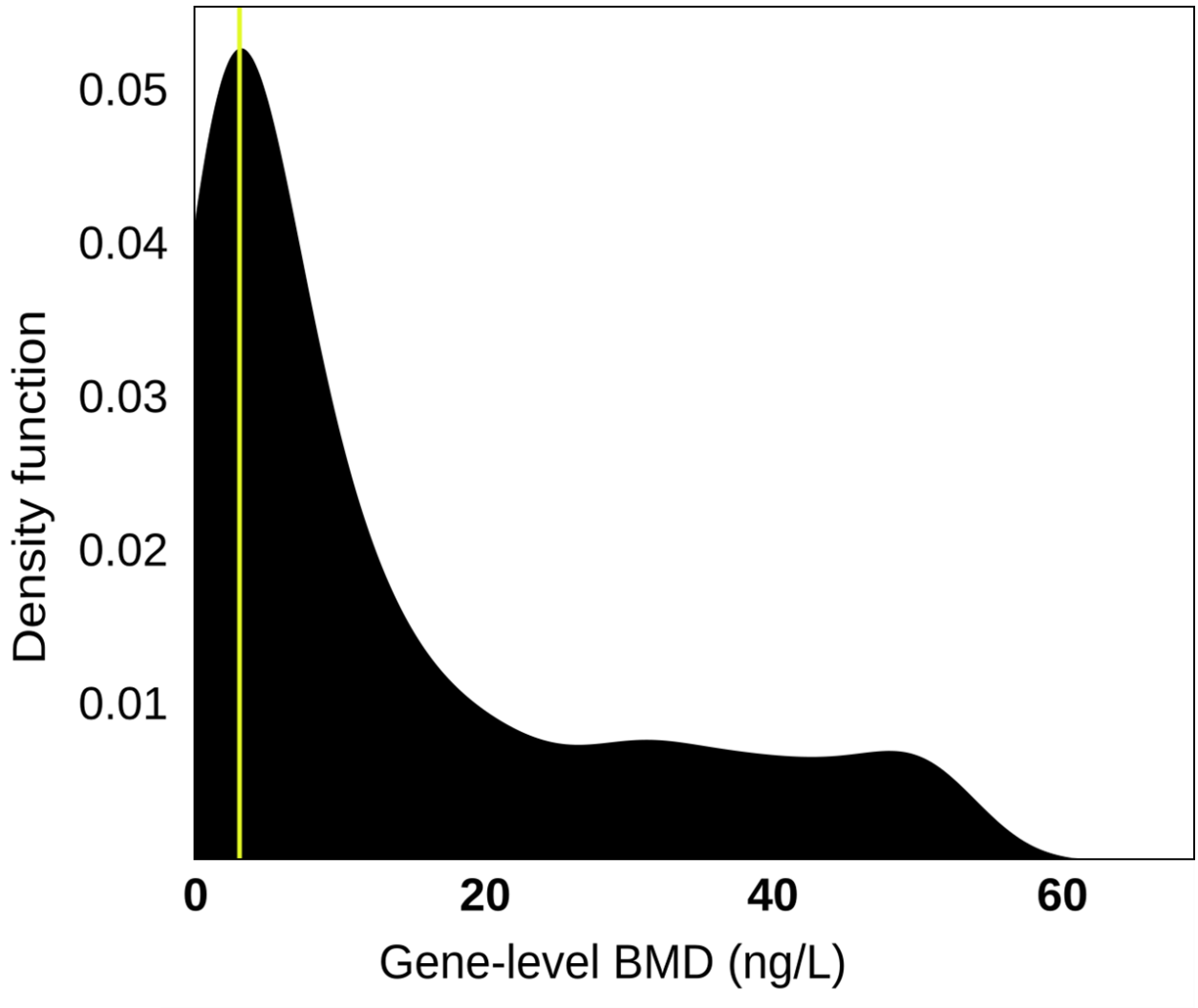

Figure C.S6. Transcriptomic BMD probability distribution (normal scale). Yellow line indicated the first mode of the geneBMD distribution ($omicBMD_{mode}$). Note that the plot is a smoothed probability distribution which would spill to the left of zero concentration and should therefore be interpreted with caution since the area at the left of zero is an artifact of curve smoothing and that there was no geneBMD below zero. The area below zero has been truncated.

APPENDIX D

D.1. Chemical analyses

Concentrations of FLX in solution were measured at SGS AXYS Analytical Services Ltd (BC, Canada). Reference fluoxetine (FLX) was obtained from Millipore Sigma (ON, Canada) while d_5-Fluoxetine (d_5-FLX) was obtained from CDN Isotopes (QB, Canada). FLX was quantified following the method previously described (Long *et al*., 2013), with minor revisions. Briefly, FLX from water samples was extracted by solid phase extraction/isotope-dilution prior to LC-MS/MS analysis. An appropriate aliquot based on expected exposure concentrations was spiked with d_5-FLX, diluted to 500 mL in reagent water, and buffered to a pH of 3.8 using a sodium acetate:acetic acid buffer. Samples were then loaded on a 1g Oasis-HLB cartridge (Waters, MA, USA) and eluted using 12 mL of methanol and 6 ml of 1:1 acetone:methanol. Sample extracts were evaporated to dryness under a stream of N_2 and reconstituted in 2 mL of methanol with 0.1% formic acid solution. FLX was quantitated using a Waters 2690 HPLC, equipped with Xterra MS C18 (Waters; 10.0 cm, 2.1 mm i.d., 3.5 µm particle size), coupled with Micromass Quattro Ultima MS/MS (Waters) operating in positive ion electrospray mode at unit resolution. Transitions used for FLX and d_5-FLX were 310 ⟶ 148 and 315 ⟶ 153, respectively. The flow rate varied from 0.15-0.3 mL/min. The column was maintained at 40°C. A gradient elution using mobile phases 0.1% formic acid buffer (A) and 1:1 acetonitrile:methanol (B) was used. The LC gradient program was as follows (time, %A): 0.0, 95%, 4.0, 95%, 22.5, 12%, 23.0, 0%, 26.0, 0%, 26.5, 95%, and 33.0, 95%. Source temperature was 120°C and the desolvation temperature was 350°C. A seven-point calibration curve ranging from 0.375-1250 ng/mL was used for quantitation using 1/x weighted linear calibration and response relative to d_5-FLX. Concentrations are expressed as µg/L FLX. For exposures in petri dishes only (0.44 and 112 µg/L FLX), since the working solutions

were from serially diluted stock solutions for all treatments, concentrations were based on the average % nominal of treatments with measured concentrations. This was done because the volumes used in petri dishes were too low for analytical testing.

D.2. Proteomics

To assure that proteomic responses were not due to non-specific toxic responses, 7 µg/L FLX treatment group was selected based on the NOEC of an in-house *a priori* early-life stage rainbow trout sub-chronic survival assay (data not shown; **SuppMat Figure File RBT**). Proteomics was conducted following Alcaraz *et al*. (submitted). Cell disruption and protein solubilization were done using SDT lysis buffer (4% Sodium dodecyl sulfate (SDS; Sigma-Aldrich), 0.1 M Dithiothreitol (DTT; Thermo Fisher Scientific, MA, USA), 0.1 M Tris/HCl (Sigma-Aldrich; pH = 7.6) in a Thermomixer® (Eppendorf, Hamburg, Germany) at 95ºC, for 2 hours. Quality of protein extracts was assessed by use of 1-D SDS-PAGE (12% gels). Protein extracts were then processed by filter-aided sample preparation (FASP) (Wiśniewski *et al*., 2009; Wiśniewski and Rakus, 2014). Briefly, proteins were alkylated using 50 mM iodoacetamide (Sigma-Aldrich) for 20 mins at RT and digested using trypsin (Sequencing grade; Promega, WI, USA) in 50 mM ammonium bicarbonate at 37ºC for 18 hrs, on a 30 kDa membrane filter unit. Resulting peptides were eluted with ammonium bicarbonate (AB) buffer and the FASP eluates were kept at -80ºC until further LC-MS/MS analysis.

FASP eluates were cleaned using 3 iterations (Yeung and Stanley, 2010) of ethylacetate extraction to remove SDS contamination, then completely dried in a SpeedVac vacuum concentrator (Thermo Fisher Scientific). Cleaned peptides were reconstituted by acid extraction using 50 µl of (1:1) 5% formic acid (LC-MS grade, >99% purity; Fisher Scientific) and 100%

acetonitrile (HPLC grade, >99.9%; Sigma-Aldrich), with 1.5 µl of 0.01% poly(ethylene glycol) (PEG; Millipore-Sigma) to reduce sample loses. The final solution was transferred to a TPX (polymethylpentane) vial and vacuum concentrated in SpeedVac vacuum concentrator to a final volume of 15 µl.

LC-MS/MS analyses were conducted using a Q Exactive™ HF-X Hybrid Quadrupole-Orbitrap™ mass spectrometer (Thermo Fisher Scientific, MA, USA) connected online to an Ultimate 3000 RSLCnano system (consisted of SRD-3400, NCS-3500RS CAP, WPS-3000 TPL RS; Thermo Fisher Scientific). Prior to chromatographic separation, tryptic digests were online concentrated and desalted on a cartridge trapping column (300 µm × 5 mm, C18 PepMap100, 5µm particles, 100 A; Thermo Fisher Scientific) using 0.1% formic acid (FA) in water. The peptides were eluted from the trapping column onto an Acclaim Pepmap100 C18 analytical column (3 µm particles, 75 µm × 500 mm; Thermo Fisher Scientific) by non-linear gradient (2-35% of mobile phase B; mobile phase A: 0.1% FA in water; mobile phase B: 0.1% FA in 80% acetonitrile). The analytical column was directly connected to the Digital PicoView® 550 (New Objective, Woburn MA, USA) ion source with sheath gas option and SilicaTip emitter (New Objective; P/N: FS360-20-15-N-20-C12) utilization. Active Background Ion Reduction Device (ABIRD; ESI Source Solutions, Woburn MA, USA) was installed to the LC-MS/MS system to isolate the experiment from variable background ion interferences. MS data were acquired in a data-dependent acquisition strategy, selecting up to top 20 precursors based on precursor abundance in the survey scan (350 - 2000 m/z). The resolution of the survey scan was 120,000 (at 200 m/z) with a target value of 4×10^5 ions and maximum injection time of 100 ms. Higher-energy collisional dissociation (HCD) MS/MS spectra were acquired with a target value of 5×10^4 and resolution of 15,000 (at 200 m/z). The maximum injection time for MS/MS was 22 ms.

Raw mass spectrometric data files were analyzed using MaxQuant v.1.6.15 (Cox and Mann, 2008; Tyanova *et al*., 2016) with built-in Andromeda search engine (Cox *et al*., 2011). Samples were mapped against the FHM reference proteome (NCBI Acc# GCA_016745375.1; 48,456 sequences; Martinson *et al*., n.d.), combined with the cRAP contaminant database (April 2021; 246 sequences). Acetyl (protein N-term), oxidation (M), oxidation (P) and deamidation (N, Q) as optional modifications, carbamidomethylation (C) as fixed modification and maximum of two enzymes miss-cleavages were set for the first and main search. Peptide identification was set to match between runs at 0.7 min match time window. Peptides and proteins with an FDR (q-value) < 1% and at least one razor peptide were selected for differential abundance analyses. Raw data were deposited in the ProteomeXchange Consortium via the Proteomics Identifications (PRIDE) (Perez-Riverol *et al*., 2019) partner repository under accession# PXD027024.

All downstream differential protein abundance analyses were done in KNIME (Berthold *et al*., 2008). Datasets were filtered to keep protein groups with 2 or more peptides, and at least two measured intensity values in both experimental groups being compared. Log2-transformed protein group intensities were quantile-normalized. Protein groups with missing quantification values on all replicates within a treatment group were filtered out. Missing values were imputed by global minimum strategy. Significance of differentially abundant (DA) protein groups was assessed using *limma* (Ritchie *et al*., 2015) with a cut-off moderated p-value of ≤ 0.05 and a minimum effect size threshold of $|FC| > 1.5$ relative to the water control group. *limma* estimates moderated p-values by using the whole dataset to shrink sample variances towards pooled estimate, which have been shown to be a practical approach in detecting DA proteins with minimal loss from false negatives (Kammers *et al*., 2015; Pascovici *et al*., 2016). Default software settings were used for analyses, unless otherwise stated.

All significant DA proteins with at least 2 peptides identified were used in the overrepresentation analyses as previously described (**Sec. 4.4.3**).

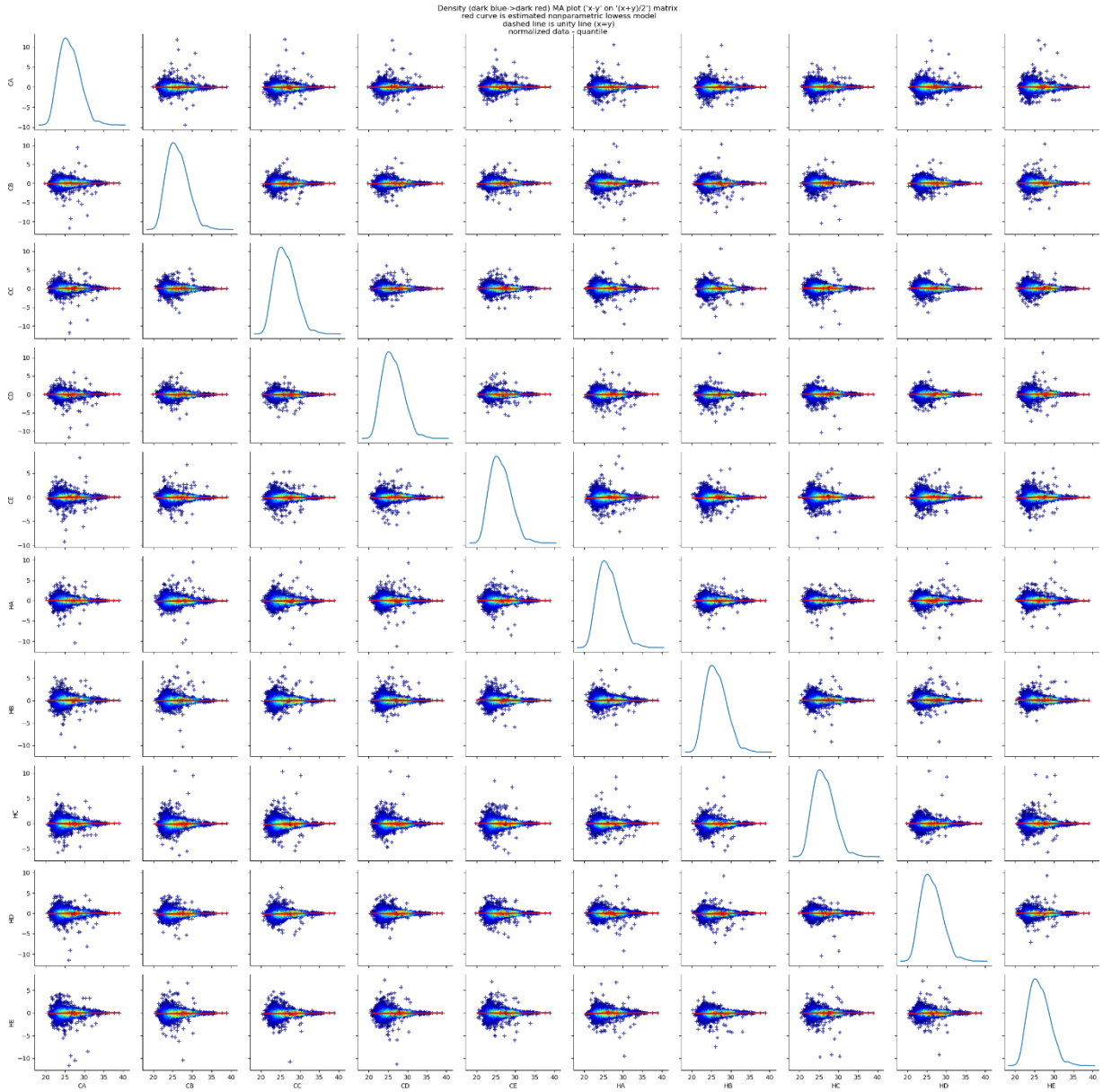

Figure D.S1. Quantile-normalized protein group intensities.

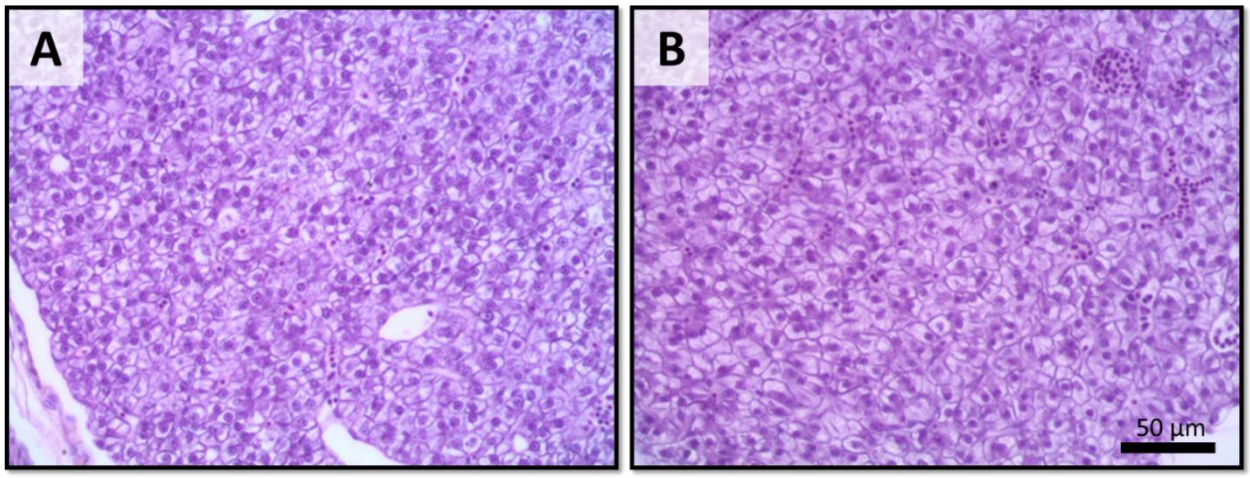

Figure D.S2. Photomicrographs of livers from FLX-exposed early-life stage (32 dpf) fathead minnows (Hematoxylin and Eosin stain). (A) Water control and (B) 10.2 µg/L FLX treatment groups. There was no apparent difference among treatment groups. Livers within bot

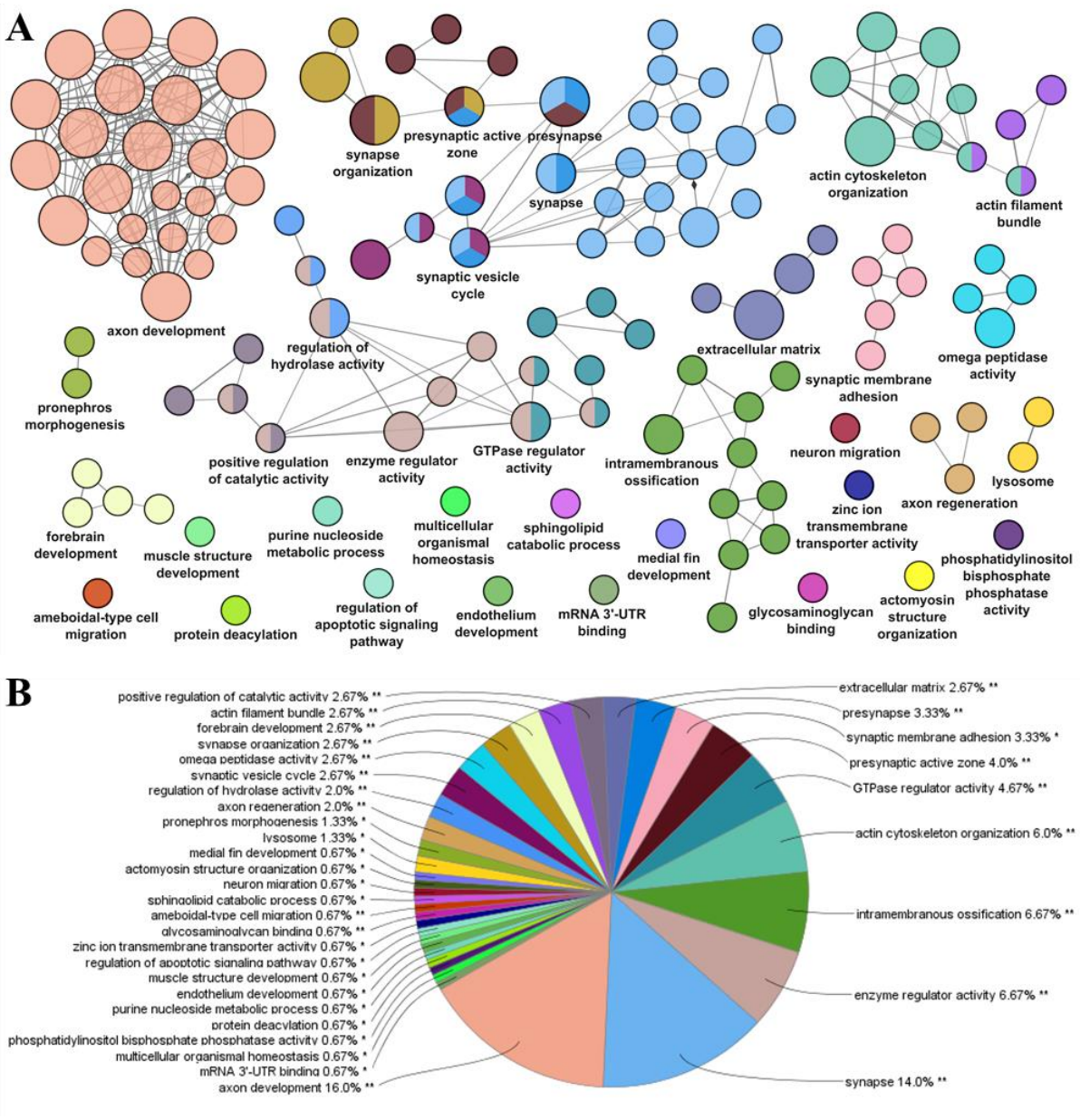

Figure D.S3. Overrepresentation analyses of significantly dysregulated transcripts from all FLX treatment groups using gene ontologies (GO: molecular function, biological process, cellular component) from *D. rerio* as reference set. Statistical test was done using two-sided hypergeometric test with p-value cut off <0.05 followed Benjamini-Hochberg correction for multiple testing and a kappa score = 0.04. (**A**) Overrepresentation network. GO parent-child terms based on similar associated genes were fused (GO Fusion). Nodes were set with a minimum of 3

genes or 4% of genes in a term. Size of the nodes reflects the statistical significance of the terms. Clustering reflects the relationships between the terms based on the similarity of their associated genes. Group leading term is the most significant term of the cluster. (**B**) Relative number of significantly overrepresented GO terms.

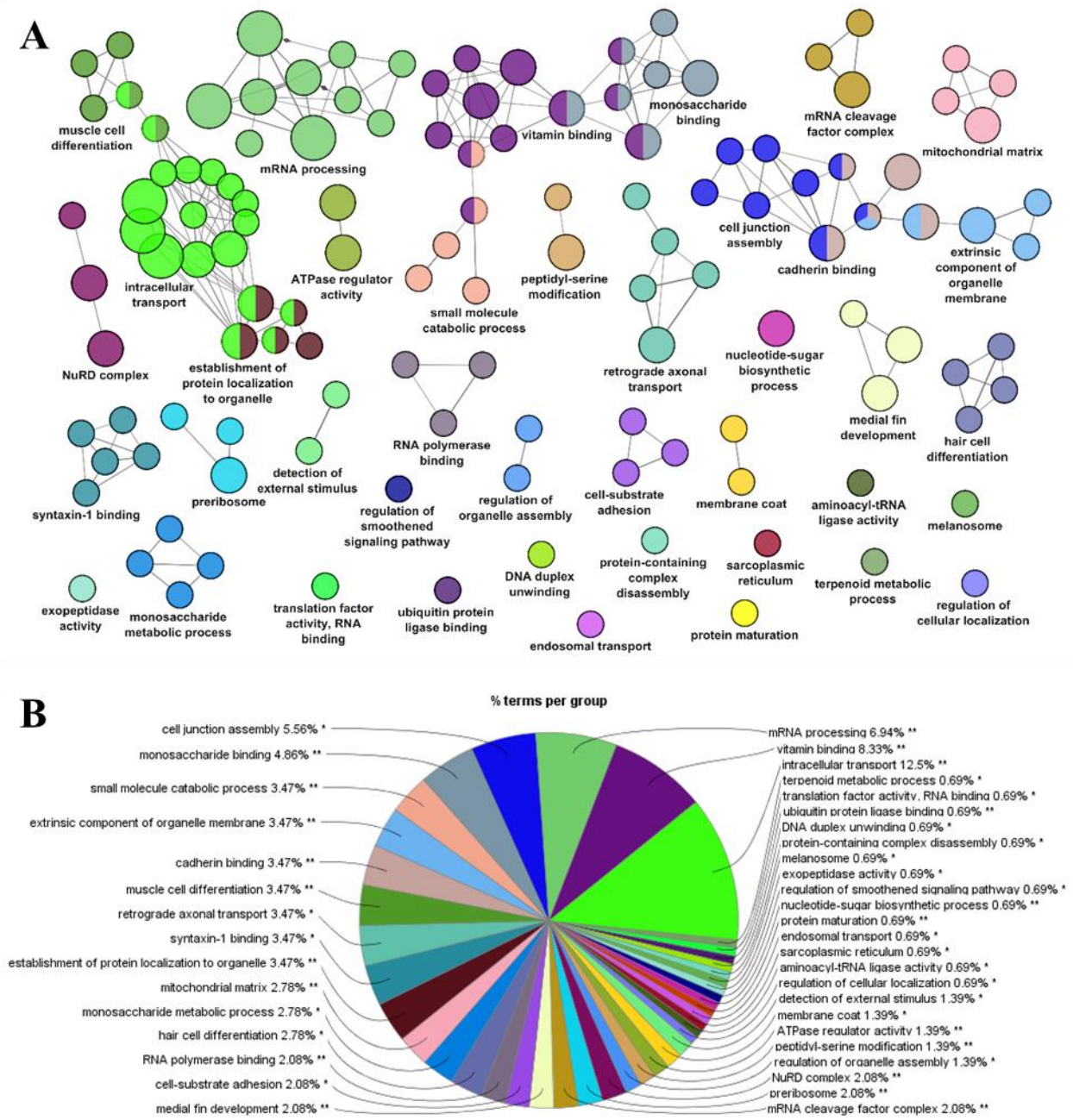

4742

4743 **Figure D.S4.** Overrepresentation analyses of significantly dysregulated proteins from the 3.38

4744 µg/L treatment group using gene ontologies (GO: molecular function, biological process, cellular

4745 component) from *D. rerio* as reference set. Statistical test was done using two-sided

4746 hypergeometric test with p-value cut off <0.05 followed Benjamini-Hochberg correction for

4747 multiple testing and a kappa score = 0.04. (**A**) Overrepresentation network. GO parent-child

terms based on similar associated genes were fused (GO Fusion). Nodes were set with a minimum of 3 genes or 4% of genes in a term. Size of the nodes reflects the statistical significance of the terms. Clustering reflects the relationships between the terms based on the similarity of their associated genes. Group leading term is the most significant term of the cluster. (**B**) Relative number of significantly overrepresented GO terms.

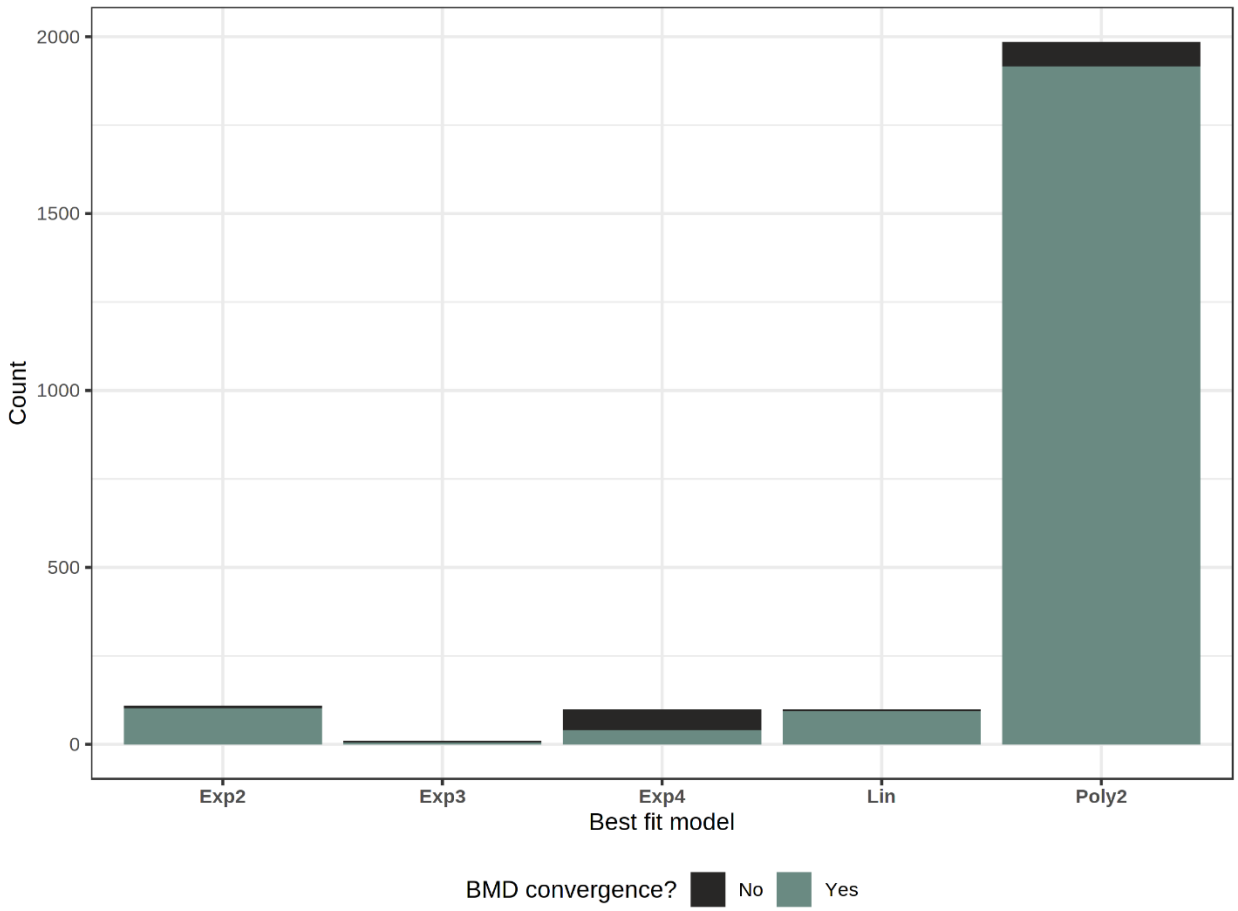

4753

4754 **Figure D.S5.** Frequency of statistical models among best fit curves based on the lowest AIC.

Table D.S1. Nominal and measured concentrations of fluoxetine in exposure solutions. Water samples were collected at 3 time-points (Day 4, 10 and 28).

Nominal (µg/L FLX)	Measured (mean) (ug/L FLX)	Measured (± stdev)	% Nominal
Water (0)	<0.01		
0.44	0.19*		42.37†
1.75	0.74	0.08	42.41
7	3.38	0.56	48.35
28	10.2	2.38	36.34
112	47.5*		42.37†

†average % nominal from measured concentrations

*estimated based on average % nominal

Table D.S2. Physico-chemical characteristics of exposure solutions. Water replacements were ~ 3x the volume of each tank per day.

Parameters	*Values (mean ± stdev)*
Temperature	22.43 ± 0.65 ^{o}C
pH	8.24 ± 0.08
Conductivity	451.77 ± 45.97 µS/cm
Dissolved oxygen (DO)	87.82 ± 1.75 %
Ammonia	≤ 0.25 mg/L*
Nitrates	≤ 1 mg/L*
Nitrite	≤ 0.1 mg/L*
Hardness	190.52 ± 6.51 mg CaCO3/L
Alkalinity	132.92 ± 5.93 mg CaCO3/L

* whenever measured NH4, NO3, or NO2 were above detection limits, tanks were drained to ~50% and fresh solutions were allowed to flow and refill the drained volume.

Table D.S3. List of common dysregulated features from differentially expressed genes and differentially abundant proteins (based on gene symbols).

List of common dysregulated features
mta3
fbln1
vwa2
cplx2l
nr2f2
LOC120466807
LOC120492116
qki2
ctnnd2a
LOC120484165
ahcyl1
mtdha
nbeaa
sdcbp2
ctsa
inpp5kb
ahsg2
epn2

4767 **APPENDIX E**

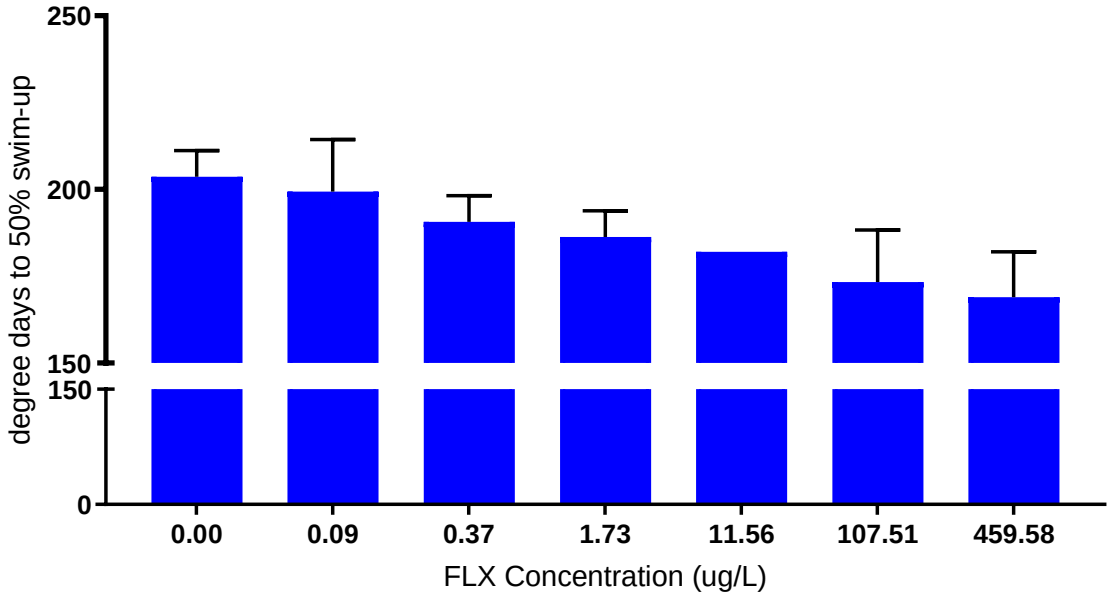

4768

4769 **Figure E.S1.** Degree days to 50% swim up of RBT exposed to FLX.

4770

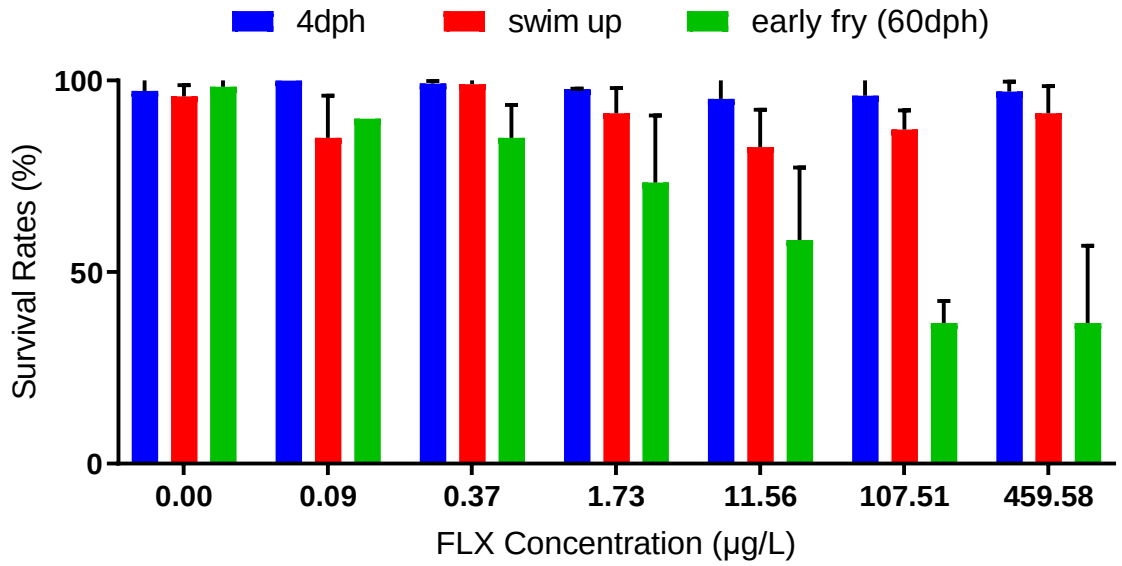

4771

4772 **Figure E.S2.** Survival rates of RBT at different life stages after continuous exposure to FLX.

Table E.S1. Survival rates of RBT at different life stages after continuous exposure to FLX.

Species	Chemical (units)	Nominal concentrations/Treatment groups (# of rep in parenthesis)	Start of exposure	End of exposure	Exposure condition	Temp (°C)	# of individuals for total RNA extraction (per rep)	Sequencing platform	Reference transcriptome	Data Source
WS	FLX (µg/L)	water control, 0.44, 1.75, 7, 28, and 112 (3 reps each)	0 dph	4 dph	static renewal	14±1	3	NextSeq500	NCBI GEO Acc# GSE79624	This study
WS	EE2 (ng/L)	0.01% DMSO solvent control, 1, 3, 10, 30, and 100 (3 reps each)	0 dph	4 dph	static renewal	14±1	3	NextSeq500	NCBI GEO Acc# GSE79624	This study
RBT	FLX (µg/L)	water control, 0.44, 1.75, 7, 28, and 112 (3 reps each)	0 dph	4 dph	flow-through	15±1	3	NovaSeq6000	GCA_002163495.1	This study
RBT	EE2 (ng/L)	0.01% DMSO solvent control, 1, 3, 10, 30, and 100 (3 reps each)	0 dph	4 dph	flow-through	15±1	3	NovaSeq6000	GCA_002163495.1	Metadata (Alcaraz et al., 2021a)
FHM	FLX (µg/L)	water control(5), 0.44(3), 1.75(5), 7(5),	<6 hpf†	4 dph	static renewal	24±1	20	NovaSeq6000	GCA_016745375.1	Metadata (Alcaraz et al.,

		28(5), and 112(3)								submitted)
FHM[‡]	EE2 (ng/L)	0.01% DMSO solvent control(5), 1(3), 4(5), 10(3)*, 20(5), and 100(5)	<6 hpf[†]	4 dph	static renewal	24±1	20	HiSeq4000	GCA_016745375.1	This study and metadata (Alcaraz et al., 2021b)

WS = white sturgeon; RBT = rainbow trout; FHM = fathead minnows

hpf = hours post-fertilization; dph = days post-hatch; Temp = temperature; reps = replicates

FLX = fluoxetine; EE2 = 17α-ethinylestradiol

[‡] sequences for 1, 4, and 10 ng/L treatment groups have not been previously reported, but exposures were nevertheless conducted at the same time as the rest of those reported in Alcaraz *et al*. (2021)

* 1 replicate failed quality control for sequencing

[†] between late cleavage and high blastula stage

Table E.S2. Summary of experimental design of the 6 separate studies reported here.

Reference/Source	Species	Chemical (units)	Method of analysis	Length of original study	Nominal concentration	Measured concentration	% Nominal	Notes
This study	WS	FLX (µg/L)	LC-MS (SM 2.1)	60 dph$^{\partial}$	Water*	0	-	Due to potential risks of pathogenic contamination from wild-caught sources, WS experiments had to be conducted in a quarantine facility with limited space, which resulted in not being able to collect sufficient water samples for FLX analyses. Hence, measured concentrations for FLX from RBT was used for WS since these experiments shared stock solutions.
					0.44	0.09$^{\beta}$	20$^{\blacktriangledown}$	
					1.75	0.37$^{\beta}$	21$^{\blacktriangledown}$	
					7	1.83±0.60	26	
					28	11.56±4.93	41	
					112	107.51±15.00	96	
This study	WS	EE2 (ng/L)	ELISA (SM 2.3)	60 dph$^{\partial}$	0.01% DMSO†	< 0.01	-	
					1	0.36±0.12	36	
					3	1.47±0.04	49	
					10	8.85±0.54	89	
					30	24.99±0.10	83	
					100	73.95±9.86	74	
This study	RBT	FLX (µg/L)	LC-MS (SM 2.1)	60 dph	Water*	0	-	
					0.44	0.09$^{\beta}$	20$^{\blacktriangledown}$	$^{\blacktriangledown}$ % nominal appeared to follow a strong 2° polynomial trend (R^2 = 0.9997); hence, % nominal was calculated using the equation of the trendline: y = -0.0015x2 + 0.8442x + 19.67
					1.75	0.37$^{\beta}$	21$^{\blacktriangledown}$	$^{\beta}$ Concentration was based on extrapolated % nominal
					7	1.83±0.60	26	
					28	11.56±4.93	41	
					112	107.51±15.00	96	
(Alcaraz et al., 2021a)	RBT	EE2 (ng/L)	ELISA (SM 2.3)	60 dph	0.01% DMSO†	< 0.01	-	
					1	1.13±0.10	113	
					3	1.57±0.33	52	
					10	6.22±1.16	62	
					30	16.34±2.45	54	
					100	55.10±9.46	55	

Alcaraz et al. (accepted)	FHM	FLX (µg/L)	LC-MS (SM 2.2)	28 dph	Water*	0.01±0.01	-	
					0.44	0.19‡	42.37Δ	‡ Extrapolated from the average % nominal from other concentrations in this particular study.
					1.75	0.74±0.08	42.41	Δ Average % nominal from those with measured concentrations above the instrument limit of detection
					7	3.38±0.56	48.35	
					28	10.2±2.38	36.34	
					112	47.5‡	42.37Δ	
This study and Alcaraz et al. (2021b)	FHM	EE2 (ng/L)	LC-MS (SM 2.4)	28 dph	0.01% DMSO†	< 0.01	-	
					1	1.07‡	106.65Δ	‡ Extrapolated from the average % nominal from other concentrations in this particular study.
					4	4.27‡	106.65Δ	Δ Average % nominal from those with measured concentrations above the instrument limit of detection
					10	10.67‡	106.65Δ	
					20	23.46±8.13	117.3	
					100	95.99±19.58	95.99	

% nominal = measured/nominal x 100

* facility water

† 0.01% DMSO as solvent control

‡, Δ, β, ∂ Extrapolations were done either due to (1) concentrations were below limits of instrument detection or (2) water samples (in petri dishes) were not enough for analytical measurements.

∂ 60 dph maximum for control and the highest concentration only. Due to the limited space in the fish quarantine facility, most of the larva had to be culled at very early life stages.